UC San Diego
Research Theses and Dissertations

Title
Novel Anticancer Agents from Ascidiacea

Permalink
https://escholarship.org/uc/item/2vh094nq

Author
Vervoort, Hélène C.

Publication Date
1999

Peer reviewed

eScholarship.org Powered by the California Digital Library
University of California

INFORMATION TO USERS

This manuscript has been reproduced from the microfilm master. UMI films the text directly from the original or copy submitted. Thus, some thesis and dissertation copies are in typewriter face, while others may be from any type of computer printer.

The quality of this reproduction is dependent upon the quality of the copy submitted. Broken or indistinct print, colored or poor quality illustrations and photographs, print bleedthrough, substandard margins, and improper alignment can adversely affect reproduction.

In the unlikely event that the author did not send UMI a complete manuscript and there are missing pages, these will be noted. Also, if unauthorized copyright material had to be removed, a note will indicate the deletion.

Oversize materials (e.g., maps, drawings, charts) are reproduced by sectioning the original, beginning at the upper left-hand corner and continuing from left to right in equal sections with small overlaps.

Photographs included in the original manuscript have been reproduced xerographically in this copy. Higher quality 6" x 9" black and white photographic prints are available for any photographs or illustrations appearing in this copy for an additional charge. Contact UMI directly to order.

ProQuest Information and Learning
300 North Zeeb Road, Ann Arbor, MI 48106-1346 USA
800-521-0600

UMI®

Reproduced with permission of the copyright owner. Further reproduction prohibited without permission.

Reproduced with permission of the copyright owner. Further reproduction prohibited without permission.

UNIVERSITY OF CALIFORNIA, SAN DIEGO

Novel Anticancer Agents from Ascidiacea

A dissertation submitted in partial satisfaction of the
requirements for the degree
Doctor of Philosophy

in

Oceanography

by

Hélène C. Vervoort

Committee in charge:

Professor William Fenical, Chair
Professor D. John Faulkner
Professor Victor Vacquier
Professor Stephen B. Howell
Professor Erkki Ruoslahti

1999

Reproduced with permission of the copyright owner. Further reproduction prohibited without permission.

UMI Number: 3035904

Copyright 1999 by
Vervoort, Helene C.

All rights reserved.

UMI Microform 3035904
Copyright 2002 by ProQuest Information and Learning Company.
All rights reserved. This microform edition is protected against
unauthorized copying under Title 17, United States Code.

ProQuest Information and Learning Company
300 North Zeeb Road
P.O. Box 1346
Ann Arbor, MI 48106-1346

Reproduced with permission of the copyright owner. Further reproduction prohibited without permission.

Copyright
Hélène C. Vervoort, 1999
All rights reserved.

Reproduced with permission of the copyright owner. Further reproduction prohibited without permission.

The dissertation of Hélène C. Vervoort is approved, and it is acceptable in quality and form for publication on microfilm:

Chair

University of California, San Diego

1999

Reproduced with permission of the copyright owner. Further reproduction prohibited without permission.

To Diane

Reproduced with permission of the copyright owner. Further reproduction prohibited without permission.

ACKNOWLEDGEMENTS

William Fenical
John Faulkner
Erkki Ruoslahti
Stephen Howell
Victor Vacquier

Renata Pasqualini, Wadih Arap, Gerrit Los; Mercedes Cueto, Marc Cummings, Tegan Eve, Felix Flachsmann, Walter Frankmoelle, Kelly Jenkins, Paul Jensen, Chris Kaufman, Niels Lindquist, Stephany Lewis, Thomas Lindel, Julia Kubanek, Bill Paplawsky, Monica Puyana, David Rowley, Jackie Trishman, Dean Wilson, Tammy Woo; Chris Blackburn, Mary-Kay Harper, Scott Mitchell, Christine Salomon, Eric Schmidt; Joe Pawlik, Mark Hay, Rosangela Epifanio, Lauri Ramundo, Nida Kalumpong, Crew of the Malaena, S. Johnson; May de las Alas, Gerald, Barbara Blouw, Dorine How; David Newman, Pat Collins, Dennis Young, Martin Haas; Gladys; Johan Lugtenburg; Jeffrey Regan; Wim en Len Vervoort

♡

California Sea Grant College Program
National Science Foundation
National Oceanic and Atmospheric Administration

Reproduced with permission of the copyright owner. Further reproduction prohibited without permission.

TABLE OF CONTENTS

Reproduced with permission of the copyright owner. Further reproduction prohibited without permission.

Reproduced with permission of the copyright owner. Further reproduction prohibited without permission.

LIST OF FIGURES

Reproduced with permission of the copyright owner. Further reproduction prohibited without permission.

Reproduced with permission of the copyright owner. Further reproduction prohibited without permission.

Reproduced with permission of the copyright owner. Further reproduction prohibited without permission.

Reproduced with permission of the copyright owner. Further reproduction prohibited without permission.

LIST OF TABLES

Reproduced with permission of the copyright owner. Further reproduction prohibited without permission.

LIST OF ABBREVIATIONS

Cbz	benzyloxycarbonyl
COSY	Correlation Spectroscopy
DAA	2,4-dinitrophenyl-5-L-alanine amide
DEPT	Distortionless Enhancement by Polarization Transfer
DMAP	4-dimethylaminopyridine
DMF	dimethylformamide
DMSO	dimethylsulfoxide
DQF-COSY	Double Quantum Filtered COSY
ECM	extracellular matrix
ECOSY	Exclusive COSY
EDC	1-(3-dimethylaminopropyl)-3-ethylcarbodiimide hydrochloride
FABMS	Fast Atom Bombardment Mass Spectroscopy
FDA	Food and Drug Administration
FDAA	1-fluoro-2,4-dinitrophenyl-5-L-alanine amide
FITC	fluorescein isothiocyanate
Fmoc	9-fluorenylmethoxycarbonyl
gHMBC	gradient Heteronuclear Multiple Bond Correlation
gHMQC	gradient Heteronuclear Multiple Quantum Coherence
GTP	guanosine 5'-triphosphate
HOBt	1-hydroxybenzotriazole
HPLC	High Performance Liquid Chromatography
MAP	microtubule-associated protein
MAb	monoclonal antibody
MDR	multiple drug resistant
MMP	matrix metalloproteinase
MTOC	microtubule organizing center
MTPA	(*R*,*S*)-methoxytrifluorophenyl acid chloride
NCI	National Cancer Institute
NMR	Nuclear Magnetic Resonance
NOE	Nuclear Overhauser Enhancement
NOESY	NOE Spectroscopy
PBS	phosphate buffered saline
Pfp	pentafluorophenyl
Su	succinimidyl
ROE	Rotating frame Overhauser Enhancement
ROESY	ROE Spectroscopy
RP	reversed phase
TFA	trifluoroacetic acid
TOCSY	Total Correlation Spectroscopy

Reproduced with permission of the copyright owner. Further reproduction prohibited without permission.

VITA

1993	Doctorandus Physical Organic Chemistry University of Leiden The Netherlands
1997-1998	Sea Grant Trainee Center for Marine Biotechnology and Biomedicine Scripps Institution of Oceanography University of California at San Diego
1999	Ph.D. Oceanography Center for Marine Biotechnology and Biomedicine Scripps Institution of Oceanography University of California at San Diego

PUBLICATIONS

H.C. Vervoort, W. Fenical; "Antimicrobial Diterpenoids from an Undescribed Soft-coral of the Genus *Xenia*", *Nat. Prod. Lett.* 6, p49-55, 1995.

H.C. Vervoort, S.E. Richards-Gross, W. Fenical, A.Y. Lee, J. Clardy; "Didemnimides A-D, Novel Predator Deterrent Alkaloids from the Caribbean Mangrove Ascidian *Didemnum conchyliatum*", *J. Org. Chem.* 62, p1486-1490, 1997.

H.C. Vervoort, J. Pawlik, W. Fenical; "Chemical Defense of the Caribbean Ascidian *Didemnum conchyliatum*", *Mar. Ecol. Prog. Ser.* 165, p221-228, 1998.

H.C. Vervoort, W. Fenical, P.A. Keifer; "Cyclized Didemnimide Alkaloid from the Caribbean Ascidian *Didemnum conchyliatum*", *J. Nat. Prod.* 62, p389-391, 1999.

H.C. Vervoort, W. Fenical, R. de A. Epifanio; "Tamandarins A and B, Novel Cytotoxic Depsipeptides from a Brazilian Ascidian of the Genus *Didemnidae*", *J. Org. Chem.* In preparation, 1999.

H.C. Vervoort, M.I. Choudhary, W. Fenical; "Patellin 7, a Novel Cytotoxic Peptide from the Philippine Ascidian *Polysynchraton* sp..", *J. Nat. Prod.* In preparation, 1999.

H.C. Vervoort, W. Fenical, G. Los, S.B. Howell; "Mechanism of Action of Diazonamide A, a Novel Antimitotic Agent.", In preparation, 1999.

Reproduced with permission of the copyright owner. Further reproduction prohibited without permission.

FIELDS OF STUDY

Major Field: Marine Natural Products Chemistry

Studies in Isolation and Structure Elucidation of Organic Compounds.
Studies in Nuclear Magnetic Resonance Spectroscopy.
Studies in Organic Synthesis.
Professors William Fenical and D. John Faulkner

Studies in Chemical Ecology.
Professors Joe Pawlik and Mark Hay

Studies in Cancer Immunology.
Professor Erkki Ruoslahti and Dr. Renata Pasqualini

Studies in Cancer Pharmacology.
Professor Stephen B. Howell and Dr. Gerrit Los

Reproduced with permission of the copyright owner. Further reproduction prohibited without permission.

ABSTRACT OF THE DISSERTATION

Novel Anticancer Agents from Ascidiacea

by

Hélène C. Vervoort
Doctor of Philosophy in Oceanography
University of California San Diego, 1999
Professor William Fenical, Chair

This thesis presents an effort to contribute to the discovery and development of structurally and mechanistically novel anticancer drugs. In order to reach this goal, it focusses on the biologically active secondary metabolites of marine invertebrates of the class Ascidiacea (phylum Chordata, subphylum Urochordata (Tunicata), class Ascidacea).

Three distinct areas of research were combined. The first part concerns the discovery of two novel, naturally occurring didemnin depsipeptides, tamandarins A and B. The tamandarins were isolated from an unidentified Brazilian ascidian of the family Didemnidae. Their structures were determined by FABMS and extensive 2D NMR spectroscopy, the absolute configurations by alkaline hydrolysis and by Marfey analysis of the acid hydrolyzates. The cytotoxic activity of tamandarin A against various human cancer cell lines was evaluated and this metabolite was found to inhibit protein biosynthesis. A qualitative discussion on the conformation of tamandarin A in solution, obtained from J-values, variable temperature experiments and NOE/ROE data, is included.

The next section reports preliminary studies aimed at gaining a better understanding of the mechanism of cytotoxic action of diazonamide A, a recently isolated ascidian metabolite that shows potent and selective anticancer activity.

The last part describes the synthesis of dianestatin 1, the first conjugate between a tumor-homing peptide and didemnin B. This work, performed in collaboration with researchers at the Burnham Institute in La Jolla, is aimed at the development of an alternative form of cancer treatment by targeted delivery of potent, non-selective cytotoxins using tumor-homing peptides.

Reproduced with permission of the copyright owner. Further reproduction prohibited without permission.

Chapter 1

Introduction

Marine invertebrates of the class Ascidiacea (phylum Chordata, subphylum Urochordata (Tunicata)) are an exceptionally rich source of novel, cytotoxic metabolites [4–11]. This study describes the isolation and medicinal chemistry of biologically active secondary metabolites produced by this group in an effort to discover and develop structurally and mechanistically novel antitumor agents. The study is divided into three distinct areas of research: marine drug discovery, preclinical pharmacology studies and synthesis.

Chapter II describes the discovery of novel cytotoxic substances from ascidians. It gives an overview of ascidian metabolites and presents the structures of two novel, cytotoxic depsipeptides, tamandarins A (**42**) and B (**43**). The tamandarins were isolated from an unidentified Brazilian ascidian of the family Didemnidae. The structures of the new cytotoxins were assigned by interpretation of FABMS data and by extensive 2D NMR analyses. The absolute configurations of the tamandarins were assigned by alkaline hydrolysis to yield their corresponding amino acids, which were then identified as their Marfey derivatives. The cytotoxicity of tamandarin A (**42**) was evaluated against various human cancer cell lines and shown to be slightly more potent than didemnin B (**11**). A discussion of the conformation of tamandarin A (**42**) in solution, obtained from NMR J-values, variable temperature experiments and NOESY/ROESY data is included.

Chapter III describes preliminary studies aimed at gaining a better understanding of the mechanism of action of newly isolated cytotoxic compounds. Specifically, it describes *in vitro* studies on the mechanism of action of diazonamide A (**75**), a recently isolated antimitotic ascidian metabolite. An *in vitro* cytotoxicity screen using the NCI's 60 cell line panel showed that this metabolite has potent and selective anticancer ac-

Reproduced with permission of the copyright owner. Further reproduction prohibited without permission.

tivity. Diazonamide A (**75**) is an unusually complex, highly modified bicyclic peptide, originally isolated from the marine ascidian *Diazona angulata* [2,3]. Incubation of cells from the 2008 human ovarian carcinoma cell line with diazonamide A (**75**) resulted in a dose dependent inhibition of cell proliferation with an IC_{50} value of 10.0 nM. Flow-cytometric analysis of 2008 cells treated with 40 nM diazonamide A (**75**) for up to 96 hours indicated that diazonamide A (**75**) causes an increase in the number of cells in the G_2-M phase of the cell cycle with a concomitant increase in the percentage of cells in mitosis. Indirect immunofluorescence studies demonstrated that treatment of 2008 human ovarian carcinoma cells with diazonamide A (**75**) results in marked depletion of cellular microtubules, similar to the effects of vinblastine (**71**).

Chapter IV describes the synthesis of dianestatin 1 (**102**), the first conjugate between a tumor-homing peptide and a marine natural product, the ascidian metabolite didemnin B (**11**). This work is aimed at the development of an alternative form of cancer treatment, the direct tumor-targeting of potent cytotoxins that, due to a lack of selectivity, cannot be used unmodified as clinical anticancer drugs. Recent research [12, 13] using phage display peptide libraries identified peptides with enhanced selectivity for the endothelial surfaces of certain body tissues, including the neovasculature of tumors. The anticancer drug doxorubicin (Adriamycin, (**67**)) was conjugated to two such peptides, allowing it to be targeted to a human breast carcinoma in a mouse model, dramatically enhancing the efficacy of the drug and reducing its toxicity [14].

Based upon this result, dianestatin 1 (**102**) was synthesized to test the experimental hypothesis that an effective anticancer agents can be created by conjugating potent but *non-selective* cytotoxins, such as didemnin B (**11**), to a tumor-homing peptide. In addition, this synthesis is prerequisite to testing the concept that conjugation to the homing peptide using an ester bond, rather than an amide bond, may result in a reagent which can regenerate the parent cytotoxin *in situ* by an expected lipase-mediated ester bond hydrolysis. *In vitro* testing has shown that the cytotoxicity of dianestatin 1 (**102**) is reduced compared to the unmodified parent compound didemnin B (**11**). Dianestatin 1 (**102**) is undergoing further biological testing. It is hoped that it will specifically home to the tumor vasculature and accumulate there to subsequently undergo enzymatic hydrolysis liberating the parent cytotoxin didemnin B (**11**).

Reproduced with permission of the copyright owner. Further reproduction prohibited without permission.

Chapter 2

Discovery of Novel Cytotoxic Agents from Ascidiacea

2.1 Introduction

Over 70% of the world surface is covered by oceans. Over the past several decades scientists have discovered that this vast body of water harbors a tremendous amount of biodiversity, expressed not only in the number of different species but also in the ecologically diverse environments in which they are found. The genetically unique biodiversity of the marine environment leads to the expression of unique biochemical pathways yielding unprecedented chemical structures.

In the terrestrial environment, human beings have roamed the earth's surface for thousands of years, sampling the plants and animals around them for their medicinal potential. The knowledge thus acquired, forming the basis of "ethno-medicine", has been transfered from generation to generation and eventually became the basis of today's pharmaceutical industry.

In the marine environment, the gathering of any information about life below the sea surface was delayed until technological advances in the 1950's, such as diving equipment and submersibles, allowed marine scientists to look below the surface and assess the potential of marine plants and animals in the treatment of human disease. In the absence of any information as to which plants and animals would be of use, they had to rely on ecological observations.

One such observation was that in the shallow tropical coral reef environments, but also in the more temperate and (ant-)arctic bottom communities, many marine

Reproduced with permission of the copyright owner. Further reproduction prohibited without permission.

organisms appear to be defended, e.g. against predation, by means of spines, shells, and exoskeletons. On the other hand, many organisms appear on physical grounds to be defenseless, delicate, and vulnerable. Yet they survive and thrive in these often very competitive environments. It is those animals that were hypothesized to have developed alternative defense mechanisms, such as noxious chemicals, and a correlation between the lack of physical defenses and the presence of secondary metabolites (metabolites not used for the primary metabolism) is often found [15].

Since the 1970's marine natural products chemists have isolated over 6000 compounds, most structurally unprecedented, often exhibiting strong bioactivities. In fact, some of the most important, recent discoveries have been from the marine environment and currently approximately 13 marine drug candidates are in clinical evaluation against cancer. Fig. 2.1 lists several of these molecules including their sources and biomedical relevance. Consistent with the concept of chemical defense, most of these molecules were isolated from soft bodied marine organisms [15].

Ascidians (phylum Chordata, subphylum Urochordata, class Ascidiacea) are solitary or colonial marine invertebrates with a general body plan as depicted in Fig. 2.2. Solitary individuals, the largest of which may reach 30 cm from base to apex, are generally much larger than the compound bodies of colonial ascidians, the dimensions of which are usually measured in millimeters. The colonies of these ascidians may, however, spread over a large surface area, sometimes as much as a square meter.

The adult ascidian body is a hollow, complex basket open to the outside through two siphons through which water is filtered. It is entirely embedded within a tunic, which forms a somewhat flexible exoskeleton. The tunic's composition is unusual in that it consists largely of polysaccharides much like the constituents of plant cellulose. The consistency of the tunic varies enormously. Some ascidians possess tough, leathery tunics whereas in others it is very soft, even slimy [16].

Historically, the search for new pharmacologically active agents from ascidians has led to the discovery of many highly cytotoxic substances and several new lead compounds, some of which have entered clinical trials to evaluate their potential as anticancer drugs. Although most of these compounds are not suitable for drug development, some are now being used as "molecular probes" providing selective inhibition of their protein targets such that they can be used to study the role of genes and their gene products in cancer and other diseases [17].

Approximately 400 natural products have been isolated from ascidians to date.

Reproduced with permission of the copyright owner. Further reproduction prohibited without permission.

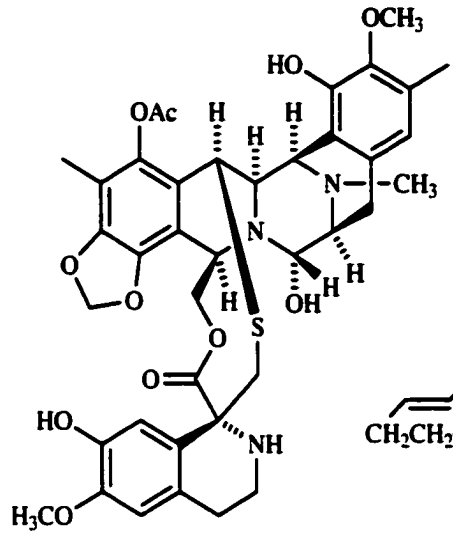

Ecteinascidin 743 (1)

Ecteinascidia turbinata (Ascidian)
Leukemia, melanoma, ovarian, Lewis lung, breast cancer

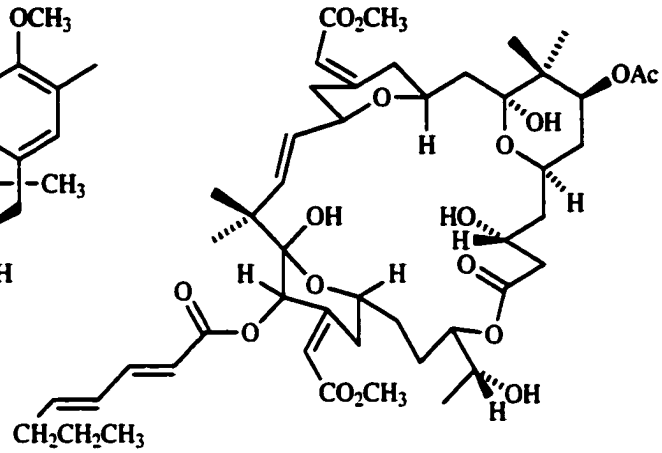

Bryostatin 1 (2)

Bugula neritina (Bryozoan)
Leukemia

Dolastatin 10 (3)

Dolabella auricularia (sea hare)
Melanoma

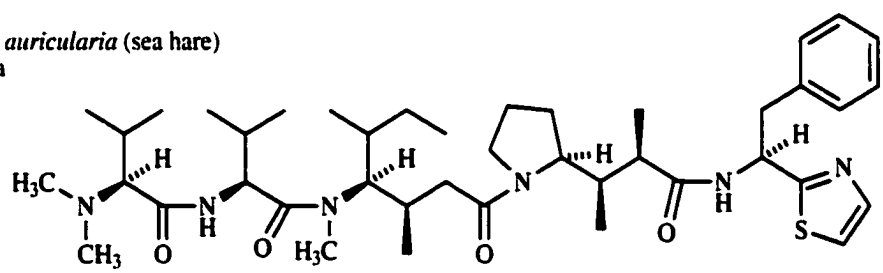

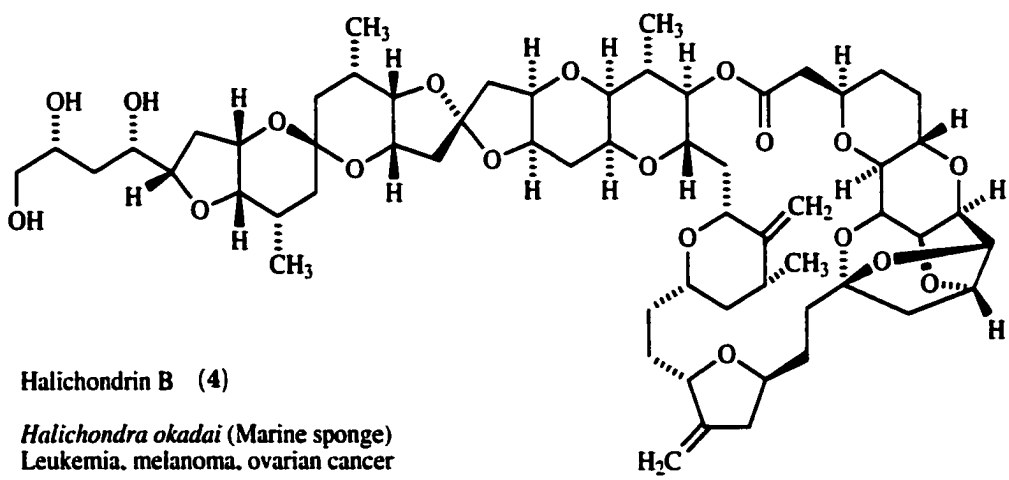

Halichondrin B (4)

Halichondra okadai (Marine sponge)
Leukemia, melanoma, ovarian cancer

Figure 2.1: Important marine natural products, their source, and biomedical relevance.

Reproduced with permission of the copyright owner. Further reproduction prohibited without permission.

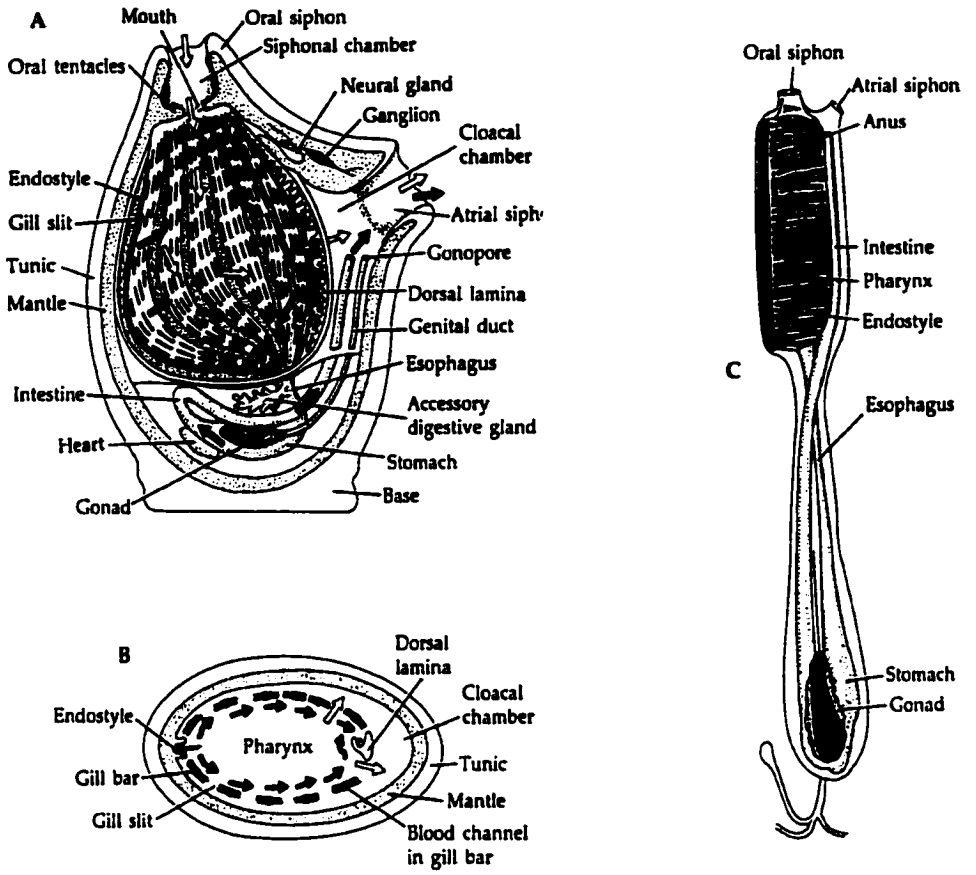

Figure 2.2: General anatomy of the ascidian. A. Solitary ascidian (cutaway view). B. The pharyngeal region of the same animal (cross section). White arrows indicate water flow; black arrows indicate path of food material. C. A single zooid from a colonial ascidian (Source: Ref. [1]).

Most of these compounds are derivatives of amino acids and thus nitrogenous in character, ranging from peptides, often with unusual amino acids, to polycyclic aromatic compounds or alkaloids [4–11, 18].

Ascidians have yielded many cytotoxic substances, including several lead structures that have entered clinical trials for the treatment of cancer. The first ascidian discovered to contain substances of potential biomedical importance, was the Caribbean mangrove ascidian *Ecteinascidia turbinata* (order Phlebobranchia, family Perophoridae). Although its extracts were found to exhibit potent cytotoxic properties as early as 1969 [19], it took almost 20 years of progress in natural products chemistry before the active components, the ecteinascidins (**1**, **5-10**) Fig. 2.3, were isolated and described [20–22]. The ecteinascidins (**1**, **5-10**) are numbered by the highest mass ob-

Reproduced with permission of the copyright owner. Further reproduction prohibited without permission.

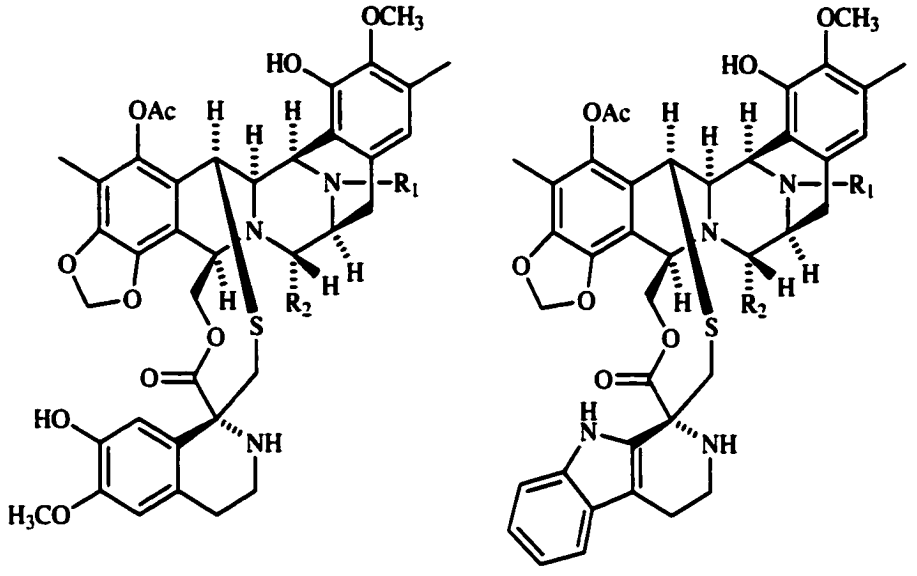

Ecteinascidin 743 (**1**) $R_1 = CH_3$, $R_2 = OH$
Ecteinascidin 729 (**5**) $R_1 = H$, $R_2 = OH$
Ecteinascidin 745 (**6**) $R_1 = CH_3$, $R_2 = H$
Ecteinascidin 759B (**7**) $R_1 = CH_3$, $R_2 = OH$, S-oxide
Ecteinascidin 770 (**8**) $R_1 = CH_3$, $R_2 = CN$
Ecteinascidin 736 (**9**) $R_1 = CH_3$, $R_2 = OH$
Ecteinascidin 722 (**10**) $R_1 = H$, $R_2 = OH$

Figure 2.3: The ecteinascidins (**1**, **5-10**), isolated from the Caribbean ascidian *Ecteinascidia turbinata*.

tained by mass spectrometry, which corresponds to the total mass of each compound minus a hydroxyl group.

Initially, the NCI started the clinical development of the ecteinascidins with ecteinascidin 729 (**5**), which showed *in vitro* activity against human solid tumor cell lines and *in vivo* activity against P388 leukemia and B16 melanoma [23]. However, comparison of *in vitro* and *in vivo* studies of ecteinascidin 729 (**5**) and ecteinascidin 743 (**1**) revealed that both compounds have similar activities against human and murine tumor models. Since ecteinascidin 743 (**1**) is more abundant in the tunicate, it was selected as the lead structure for further development.

The ecteinascidins (**1**, **5-10**), Fig. 2.3, were first isolated form the Caribbean mangrove ascidian *Ecteinascidia turbinata* [19, 24]. They are tetrahydroquinoline alkaloids, most closely related to the saframycins, originally isolated from a cultured *Streptomycete* species [25]. Ecteinascidin 743 (**1**) showed significant activity against murine (L1210) leukemia *in vitro* (IC_{50}=0.5 ng/mL), and *in vivo* activities against P388 lymphocytic leukemia and human mammary tumors [20, 26]. Ecteinascidin 743 (**1**) inhibits

Reproduced with permission of the copyright owner. Further reproduction prohibited without permission.

DNA synthesis and DNA polymerase as well as RNA synthesis and RNA polymerase [27]. It alkylates DNA at the minor groove by covalent binding to the exocyclic amino group at position 2 of guanine [28]. Ecteinascidin 743 (**1**) was also found to block cell cycle progression at late S/G_2 [29] and it interacts with the microtubule network, although it does not seem interacts directly with tubulin [30].

During preliminary testing, the ecteinascidins showed potent antileukemia activity (L1210) *in vitro*, and *in vivo* activity against P388 lymphocytic leukemia, B16 melanoma, M5076 ovarian carcinoma, Lewis lung carcinoma, and several human tumor xenograft models in mice [26]. In subsequent studies, ecteinascidin 743 (**1**) showed selectivity against advanced stage MX-1 human mammary tumors in mice with over 90% of the mice becoming tumor free following treatment with ecteinascidin 743 (**1**) [31]. Based upon these results and further preclinical testing, ecteinascidin 743 (**1**) was advanced to clinical trials in three European countries and the USA [32–38].

Thus far, ecteinascidin 743 (**1**) has demonstrated incomplete cross-resistance with paclitaxel (taxol, **73**), alkylating agents, doxorubicin (**67**) and cisplatin (**49**). The activity of ecteinascidin 743 (**1**) in breast, non-small-cell lung, and ovarian cancers is also very promising, as well as its potential in sarcoma, melanoma and renal tumors [39]. In addition, ecteinascidin 743 (**1**) has shown to be a potent drug against ovarian carcinoma xenografts, being equally active or more efficacious than cisplatin (**49**) in the same tumor line [40].

Didemnid ascidians (order Aplousobranchia, family Didemnidae) have proven to be a particularly rich source of chemically diverse natural products with potent biological activities. Some of the most potent among these are the didemnins (**11**), Fig. 2.4, namenamicin (**14**), the bistratenes (**15–16**), the patellazoles (**17–19**), and varacin (**20**), Fig. 2.6.

The didemnins (derivatives of **11**, Fig. 2.4) are potent cytotoxic depsipeptides, acting by the inhibition of protein biosynthesis [41,42]. Among the didemnins, didemnin B (**11**) is one of the most potent members of its class [43–53]. Didemnin B, isolated from the Caribbean tunicate *Tridemnum solidum*, showed significant *in vivo* activity in mice [43–46, 54]. Didemnin B was the first marine derived compound to be extensively investigated clinically. Unfortunately, dose-limiting toxicities, *i.e.*, neuromuscular and cardiac toxicities, preclude its use at clinically relevant doses and didemnin B was eventually discarded for further development against cancer.

In the search for other novel didemnin depsipeptides, a structure closely related

Reproduced with permission of the copyright owner. Further reproduction prohibited without permission.

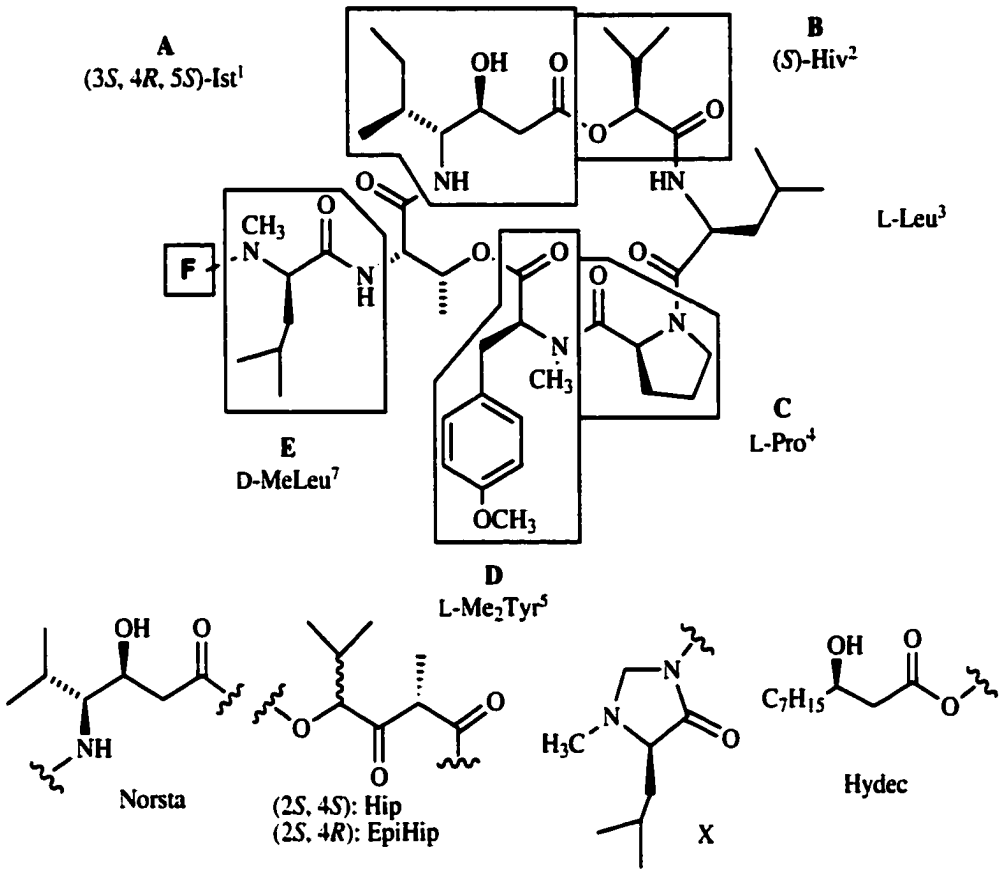

		A	B	C	D	E	F
Tamandarin	A (**42**)	Ist	Hiv	Me_2Tyr	L-Pro	MeLeu	-Pro-Lac
	B (**43**)	Norsta	Hiv	Me_2Tyr	L-Pro	MeLeu	-Pro-Lac
Didemnin	A	Ist	Hip	Me_2Tyr	L-Pro	MeLeu	-H
	B (**11**)	Ist	Hip	Me_2Tyr	L-Pro	MeLeu	-Pro-Lac
	C	Ist	Hip	Me_2Tyr	L-Pro	MeLeu	-Lac
	D	Ist	Hip	Me_2Tyr	L-Pro	MeLeu	-Pro-Lac-$(Gln)_3$-pGlu
	E	Ist	Hip	Me_2Tyr	L-Pro	MeLeu	-Pro-Lac-$(Gln)_2$-pGlu
	G	Ist	Hip	Me_2Tyr	L-Pro	MeLeu	-CHO
	M/H	Ist	Hip	Me_2Tyr	L-Pro	MeLeu	-Pro-Lac-Gln-pGlu
	N	Ist	Hip	Tyr	L-Pro	MeLeu	-Pro-Lac
	X	Ist	Hip	Me_2Tyr	L-Pro	MeLeu	-Pro-Lac-$(Gln)_3$-Hydec
	Y	Ist	Hip	Me_2Tyr	L-Pro	MeLeu	-Pro-Lac-$(Gln)_4$-Hydec
[D-Pro⁴]-didemnin	B	Ist	Hip	Me_2Tyr	D-Pro	MeLeu	-Pro-Lac
Nordidemnin	A	Norsta	Hip	Me_2Tyr	L-Pro	MeLeu	-H
	B (**12**)	Norsta	Hip	Me_2Tyr	L-Pro	MeLeu	-Pro-Lac
	N	Norsta	Hip	Tyr	L-Pro	MeLeu	-Pro-Lac
Methylenedidemnin	A	Ist	Hip	Me_2Tyr	L-Pro	X	-H
Epididemnin	A_1	Ist	EpiHip	Me_2Tyr	L-Pro	MeLeu	-H
Acyclodidemnin	A	Ist	Hip	Me_2Tyr	L-Pro	MeLeu	-H
Dehydrodidemnin	B (**13**)	Ist	Hip	Me_2Tyr	L-Pro	MeLeu	-Pro-Pyr

Figure 2.4: Naturally occurring didemnin congeners. Tamandarins A (**42**) and B (**43**) were isolated during this study.

Reproduced with permission of the copyright owner. Further reproduction prohibited without permission.

	A	B	C	E	F
N^{α}-acetyl-didemnin A	Ist	Hip	Me_2Tyr	D-MeLeu	-*n*-CH_3CO-
N^{α}-propionyl-didemnin A	Ist	Hip	Me_2Tyr	D-MeLeu	-*n*-CH_3CH_2CO-
N^{α}-*n*-butyryl-didemnin A	Ist	Hip	Me_2Tyr	D-MeLeu	-*n*-$CH_3(CH_2)_2CO$-
N^{α}-pentanoyl-didemnin A	Ist	Hip	Me_2Tyr	D-MeLeu	-*n*-$CH_3(CH_2)_3CO$-
N^{α}-hexanoyl-didemnin A	Ist	Hip	Me_2Tyr	D-MeLeu	-*n*-$CH_3(CH_2)_4CO$-
N^{α}-octanoyl-didemnin A	Ist	Hip	Me_2Tyr	D-MeLeu	-*n*-$CH_3(CH_2)_6CO$-
N^{α}-dodecanoyl-didemnin A	Ist	Hip	Me_2Tyr	D-MeLeu	-*n*-$CH_3(CH_2)_{10}CO$-
N^{α}-octadecanoyl-didemnin A	Ist	Hip	Me_2Tyr	D-MeLeu	-*n*-$CH_3(CH_2)_{16}CO$-
OAc-didemnin A	OAc-Ist	Hip	Me_2Tyr	D-MeLeu	-H
[H_2-Hip^3]-didemnin A	Ist	H_2-Hip	Me_2Tyr	D-MeLeu	-H
N^{α}-Pro-didemnin A	Ist	Hip	Me_2Tyr	D-MeLeu	-Pro
N^{α}-D-Pro-didemnin A	Ist	Hip	Me_2Tyr	D-MeLeu	-D-Pro
N^{α}-Leu-didemnin A	Ist	Hip	Me_2Tyr	D-MeLeu	-Leu
N^{α}-OHPro-didemnin A	Ist	Hip	Me_2Tyr	D-MeLeu	-4-OHPro
N^{α}-dehydroPro-didemnin A	Ist	Hip	Me_2Tyr	D-MeLeu	-3,4-dehydroPro
Z-didemnin A	Ist	Hip	Me_2Tyr	D-MeLeu	-Z
Z-[(3*R*,4*R*,5*S*)-Ist^2]-didemnin A	Ist	Hip	Me_2Tyr	D-MeLeu	-Z
Z-[(3*S*,4*R*,5*R*)-Ist^2]-didemnin A	Ist	Hip	Me_2Tyr	D-MeLeu	-Z
Z-[(3*S*,4*S*,5*S*)-Ist^2]-didemnin A	Ist	Hip	Me_2Tyr	D-MeLeu	-Z
OHPro^8-didemnin B	Ist	Hip	Me_2Tyr	D-MeLeu	-4-OH-Pro-Lac
dehydroPro^8-didemnin B_2	Ist	Hip	Me_2Tyr	D-MeLeu	-3,4-dehydroPro-Lac
[*N*-MeLeu^5]-didemnin B	Ist	Hip	L-MeLeu	D-MeLeu	-Pro-Lac
Man^9-didemnin B	Ist	Hip	Me_2Tyr	D-MeLeu	-Pro-Man
Hpp^9-didemnin B	Ist	Hip	Me_2Tyr	D-MeLeu	-Pro-Hpp
[L-*N*-MeLeu^7]-nordidemnin B	Ist	Hip	Me_2Tyr	L-MeLeu	-Pro-Lac
Pal^9-didemnin B	Ist	Hip	Me_2Tyr	D-MeLeu	-Pro-$CO(CH_2)_{14}CH_3$
[Phth-Ala^9]-didemnin B	Ist	Hip	Me_2Tyr	D-MeLeu	-Pro-Phth-Ala
[AnhIst^2][Phth-Ala^9]-didemnin B	AnhydroIst	Hip	Me_2Tyr	D-MeLeu	-Pro-Phth-Ala
[Hip^{3}oxime]-didemnin B	Ist	Hip oxime	Me_2Tyr	D-MeLeu	-Pro-Lac
[iodoMe_2Tyr^6]-didemnin B	Ist	Hip	iodoMe_2Tyr	D-MeLeu	-Pro-Lac
[H_6-Me_2Tyr^6]-didemnin B	Ist	Hip	H_6-Me_2Tyr	D-MeLeu	-Pro-Lac
[H_6-*N*-MePhe^6]-didemnin B	Ist	Hip	H_6-*N*-MePhe	D-MeLeu	-Pro-Lac
[acetyl^9]-didemnin B	Ist	Hip	Me_2Tyr	D-MeLeu	-Pro-CH_3CO-
[propionyl^9]-didemnin B	Ist	Hip	Me_2Tyr	D-MeLeu	-Pro-CH_3CH_2CO-
[isobutyryl^9]-didemnin B	Ist	Hip	Me_2Tyr	D-MeLeu	-Pro-isobutyryl
[isobutyryl^9-D-Pro^8]-didemnin B	Ist	Hip	Me_2Tyr	D-MeLeu	-D-Pro-isobutyryl
[Ala^8]-didemnin B	Ist	Hip	Me_2Tyr	D-MeLeu	-Ala-Lac
[D-Pro^9]-didemnin B	Ist	Hip	Me_2Tyr	D-MeLeu	-D-Pro-Lac
O-pGlu-didemnin B	Ist	Hip	Me_2Tyr	D-MeLeu	-Pro-Lac-pGlu
[Gly^{10}]-didemnin B (**97**)	Ist	Hip	Me_2Tyr	D-MeLeu	-Pro-Lac-Gly
didemnin B-[Gly^{10}] (**98**)	Ist-Gly	Hip	Me_2Tyr	D-MeLeu	-Pro-Lac

Figure 2.5: Semi-synthetic didemnin congeners. [Gly^{10}]didemin B (**97**) and didemnin B[Gly^{10}] (**98**) were synthesized during this study.

Reproduced with permission of the copyright owner. Further reproduction prohibited without permission.

to that of didemnin B (**11**) was discovered: dehydrodidemnin B (aplidine) (**13**), Fig. 2.4. This molecule was isolated from the Mediterranean ascidian *Aplidium albicans* [52] and is composed of a pyruvyl (Pyr^9) group instead of the lactic acid (Lac^9) group found in didemnin B (**11**).

Dehydrodidemnin B (Aplidine) (**13**), Fig. 2.4, like didemnin B (**11**), is a potent inhibitor of protein biosynthesis [55]. When dehydrodidemnin B (**13**) was tested against several types of tumor cells *in vitro* and in *in vivo* studies in mice, it showed a remarkable gain in *in vitro* and *in vivo* activities compared to didemnin B (**11**) [56,57]. Dehydrodidemnin B also showed activity against breast, melanoma and non-small-cell lung cancer and the compound induced only mild bone marrow toxicity. These results indicate that, in contrast to didemnin B (**11**), a therapeutic window between tolerable toxicity and pharmacological activity may indeed exist for dehydrodidemnin B (**13**) [58].

Namenamicin (**14**), Fig. 2.6, was isolated from the Fijian ascidian *Polysyncraton lithostrotum*. In a 26 cell line human tumor panel, the crude extract of this ascidian showed a similar cytotoxicity profile to calicheamicin, a microbial cytotoxin isolated from the fermentation broth of the actinomycete *Micromonospora echinospora* subsp. *calichensis* [59,60]. Calicheamicin and namenamicin (**14**) both carry the enediyne functional group, often called the "enediyne warhead". When triggered by reduction, this functional group is capable of generating a biradical which causes double-strand DNA cleavage. Namenamicin (**14**) shows potent *in vitro* cytotoxicity with a mean IC_{50} value of 3.5 ng/mL and *in vivo* antitumor activity in a P388 leukemia model in mice (ILS 40% 3 μg/kg). DNA cleavage experiments have indicated that namenamicin (**14**) cleaves DNA with a slightly different recognition pattern than calicheamicin [61].

The bistratenes (**15–16**), Fig. 2.6, are potent cytotoxins isolated from the tropical ascidian *Lissoclinum bistratum*. Their initial discovery illustrates the potency of these polyethers and the need for caution when working with "all-natural" substances: "A few minutes after handling the lyophilized powder of a New Caledonia ascidian *Lissoclinum bistratum*, a laboratory worker experienced symptoms of intoxication. These effects, felt to a lesser degree by a second person in the same room, were described as being "like in a state of shock, at first, followed by paralysis or numbness around the mouth and heaviness in the limbs..." [62]. Bistratene A (**15**) is the most potent among the bistratenes with cytotoxicities of 0.01-0.1 μg/mL in non-small-cell lung carcinoma NSCLC-N6 cells, KB cells, P388 leukemia, MRC5CV1 fibroblasts, and T24 bladder carcinoma cells [62–64]. Bistratene A (**15**) induces (incomplete) differentiation and growth arrest in G_2/M phase

Reproduced with permission of the copyright owner. Further reproduction prohibited without permission.

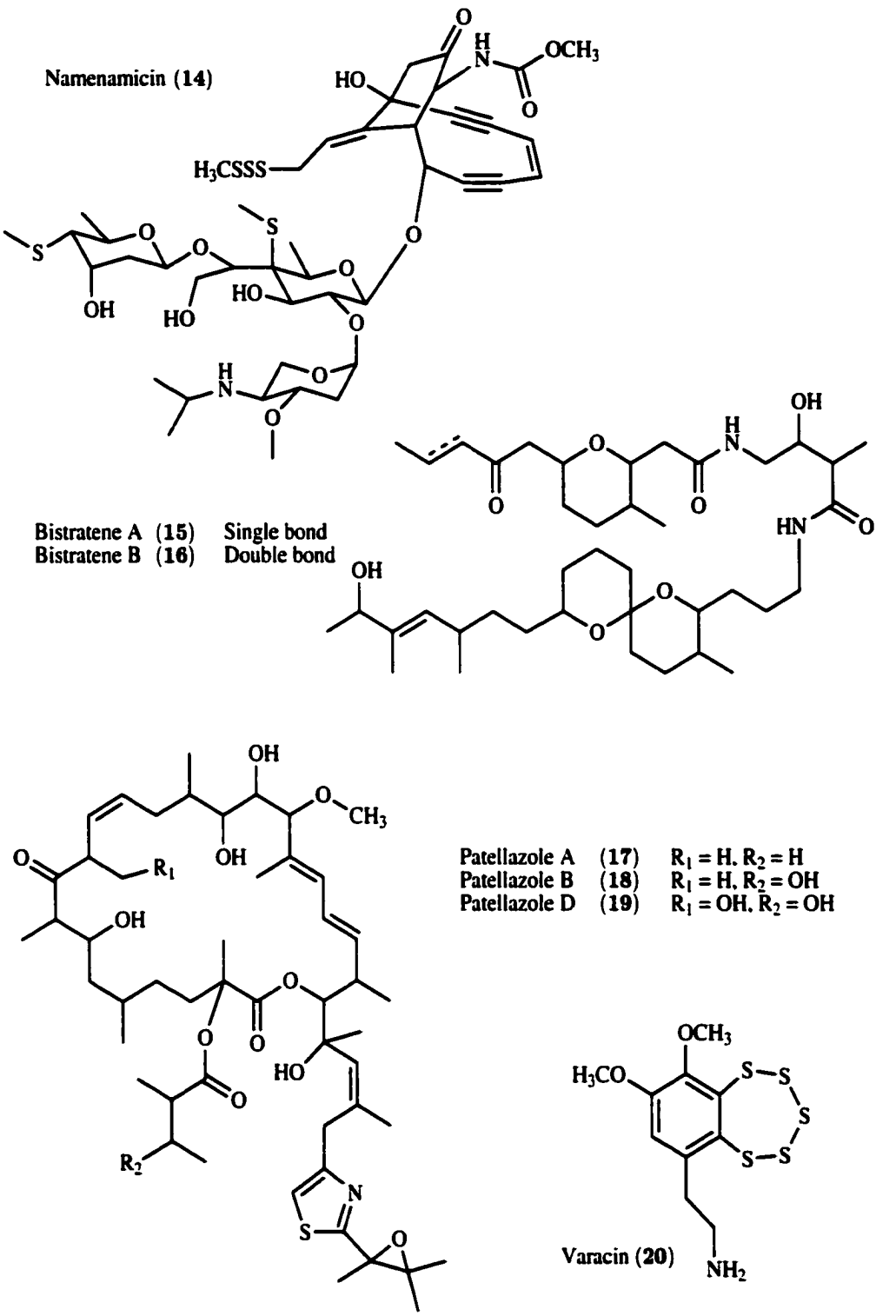

Figure 2.6: Some of the most potent cytotoxins isolated from ascidians to date.

Reproduced with permission of the copyright owner. Further reproduction prohibited without permission.

of human leukemia (HL-60) cells [65]. It is also a specific activator of protein kinase C (PKC) [66] causing phosphorylation of the focal adhesion protein talin and redistribution of actin microfilaments in fibroblasts [67].

The patellazoles (**17–19**), Fig. 2.6, were first isolated form the Fijian ascidian *Lissoclinum patella* [68, 69]. These molecules are unique thiazole containing polyketide metabolites with mean IC_{50} values of 10^{-3}-10^{-6} μg/mL in the NCI *in vitro* 60 cell line screen. Patellazole A (**17**), the most potent of the three, showed *in vitro* activity in KB cells at 300 pg/mL.

Varacin (**20**), Fig. 2.6, a member of the benzopentathiepin class, is a biologically active polysulfide isolated from *Lissoclinum vareau*. Varacin (**20**) exhibits significant antifungal and cytotoxic activity, and is 100 times more potent *in vitro* than 5-fluorouracil (**62**) towards the HCT 116 human colon adenocarcinoma. Preliminary assays suggest that its cytotoxicity is mediated through damaging DNA [70].

The molecules shown above are among the most potent metabolites isolated from ascidians to date. However, the genus *Lissoclinum* is most well known for the production of a large number of unusual thiazol and thiazoline containing peptides, such as the lissoclinamides (**21–28**) [71–75], Fig. 2.7, the ulithiacyclamides (**29–30**) [72, 76], and the patellamides (**31–35**), Fig. 2.8, [72, 77–80]. Some of these peptides also exhibit potent cytotoxicity for example ulithiacyclamide A (**29**) which is the most potent among them with IC_{50} values between 0.01-0.35 μg/mL [75, 81]. However, most of these molecules exhibit much weaker cytotoxicities with IC_{50} values around or above 1 μg/mL.

Another ascidian genus that is worth mentioning in the context of the interesting bioactivities of its natural products, is the genus *Eudistoma*. A unidentified purple *Eudistoma* species from the Red Sea has yielded six alkaloids, Fig. 2.9, segoline A (**36**), segoline B (**37**), isosegoline (**38**) norsegoline (**39**), debromoshermilamine (**40**), and eilatin (**41**) that all have a fused tetracyclic pyrido(2,3,4-kl)acridine ring system. The pyridoacridine ring system is a common theme among aromatic alkaloids from ascidians and other marine organisms including sponges and anemones.

The six metabolites, and in particular eilatin (**41**), possess potent growth regulatory properties in cultured neuroblastoma and fibroblast cells and they affect cell shape and adhesion. A single application of these compounds, at micromolar concentrations, is sufficient to completely block cell multiplication and to induce and sustain differentiation and reverse transformation. In addition, the *Eudistoma* alkaloids may act on the cAMP signaling system [82]. Eilatin (**41**) is the most potent metabolite within

Reproduced with permission of the copyright owner. Further reproduction prohibited without permission.

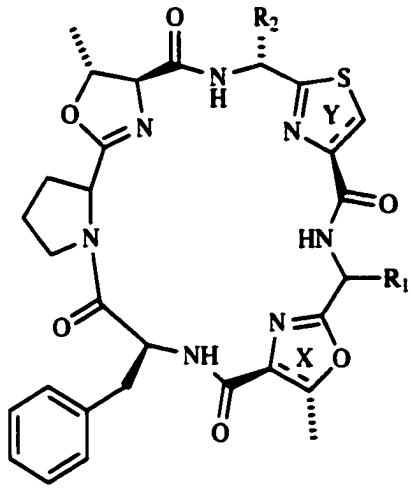

Lissoclinamide 1 (**21**) X = Y = thiazole, R_1 = D-Ile, R_2 = L-Val
Lissoclinamide 2 (**22**) X = thiazole, Y = thiazoline, R_1 = D-Ala, R_2 = D-Ile
Lissoclinamide 3 (**23**) X = thiazole, Y = thiazoline, R_1 = L-Ala, R_2 = D-Ile
Lissoclinamide 4 (**24**) X = thiazole, Y = thiazoline, R_1 = L-Phe, R_2 = D-Val
Lissoclinamide 5 (**25**) X = Y = thiazole, R_1 = L-Phe, R_2 = D-Val
Lissoclinamide 6 (**26**) X = thiazole, Y = thiazoline, R_1 = D-Phe, R_2 = D-Val
Lissoclinamide 7 (**27**) X = Y = thiazoline, R_1 = D-Phe, R_2 = D-Val
Lissoclinamide 8 (**28**) X = thiazole, Y = thiazoline, R_1 = D-Phe, R_2 = L-Val

Figure 2.7: Several cytotoxic thiazole/thiazoline- and oxazoline-containing peptides from ascidians.

this group of growth regulators and in the future it may be used in conjunction with currently available agents in *ex vivo* treatment of bone marrow leukemia [83,84].

As is demonstrated by the examples above and the large number of anticancer substances that continues to be reported from ascidians, secondary metabolites from ascidians remain an important resource for novel anticancer agents.

Reproduced with permission of the copyright owner. Further reproduction prohibited without permission.

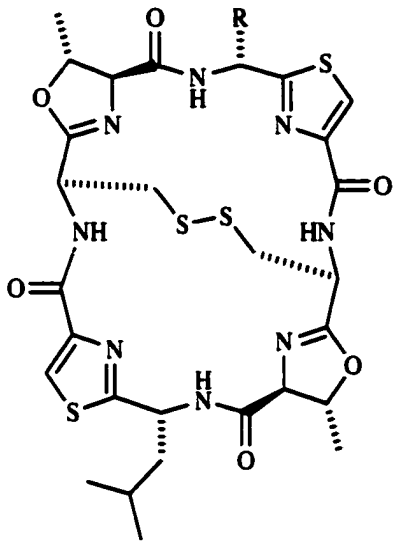

Ulithiacyclamide A(**29**) R = D-Leu
Ulithiacyclamide B(**30**) R = D-Phe

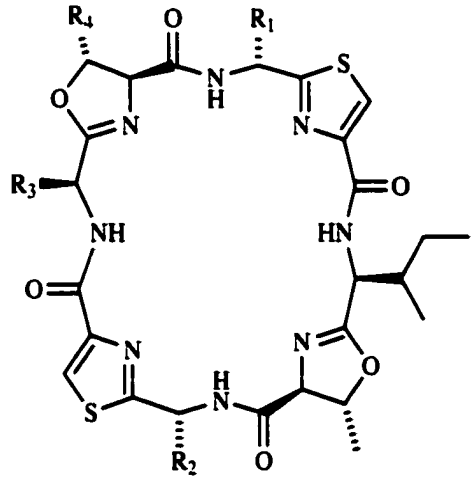

Patellamide A (**31**) $R_1 = R_2$ = D-Val, R_3 = D-Ile, R_4 = H
Patellamide B (**32**) R_1 = D-Ala, R_2 = D-Phe, R_3 = D-Leu, R_4 = Me
Patellamide C (**33**) R_1 = L-Ala, R_2 = D-Phe, R_1 = L-Ala, R_2 = D-Ile
Patellamide D (**34**) R_1 = D-Ala, R_2 = D-Phe, R_3 = L-Ile, R_4 = Me
Patellamide E (**35**) $R_1 = R_3$ = L-Val, R_2 = D-Phe, R_4 = Me

Figure 2.8: Several cytotoxic thiazole/thiazoline- and oxazoline-containing peptides from ascidians (Continued).

Reproduced with permission of the copyright owner. Further reproduction prohibited without permission.

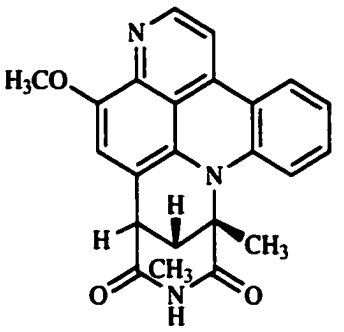

Segoline A (**36**)

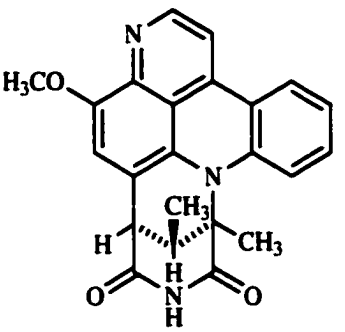

Segoline B (**37**)

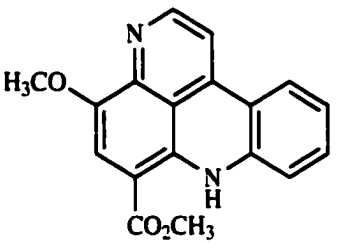

Norsegoline (**39**)

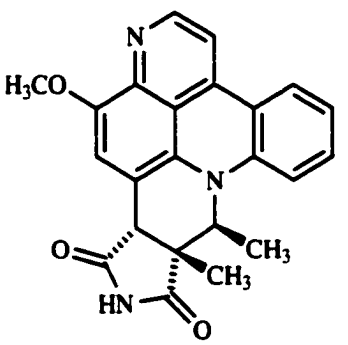

Isosegoline A (**38**)

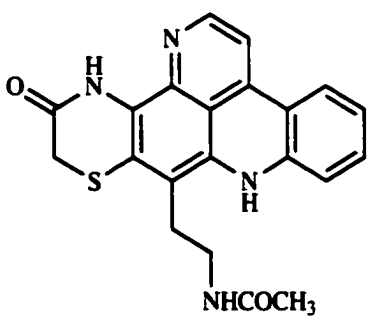

Debromoshermilamine (**40**)

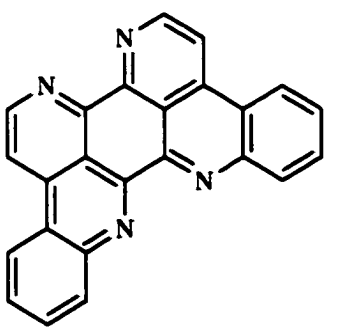

Eilatin (**41**)

Figure 2.9: Six alkaloids containing the fused tetracyclic pyrido(2,3,4-kl)acridine ring system, isolated from a Red Sea ascidian, *Eudistoma* sp.

Reproduced with permission of the copyright owner. Further reproduction prohibited without permission.

2.2 Tamandarins A and B, Novel Cytotoxic Depsipeptides from a Brazilian Ascidian of the Genus Didemnidae

As part of an ongoing program to explore marine ascidians for their applications in cancer drug discovery, we encountered an unidentified didemnid ascidian on a shallow-water reef near the Brazilian village of Tamandaré. The crude extract of this animal showed potent growth inhibitory activity in our primary cytotoxicity assay employing the HCT 116 human colon adenocarcinoma cell line. Subsequent bioassay-guided fractionation using sephadex LH-20 and RP (C_{18}) HPLC, yielded two cytotoxic depsipeptides, the major metabolite assigned as tamandarin A (**42**), and a minor metabolite tamandarin B (**43**).

Analysis of spectral data revealed that tamandarins A (**42**) and B (**43**) are closely related to didemnin B (**11**) and nordidemnin B (**12**), respectively. The molecules were found to differ only by the presence of hydroxyisovaleric acid (Hiv^2) instead of the hydroxyisovalerylpropionic acid (Hip^2) unit which is present in all other naturally occurring didemnin congeners. Tamandarin B (**43**) was found to contain a norstatine (Nst^1) residue instead of the isostatine (Ist^1) residue of tamandarin A (**42**). This chapter describes the isolation and structure elucidation of tamandarins A (**42**) and B (**43**), and provides preliminary pharmacological information for tamandarin A (**42**). A comparison of the conformation of this metabolite in solution versus that of didemnin B (**11**) is also presented.

2.2.1 Constitution of Tamandarins A and B

Tamandarin A (**42**) was obtained as a greenish white solid. Mass spectral analysis (FABMS) of this metabolite showed a pseudomolecular ion consistent with the molecular formula $C_{54}H_{87}N_7O_{14}$. The ^1H NMR spectrum of tamandarin A (**42**), Table 2.1, in $CDCl_3$ (300 MHz), showed several characteristic features that strongly resembled those of didemnin B (**11**). Three NH protons were visible in the amide hydrogen region (δ 7.3-7.8 ppm), and a *para*-substituted phenyl ring was apparent (δ 7.07, d, 2H, 8.4 Hz; δ 6.84, d, 2H, 8.7 Hz). However, only ten well resolved apparent α-hydrogens were visible (δ 3.8-5.5 ppm) whereas didemnin B (**11**) possesses eleven. Three methyl groups on heteroatoms (δ 3.79, s, 3H, OCH_3; δ 3.11, s, 3H, NCH_3; δ 2.58, s, 3H, NCH_3) were observed, but only ten additional methyl groups could be accounted for (δ 0.8-1.5 ppm) while didemnin B (**11**) has eleven. These findings indicated that tamandarin A (**42**) is

Reproduced with permission of the copyright owner. Further reproduction prohibited without permission.

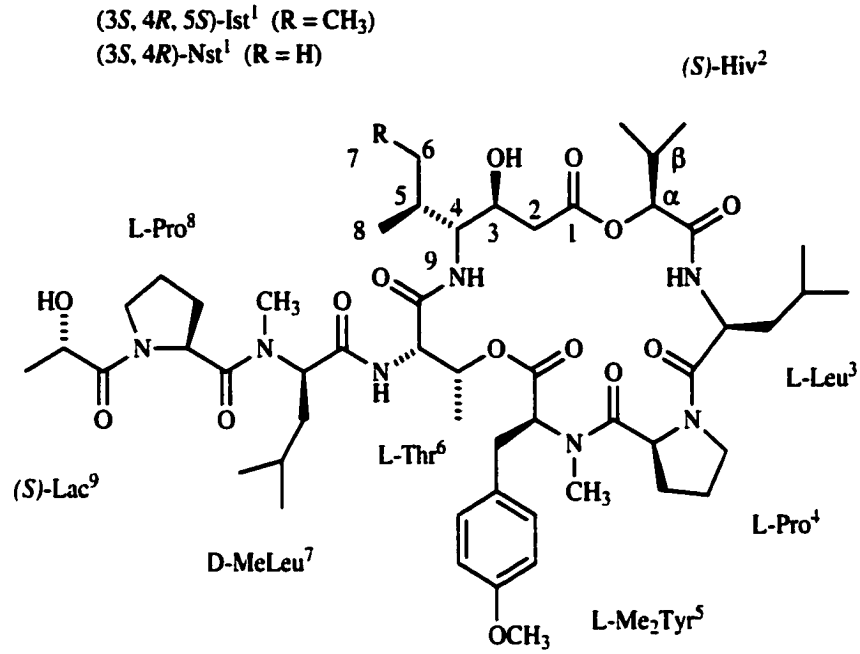

Tamandarin A (**43**)
Tamandarin B (**42**)

Figure 2.10: The tamandarins (**42–43**). isolated from a Brazilian didemnid ascidian.

a novel didemnin congener. Tandem mass spectral analysis (MS/MS, Fig. 2.13, was undertaken to establish the relationship between those two molecules. The fragmentation pattern of the parent ion at 1056 amu's ($M+H^+$) showed the loss of a lactic acid (Lac^9) and a proline (Pro^8) as one unit, 169 (m/z 887) and loss of 127 (m/z 760) for a *N*-methyl leucine ($MeLeu^7$) unit, indicating that tamandarin A(**42**) possesses the same side chain as didemnin B (**11**). Hence, the noted modifications must be within the macrocyclic ring. The ^{13}C NMR spectrum of tamandarin A (**42**) shows 54 carbon resonances including nine carbonyl carbons (δ 168-175 ppm). Unlike didemnin B (**11**), tamandarin A (**42**) did not possess a ketone, the carbonyl shift of the former being observed at approximately 200 ppm. Six carbon resonances appeared in the aromatic region, with the phenyl ring carbons overlapping (δ 114-160 ppm). The remaining 39 carbons resonances were all in the aliphatic region. A DEPT and an gHMQC experiment established the multiplicities of each carbon and all one bond ^1H-^{13}C correlations, in agreement with the molecular formula. The spin systems of Lac^9, Pro^4 and Pro^8 units, a leucine (Leu^3) and $MeLeu^7$ unit, a threonine (Thr^6) unit and parts of the Ist^1 and *N,O*-dimethyltyrosine (Me_2Tyr^5) were identified by correlations observed in a double quantum filtered COSY experiment

Reproduced with permission of the copyright owner. Further reproduction prohibited without permission.

(DQF-COSY). In addition, a Hiv^2 unit was identified, but the propionic acid of Hip^2 of didemnin B (**11**) was clearly absent in tamandarin A (**42**).

As was pointed out by Kessler *et al.* for didemnin B (**11**), several correlations within Ist^1 (C5H to C6H) and Leu^3 and $MeLeu^7$ (CβH to CγH) do not appear in the COSY spectrum [85,86]. These correlations were not observed for tamandarin A (**42**), but they were obtained from a TOCSY experiment which also confirmed the proposed units.

A ROESY experiment established the sequence of the amino acids and confirmed the absence of the propionic acid in the Hip^2 unit. An gHMBC experiment provided additional sequence data and allowed all carbonyl functionalities, except for the Leu^3 CO carbon, to be assigned. This experiment also confirmed the ester bonds between the Ist^1 and the Hiv^2, and between Thr^6 and Me_2Tyr^5 units. On the basis of these data, tamandarin A (**42**) was confidently assigned as possessing a hydroxyisovaleric acid (Hiv^2) instead of the hydroxyisovalerylpropionic acid (Hip^2) found in didemnin B (**11**).

Tamandarin B (**43**), obtained as an amorphous white solid, showed a FABMS pseudomolecular ion consistent with the molecular formula $C_{53}H_{82}N_7O_{14}$. The lower mass of this metabolite, shifted by 14 units as compared with tamandarin A (**42**), suggested that the difference is the absence of a methylene group. The ^1H NMR spectrum of tamandarin B (**43**) (Table 2.2) was almost identical to that of tamandarin A (**42**), except for a small downfield shift ($\Delta\delta$ = 0.2 ppm) in one of the hydrogens in the amide region (δ 7.2-7.8 ppm) and slight upfield shifts ($\Delta\delta$ = 0.05 ppm) of two hydrogens in the α-hydrogen region (δ 3.8-5.5 ppm). Perhaps most importantly, the latter protons showed a change in coupling pattern. In addition, a hydrogen at δ 1.20 ppm, showing an obvious multiplet structure in the ^1H spectrum of tamandarin A (**42**), was lacking. These observations indicated that tamandarin B (**43**) contains a Nst^1 residue instead of the Ist^1 residue of tamandarin A (**42**).

With some difficulty from overlapping shifts, the replacement of the triplet methyl signal of tamandarin A (**42**) at δ 0.92 ppm with a doublet methyl in tamandarin B (**42**) at δ 0.97 ppm was resolved. The ^{13}C NMR spectrum of tamandarin B (**43**) was nearly identical to that of tamandarin A (**42**), except for the lack of one methylene resonance in the aliphatic region. DEPT and gHMQC experiments confirmed the multiplicity of each carbon and showed all one bond ^1H-^{13}C correlations in agreement with the molecular formula. COSY and TOCSY experiments established the connectivities

Reproduced with permission of the copyright owner. Further reproduction prohibited without permission.

within the Nst^1 residue and confirmed the presence of the Lac^9 unit and the same remaining amino and hydroxy acids as in tamandarin A (**42**). Determination of the amino acid sequence and assignment of all carbonyl functionalities of tamandarin B (**43**) was accomplished by means of ROESY and gHMBC experiments. Tamandarin B (**43**) was confidently assigned as differing from tamandarin A (**42**) by the presence of the amino acid Nst^1 instead of the Ist^1 unit of tamandarin A (**42**).

Reproduced with permission of the copyright owner. Further reproduction prohibited without permission.

Figure 2.11: ^{1}H NMR spectrum of tamandarin A (**42**) ($CDCl_3$, 300MHz).

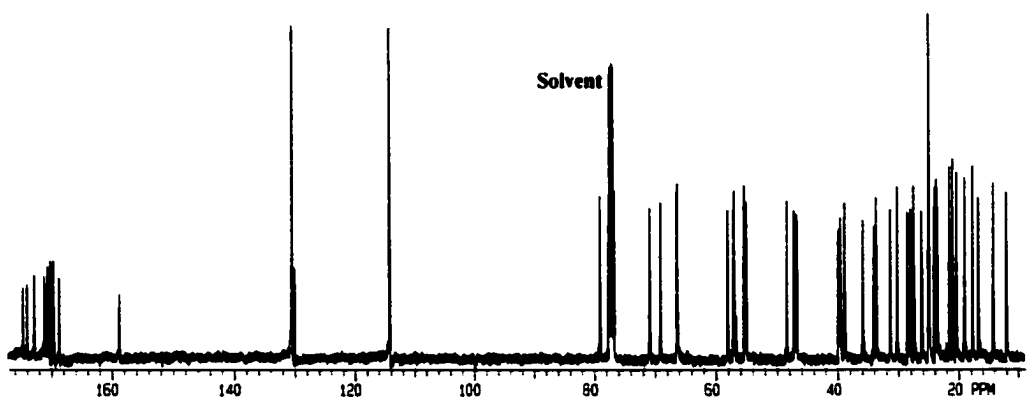

Figure 2.12: ^{13}C NMR spectrum of tamandarin A (**42**) ($CDCl_3$, 100MHz).

Reproduced with permission of the copyright owner. Further reproduction prohibited without permission.

Table 2.1: NMR Assignments for Tamandarin A (**42**).

(3*S*, 4*R*, 5*S*)-Ist[1]						
1	174.7	(C)				5.03, 3.25, 2.44
2	39.9	(CH_2)	2.44	(dd, 17.0, 8.1, 1H)	3.25, 3.91	4.03
			3.25	(br d, 17.0, 1H)	2.44, 3.91	
3	69.1	(CH)	3.91	(br tr, 9.6, 8.1, 1H)	2.44,3.25	2.44
3-OH			n.o.			
4	55.4	(CH)	4.03	(tr d, 2×9.6, 3.4, 1H)	7.36, 1.96	3.91, 3.25, 1.20
5	33.8	(CH)	1.96	(m, 1H)	4.03, 0.88	1.40, 1.20
6	27.6	(CH_2)	1.20	(dd, 13.8, 6.9, 1H)	1.40, 0.92	
			1.40	(m, 1H)	1.20, 0.92	
7	12.0	(CH_3)	0.92	(tr, 2×6.9, 3H)	1.20, 1.40	1.40, 1.20
8	14.3	(CH_3)	0.88	(d, 6.3, 3H)	1.96	4.03, 1.40, 1.20
9			7.36	(br d, 9.6, 1H)	4.03	
(*S*)-Hiv[2]						
CO	169.8	(C)				5.03
α	79.1	(CH)	5.03	(d, 4.8, 1H)	2.26	
β	30.3	(CH)	2.26	(m, 1H)	1.03, 1.04	5.03
β-CH_3	17.8	(CH_3)	1.04	(d, 6.6, 3H)	2.26	5.03, 2.26
β-CH_3	19.1	(CH_3)	1.03	(d, 6.6, 3H)	2.26	5.03, 2.26
L-Leu[3]						
CO	170.6	(C)				
α	48.5	(CH)	4.88	(tr d, 2×9.6, 1.6, 1H)	1.25, 1.50, 7.77	
β	39.6	(CH_2)	1.25	(m, 1H)	1.50, 4.88	0.95, 0.91
			1.50	(m, 1H)	1.25, 4.88	
γ	25.0	(CH)	1.55	(m, 1H)	0.95, 0.91	0.95, 0.91
γ-CH_3	21.1	(CH_3)	0.95	(d, 6.3, 3H)	1.55	
γ-CH_3	24.0	(CH_3)	0.91	(d, 6.3, 3H)	1.55	
NH			7.77	(br d, 9.6, 1H)	4.88	
L-Pro[4]						
CO	171.3	(C)				2.10, 1.77
α	57.2	(CH)	4.65	(dd, 7.8, 3.6, 1H)	1.77, 2.10	
β	28.2	(CH_2)	1.77	(m, 1H)	2.10, 4.65	4.65, 3.65
			2.10	(m, 1H)	1.77, 4.65	
γ	25.1	(CH_2)	2.10	(m, 2H)	3.65	4.65, 3.65, 2.10
δ	46.9	(CH_2)	3.65	(m, 2H)	2.10	1.77
L-Me_2Tyr[5]						
CO	168.7	(C)				5.42, 3.59, 3.13
α	66.4	(CH)	3.59	(dd, 10.8, 4.1, 1H)	3.13, 3.40	3.40, 3.13
β	34.1	(CH_2)	3.13	(dd, 14.6, 10.8, 1H)	3.40, 3.59	7.07, 3.59
			3.40	(dd, 14.6, 4.1, 1H)	3.13, 3.59	
γ	130.3	(C)				3.59, 3.40, 3.13
δ	130.5	(CH)	7.07	(d, 8.6, 2H)	6.84	3.40, 3.13
ϵ	114.3	(CH)	6.84	(d, 8.6, 2H)	7.07	7.07

...continued on next page

Reproduced with permission of the copyright owner. Further reproduction prohibited without permission.

...continued from previous page

ζ	158.8	(C)				7.07, 3.79
γ-CH_3	55.5	(CH_3)	3.78	(s, 3H)		
N-CH_3	38.9	(CH_3)	2.58	(s, 3H)		
L-Thr[6]						
CO	170.3	(C)				7.36, 4.03
α	58.1	(CH)	4.26	(dd, 5.4, 1.4, 1H)	7.47, 5.42	5.42
β	70.9	(CH)	5.42	(q d, 6.0, 1.4, 1H)	1.35, 4.26	7.47, 4.26, 1.35
β-CH_3	16.7	(CH_3)	1.35	(d, 6.0, 3H)	5.42	5.42, 4.26
NH			7.46	(br d, 5.4, 1H)	4.26	
D-MeLeu[7]						
CO	170.8	(C)				7.47, 1.88
α	55.1	(CH)	5.30	(dd, 11.4, 3.6, 1H)	1.88, 1.66	3.11, 1.66
β	35.9	(CH_2)	1.88	(m, 1H)	1.66, 1.35, 5.30	
5.30						
			1.66	(m, 1H)	1.88, 1.35, 5.30	
γ	25.0	(CH)	1.35	(m, 1H)	0.84, 0.91	5.30
β-CH_3	23.7	(CH_3)	0.91	(d, 6.9, 3H)	1.35	
β-CH_3	21.5	(CH_3)	0.84	(d, 6.9, 3H)	1.35	1.88, 1.66
N-CH_3	31.5	(CH_3)	3.11	(s, 3H)		5.30
L-Pro[8]						
CO	172.9	(C)				5.30, 3.11
α	56.9	(CH)	4.72	(br t, 2×7.5, 1H)	2.22, 1.96	3.59
β	28.6	(CH_2)	1.96	(m, 1H)	2.22	4.72, 1.96
			2.22	(m, 1H)	1.96	
γ	26.2	(CH_2)	1.96	(m, 1H)	2.22	3.59
			2.22	(m, 1H)	1.96	
δ	47.2	(CH_2)	3.65	(m, 1H)	3.65, 2.22, 1.96	2.22
			3.59	(dd, 10.8, 3.9, 1H)	3.59, 2.22, 1.96	
(*S*)-Lac[9]						
CO	174.0	(C)				4.38
α	66.3	(CH)	4.38	(br q, 6.9, 1H)	1.43	1.43
α-CH_3	20.5	(CH_3)	1.43	(d, 6.9, 3H)	4.38	4.38
α-OH			n.o.			

a) ^1H and ^{13}C NMR shifts were referenced to $CDCl_3$ (^1H δ 7.27 and ^{13}C δ 77.2 ppm).

Reproduced with permission of the copyright owner. Further reproduction prohibited without permission.

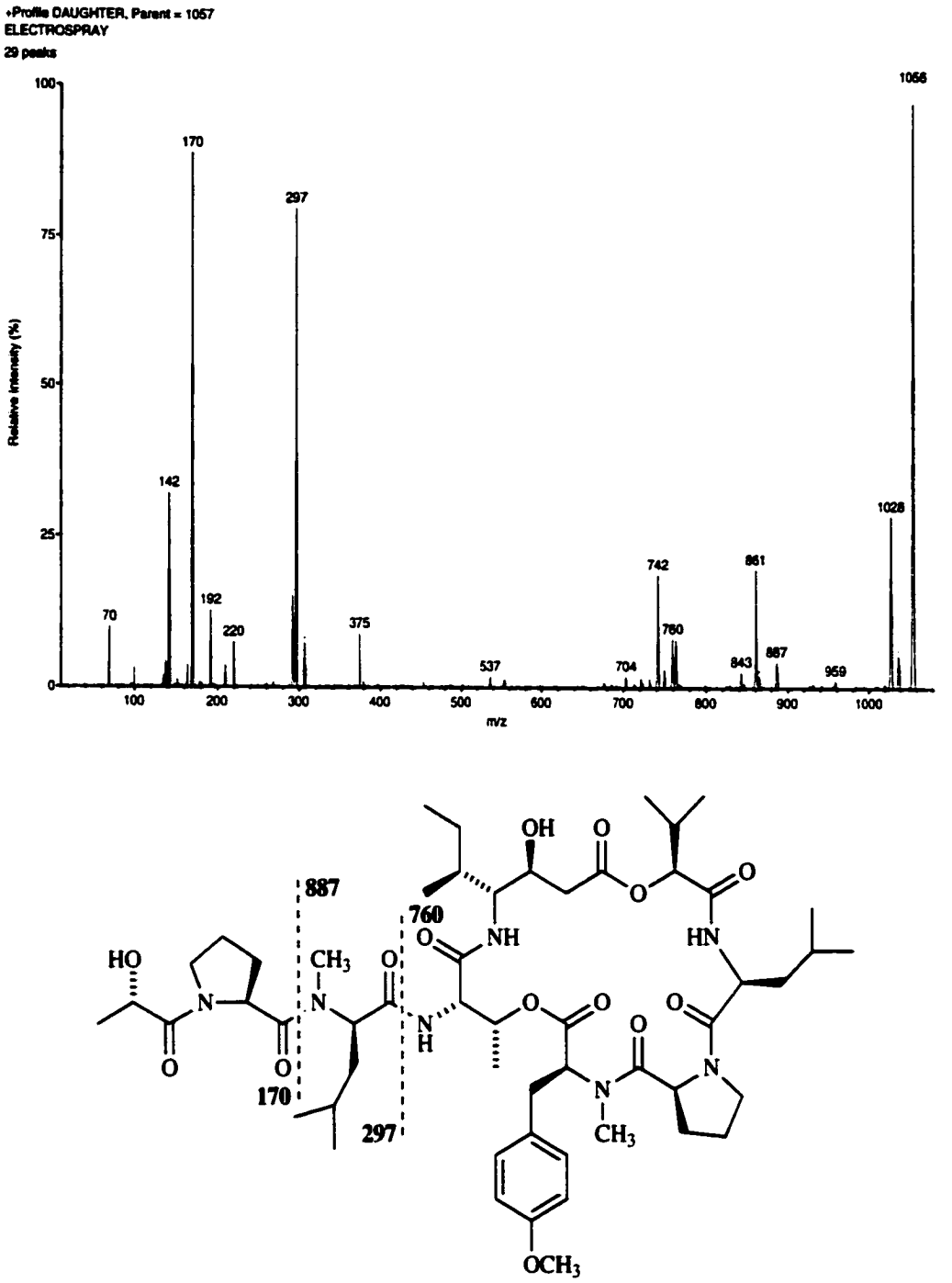

Figure 2.13: Top: Tandem mass spectrometry (MS/MS) fragmentation pattern of tamandarin A (**42**). Bottom: Structure of tamandarin A (**42**) showing fragment ions obtained by MS/MS (m/z 1057 $[M+H]^+$).

Reproduced with permission of the copyright owner. Further reproduction prohibited without permission.

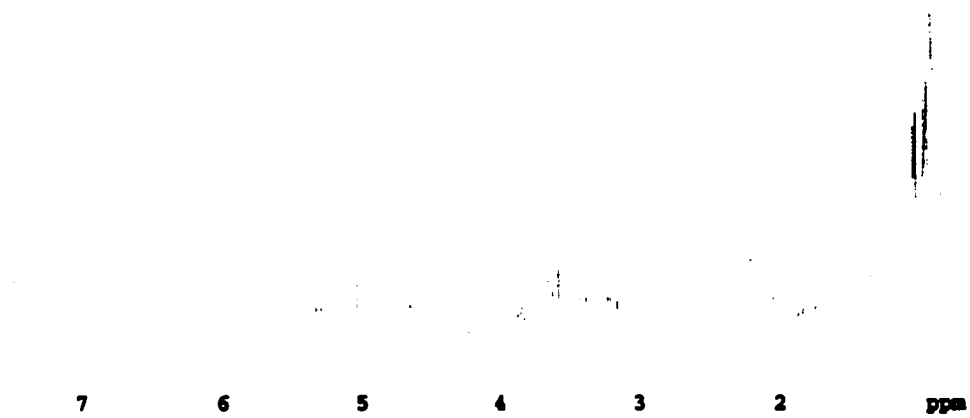

Figure 2.14: ^{1}H NMR spectrum of tamandarin B (**43**) ($CDCl_3$, 300MHz).

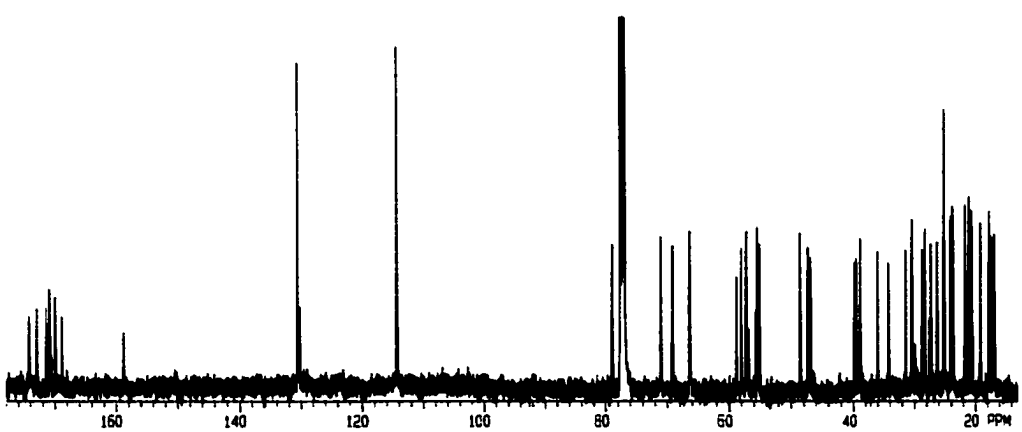

Figure 2.15: ^{13}C NMR spectrum of tamandarin B (**43**) ($CDCl_3$, 100MHz).

Reproduced with permission of the copyright owner. Further reproduction prohibited without permission.

Table 2.2: NMR Assignments for Tamandarin B (**43**).

(3*R*, 4*S*)-Nst[1]						
1	174.2	(C)				3.25, 2.48
2	39.7	(CH_2)	2.48	(dd, 17.0, 7.5, 1H)	3.96, 3.34	
			3.25	(dd, 17.0, 2.7, 1H)	3.96, 3.48	
3	69.2	(CH)	3.96	(m, 1H)	3.86, 3.25, 2.48	2.48
3-OH			3.34	(m, 1H)	3.96	
4	58.8	(CH)	3.86	(dd, 8.8, 5.0, 1H)	7.56, 3.96, 2.13	0.97, 0.91
5	27.3	(CH)	2.13	(m, 1H)	3.86, 0.97, 0.91	0.97, 0.91
6	17.3	(CH_3)	0.91	(d, 6.9, 3H)	2.13	0.97
7						
8	20.7	(CH_3)	0.97	(d, 6.9, 3H)	2.13	0.91
9			7.56	(br d, 8.8, 1H)	3.86	
(*S*)-Hiv[2]						
CO	169.9	(C)				5.04
α	78.9	(CH)	5.04	(d, 4.5, 1H)	2.25	1.04
β	30.4	(CH)	2.25	(m, 1H)	1.05, 1.04	5.04, 1.05, 1.04
β-CH_3	17.7	(CH_3)	1.05	(d, 6.9, 3H)	2.25	1.04
β-CH_3	19.2	(CH_3)	1.04	(d, 6.9, 3H)	2.25	1.05
L-Leu[3]						
CO	171.3	(C)				
α	48.5	(CH)	4.89	(tr d, 9.8, 9.8, 1.6, 1H)	7.78	
β	39.5	(CH_2)	1.33	(m, 1H)	1.51	0.96, 0.92
			1.51	(m, 1H)	1.33	
γ	25.1	(CH)	1.59	(m, 1H)	0.96, 0.92	0.96, 0.92
γ-CH_3	21.7	(CH_3)	0.96	(d, 6.9, 3H)	1.59	0.92
γ-CH_3	24.0	(CH_3)	0.92	(d, 6.9, 3H)	1.59	0.96
NH			7.78	(br d, 9.9, 1H)	4.89	
L-Pro[4]						
CO	170.9	(C)				3.60, 2.59, 1.84
α	57.2	(CH)	4.65	(dd, 7.5, 4.1, 1H)	2.05, 1.84	
β	28.2	(CH_2)	1.84	(m, 1H)	2.05	4.65
			2.05	(m, 1H)	1.84	
γ	25.1	(CH_2)	2.05	(m, 2H)	3.67	4.65
δ	46.9	(CH_2)	3.67	(m, 2H)	2.05	
L-Me_2Tyr[5]						
CO	168.8	(C)				5.42, 3.60
α	66.5	(CH)	3.60	(dd, 10.8, 4.0, 1H)	3.40, 3.16	3.41, 3.16, 2.59
β	34.2	(CH_2)	3.16	(dd, 14.1, 10.5, 1H)	3.40, 3.60	3.60
			3.40	(dd, 14.1, 4.0, 1H)	3.60, 3.16	
γ	130.0	(C)				6.85, 3.60, 3.41
						3.16
δ	130.6	(CH)	7.08	(d, 8.3, 2H)	6.85	6.85, 3.41, 3.16
ϵ	114.3	(CH)	6.85	(d, 8.3, 2H)	7.08	6.85

...continued on next page

Reproduced with permission of the copyright owner. Further reproduction prohibited without permission.

...continued from previous page

ζ	158.8	(C)				7.08, 6.85, 3.80
γ-CH_3	55.5	(CH_3)	3.80	(s, 3H)		
N-CH_3	38.9	(CH_3)	2.59	(s, 3H)		3.60
L-Thr[6]						
CO	170.8	(C)				7.56
α	58.0	(CH)	4.31	(dd, 5.6, 1.4, 1H)	7.49, 5.42	1.38
β	71.0	(CH)	5.42	(qd, 6.5, 1.4, 1H)	4.32, 1.38	7.49, 4.31, 1.38
β-CH_3	16.8	(CH_3)	1.38	(d, 6.5, 3H)	5.42	
NH			7.49	(br d, 5.6, 1H)	4.31	
D-MeLeu[7]						
CO	170.7	(C)				7.49
α	55.1	(CH)	5.31	(dd, 11.4, 3.6, 1H)	1.88, 1.67	3.11
β	36.8	(CH_2)	1.88	(m, 1H)	1.67	0.92, 0.85
			1.67	(m, 1H)	1.88	
γ	25.1	(CH)	1.38	(m, 1H)	1.88, 1.67	0.92, 0.85
					0.85	
β-CH_3	23.7	(CH_3)	0.92	(d, 6.9, 3H)	1.38	0.85
β-CH_3	21.6	(CH_3)	0.85	(d, 6.9, 3H)	1.38	1.88, 1.67, 0.92
N-CH_3	31.4	(CH_3)	3.11	(s, 3H)		5.31
L-Pro[8]						
CO	172.9	(C)				5.31, 3.11
	57.0	(CH)	4.73	(br t, 7.8, 7.8, 1H)	2.13, 1.97	
	28.6	(CH_2)	1.97	(m, 1H)	2.13	
			2.13	(m, 1H)	1.97	
γ	26.2	(CH_2)	1.97	(m, 1H)	2.13	4.73
			2.13	(m, 1H)	1.97	
δ	47.3	(CH_2)	3.67	(m, 1H)	1.97	
			3.60	(dd, 10.8, 4.1, 1H)	2.13	
(*S*)-Lac[9]						
CO	174.1	(C)				1.44
	66.3	(CH)	4.39	(br q, 6.9, 1H)	3.44, 1.44	1.44
α-CH_3	20.5	(CH_3)	1.44	(d, 6.9, 3H)	4.39	
α-OH			3.44	(m, 1H)	4.39	

a) ^1H and ^{13}C NMR shifts were referenced to $CDCl_3$ (^1H δ 7.27 and ^{13}C δ 77.2 ppm).

Reproduced with permission of the copyright owner. Further reproduction prohibited without permission.

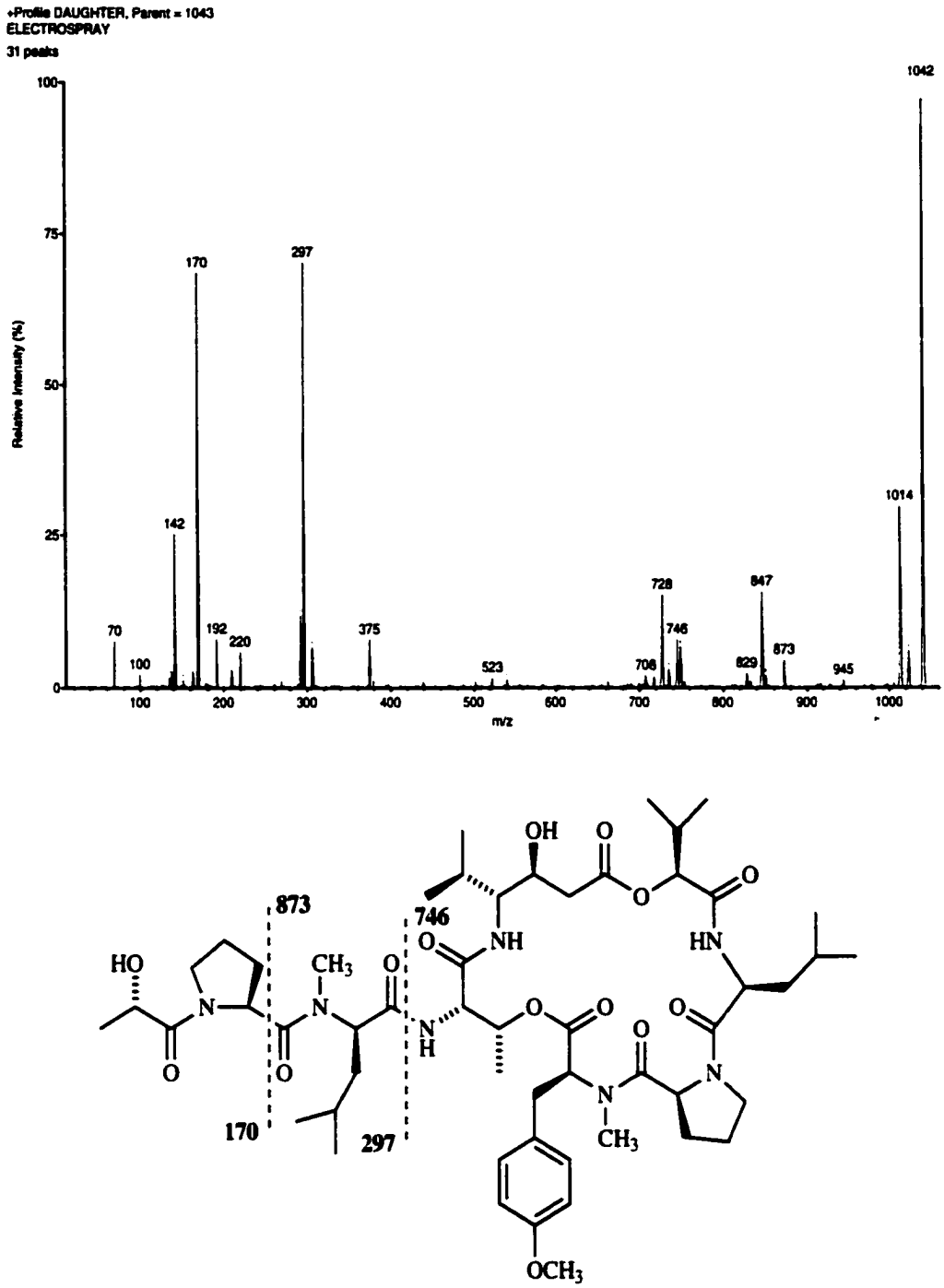

Figure 2.16: Top: Tandem mass spectrometry (MS/MS) fragmentation pattern of tamandarin B (**43**). Bottom: Structure of tamandarin B (**42**) showing fragment ions obtained by MS/MS (m/z 1043 $[M+H]^+$).

Reproduced with permission of the copyright owner. Further reproduction prohibited without permission.

2.2.2 Stereochemistry of Tamandarins A and B

Hydrolysis of tamandarin A (**42**) under mild alkaline conditions (1N NaOH in MeOH, 1h, RT, Fig. 2.17) yielded the northern and southern peptide fragments **46** and **44**, which were converted to their methyl esters by reaction with diazomethane. In a similar reaction, didemnin B (**11**) was hydrolyzed to yield the analogous peptide fragments. Comparison of the ^{1}H NMR spectra, optical rotations and tandem mass spectrometry results of the tamandarin A (**42**) peptides with those obtained from didemnin B (**11**) [87] revealed that the northern fragments of both peptides are identical ($[\alpha]_D$ = +410, c = 0.07). The chiralities of the amino acid residues in the northern fragment (**44**) were thus established as (S)-Lac^9, L-Pro^8, D-MeLeu^7, L-Thr^6 and (3S,4R,5S)-Ist^1. The chiralities of the amino acids constituting the southern peptide fragment (**46**) of tamandarin A (**42**) were obtained by acid-catalyzed hydrolysis and preparation of the corresponding Marfey derivatives (Fig. 2.21) and HPLC analysis (Fig. 2.22) using D and L amino acid standards (Marfey's derivatives) [88]. All comparable amino acids in this fragment were shown to have absolute configurations identical with those in didemnin B (**11**); L-Me$_2$Tyr^5, L-Pro^4 and L-Leu^3. Acid hydrolysis of the southern peptide fragment (**46**) did not cleave the methyl ester link of L-Me$_2$Tyr. Therefore, a mixture of Marfey derivatives of D- and L- Me$_2$Tyr-methyl ester (Me$_3$Tyr) was prepared and used in the HPLC analysis (Fig. 2.20).

The absolute stereochemistry of the Hiv^2 unit could not be obtained from the Marfey derivative HPLC analysis. Instead, the stereochemistry of the Hiv^2 unit was determined by analysis of the ^{1}H NMR spectra of the diastereomeric (R)- and (S)-Mosher ester derivatives of the southern peptide fragment (**46**) [89, 90]. In the (S)-MTPA ester, Fig. 2.23, all protons in the Hiv^2 unit were more highly shielded (appeared further upfield) whereas the α- and amide hydrogens in the neighboring leucine unit were less highly shielded (and appeared further downfield). The reverse was true for the (R)-MTPA ester of the southern peptide fragment (**46**), permitting the identification of the absolute stereochemistry of the hydroxyisovaleric acid as (S)-Hiv^2.

Similar to tamandarin A (**42**), hydrolysis of tamandarin B (**43**) yielded the northern and southern peptide fragments, (**45**) and (**46**), which were also converted to the methyl esters with diazomethane. Likewise, hydrolysis of nordidemnin B (**12**) yielded

Reproduced with permission of the copyright owner. Further reproduction prohibited without permission.

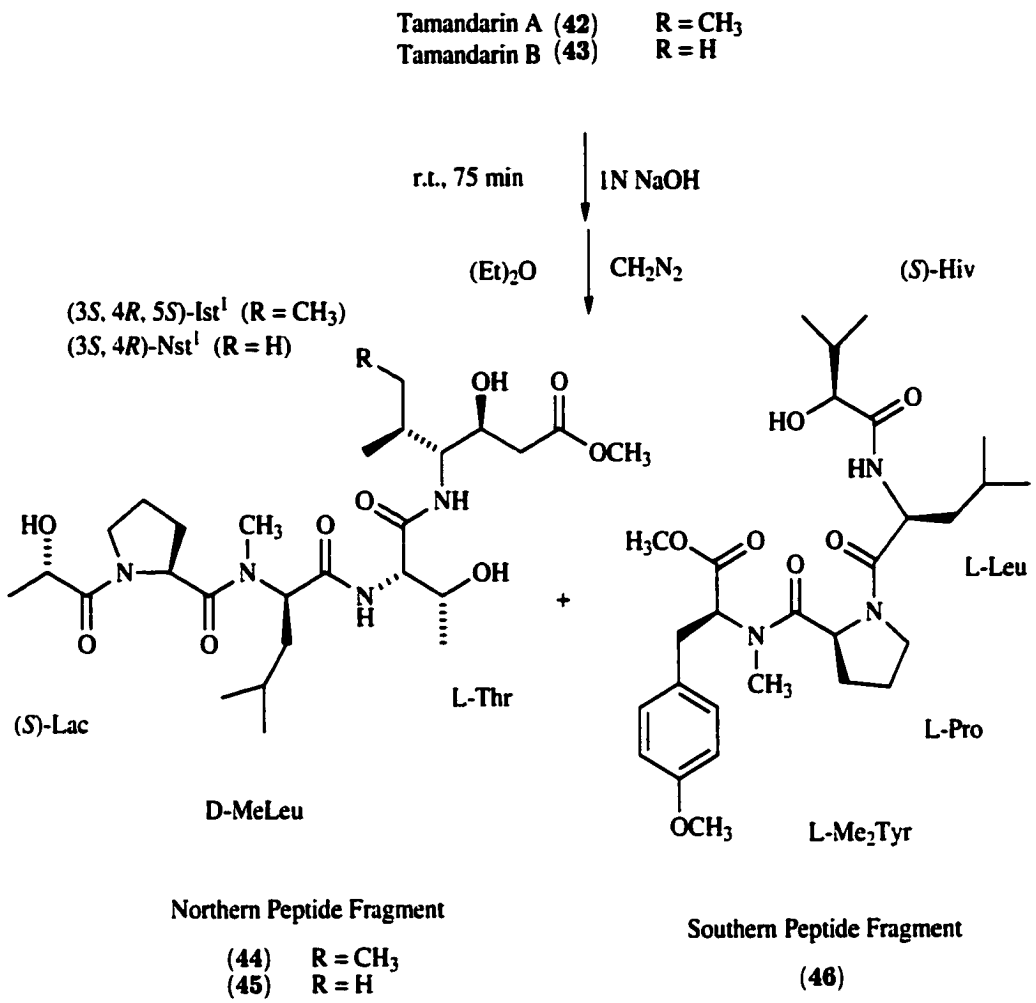

Figure 2.17: Mild alkaline hydrolysis of tamandarin A (**42**) and tamandarin B (**43**) yields northern peptide fragments (**44**) and (**45**) and a southern peptide fragment (**46**).

peptide fragments which were compared to those from tamandarin B (**43**). The northern peptide fragment, (**45**) of tamandarin B (**43**) ($[\alpha]_D$ = +24deg, c = 0.05) was found to be identical to the northern fragment of nordidemnin B (**12**), thus indicating the absolute configurations of the amino acids to be identical: (*S*)-Lac[9], L-Pro[8], D-MeLeu[7], L-Thr[6] and (3*S*, 4*R*)-Nst[1]. The southern peptide fragment (**46**) from tamandarin B (**43**) showed the same ^{1}H NMR spectrum and optical rotation as the southern peptide fragment (**46**) from tamandarin A (**42**), indicating the chiralities of the amino acids to be identical (L-Me$_2$Tyr[5], L-Pro[4], L-Leu[3] and (*S*)-Hiv[2]).

Reproduced with permission of the copyright owner. Further reproduction prohibited without permission.

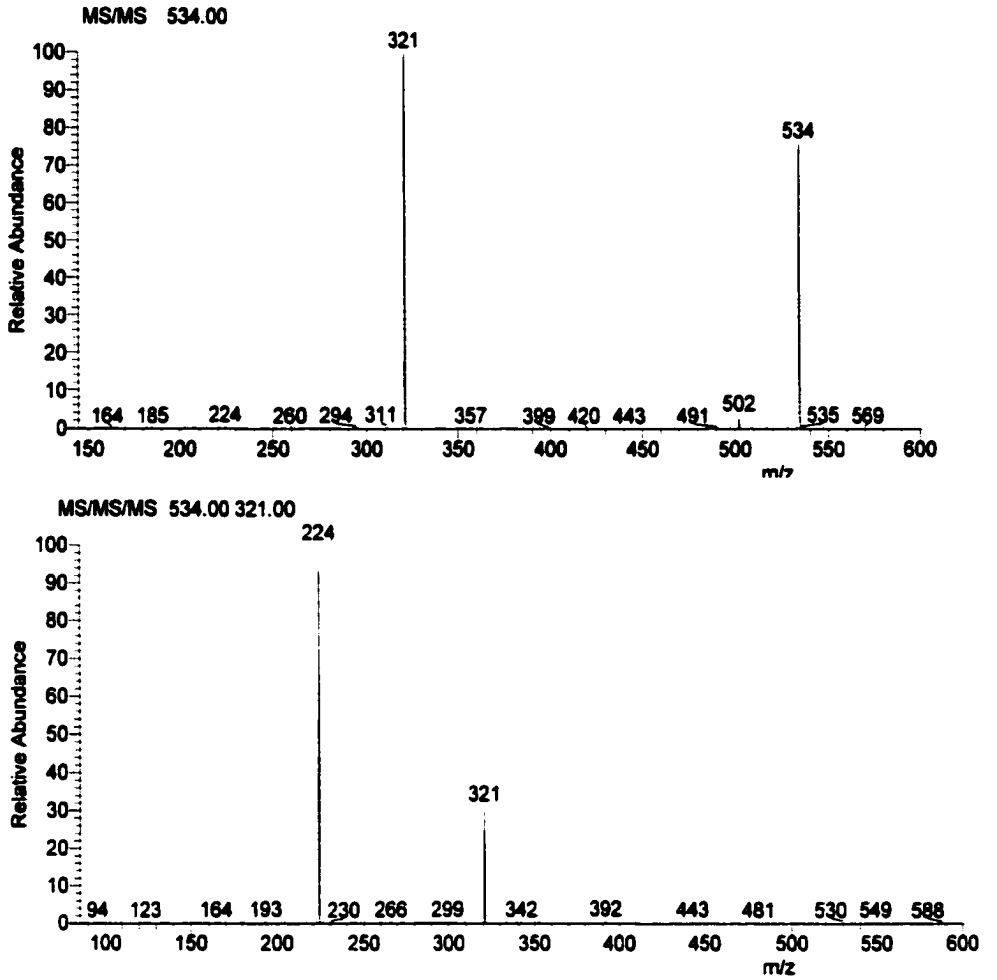

Figure 2.18: Tandem mass spectrometry (MS/MS) fragmentation pattern of the southern peptide fragment of tamandarin A (**42**).

Reproduced with permission of the copyright owner. Further reproduction prohibited without permission.

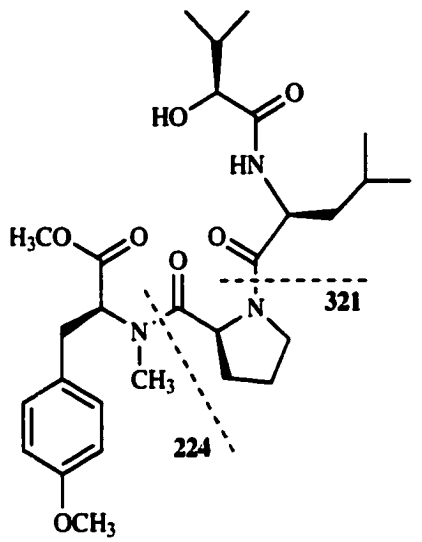

Figure 2.19: Structure of the southern peptide fragment (**46**) of tamandarin A (**42**) showing fragment ions obtained by MS/MS (m/z 543 $[M+H]^+$).

Reproduced with permission of the copyright owner. Further reproduction prohibited without permission.

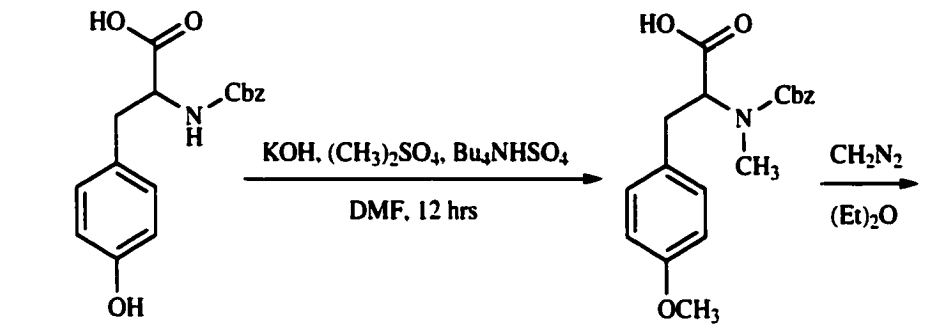

D/L-Tyrosine-*N*-Cbz

N-Cbz-*N*,*O*-dimethyl-D/L-tyrosine (**47**)
Li *et al. J. Amer. Chem. Soc.* **1990**, *21*, 7668.

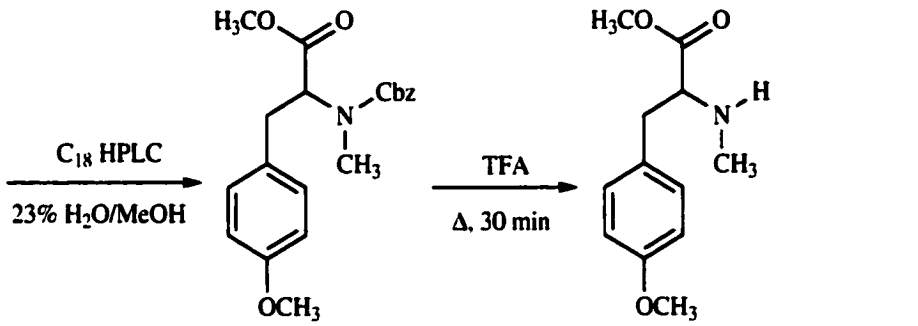

84%

N,*O*-dimethyl-D/L-tyrosine methyl ester(**48**)

Figure 2.20: Preparation of the *N*,*O*-dimethyltyrosine-methyl ester (Me_3Tyr) standard for Marfey derivatization and HPLC analysis.

Reproduced with permission of the copyright owner. Further reproduction prohibited without permission.

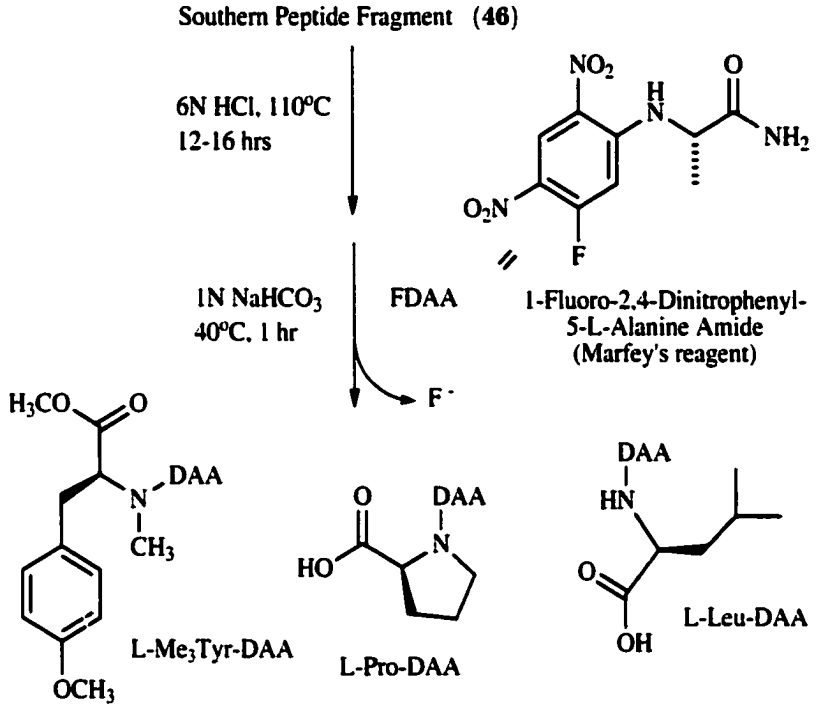

Figure 2.21: Hydrolysis and Marfey derivatization of the southern peptide fragment (**46**) of tamandarins A (**42**) and B (**43**).

Reproduced with permission of the copyright owner. Further reproduction prohibited without permission.

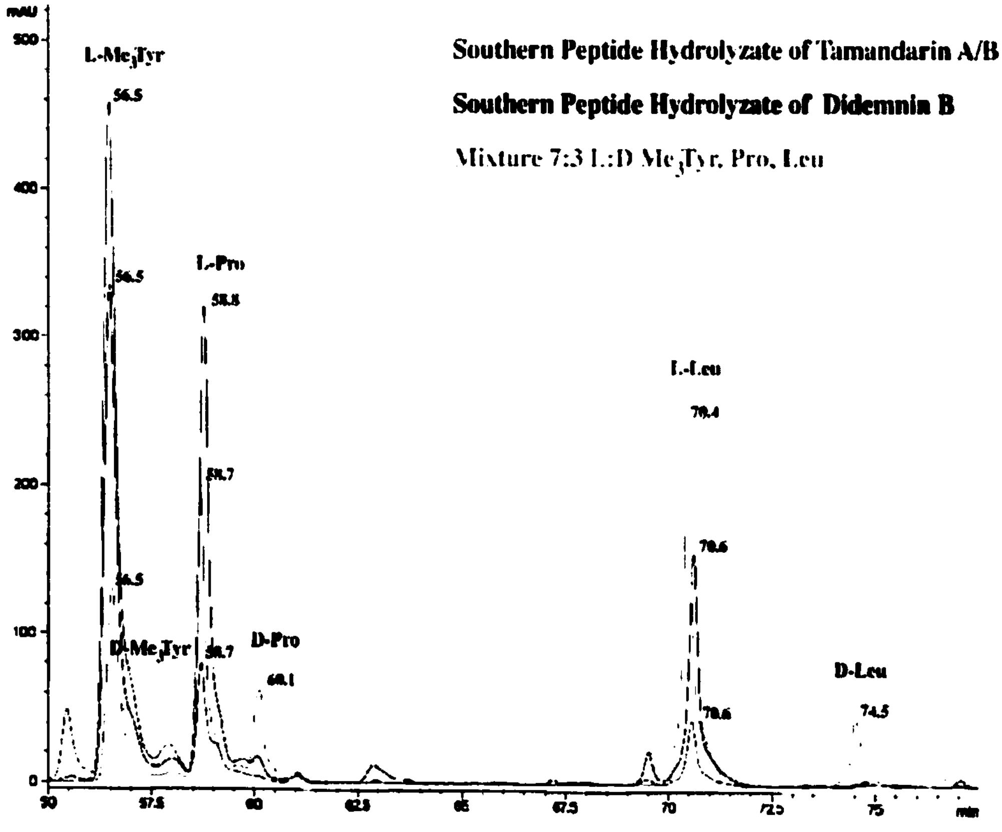

Figure 2.22: HPLC analysis of Marfey derivatives of the southern peptide hydrolyzates of tamandarins A (**42**) and B (**43**), didemnin B (**11**), and a mixture of standard amino acids. Marfey derivatives of the amino acids are separable by HPLC and comparison of retention times with standard samples determines their chirality (D or L).

Reproduced with permission of the copyright owner. Further reproduction prohibited without permission.

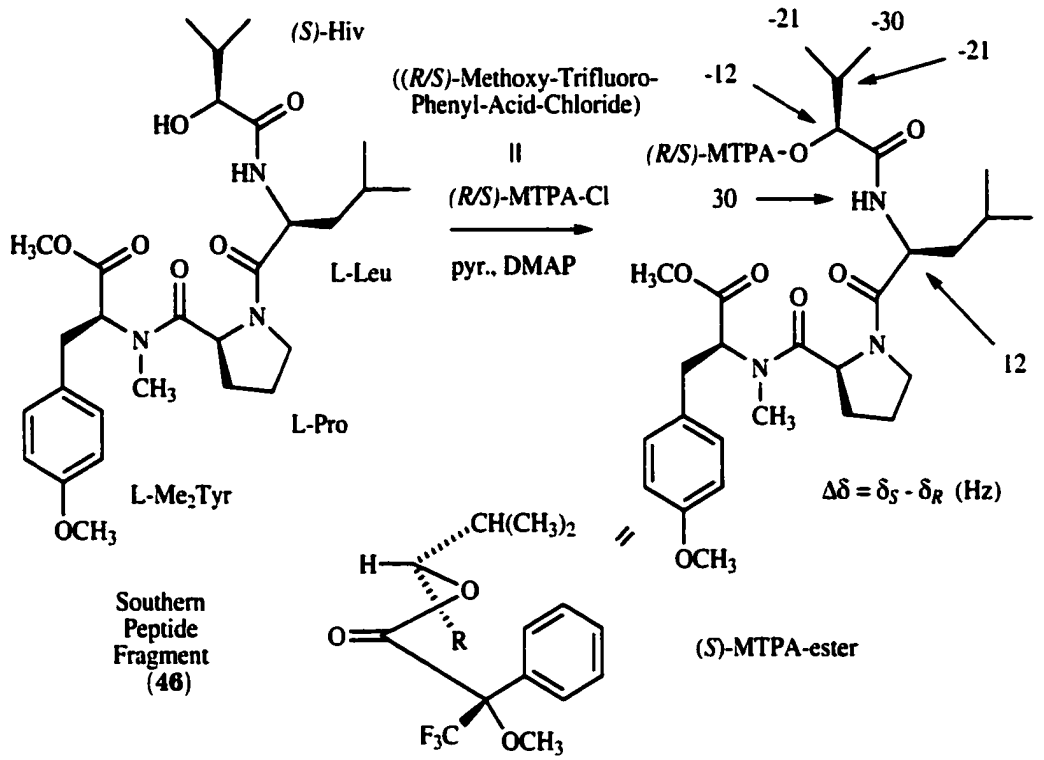

Figure 2.23: Mosher ester analysis of the southern peptide fragment (**46**) of tamandarins A (**42**) and B (**43**). ^{1}H NMR chemical shift differences ($\Delta\delta$) between the (*R*)- and (*S*)-MTPA esters indicate that the chirality of the Hiv unit is (*S*). The (*S*)-MTPA ester is drawn for clarity.

Reproduced with permission of the copyright owner. Further reproduction prohibited without permission.

2.2.3 Pharmacology of Tamandarin A

Cytotoxicity

Tamandarin A (**42**) was evaluated for its cytotoxicity (Fig. 2.24) against three cell lines, pancreatic carcinoma BX-PC3 (A), prostatic carcinoma DU145 (B), and head and neck carcinoma UMSCC10b (C). These bioassays were clonogenic (colony forming) assays performed under continuous exposure to tamandarin A (**42**) and didemnin B (**11**). The concentrations causing a 50% reduction in overall cell survival (IC_{50}, Table 2.3) were 1.79 ng/mL, 1.36 ng/mL and 0.99 ng/mL, respectively (versus 2.00 ng/mL, 1.53 ng/mL and 1.76 ng/mL, resp., for didemnin B (**11**)). Although the cell lines differed slightly in sensitivities the two compounds show virtually the same pattern of activity and potency.

Table 2.3: IC_{50} values for Tamandarin A (**42**) and Didemnin B (**11**), determined by clonogenic (colony forming) assays using three cancer cell lines.

	Tamandarin A (**42**) (ng/mL)	Didemnin B (**11**) (ng/mL)
Pancreatic carcinoma BX-PC3	1.79	2.00
Prostatic cancer DU-145	1.36	1.53
Head and Neck carcinoma UMSCC10b	0.99	1.76

Protein Synthesis Inhibition

Although the mechanism of cytotoxic action of tamandarin A (**42**) has not been thoroughly studied, it appears that the molecule behaves in a similar fashion to didemnin B (**11**). Recent research in the laboratory of Dr. Peter Toogood at the University of Michigan, has shown that tamandarin A (**42**) inhibits protein biosynthesis in rabbit reticulocyte cell lysates with an IC_{50} value of 1.3 μM. This is approximately 3 times more potent than didemnin B (**11**) in the same assay.

Reproduced with permission of the copyright owner. Further reproduction prohibited without permission.

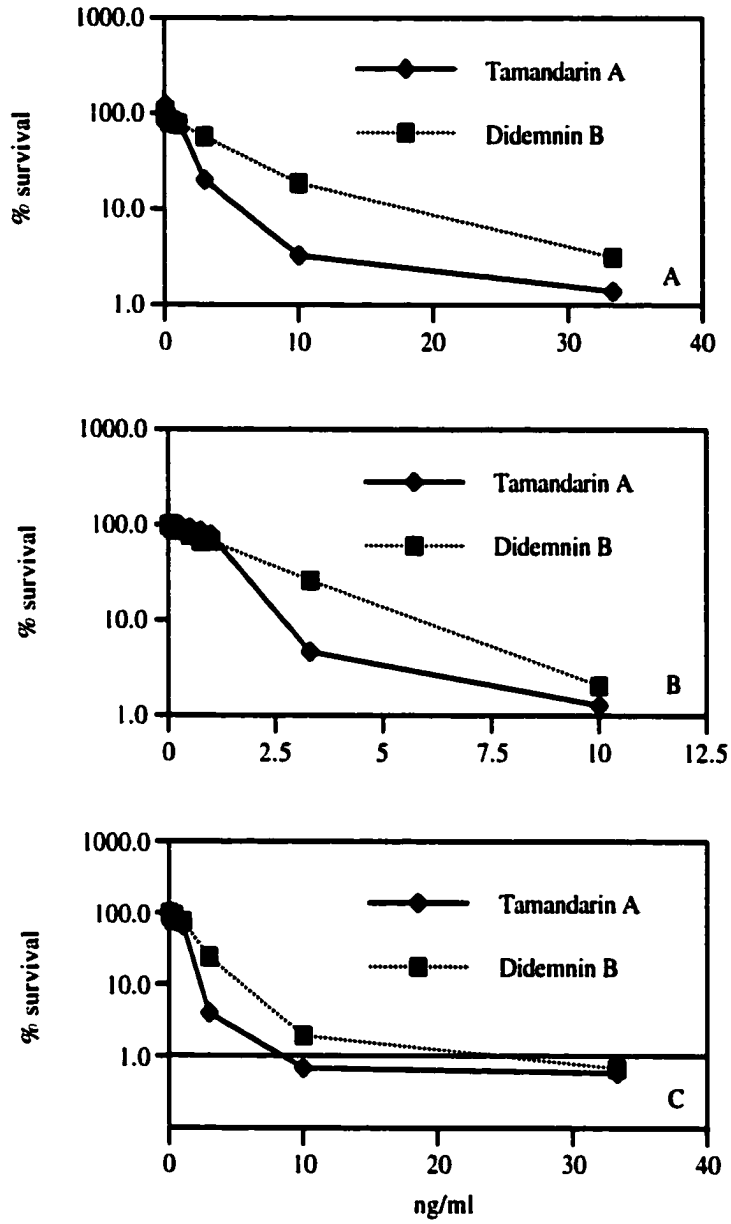

Figure 2.24: Dose-response curves for tamandarin A (**42**) and didemnin B (**11**) in clonogenic (colony forming) assays, using the cell lines (A) pancreatic carcinoma BX-PC3, (B) prostatic cancer DU-145, (C) head and neck carcinoma UMSCC10b.

2.2.4 Solution Conformation of Tamandarin A

Given the comparison of tamandarin A (**42**) with didemnin B (**11**), studies were undertaken to document the tertiary structure of this molecule. Several independent studies on the conformation of didemnin B (**11**) showed that it exhibits conformational

Reproduced with permission of the copyright owner. Further reproduction prohibited without permission.

constancy from crystal to solution structure and over a range of polar and apolar solvents [53,86,87,91-93]. Each study showed the molecule to exist in a globular shape, stabilized by at least three intramolecular hydrogen bonds. The strongest hydrogen bond is a transannular interaction linking Leu^3 CO and Ist^1 NH. This gives the macrocyclic ring the shape of a distorted "figure-eight", rather than the flat antiparallel β-sheet type arrangement more commonly observed in cyclic depsipeptides. The linear portion of didemnin B (**11**) is involved in a β II-type turn, a structural feature often observed in linear peptides, in which 4 amino acids are stabilized in a well defined conformation by hydrogen bonding between amino acids i (H-donor) and $i + 3$ (H-acceptor). The β-turn in didemnin B (**11**) encompasses residues Thr^6, $MeLeu^7$, Pro^8 and Lac^9 with hydrogen bonding interaction consistently found between Thr^6 NH and Lac^9 CO. The third hydrogen bond in didemnin B (**11**) was identified between $MeLeu^7$ CO in the linear portion of the molecule and Leu^3 NH in the macrocycle, orienting the folded linear chain back over the macrocyclic ring, resulting in its overall globular shape.

To assess the effects of the ring modifications in tamandarin A (**42**), conformational studies were undertaken using J-values from 1D ^1H or 2D ECOSY NMR spectra, NH chemical shifts and their temperature dependence (Table 2.5), and NOE/ROE correlations obtained from 2D NOESY and ROESY experiments (Table 2.4). An effort was made to identify the major differences in shape between tamandarin A (**42**) and didemnin B (**11**) brought about by the presence of a Hiv^2 group in tamandarin A (**42**). All NMR experiments (except the variable temperature experiments) were carried out in $CDCl_3$ in which one set of signals and therefore a single conformer of tamandarin A (**42**) was observed in solution. In this solvent, all ^1H and ^{13}C chemical shifts were assigned as described earlier. ^1H chemical shift values for tamandarin A (**42**) differed from those of didemnin B (**11**) in the same solvent by no more than +/- 0.23 ppm. ^{13}C chemical shifts between the two molecules differed up to 2.7 ppm, except in Ist^1 where C1 appeared at δ 39.9 ppm in tamandarin A (**42**) versus δ 29.7 ppm in didemnin B (**11**).

Tamandarin A (**42**) appeared rigid as could be deduced from the vicinal coupling constants $^3J_{NH-C4H}$ in Ist^1 (9.6 Hz), Leu^3 (9.6 Hz) and Thr^6 (5.4 Hz), which indicated a single dominant conformation rather than freely interconverting residues for which average J-values of 6-8 Hz would be seen. On the basis of these coupling constants,

Reproduced with permission of the copyright owner. Further reproduction prohibited without permission.

trans conformations were assigned to the NH-C4H and NH-CαH bonds in Ist^1 and Leu^3, respectively, versus a *gauche* conformation for Thr^6. Additional vicinal coupling constants for Thr^6, $^3J_{C\alpha H-C\beta H}$ = 1.4 Hz and $^3J_{C\beta H-C\beta H_3}$ = 6.0 Hz, and ROE enhancements between Thr^6 NH and Thr^6 CβH and β-CH$_3$, determined that the conformation of this unit is practically identical to that of Thr^6 in didemnin B (**11**) [87]. The diastereotopic protons Ist^1 C2H$_2$ were assigned on the basis of vicinal coupling constants $^3J_{C2Ha-C3H}$ = 8.1 Hz and $^3J_{C2Hb-C3H}$ = ~0 Hz, and their values together with the chemical shift difference between them is another indication of the rigidity of the molecule. For the Ist^1 unit, where one could expect significant conformational changes, additional coupling constants of $^3J_{C2Ha-C2Hb}$ = 17.0 Hz, $^3J_{C3H-C4H}$ = 9.6 Hz, $^3J_{C4H-C5H}$ = 3.4 Hz, $^3J_{C6H-C7H}$ = 6.9 Hz, $^3J_{C5H-C8H}$ = 6.3 Hz were observed. These values, together with NOE enhancements between Ist^1 NH and Ist^1 C8H$_3$ and C3H, and between Ist^1 C4H and Ist^1 C7H$_3$ and C5H, determined the conformation to be practically identical to Ist^1 in didemnin B (**11**) as well [87].

All remaining peptide bonds in tamandarin A (**42**) were assigned *trans* conformations as in didemnin B (**11**), on the basis of NOE/ROE enhancements between NH or NCH$_3$ and the α protons of the preceding amino acids. In the case of Pro^4 and Pro^8, lacking such correlations, *trans* peptide bonds were assigned based on enhancements between Pro^4 CβH$_2$ and Leu^3 CβH, and between Pro^8 CβH2 and Lac^9 CαH. A *trans* conformation was confidently assigned to the bond Hiv^2-Leu^3, based on an enhancement between Hiv^2 CαH and Leu^3 NH. Based on an NOE/ROE enhancement observed between MeLeu^7 NCH$_3$ and Thr^6 NH, a similar conclusion was reached for the MeLeu^7-Thr^6 peptidic bond, where NOE/ROE correlations between MeLeu^7 NCH$_3$ and Thr^6 CαH were lacking.

The temperature dependence of amide proton chemical shifts is generally considered to be well correlated with their inaccessibility to solvent and hence their potential to be involved in intramolecular hydrogen bonds. Many studies on amide proton T-dependence in a variety of solvents has led to the view that $\Delta\delta/\Delta T$ coefficients higher than 5 $\times$ 10^{-3} ppm/°K in polar solvents indicate amide protons that are solvated, as in the case of linear extended peptide conformations. Conversely, a coefficient of 4.0 $\times$ 10^{-3} ppm/°K is considered the upper limit for internal protons that are inaccessible to

Reproduced with permission of the copyright owner. Further reproduction prohibited without permission.

Table 2.4: Observed NOE/ROE correlations for Tamandarin A (**42**)

Ist[1]	Hiv[2]	Leu[3]	Pro[4]	Me_2Tyr^5	Thr[6]	MeLeu[7]	Pro[8]	Lac[9]
NH - - $C8H_3$					NH - - - - - - - - - - - - - -		CαH	
NH - - C3H		CαH - - - -	$CβH_2$				$CβH_2$ - - - - -	CαH
C4H - - $C7H_3$	CαH - - - -	NH				NCH_3 - - - -	CαH	
C4H - - C5H			CαH - - - - - -	NCH_3	NH - - - - -	NCH_3		
$C2H_b$ - - - - - - - - - - - - - -		NH		CαH - - - - - - -	NH			
					NH - - CβH			
					NH - - β-CH_3			
		NH -			CαH			
		$CβH_a$ -			CαH			
NH -					CαH			
$C6H_3$ -				NCH_3				
$C6H_3$ -			CαH					
	$CγH_3$ -					$CβH_3$		

solvent and thus might be involved in hydrogen bonds [94, 95].

The temperature coefficients (Table 2.5) for the amide proton chemical shifts of tamandarin A (**42**) were determined in DMSO-d_6. In this solvent several conformers of tamandarin A (**42**) can be observed. The major conformer of tamandarin A (**42**) was assumed to be conformationally constant in solvents ranging from $CDCl_3$ to DMSO-d_6, analogous to what has been found for didemnin B (**11**) [87]. On this assumption, the amide proton chemical shifts of the major conformer were assigned on the basis of their couplings constants. Temperature dependence was measured over the range 298 to 388°K. The Ist[1] and Leu[3] NHs were found to be practically T-independent with very small $\Delta\delta/\Delta T$ coefficients of 9×10^{-4} and 4×10^{-5} ppm/°K, respectively. The Thr[6] NH showed T-dependence with the larger $\Delta\delta/\delta T$ coefficient of 2.8×10^{-3} ppm/°K. All these coefficients, however, are less than 4.0×10^{-3} ppm/°K, hence the amide protons of tamandarin A (**42**) exist in inaccessible environments and could be involved in hydrogen bonds. Since only a limited number of possible hydrogen bonds can be formed in the molecule, these results pointed toward a hydrogen bond situation very similar to that of didemnin B (**11**). A weak ROE correlation between Leu[3] NH and Ist[1] C2Hb, together with the small temperature coefficient for Ist[1], indicate the involvement of Leu[3] in a transannular hydrogen bonding interaction with Ist[1]. Additional ROE correlations

Reproduced with permission of the copyright owner. Further reproduction prohibited without permission.

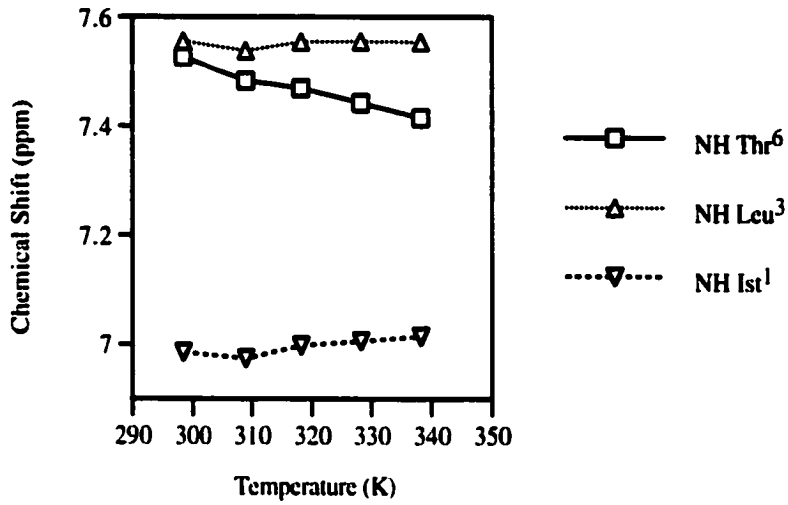

Figure 2.25: Temperature dependence of NH protons of tamandarin A (**42**), DMSO-d_6, 300 MHz.

between Ist^1 $C6H_3$ and Me_2Tyr^5 NCH_3, and Ist^1 $C6H_3$ and Pro^4 CαH, are consistent with such a hydrogen bridge across the macrocyclic ring. Transannular ROE correlations between Thr^6 CαH and Leu^3 CβHa, and Hiv^2 CγH_3 and $MeLeu^7$ CβHa confirmed the internal orientation of the Leu^3 NH. These ROE correlations, consistent with the solvent inaccessibility of the Leu^3 NH, suggest orientation of part of the linear portion of the molecule back over the cyclic backbone and possible stabilization by hydrogen bonding. Strong interresidue ROE and NOE correlations were observed in the linear portion of the molecule, in particular between Pro^8 CαH and Thr^6 NH, $MeLeu^7$ NCH_3 and Thr^6 NH, and $MeLeu^7$ NCH_3 and Pro^8 CαH. These correlations are indicative of a β II turn in the linear side-chain of the molecule, stabilized by a hydrogen bond between Thr^6 NH and Lac^9 CO. The corner positions of the turn are occupied by Pro^8 in the (i+1) position and $MeLeu^7$ in the (i+2) position, bringing Pro^8 CO and $MeLeu^7$ CαH coplanar as can been concluded from the low-field chemical shift, δ 5.30 ppm, of the latter.

Table 2.5: Temperature dependence (ppm/°K) of NH protons of Tamandarin A (**42**).

	Ist^1	Leu^3	Thr^6
$\Delta\delta/\Delta T$	9×10^{-4}	4×10^{-5}	2.8×10^{-3}

Reproduced with permission of the copyright owner. Further reproduction prohibited without permission.

The conformations of the side-chain amino acids of tamandarin A (**42**) were analyzed by means of vicinal coupling constants $^3J_{C\alpha H-C\beta H}$ and analysis of their corresponding dihedral angles χ_1. As was described earlier, based on coupling constants, the conformations of Ist[1] and Thr[6] were found identical to these units in didemnin B (**11**), which both in the crystal and solution structure adopt dihedral angles χ_1 of ~60° and ~155°, respectively. Hiv[2], in which one might expect the greatest changes to appear, showed a vicinal coupling constant $^3J_{C\alpha H-C\beta H}$ of 4.8 Hz (versus ~3.5 Hz in didemnin B (**11**)) which indicated a gauche conformation about the Cα-Cβ bond. Although the sign of χ_1 could not be unambiguously determined, the identical chemical shifts of the *pro-R* and *pro-S* methyl groups, and thus their equal proximity to the neighboring carbonyl, seems to favor χ_1 = 60°, as in didemnin B (**11**). Vicinal coupling constants $^3J_{C\alpha H-C\beta H}$ and $^3J_{C\alpha H-C\beta H'}$ in Leu[3] (9.6 and 1.6 Hz), Pro[4] (3.6 and 7.8 Hz), Me_2Tyr[5] (10.8 and 4.1 Hz) and MeLeu[7] (3.6 and 11.4 Hz) were extracted from the 1D ^{1}H NMR spectrum of tamandarin A (**42**). These values are virtually identical with those found in didemnin B (**11**), indicating the conformations about the Cα-Cβ bonds to be identical in both molecules. Therefore, the side-chain of Leu[3] in tamandarin A (**42**) appears to be highly restrained as in didemnin B (**11**), although the expected strong NOE correlations between Leu[3] CβH and Pro[4] CγH were not observed. Coupling constants for Pro[4] seemed to indicate an '*endo*' configuration with respect to ring puckering, in which Cγ and CO point in the same direction, as in didemnin B (**11**). Vicinal coupling constants $^3J_{C\alpha H-C\beta H}$ and $^3J_{C\alpha H-C\beta H'}$ for Pro[8] of both 7.5 Hz are quite different from those observed in Pro[4]. The measured values correspond to a dihedral angle and ring puckering identical to Pro[8] in didemnin B (**11**), which adopts an '*exo*' configuration (Cγ and CO pointing in opposite directions, Fig. 2.26-Fig. 2.27).

2.3 Discussion

Tamandarin A (**42**) and B (**43**) are novel didemnin depsipeptides, a well known class of cyclic, highly active antiviral, antitumor and immunosuppressive peptides. To date, eighteen naturally occurring congeners (Fig. 2.4) have been isolated from the Caribbean tunicate *Tridemnum solidum* (class Ascidiacea, order Aplousobranchia,

Reproduced with permission of the copyright owner. Further reproduction prohibited without permission.

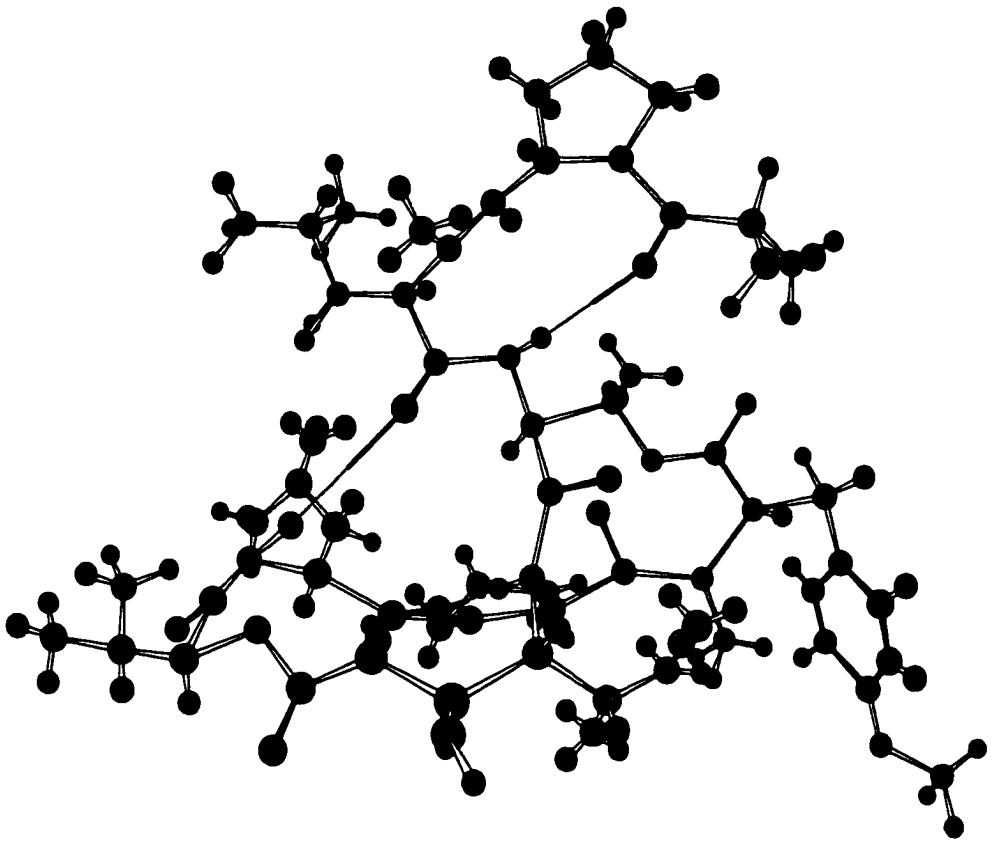

Figure 2.26: Perspective drawing of the solution conformation of tamandarin A (**42**).

family Didemnidae), the Mediterranean species *Trididemnum cyanophorum* and *Aplidium albicans* (order Aplousobranchia, family Polyclinidae) and the unidentified Brazilian ascidian (family Didemnidae) in this study [43–53]. Didemnin B (**11**) is among the most potent members of this class of molecules, rivaled by tamandarin A (**42**) in some assays. Didemnin B (**11**) was early shown to be active against several DNA and RNA viruses *in vitro* and *in vivo*, but is unfortunately ineffective against the AIDS causing virus HIV [43,96,97].

In several *in vitro* and *in vivo* assays, didemnin B (**11**) showed antiproliferative activity of T-lymphocytes with a potency stronger than cyclosporin A, at present the most important immunosuppressive agent used clinically [98–103]. During further evaluation of the antiproliferative activity of didemnin B (**11**) for the purpose of prolonging organ allograft survival, it was generally found that didemnin B (**11**) displays some immunosuppressive activity *in vivo*, but possesses a very narrow therapeutic index

Reproduced with permission of the copyright owner. Further reproduction prohibited without permission.

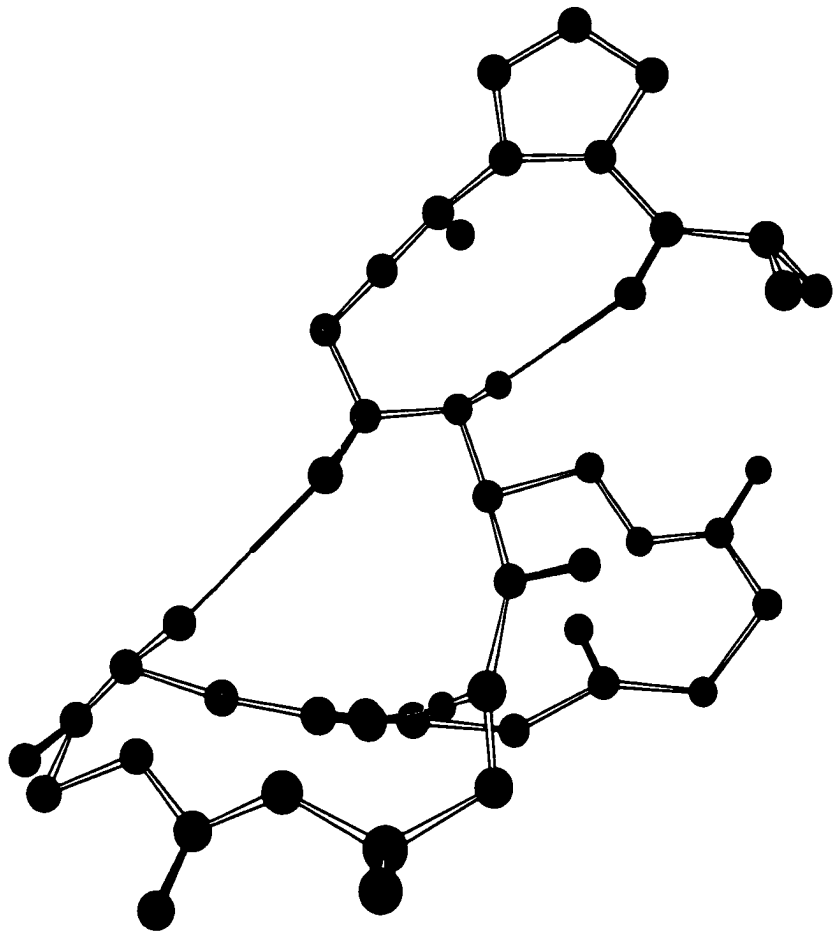

Figure 2.27: Perspective drawing of the solution conformation of tamandarin A (**42**), backbone and hydrogen bonds only.

as it displays significant toxicity at therapeutic dosages [104–109].

Didemnin B (**11**) was also shown to be cytotoxic toward B16 melanoma, both *in vitro* and *in vivo*, and P388 leukemia *in vivo* and L1210 *in vitro* [110]. On the basis of these results, and activity observed against a number of human tumor stem cell lines, didemnin B (**11**) was the first marine cytotoxin to enter clinical trials as an antineoplastic agent [111–118]. Phase I and II clinical trials were conducted against melanoma and cancers of the ovaries, cervix, prostate, lung, breast and kidney [119–129]. Invariably, didemnin B (**11**) was found to be toxic but inactive in most of the trials completed. Didemnin B (**11**) showed no significant antitumor activity against these cancers and further clinical trials were canceled [130].

Based on the structural and biological similarity to didemnin B (**11**), taman-

Reproduced with permission of the copyright owner. Further reproduction prohibited without permission.

darin A (**42**) can be expected to show potent antiviral, immunosuppressive and antitumor activities. Indeed, clonogenic cytotoxicity assays showed that colony formation under continuous exposure is equally strongly inhibited by tamandarin A (**42**) as by didemnin B (**11**).

The possible mechanisms through which didemnin B (**11**) may exert its antiviral, antitumor and immunomodulating activities have been studied extensively. Both in cellular (*in vivo* and in vitro) [41, 131] and cell-free assays [42], didemnin B (**11**) was found to inhibit protein and DNA synthesis, and to a lesser extent RNA synthesis. Evidence has been provided that inhibition of peptide synthesis by didemnin B (**11**) occurs by stabilization of aminoacyl-tRNA binding to the ribosomal A-site, preventing translocation of phenylalanyl-$tRNA^{phe}$ from the A- to the P-site but not preventing peptide bond formation [132]. Consistent with these findings, it was previously found that didemnin B (**11**) binds to elongation factor 1α in a GTP dependent manner and formation of the didemnin B (**11**)-GTP- EF1α complex may be responsible for the observed inhibition of protein synthesis [133]. The structural similarity of tamandarin A (**42**) with didemnin B (**11**) suggests that they work through the same mechanism of action. Accordingly, tamandarin A (**42**) was found to be a three-fold more potent inhibitor of protein biosynthesis in cell-free assays than didemnin B (**11**).

In view of their potent biological properties, numerous synthetic and structure-activity studies have been performed on the didemnins. The total synthesis of didemnins A, B, C [134–139] and nordidemnin B (**12**) [140–143] have been reported, as well as the (semi-)synthesis of approximately 40 "unnatural" analogs of didemnin B (**11**) (Fig. 2.5) and its parent structure didemnin A [56, 144]. Antitumor, antiviral and immunosuppressive activities of the structures were assessed *in vitro* and *in vivo* and several compounds with increased potency over didemnin B (**11**) were discovered. Structure-activity studies identified several parts of the molecule as potentially important in drug-receptor interactions. Whereas modifications of the linear side-chain resulted in increased potency in certain cases, stereocenters and functionalities of the cyclic depsipeptide core were deemed essential for bioactivity [145–147]. It was proposed that the keto group of the Hip^2 unit plays a major role in the bioactivities of the didemnins, since its reduction to the alcohol resulted in loss of bioactivity [46]. This proposal seems incorrect however,

Reproduced with permission of the copyright owner. Further reproduction prohibited without permission.

since tamandarin A (**42**), which lacks this group, shows potent cytotoxicity and protein synthesis inhibition, at levels comparable to didemnin B (**11**).

The solution conformation of tamandarin A (**42**), described in this paper, indicates that the lack of the propionic acid unit of didemnin B (**11**), results in only minor conformational modifications. Whereas the cyclic peptide ring in didemnin B (**11**) is 23-membered, the ring in tamandarin A (**42**) is 21-membered. The effect of this change seems to be spread out over the entire molecule, resulting in little overall change. The backbone configuration of tamandarin A (**42**) appears to be stabilized by the same three hydrogen bonds, Ist^1 NH-Leu^3 CO, Leu^3 NH-$MeLeu^7$ CO and Lac^9 CO-Thr^6 NH, yielding the same "bent figure eight"-shape of the cyclic peptide ring and the side-chain folding back over the cyclic portion of the molecule. The conformations of the amino acid side-chains in tamandarin A (**42**) appear identical to those in didemnin B (**11**) as well, indicating again no major increase or decrease in local crowding due to the reduced size of the cyclic peptide.

Although the didemnin class of cyclic depsipeptides may not yield a clinically useful antitumor drug with utility in conventional chemotherapy, these molecules remain of great interest for the development of novel cancer treatments. In view of the exceptional potency of these cyclic peptides, they may become useful in future applications in which antitumor compounds are delivered directly to the tumor by means of an alternative transport system. Such targeted systems can potentially avoid the problem of toxicity toward normal tissues. Carrier systems that have been reported include monoclonal antibodies, lyposomes, viral particles and tumor homing peptides.

2.4 Experimental

General

NMR spectra were recorded on a Varian Unity Inova at 300 MHz (^{1}H) and a Varian Gemini at 100 MHz (^{13}C) in $CDCl_3$. In this solvent only one conformation is apparent. FAB mass spectral analysis and tandem mass spectral analysis were performed by K. S. Chatman at the Scripps Research Institute, La Jolla, CA. High-performance liquid chromatography was carried out isocratically, using a reversed-phase (C_{18}) Rainin Dy-

Reproduced with permission of the copyright owner. Further reproduction prohibited without permission.

namax 60 Å column (I.D. 10 mm) and a Waters R401 differential refractometer. Optical rotations were determined on an Autopol III Automatic Polarimeter (Rudolph Research, Flanders NJ). UV spectra were measured on a Perkin-Elmer Lambda 3B UV/VIS Spectrophotometer and IR spectra on a Perkin-Elmer 1600 Series FTIR Spectrophotometer.

Isolation of Tamandarins A and B

Approximately 112 grams of wet ascidian were collected in March 1996 at a depth of 10 meters on a small reef off the coast of the village Tamandaré, Mamucabinha, Brazil. The specimen was immediately frozen and, upon lyophilization, yielded approximately 465 grams of dry material. The dry material was extracted three times with a mixture of dichloromethane and methanol (1:1). The crude extract obtained (26.6 grams) showed potent growth inhibitory activity at or below 0.03 μg/mL in the primary *in vitro* cytotoxicity assay using the HCT 116 cell line. The dark oil was partitioned between isooctane and methanol, the methanol fraction was dried *in vacuo* and further partitioned between water and ethyl acetate, water and dichloromethane, and water and butanol. The ethyl acetate and dichloromethane fractions appeared very similar in contents by TLC analysis and contained the bulk of the cytotoxic activity. The fractions were combined for subsequent size exclusion chromatography employing Sephadex LH-20 resin using a mixture of hexane, toluene and methanol (3:1:1). This method has proven to be an excellent technique for the separation of medium sized peptides, such as the tamandarins, from complex organic mixtures. The procedure yielded 21 fractions, all of which showed potent inhibition in the cytotoxicity assay at or below 0.03 μg/mL. However, by ^{1}H NMR, one fraction appeared to be clearly enriched with peptidic metabolites. Without further fractionation, 75 mg of tamandarin A (**42**) accompanied by 10 mg of tamandarin B (**43**) were purified from the fraction by RP (C_{18}) HPLC using 23% water in methanol.

Tamandarin A (42) White amorphous solid or transparent glass. $[\alpha]_D$ = -35°, c = 0.11; IR (KBr) 3495, 3342, 2966, 2872, 1743, 1649, 1537, 1514, 1455, 1249, 1173, 1079, 1032 cm^{-1}; UV (CH_2Cl_2) λ_{max} 228 nm (ϵ 24500), 276 nm (ϵ 4000), 283 nm (ϵ 3400); HRFABMS (NBA/CsI matrix) m/z 1187.5074 $[MCs+2H]^+$, calcd for $C_{54}H_{84}N_7O_{14}$,

Reproduced with permission of the copyright owner. Further reproduction prohibited without permission.

1187.5131 (Δ = 4.8 ppm); ^{1}H and ^{13}C NMR data ($CDCl_3$) are shown in Table 2.1.

Tamandarin B (43) White amorphous solid or transparent glass. $[\alpha]_D$ = -29°, c = 0.11; IR (KBr) 3472, 3342, 2966, 2872, 1742, 1661, 1637, 1531, 1514, 1449, 1249, 1173, 1078, 1032 cm^{-1}; UV (CH_2Cl_2) λ_{max} 227 nm (ϵ 14400), 277 nm (ϵ 1500), 283 nm (ϵ 1200); HRFABMS (NBA/CsI matrix) m/z 1173.4916 $[MCs+2H]^+$, calcd for $C_{53}H_{82}N_7O_{14}$, 1173.4974 (Δ = 4.9 ppm); ^{1}H and ^{13}C NMR data ($CDCl_3$) are shown in Table 2.2.

Mild Alkaline Hydrolysis of Tamandarins A (42) and B (43) A sample of tamandarin A (**42**) (5 mg) was dissolved in cooled (4°C) methanol (500 μL) and hydrolyzed by adding 30 μL 1N sodium hydroxide at room temperature. The disappearance of starting material was monitored by TLC analysis. After 75 minutes, the reaction was quenched by acidification with 30 μL 1N hydrochloric acid. The crude reaction mixture was methylated by addition of diazomethane in ether until the yellow coloration persisted and gas formation ceased (approximately 1.5 mL). The resulting solution was evaporated to dryness and the residue was chromatographed on a silica gel column (1 gram) using 5% methanol in dichloromethane. The two major peptide fragments (northern fragment (**44**) and southern fragment (**46**)) were purified by RP (C_{18}) HPLC using 23% water in methanol. The procedure was repeated with 5 mg didemnin B (**11**) to obtain two reference peptidic fragments (northern fragment (**44**) and a southern fragment). ^{1}H NMR spectra, FABMS spectra, and optical rotations were recorded for the four peptides obtained.

Tamandarin B (**43**), 5 mg, was hydrolyzed using the same method to yield two peptide fragments (a northern fragment (**45**) and a southern fragment (**46**)), as was 1 mg nordidemnin B (**12**) to obtain reference peptide fragments (a northern fragment (**44**) and a southern fragment). ^{1}H NMR, FABMS spectra and optical rotations were recorded for the four peptides.

Northern Peptide Fragment from Tamandarin A (44) White, amorphous solid or transparent glass. $[\alpha]_D$ = +41°, c = 0.07; HRFABMS (NBA/CsI matrix) m/z 719.2658 $[MCs+2H]^+$, calcd for $C_{28}H_{50}N_4O_9$, 719.2632 (Δ = 3.6 ppm); ^{1}H NMR ($CDCl_3$,

Reproduced with permission of the copyright owner. Further reproduction prohibited without permission.

determined by ^{1}H and COSY experiments): (*S*)-Lac: δ 4.41 (m, 1H), 1.18 (d, 3H, J = 6.3 Hz); L-Pro: δ 4.75 (br tr, 1H, J = 6.6 Hz), 3.64 (m, 2H), 2.23 (m, 2H), 1.97 (m, 2H); D-MeLeu: δ 5.36 (dd, 1H, J = 10.2, 5.1 Hz), 3.08 (s, 3H), 1.96 (m, 1H), 1.90 (m, 1H), 1.43 (m, 1H), 0.97 (d, 3H, J = 6.6 Hz), 0.93 (d, 3H, J = 6.6 Hz); L-Thr: δ 7.37 (d, 1H, J = 7.8 Hz), 4.37 (m, 2H), 1.37 (d, 3H, J = 6.6 Hz); (3*S*, 4*R*, 5*S*)-Ist: δ 6.62 (br d, 1H, J = 10.8 Hz), 4.16 (d tr, 1H, J = 6.0, 5.3 Hz), 4.04 (m, 1H), 3.70 (s, 3H), 2.54 (s, 1H), 2.52 (d, 1H, J = 6.3 Hz), 1.91 (m, 1H), 1.37 (m, 1H), 1.20 (m, 1H), 0.93 (d, 3H, J = 8.1 Hz), 0.91 (tr, 3H, J = 6.8 Hz).

Southern Peptide Fragment from Tamandarins A and B (46) White amorphous solid or transparent glass. $[\alpha]_D$ = -100°, c = 0.03; HRFABMS (NBA/CsI or NaI matrix) m/z 666.2179 $[MCs+H]^+$, calcd for $C_{28}H_{43}N_3O_7$, 666.2155 (Δ = 3.6 ppm) and m/z 534.3160 $[M+H]^+$, calcd for $C-28H_{43}N_3O_7$, 534.3179 (Δ = 3.6 ppm); ^{1}H NMR ($CDCl_3$, determined by ^{1}H and COSY experiments): L-Me_3Tyr: δ 2.93 (s, 3H), 3.01 (dd, 1H, J = 14.4, 9.3 Hz), 3.27, (dd, 1H, J = 14.7, 6.0 Hz), 3.80 (s, 3H), 3.69 (s, 3H), 5.03 (dd, 1H, J = 9.3, 6.3 Hz), 6.83 (d, 2H, J = 8.7 Hz), 7.12 (d, 2H, J = 8.4 Hz); L-Pro: δ 1.87 (m, 1H), 2.16 (m, 3H), 3.68 (m, 1H), 3.82 (m, 1H), 4.78 (m, 1H); L-Leu: δ 0.98 (tr, 6H, J = 6.3 Hz), 1.67 (m, 1H), 1.71 (m, 2H), 4.78 (m, 1H), 6.99 (d, 1H, J = 8.7 Hz); (*S*)-Hiv: δ 0.87 (d, 3H J = 6.9), 1.03 (d, 3H, J = 6.9 Hz), 2.16 (m, 1H), 3.96 (d, 1H, J = 3.0 Hz).

Northern Peptide Fragment of Tamandarin B (45) White amorphous solid or transparent glass. $[\alpha]_D$ = +24°, c = 0.05; HRFABMS (NBA/NaI matrix) m/z 595.3302 $[MNa+2H]^+$, calcd for $C_{27}H46N_4O_9$, 595.3319 (Δ = 2.9 ppm); ^{1}H NMR ($CDCl_3$, determined by ^{1}H and COSY experiments): (*S*)-Lac: δ 1.21 (d, 3H, J = 6.3 Hz), 4.45 (m, 1H); L-Pro: 1.99 (m, 2H), 2.26 (m, 2H), 3.68 (m, 2H), δ 4.78 (br tr, 1H, J = 7.2 Hz); D-MeLeu: δ 0.93 (d, 3H, J = 6.6 Hz), 0.97 (d, 3H, J = 7.2 Hz), 1.48 (m, 1H), 1.68 (m, 1H), 1.94 (m, 1H), 3.11 (s, 3H), 5.38 (dd, 1H, J = 10.5, 4.8 Hz); L-Thr: δ 1.40 (d, 3H, J = 6.9 Hz), 4.41 (m, 2H), 7.41 (br d, 1H, J = 7.2 Hz); (3*S*, 4*R*)-Nst: δ 0.98 (tr, 3H, J = 6.6 Hz), 0.99 (d, 3H, J = 6.9 Hz), 1.99 (m, 1H), 2.52 (d, 1H, J = 6.0 Hz), 2.54 (s, 1H), 3.72 (s, 3H), 3.95 (m, 1H), 4.21 (m, 1H), 6.66 (br d, 1H, J = 10.5 Hz).

Reproduced with permission of the copyright owner. Further reproduction prohibited without permission.

Preparation of *N,O*-dimethyltyrosine-methyl ester (Me_3Tyr) (47) *N,O*-dimethyltyrosine-methylester was obtained by deprotection of *N*-Cbz-*N,O*-dimethyltyrosine-methyl ester (**48**) (1 mg, see further) in refluxing TFA (1 mL) for 30 minutes. Reaction progress was monitored by TLC analysis. The reaction mixture was cooled, evaporated to dryness and traces of TFA were removed by repeated evaporation from water. The crude *N,O*-dimethyltyrosine-methyl ester was then converted to its Marfey derivative without further purification.

Preparation of *N*-Cbz-*N,O*-dimethyltyrosine-methyl ester (48) A mixture of 100 mg (0.32 mmol) *N*-Cbz-tyrosine (D:L = 3:7) was dimethylated analogous to methods described previously.[1] The protected amino acid was dissolved in 5 mL DMF (reagent grade) and 10 mg Bu_4NHSO_4 (20% by weight) was added. Portions of 180 mg finely powdered KOH and 300 μL dimethylsulfate were added three times over a period of 16 hrs, during which the reaction mixture was stirred vigorously at room temperature. The reaction mixture was cooled to 0°C, diluted with 20 mL diethylether and 30 mL water was added. The aqueous layer was separated and the organic layer was extracted twice with 30 mL saturated $NaHCO_3$ solution. The aqueous layers were combined, acidified with $KHSO_4$ (1M) to pH 1 and extracted three times with ethyl acetate. The organic layers were combined, dried over $MgSO_4$, filtered and dried *in vacuo*. The crude reaction mixture was dissolved in 1 mL absolute methanol, cooled in ice and methylated with CH_2N_2 in ether. The solvent was evaporated under a stream of nitrogen and *N*-Cbz-*N,O*-dimethyltyrosine- methyl ester was purified by RP (C_{18}) HPLC using 23% water in methanol.

Compound (**47**) was obtained as a colorless oil: ^{1}H NMR ($CDCl_3$): δ 2.85 and 2.83 (s, 3H, rotational isomers), 2.97 (dd, 1H, J = 11.9 Hz), 3.28 (tr d, 1H, J = 14.2, 5.7 Hz), 3.75 and 3.68 (s, 3H, rotational isomers), 3.79 (s, 3H), 4.77 and 4.98 (dd, 1H, J = 5.1, 10.2 Hz, rotational isomers), 5.05 (d, 1H, J = 5.7 Hz), 5.12 (d, 1H, 5.7 Hz), 6.78 (d, 1H, J = 7.9 Hz), 6.82 (d, 1H, J = 8.0 Hz), 7.04 (d, 1H, J = 7.9 Hz), 7.13 (d, 1H, J = 8.0 Hz), 7.24 (m, 1H), 7.33 (m, 4H).

[1]The method as described in [139] followed by methylation with diazomethane yielded only *O*-methyltyrosine-methyl ester. For dimethylation to occur the modified reaction scheme, Fig. 2.20, was used

Reproduced with permission of the copyright owner. Further reproduction prohibited without permission.

Acid Catalyzed Hydrolysis of Southern Peptide Fragment (46) The southern peptide fragment (**46**), 1 mg, in 0.5 ml 6N HCl was heated at 105°C for 16 hrs in a sealed vial. The cooled reaction mixture was evaporated to dryness and traces of HCl were removed from the residual hydrolysate by repeated evaporation from H_2O.

Amino Acid Analysis of Southern Peptide (46) using Marfey's Method The previously obtained crude hydrolysate of the southern peptide fragment (**46**), or the crude *N,O* -dimethyltyrosine-methyl ester (Me_3Tyr) or a small amount of standard free amino acid (D:L = 3:7), in 50 μL of water/acetone was mixed with 100 μL of a 1% solution of FDAA (Marfey's reagent = 1-Fluoro-2,4-Dinitrophenyl-5-L-Alanine Amide) in acetone. Sodium bicarbonate (20 μL, 1 M) was added to this mixture and the resultant solution was heated at 40°C for one hour and then allowed to cool. After addition of 10 μL of 2M HCl, the resulting solution was evaporated, the residue was dissolved in 0.5 ml of DMSO and analyzed by Diode Array HPLC. The analysis was performed under the following conditions: solvent A, 0.1% TFA in H_2O; solvent B, 0.1% TFA in methanol; gradient flow rate of A + B at 1 mL/min., 100/0 to 80/20 in 45 min. and from 80/20 to 40/60 in 45 min.; column, Hewlett Packard ODS Hypersil 5μ, 200 mm x 4.6 mm; UV detection at 340 nm. The peaks were identified by comparison with a mixture of D/L-standard amino acid-DAA derivatives (D:L = 3:7). Retention times (min.): L-Me_3Tyr-DAA (56.5), L-Pro-DAA (58.8), L-Leu-DAA (70.5).

Mosher Ester Analysis of Hiv^2 in Southern Peptide Fragment (46) The southern peptide fragment (**46**), 1 mg, was dissolved in 200 μL dichloromethane. Dry pyridine (100 μL, predried over 4 Å molecular sieves) was added, followed by 0.5 mg 4-(dimethylamino)pyridine. Approximately 5 μL (*R*)- or (*S*)-MTPA acid chloride (*R*)- or (*S*)-α-methoxy-α-(trifluoromethyl)phenylacetyl chloride) was added and the solution was left to sit at room temperature. Reaction progress was monitored by Si gel TLC analysis. After three days, 3 mL saturated $NaHCO_3$ solution and 3 mL diethylether were added and the solution was stirred vigorously for 30 minutes to hydrolyze excess MTPA-acid chloride. The organic phase was separated and the aqueous phase was extracted with 3 mL diethylether. The organic phases were combined, washed three times with 3 ml 5% aqueous $NaHCO_3$ to remove pyridine, three times with 3 mL saturated

Reproduced with permission of the copyright owner. Further reproduction prohibited without permission.

NaCl solution, dried over $MgSO_4$ and dried *in vacuo*. The (*R*)- or (*S*)-MTPA ester of southern peptide fragment (**46**) was purified by taking the reaction mixture over a 1 inch silica flash column in a Pasteur pipette using 3:1 isooctane/ethyl acetate.

(*R*)-MTPA Ester of the Southern Peptide Fragment (46) ^{1}H NMR ($CDCl_3$), determined by ^{1}H and COSY experiments): L-Me_3Tyr: δ 2.94 (s, 3H), 3.02 (dd, 1H, J = 14.1, 9.4 Hz), 3.25, (dd, 1H, J = 14.1, 6.5 Hz), 3.77 (s, 3H), 3.70 (s, 3H), 5.01 (dd, 1H, J = 9.4, 6.5 Hz), 6.82 (d, 2H, J = 9.2 Hz), 7.13 (d, 2H, J = 9.2 Hz); L-Pro: δ 1.90 (m, 1H), 2.15 (m, 3H), 3.70 (m, 1H), 3.77 (m, 1H), 4.80 (m, 1H); L-Leu: δ 0.90 (tr, 6H, J = 6.3 Hz), 1.40 (m, 1H), 1.52 (m, 1H), 1.56 (m, 1H), 4.72 (m, 1H), 6.35 (br d, 1H, J = 9.2 Hz); (*S*)-Hiv-(*R*)-MTPA: δ 0.97 (d, 3H J = 7.5), 1.00 (d, 3H, J = 7.5 Hz), 2.35 (m, 1H), 3.58 (s, 3H), 5.20 (d, 1H, J = 3.9 Hz), 7.42 (m, 3H), 7.58 (d, 2H, J = 6.6 Hz).

(*S*)-MTPA Ester of the Southern Peptide Fragment (46) ^{1}H NMR data as determined by ^{1}H and COSY experiments: L-Me_3Tyr: δ 2.95 (s, 3H), 3.04 (dd, 1H, J = 14.1, 9.0 Hz), 3.27, (dd, 1H, J = 14.1, 6.3 Hz), 3.85 (s, 3H), 3.69 (s, 3H), 5.01 (dd, 1H, J = 9.0, 6.3 Hz), 6.81 (d, 2H, J = 9.4 Hz), 7.12 (d, 2H, J = 9.4 Hz); L-Pro: δ 1.90 (m, 1H), 2.15 (m, 3H), 3.69 (m, 1H), 3.85 (m, 1H), 4.80 (m, 1H); L-Leu: δ 0.90 (tr, 6H, J = 6.3 Hz), 1.40 (m, 1H), 1.50 (m, 1H), 1.58 (m, 1H), 4.76 (m, 1H), 6.45 (br d, 1H, J = 9.3 Hz); (*S*)-Hiv-(*R*)-MTPA: δ 0.90 (d, 6H J = 7.5), 2.28 (m, 1H), 3.58 (s, 3H), 5.16 (d, 1H, J = 4.5 Hz), 7.44 (m, 3H), 7.63 (d, 2H, J = 7.5 Hz).

Reproduced with permission of the copyright owner. Further reproduction prohibited without permission.

Chapter 3

Preclinical Development of Novel Anticancer Agents

3.1 Introduction

3.1.1 Current chemotherapy

Cytotoxic drugs have played, and will continue to play, a major role in anticancer therapy. They are the treatment of choice, especially in view of the propensity of cancer to metastasize, and they are often combined with radiation therapy and surgery.

In certain groups of patients, suffering from otherwise highly lethal forms of cancer, available drugs may effect cures in 50-70% of the cases. These diseases include some forms of leukemia and lymphoma, and a few other rare solid tumor types. For these forms of cancer, "standard therapies" are relatively well defined and widely accepted in oncology. However, in patients with more common tumors such as those of the head and neck, lung, colon, or breast, a much smaller percentage is actually cured and for those cases cytotoxic drugs are often used only to prolong life or enhance its quality.

Chemotherapy involves the systemic administration of cytotoxic drugs that travel through the body via the blood circulatory system. Approximately 90 cytotoxic or antiproliferative drugs and 25 hormonal agents are currently available for cancer therapy in the United States Table 3.1. They include the alkylating agents, the antimetabolites, the DNA binders, and the antimitotic agents, Table 3.2.

Reproduced with permission of the copyright owner. Further reproduction prohibited without permission.

Table 3.1: Anticancer Agents Available in the USA (May 1999).

Biologic Agents		
Aldesleukin	Interferon-1α	Nartograstrim
Denileukin diftitox	Interferon α-2a	Pegaspargase
Herceptin	Interleukin-2	Rituximab
Natural Products		
Actinomycin D	Masoprocol	Streptozocin
Asparaginase	Mithramycin	Topotecan
Angiotensin II	Mitomycin C	Testosterone
Bleomycin (**66**)	Taxol (Paclitaxel) (**73**)	Vinblastine (**71**)
Daunomycin (**68**)	Pentostatin	Vincristine (**72**)
Doxorubicin (**67**)		
Semisynthetic Natural Product Derivatives		
Bicalutamide	Formestane	Leuprolide acetate
Cladribine	Hydroxyprogesterone	Pirarubicin
Cytarbine ocfosfate	Idarubicin	Prednisolone
Dromostanolone	Irinotecan	Prednisone
Epirubicin HCl	Medroxyprogesterone acetate	Testolactone
Estramustine	Megestrol acetate	Triamcinolone
Ethinyl estradiol	Methylprednisolone	Valrubicin
Etoposide (VP-16) (**69**)	Methyltestosterone	Vinorelbine
Fluoxymesterone	Miltefosine	Zinostatin stimalamer
Synthetic Agents		
Amsacrine	Diethylstilbestrol	Mitotane
Bisantrene	Flutamide	Nilutamide
Busulfan (**58**)	Fotemustine	Pipobroman
Camostat mesylate	Hexamethylmelamine	Porfimer sodium
Carboplatin (**50**)	Hydroxyurea	Procarbazine
Carmustine (**56**)	Ifosfamide (**54**)	Ranimustine
Chlorambucil (**52**)	Levamisole	Sobuzoxane
Chlorotrianisene	Lomustine (**57**)	Thio-TEPA (**59**)
Cisplatin (**49**)	Lonidamine	Toremifene
Cyclophosphamide (**55**)	Mechlorethamine (**51**)	Triethylenemelamine
Cacarbazine	Melphalan (**53**)	Uracil mustard
Synthetic Agents based on Natural Product Model		
Aminoglutethimide	Fludarabine (**65**)	Methotrexate (**60**)
Capecitabine	5-Fluorouracil (**62**)	Mitoxantrone
Cytarabine	Gemcitabine (**64**)	Tamoxifen
Doxifluridine	Goserelin acetate	Toremifene
Enocitabine	Leuprolide	Taxotere (Docetaxel) (**74**)
Floxuridine	6-Mercaptopurine (**61**)	6-Thioguanine (**63**)

Reproduced with permission of the copyright owner. Further reproduction prohibited without permission.

Table 3.2: Anticancer Agents by Mechanism of Action. (Commercial and Investigative)

Alkylating Agents

Asaley	Diaziquone	PCNU
Busulfan (**58**)	Fluorodopan	Piperazine
Carboplatin (**50**)	Hepsulfam	Piperazinedione
(Carboxyphthalato)Pt	Hycanthone	Pipobroman
Carmustine (**56**)	Iproplatin	Spiromustine
Chlorambucil (**52**)	Lomustine (**57**)	Teroxirone
Chlorozotocin	Mechlorethamine (**51**)	Tetraplatin
Cisplatin (**49**)	Melphalan (**53**)	Thio-TEPA (**59**)
Clomesone	Methyl CCNU	Triethylenemelamine
Cyanomorpholinodoxorubicin	*N*-Methylmitomycin C	Uracil mustard
Cyclodisone	Mitomycin C	Yoshi-864
Dianhydrogalactitol	Mitozolamide	

Antimitotic Agents

Allocolchicine	Maytansine	Thiocolchicine
Colchicine der.	Rhizoxin	Trityl cysteine
Colchicine	Taxol (Paclitaxel) (**73**)	Vinblastine (**71**)
Dolastatin 10 (**3**)	Taxotere (Docetaxel) (**74**)	Vincristine (**72**)
Halichondrin B (**4**)		

Topoisomerase I Inhibitors

Aminocamptothecin	Camptothecin der. 1-20	Morpholinodoxorubicin
Camptothecin	Camptothecin, Na salt	

Topoisomerase II Inhibitors

Amonafide	Daunorubicin (**68**)	Mitoxantrone
Amsacrine	Deoxydoxorubicin	Oxanthrazole
Anthrapyrazole der.	Doxorubicin (**67**)	Pyrazoloacridine
N,N-Dibenzyl daunomycin	Etoposide (VP-16) (**69**)	Rubidazone
Bisantrene HCL	Menogaril	Tenoposide (VM-26) (**70**)

RNA/DNA Antimetabolites

Acivicin	Dichlorallyl lawsone	Methotrexate der.
L-Alanosine	5,6-Dihydro-5-azacytidine	*N*-(Phosphonoacetyl)-L-Asp
Aminopterin der. 1-3	5-Fluorouracil (**62**)	Pyrazofurin
An antifol 1,2	Ftorafur (pro-drug)	Triazinate
5-Azacytidine	Methotrexate (**60**)	Trimetrexate
Brequinar		

DNA Antimetabolites

Aphidicolin glycinate	3-HP	Pyrazoloimidazole
Ara-C	5-HP	α-TGDR
5-Aza-2'-deoxycytidine	Hydroxyurea	β-TGDR
Cyclocytidine	Inosine glycodialdehyde	Thioguanine
2'-Deoxy-5-fluorouridine	Macbecin II	Thiopurine
Guanazole		

Reproduced with permission of the copyright owner. Further reproduction prohibited without permission.

Alkylating Agents Alkylating agents, Fig. 3.1, exert their cytotoxic effect on the cell through the formation of covalent bonds with biological macromolecules such as proteins and DNA. The chemistry of these compounds is nicely illustrated by the smallest of the alkylating agents, mechlorethamine (**51**). This molecule carries two CH_2CH_2Cl groups linked to a nitrogen atom which together are called the mustard group. In aqueous solution this group undergoes a nucleophilic substitution reaction resulting in the loss of chlorine under the formation of a covalent bond with the incoming nucleophilic group. Nucleophiles are present in ample amount throughout the cell, but most important is their interaction with the nitrogenous bases in DNA. Bifunctional nitrogen mustards like mechlorethamine (**51**) are most potent since they can form interstrand cross links in DNA. Other alkylating agents include the nitrosoureas (**56**) and (**57**), busulfan (**58**), and thio-TEPA (**59**). Cisplatin (**49**) and analogs are often grouped among the classical alkylating agents due to their very similar mechanism of action, the formation of DNA crosslinks.

Antimetabolites Antimetabolites, Fig. 3.2, are agents that disrupt the normal metabolism of the cell due to their structural similarity with normal intermediates in the synthesis of precursors of biomolecules such as DNA and RNA. They serve as substrates for enzymes such that a nonfunctional product is obtained, or they block the functioning of enzymes directly, or both. The target enzyme is preferably involved in a key step in the metabolism of the cell and is usually an enzyme involved in the synthesis of DNA and RNA, although other target enzymatic processes have been identified as well. Well known antimetabolites include the pyrimidine analogs such as 5-fluorouracil (**62**), antifolates such as methotrexate (**60**), and cytidine analogs such as gemcitabine (**64**).

DNA binders There is currently no satisfactory classification of these cytotoxic drugs. They are often natural products or their derivatives. Some are DNA binders like bleomycin (**66**) Fig. 3.3, that in contrast to the alkylating agents bind DNA and RNA through intercalation rather than covalent bonding. Others inhibit topoisomerase I or II, e.g. doxorubicin (**67**) and etoposide (**69**). Daunorubicin (**68**) and its derivative doxorubicin (**67**), were originally isolated from a *Streptomyces* species, and the bleomycin family, a mixture a glycopeptides, is derived from *Streptomyces verticillis.*

Reproduced with permission of the copyright owner. Further reproduction prohibited without permission.

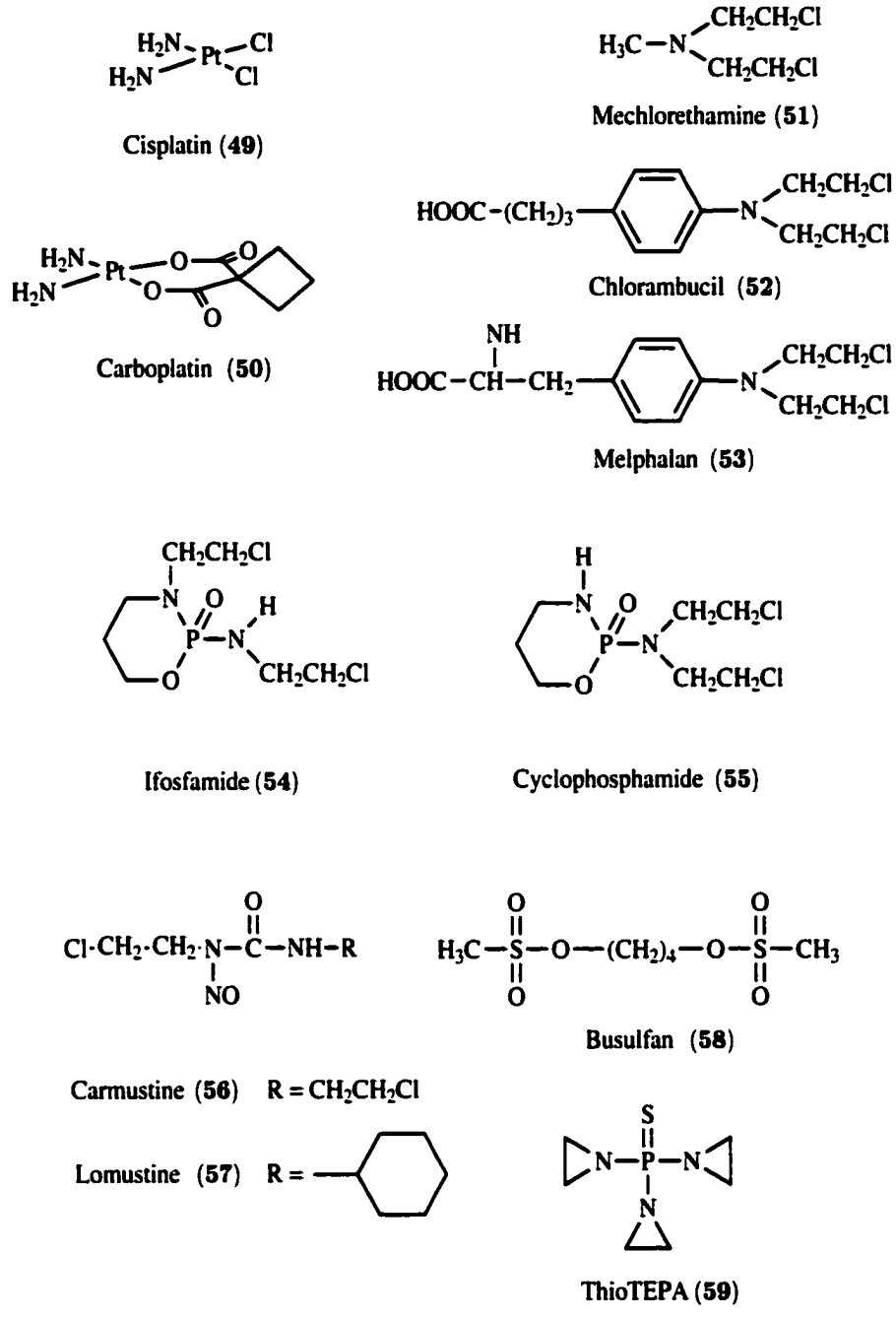

Figure 3.1: Alkylating agents exert their cytotoxic effect on the cell through the formation of covalent bonds with biological macromolecules such as proteins and DNA.

Reproduced with permission of the copyright owner. Further reproduction prohibited without permission.

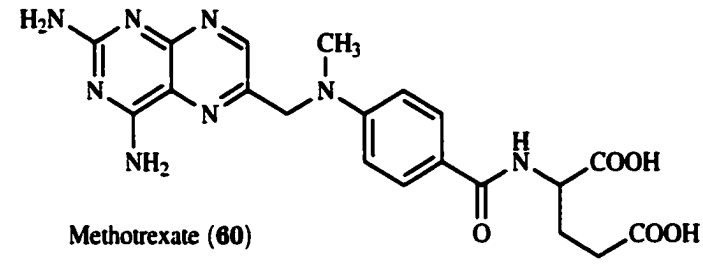

Methotrexate (**60**)

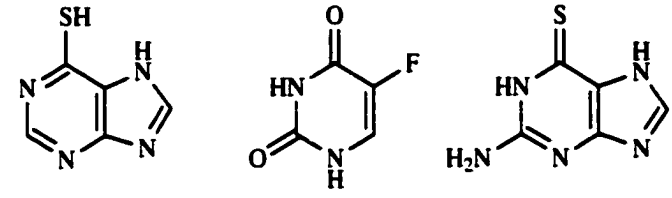

6-Mercaptopurine (**61**) 5-Fluorouracil (**62**) 6-Thioguanine (**63**)

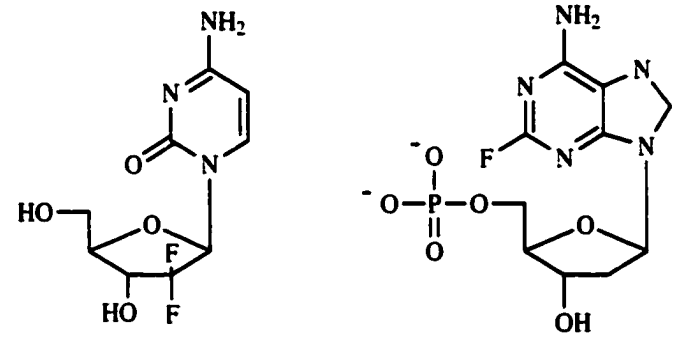

Gemcitabine (**64**) Fludarabine (**65**)

Figure 3.2: The antimetabolites are agents that disrupt the normal metabolism of the cell due to their structural similarity with normal intermediates in the synthesis of precursors of biomolecules such as DNA and RNA.

Antimitotic Agents Vinblastine (**71**), Fig. 3.4, and its analogs have been used in chemotherapy for over three decades [148–150]. These molecules were isolated from the plant *Catharanthus roseus* formerly (*Vinca rosea*) [151–156] commonly known as the Madagascar periwinkle [151–156].

A newer class of drugs is the taxanes, represented in the clinic by paclitaxel (Taxol) (**73**) [157–161] and its semi-synthetic analog docetaxel (Taxotere) (**74**) [162–164] which have recently been approved for the treatment of refractory ovarian, metastatic breast, non-small cell lung, and head and neck cancer [165]. The taxanes are complex

Reproduced with permission of the copyright owner. Further reproduction prohibited without permission.

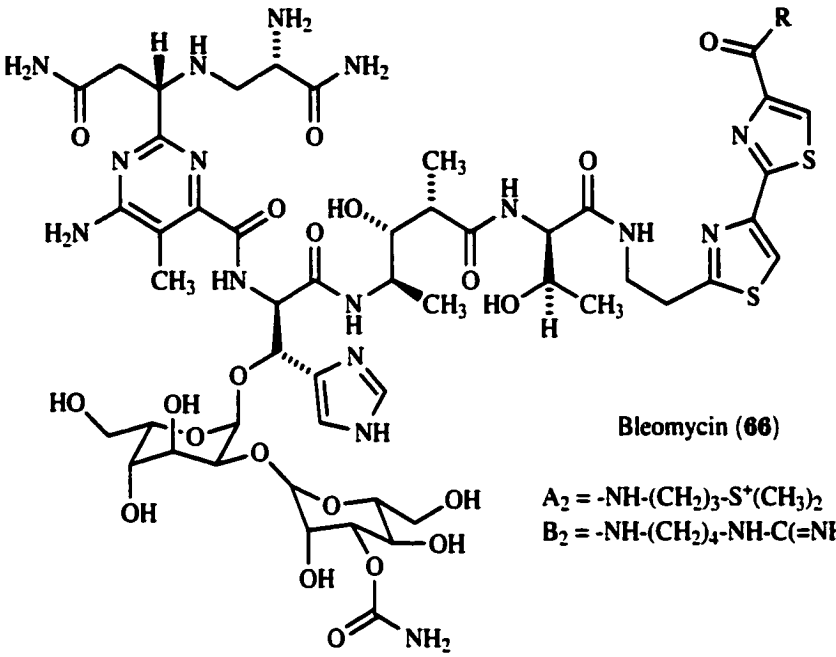

Bleomycin (**66**)

A_2 = -NH-$(CH_2)_3$-$S^+(CH_3)_2$
B_2 = -NH-$(CH_2)_4$-NH-C(=NH)NH_2

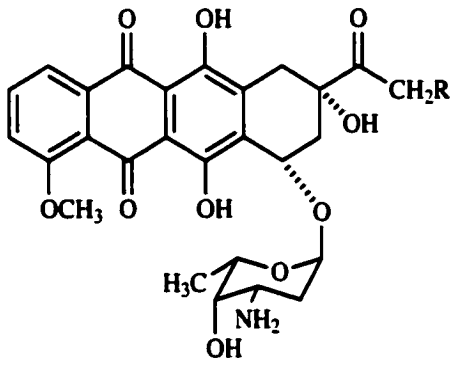

Doxorubicin (**67**) R = OH
Daunorubicin (**68**) R = H

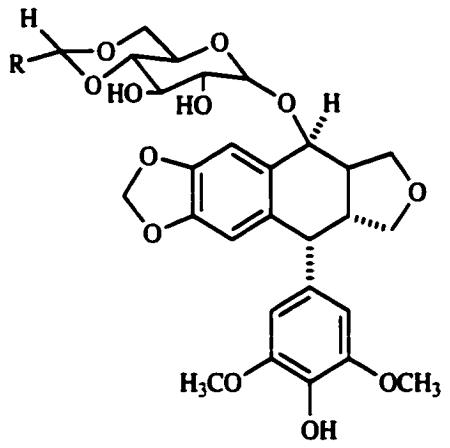

Etoposide (VP-16)(**69**) R = CH_3

Tenoposide (VM-26)(**70**) R =

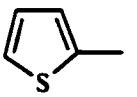

Figure 3.3: Anticancer drugs that bind DNA and RNA through intercalation or inhibit topoisomerase I or II.

Reproduced with permission of the copyright owner. Further reproduction prohibited without permission.

esters, originally isolated from the Pacific Yew, *Taxus brevifolia*, [166]. Paclitaxel (**73**) and its natural analogs have since been found in many members of the *Taxus* family [167] and from an associated fungus, although in small amounts [168]. Although they bind to different sites on tubulin, vinblastine (**71**) and paclitaxel (**73**) are now believed to exert their antimitotic activity through the stabilization of mitotic spindle microtubule dynamics. Ultimately, disruption of mitotic spindle formation leads to mitotic arrest and the inhibition of cell proliferation.

Most of these drugs operate on human cells by interfering in various stages of the cell cycle. Unfortunately, few of the available drugs have clinical antitumor activity against the most common forms of cancer. These poorly responsive cancers are typically comprised of slowly proliferating cells. Most available drugs are effective predominantly against rapidly proliferating tumors and most are therefore toxic to rapidly proliferating normal tissues, such as the bone marrow, the gut endothelium, and hair follicles. Also, tumors that are initially sensitive to a drug often rapidly become resistant, not only to the originally administered drug but frequently also to other antitumor drugs to which resistance may occur by a common mechanism.

Most of the available cytotoxic drugs if administered alone are minimally effective against even the most responsive tumors. Consequently, almost all chemotherapy regimes use combinations of antitumor drugs with the desired antitumor activity, preferably with different mechanisms of action, nonoverlapping toxicities, and no cross-resistance.

Unfortunately, the available cytotoxic drugs are, as a group, relatively similar, both with respect to their spectrum of clinical antitumor activity and toxicity, but also with respect to their mechanism of action. A majority of the current investigational cytotoxic drugs appear to offer few additional prospects for broader clinical antitumor activity or diversity of mechanism of action.

The exceptions are paclitaxel (**73**) and docetaxel (**74**) that are believed to act with a completely unique mechanism of action (see Discussion section). Regardless of their mechanism of action, their favorable pharmacological properties have recently led to their approval as clinical anticancer drugs and these drugs have provided much progress in the treatment of ovarian, breast, and several other cancers [169,170].

Reproduced with permission of the copyright owner. Further reproduction prohibited without permission.

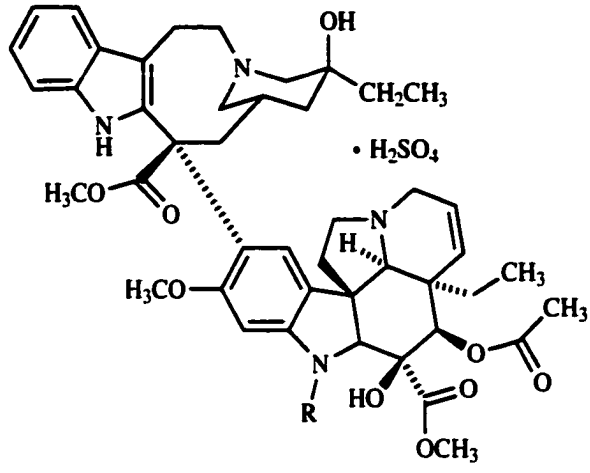

Vinblastine (sulfate) (**71**) R = CH_3
Vincristine (sulfate) (**72**) R = CHO

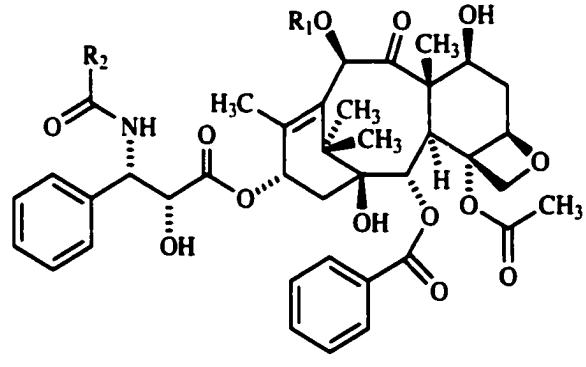

Paclitaxel (Taxol) (**73**) R_1 = $COCH_3$, R_2 = Phe
Docetaxel (Taxotere) (**74**) R_1 = OH, R_2 = O-$C(CH_3)_3$

Figure 3.4: Although they bind to different sites on tubulin, antimitotic anticancer drugs are now believed to exert their antimitotic activity through the stabilization of mitotic spindle microtubule dynamics.

Despite the limitations of the current drugs, the use of existing and investigational anticancer drugs continues to be optimized. However, a major breakthrough in effective cancer chemotherapy will require the discovery and development of completely new anticancer drugs with unprecedented antitumor activities, specificities, and mechanisms of action.

Reproduced with permission of the copyright owner. Further reproduction prohibited without permission.

3.1.2 Anticancer Drug Development

Since the 1950's, anticancer drug discovery and development has been supported significantly by the NCI. The NCI strategies in anticancer drug research and development fall within the four general categories of chance observations, targeted design, analog development and screening [171].

Chance Observations

Some key discoveries in the development of current chemotherapeutic agents, originate from chance observations of toxic effects of certain chemicals on normal tissues or cells and subsequent experimental follow-up. Examples are the nitrogen mustards (**51**)-(**57**), *Vinca* alkaloids (**71**)-(**72**) and cisplatin (**49**), as well as certain discoveries in the development and use of hormonal agents in cancer treatment.

Targeted Design

A few antitumor drugs have actually been designed to interfere with a known essential cellular target. Some examples are the antimetabolites 6-mercaptopurine (**61**), 6-thioguanine (**63**) and 5-fluorouracil (**62**). Our increasing knowledge of the cellular and molecular biology of cell growth and proliferation has offered many potential new targets for drug design and synthesis. In particular, drug are being designed to interrupt intracellular signaling pathways which mediate the effects of growth factors, proto-oncogenes, and tumor-suppressor genes on normal and malignant cell functions. Drug design strategies might, for example, focus on growth-factor receptor blockers [172], inhibitors of oncogene expression (e.g., antisense oligodeoxynucleotides [173–177]), "nonfunctional" synthetic analogs of important intermediates in the signal transduction cascade, or modulators of the activity of the enzymes involved.

An exciting new approach in this area is the design of inhibitors of angiogenesis, the formation of new blood vessels induced by tumors to support their growth. Strategies might for examples focus on matrix metalloproteinase (MMP) inhibitors or inhibitors of angiogenic factors released by the tumor. This approach is outlined in more detail in Chapter IV.

Reproduced with permission of the copyright owner. Further reproduction prohibited without permission.

Analog Development

When a pure compound is discovered that shows an interesting pattern of differential cytotoxicity, a typical next step is the screening of analogs or other related compounds to find the optimal candidates for *in vivo* testing. Analog development involves the synthetic modification of a lead structure with the goal of improving its antitumor properties or pharmacokinetics, or to reduce its toxicity. This offers usually only incremental but useful improvements over the original leads. Very rarely does an analog exhibit a fundamentally different mechanism of action from the parent compound and the majority of the investigational cytotoxic drugs are analogs previously known classes of antitumor compounds.

Screening

The products of chance observations, targeted synthesis, and analog development, are evaluated in screening systems at the molecular, biochemical, and cellular levels, both *in vitro* and *in vivo*. However, the screening of extracts of natural products, is still the most fruitful endeavor for the discovery and identification of new natural product antitumor lead structures. New active compounds can become direct candidates for drug development or can serve as templates for analog synthesis in order to identify better candidates for drug development based on the new lead structure.

From 1955 to 1985, the screening and the selection of compounds for preclinical and clinical development relied predominantly on the NCI's *in vivo* screen using L1210 and P388 murine leukemias and certain other tumor models that were transplantable into mice [171, 178, 179]. This model was used almost exclusively as the primary screen and, with a few exceptions, agents that showed no activity were not selected for further evaluation in additional tumor models or alternative screens [171].

However, the nature of the screening system determines the extent to which new chemotypes will be discovered that differ form the available agents. For this reason a relatively large number of clinically available anticancer drugs shows activity against leukemias and only a subset of solid tumor types. During the 1980's the NCI replaced its *in vivo* leukemia primary screen with a new *in vitro* primary screening model that has been operational since 1990 [171, 179]. The new screen uses sixty human tumor cell

Reproduced with permission of the copyright owner. Further reproduction prohibited without permission.

lines, including drug resistant cell lines, organized into disease-specific subpanels. The subpanels represent diverse histologies such as leukemias, melanomas, and tumors of the lung, colon, kidney, ovary, and brain.

In the sixty cell line primary screen, the growth inhibitory activity of each sample, either a crude extract or a pure compound is tested in a 48 hour, continuous exposure protocol using five concentration values, differing by factors of ten. At the end of the experiment sixty dose-response curves are obtained. The data are usually graphically displayed in the "mean-graph format" [171,178,179] in which three different response levels are displayed, GI_{50}, TGI, and LC_{50}, as calculated from the dose-response curve for each cell line.

These levels are defined in terms of the *percentage growth*

$$PG \equiv 100 \times \frac{N-T}{N-U}, \tag{3.1}$$

where

N = total number of cells in wells (treated or not) *before* incubation,

T = number of cells in treated wells *after* incubation,

U = number of cells in untreated wells *after* incubation.

The fifty-percent growth inhibition level GI_{50} is the drug concentration that results in $PG = 50\%$, *i.e.*, a 50% tumor cell growth inhibition when compared to the untreated control at the *end* of incubation. The total growth inhibition level TGI reflects the cytostatic ability of the drug, or the concentration at which the number of tumor cells remaining at the end of the incubation is the *same* as that at the beginning of the incubation, *i.e.*, $PG = 0\%$. The lethal concentration level LC_{50} is the level that is most clinically relevant. At this concentration, there is a 50% reduction in the number of treated tumor cells in reference to the untreated control at the *start* of the incubation, *i.e.*, $PG = -50\%$.

Thus, the three mean graph profiles provide a characteristic fingerprint for a given compound or extract, with bars projecting to the right indicating more sensitive cell lines and bars projecting to the left less sensitive ones. Over time, the mean graphs have become a significant source of information on the biologic and mechanistic characteristics of antitumor agents. Independent of chemical structure, compounds with a

Reproduced with permission of the copyright owner. Further reproduction prohibited without permission.

similar mechanism of action will show very similar mean graph profiles. On the other hand, compounds (or extracts) that yield a completely novel mean graph pattern, for example a high degree of selectivity for a certain subpanel, are likely to exhibit (or contain compounds that exhibit) a novel mechanism of action. In addition, the selectivity pattern displayed by the mean graph profile and its similarity, or lack thereof, with other anticancer agents, may be used cautiously in predicting the possible outcome of further clinical development of a compound.

The NCI has established a database of mean graph profiles of approximately 175 agents, Table 3.3, on which a considerable amount of information is available about their antitumor properties and mechanism of action. These compounds represent the different biological and mechanistic classes of clinically used antitumor drugs and several other important agents in cancer drug development. The mean graph profile of a newly isolated structure or crude extract can be used as a "seed" in the comparison with the standard agent database using the COMPARE[1] program [171,178,179] and similarity of pattern to that of the seed is expressed quantitatively as a Pearson correlation coefficient (PCC). In general, compounds within the same mechanistic class, Table 3.2, reliably create mean graph patterns that are grouped by COMPARE.

Thus, the NCI primary *in vitro* screen is a useful tool in the discovery of novel lead structures or the development of chemical analogs of existing ones. In addition, the screen can play an important role in the discovery and development of mechanistic analogs, compounds that share a mechanism of action, since such compounds show similar mean graph profiles regardless of their structural relation.

As a mechanistic class, antimitotic agents deserve some special attention. These drugs, Table 3.2, are of considerable interest in cancer drug discovery in general and marine drug discovery in particular [15, 180] since they, as a group, have provided a reliable source of clinical antitumor activity. The NCI's sixty cell line primary screen can recognize the class of antimitotic agents by their very similar mean graph profiles and thus their mechanistic similarity. It cannot however differentiate among individual members of the class, because although they represent different sites of interaction with tubulin or microtubules, they may not represent fundamentally different mechanistic

[1]See NCI website http://dtp.nci.nih.gov

Reproduced with permission of the copyright owner. Further reproduction prohibited without permission.

Table 3.3: NCI Standard Anticancer Agent Database.

ARA AC	Dichloroallyl lawsone	Nitroestrone
ARA-6-MP	Didemnin B (**11**)	Nitrogen mustard
AZQ	Diglycoaldehyde	Nitroimidazole)
Acivicin	Dihydro-5-azacytidine	O6-Methylguanine
Aclacinomycin A	Dihydrolenperone	Oxanthrazole
Acodazole HCl	Doxorubicin (**67**)	PALA
Actinomycin	Echinomycin	PCNU
Amonafide	Emofolin sodium	Pancratiastatin
Amsacrine	Etoposide (VP-16) (**69**)	Penclomedine
Anguidine	Flavoneacetic acid	Pentamethylmelamine
Anthrapyrazole	Flavoneacetic acid ester	Phyllanthoside
Aphidicolin glycinate	Fludarabine (**65**)	Pibenzimol hydrochloride
Asaley	Fluorodopan	Piperazine alkylator
L-Asparaginase	5-Fluorouracil (**62**)	Piperazinedione
5-Azacytidine	Fostriecin	Pipobroman
5-Azadeoxycytidine	Ftorafur	Porfiromycin
Bactobolin	5-FUDR	Procarbazine
Batracylin	Gallium nitrate	Pyrazine diazohydroxide
Bisantrene HCl	Glycoxalic acid	Pyrazofurin
Bispyridocarbazolium DMS	Guanazole	Pyrazoloacridine
Bleomycin (**66**)	HMBA	Pyrimidine-5-glycodialdehyde
Brequinar	Hepsulfam	Pyrrolizine dicarbamate
Bruceantin	Hexamethylenemelanime	R-Methylformamide
Bryostatin 1 (**2**)	Homoharringtonine	Rapamycin
Busulfan (**58**)	3-HP	Rhizoxin
CHIP	5-HP	Rifamycin SV
Caracemide	Hycanthone	Rubidazone
Carboplatin (**50**)	Hydrazine sulfate	S-Trityl-L-cysteine
(Carboxyphthalato)Pt	Hydroxyurea	Spirogermanium
Carmethizole	ICRF-1	Spirohydantoin mustard
Carmustine (**56**)	ICRF-159	Streptozoticin
Chlorambucil (**52**)	IMPY	Tamoxifen
Chlorozotocin	Ifosfamide (**54**)	Taxol (Paclitaxel) (**73**)
Chromomycin A3	Indicine N-oxide	Teniposide (VM-26) (**70**)
Cisplatin (**49**)	4-Ipomeanol	Teroxirone
Cl-Quinoxaline sulfonamide	L-Alanosine	δ-1-Testololactone
Clomesone	L-Buthionine sulfoximine	Tetraplatin
Cyanomorpholino-ADR	L-Cysteine analogue	Tetrocarcin A sodium salt
8Cl-Cyc-AMP	Largomycin	α-TGDR
Cyclocytidine	Lomustine (**57**)	β-TGDR
Cyclodisone	MX2 HCl	Thalicarpine
Cyclopentenylcytosine	Macbecin II	Thiadiazole
Cyclophosphamide (**55**)	Maytansine	6-Thioguanine (**63**)
Cytembena	Melphalan (**53**)	Thio-TEPA (**59**)
Cytosine arabinoside	Menogaril	Thymidine
D-Tetrandrine	Merbarone	Tiazofurin
DON	6-Mercaptopurine (**61**)	Topotecan
DTIC	Methotrexate (**60**)	Triazinate
Daunorubicin (**68**)	Methyl-CCNU	Triciribine phosphate
o,p'-DDD	Methyl-GAG	Triethylenemelamine
2'-Deoxycoformycin	Mitindomide	Trimethyl TMM
Deoxydoxorubicin	Mitomycin C	Trimetrexate
Deoxyspergualin	Mitoxantrone	Uracil mustard
3-Deazaguanine	Mitozolamide	Vinblastine (sulfate) (**71**)
3-Deazauridine	Mitramycin	Vincristine (sulfate) (**72**)
Dianhydrogalatitol	Morpholino-ADR	Yoshi-864
N,N-Dibenzyldaunomycin	Neocarzinostatin	

Reproduced with permission of the copyright owner. Further reproduction prohibited without permission.

classes (see Discussion section in this Chapter).

Five known antitubulin agents are in the standard agent database. These are vinblastine (**71**), vincristine (**72**), maytansine, rhizoxin, and paclitaxel (**73**). COMPARE analyses using any of the five tubulin agents will give the other four tubulin agents as the closest matches, followed by compounds with no known mechanistic similarity.

3.1.3 Mechanism of Action of Diazonamide A, a Novel Antimitotic Agent

The diazonamides A-D (**75**)-(**78**) were originally isolated by Lindquist et al. [2, 3] as the secondary metabolites of the Philippine ascidian *Diazona chinensis*, later correctly identified as *Diazona angulata* (phylum Chordata, subphylum Urochordata, class Ascidiacea, order Phlebobranchia)[2]. Sufficient material was obtained to elucidate their unusually complex structures and to identify their potent *in vitro* cytotoxic activities against the human colon adenocarcinoma HCT 116 and B-16 murine melanoma (IC_{50} less than 15 ng/mL). However, no material was available for further study of their promising pharmacological properties.

In spite of numerous efforts toward the synthesis of the diazonamides [181–186], the compounds remained unavailable until 1997 when, as part of an NCI collecting program in the Philippines, *Diazona angulata*, Fig. 3.6, was re-discovered. The crude organic extract of one out of seven recollected specimens entered the NCI's sixty cell line *in vitro* cytotoxicity test. The selectivity pattern of this specimen, Fig. 3.7, was computer analyzed and compared with those in the NCI anticancer standard database Table 3.3. Pearson correlation coefficients (PCCs) of 0.816 and 0.915 with paclitaxel (**73**) and vinblastine (**71**), respectively, were observed (Table 3.4). From this specimen 7.0 mg diazonamide A (**75**), the major metabolite and the most potent among the diazonamides, was re-isolated and the selectivity pattern of the pure compound, Fig. 3.8 again showed a high degree of similarity with that of paclitaxel (**73**) and vinblastine (**71**) (PCCs of 0.618 and 0.696, respectively) and other antimitotic agents (Table 3.5).

The following sections describe the first studies towards identifying the antim-

[2]The animal was originally identified as *Diazona chinensis* but was later reassigned as *D. angulata* by Dr. Françoise Monniot, Muséum National d'Histoire Naturelle, Laboratoire de Biologie des Invertébré Marins et Malacologie, Paris, France

Reproduced with permission of the copyright owner. Further reproduction prohibited without permission.

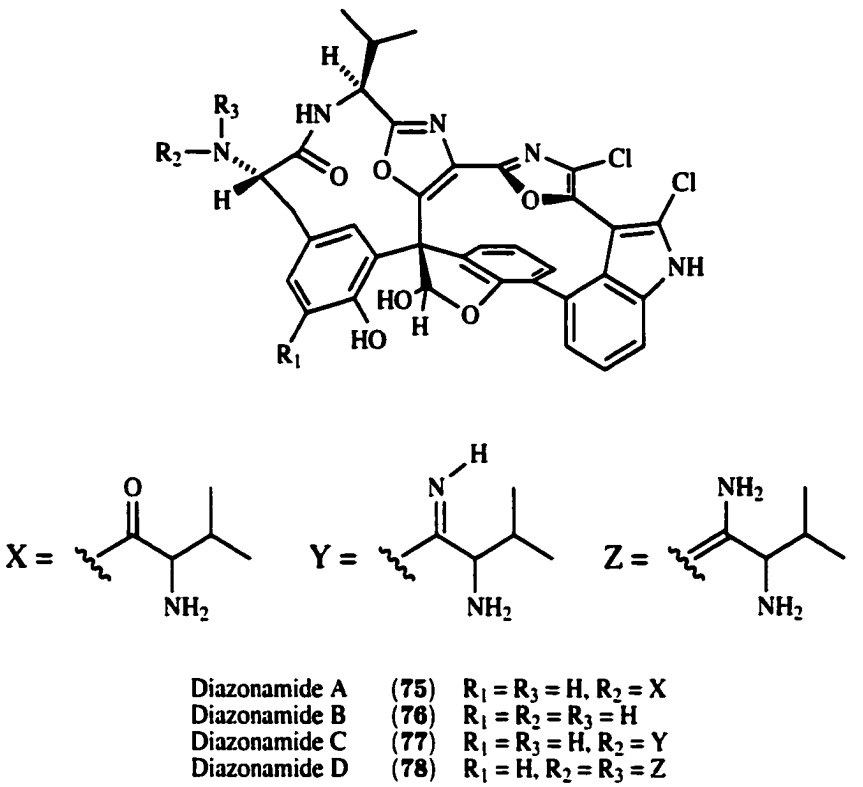

Figure 3.5: The diazonamides A-D (**75–78**), originally isolated from *Diazona angulata* [2,3].

Table 3.4: COMPARE results. Seed: Organic crude of *Diazona angulata*

GI_{50}		TGI		LC_{50}	
Compound	PCC	Compound	PCC	Compound	PCC
Vinblastine (**71**)	0.915	Vinblastine (**71**)	0.802	Maytansine	0.771
Paclitaxel (**73**)	0.816	Rhizoxin	0.753	Vinblastine (**71**)	0.739
MDR	0.783	Maytansine	0.743	Vincristine (**72**)	0.685
MDR	0.746	Paclitaxel (**73**)	0.647	β-TGDR	0.618
Maytansine	0.682	Vincristine (**72**)	0.610	6-Thioguanine (**63**)	0.591
Neocarzinostatin	0.622	S-trityl-L-cysteine	0.601	α-TGDR	0.577
S-trityl-L-cysteine	0.662	MDR	0.524	Rhizoxin	0.577
Vincristine (**72**)	0.616	5-Azadeoxycytidine	0.450	Bactobolin	0.530
Actinomycin	0.571	Neocarzinostatin	0.397	Tetraplatin	0.523
Bisantrene	0.554	Iproplatin	0.379	Oxanthrazole	0.509
Triazinate	0.533	Phyllanthoside	0.374	(Carboxyphthalato)Pt	0.477

itotic mechanism of action of diazonamide A (**75**). The work reported here shows that this highly modified bicyclic peptide is a potent inhibitor of cell proliferation, induces

Reproduced with permission of the copyright owner. Further reproduction prohibited without permission.

Table 3.5: COMPARE results. Seed: Diazonamide A (**75**)

GI_{50}		TGI		LC_{50}	
Compound	PCC	Compound	PCC	Compound	PCC
Vinblastine (**71**)	0.696	Vinblastine (**72**)	0.679	Mitindomide	0.992
Maytansine	0.622	Maytansine	0.615	Tetraplatin	0.961
Paclitaxel (**73**)	0.618	Vincristine (**72**)	0.610	5-FUDR	0.929
Vincristine (**72**)	0.598	Rhizoxin	0.593	L-Alanosine	0.815
Bis-pyridocarbazolium DMS	0.585	α-TGDR	0.560	Cisplatin (**49**)	0.791
Rhizoxin	0.580	Pibenzimol HCl	0.547	Topo1A	0.782
S-trityl-L-cysteine	0.430	Macbecin II	0.531	Dichloroally lawsone	0.780
Triazinate	0.390	Paclitaxel (**73**)	0.509	β-TGDR	0.764
Didemnin B (**11**)	0.388	Tetraplatin	0.464	Yoshi-864	0.707
Triazinate	0.368	6-Thioguanine (**63**)	0.407	(Carboxyphthalato)Pt	0.701
Macbecin II	0.359	Triazinate	0.402	Oxanthrazole	0.679

mitotic arrest, and inhibits the functioning of cellular microtubules and mitotic spindles in a manner analogous to vinblastine (**71**).

Reproduced with permission of the copyright owner. Further reproduction prohibited without permission.

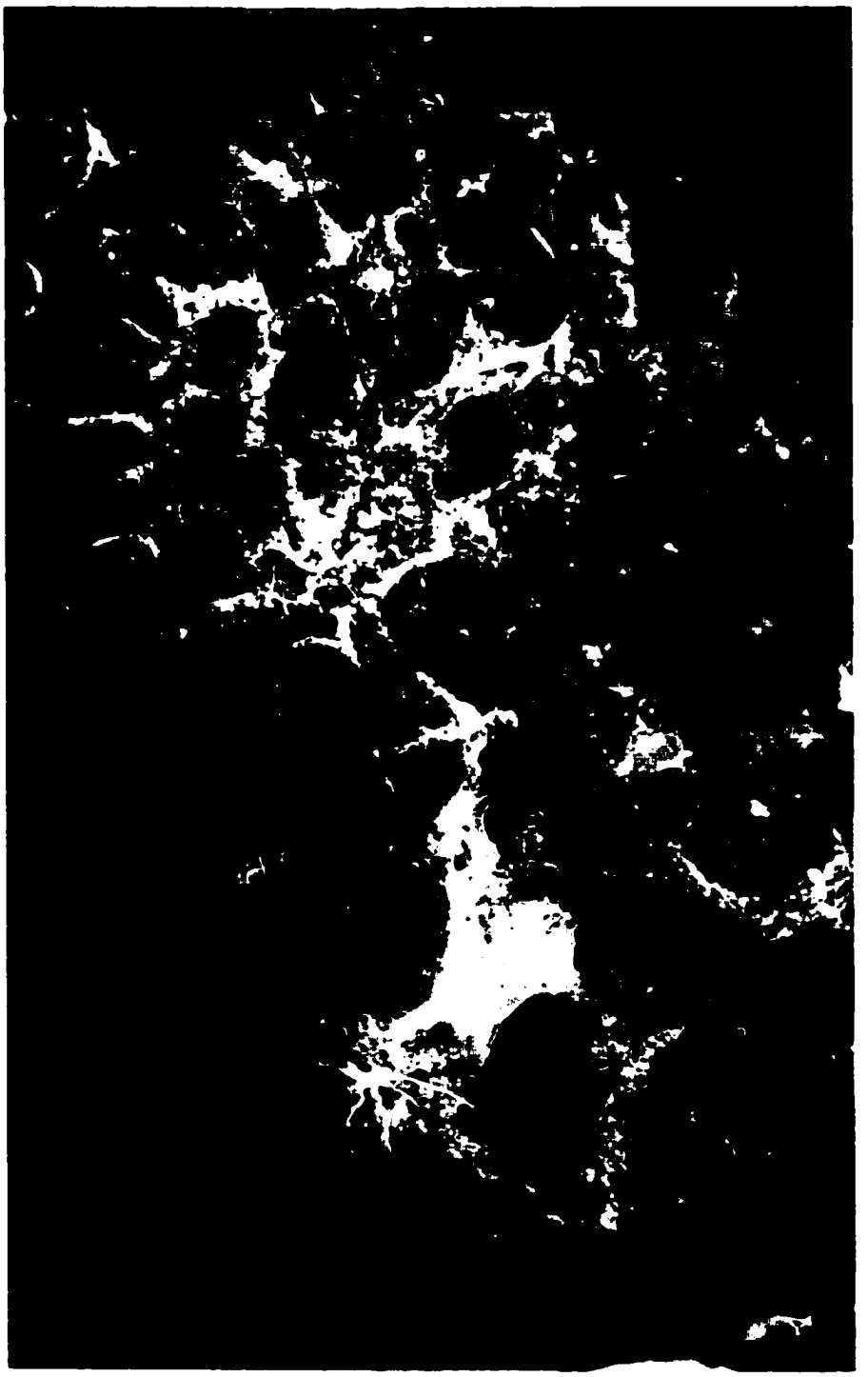

Figure 3.6: *Diazona angulata* (order Phlebobranchia, family Cionidae) from which diazonamide A (**75**) was re-isolated (Photograph by Pat Collins, NCI).

Reproduced with permission of the copyright owner. Further reproduction prohibited without permission.

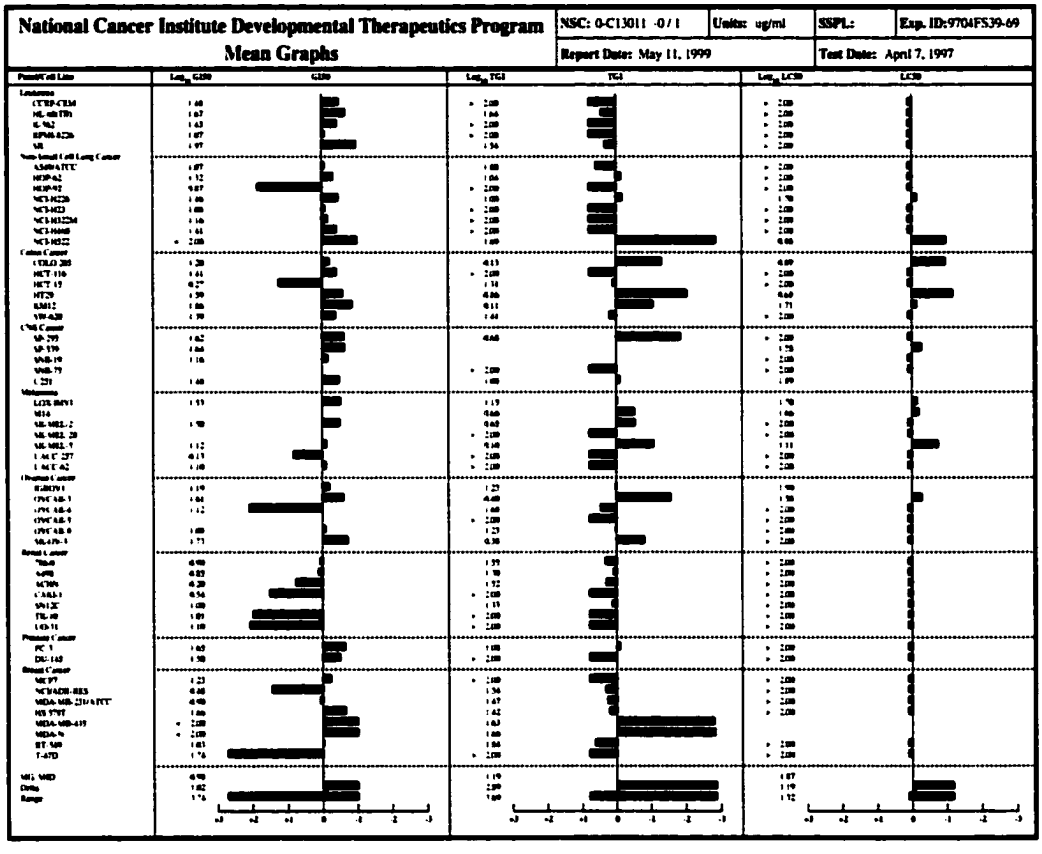

Figure 3.7: GI_{50}, TGI, and LC_{50} mean-graph profiles for the crude organic extract of a *Diazona angulata* specimen. The selectivity profile shows a high degree of similarity with that of antimitotic agents such as vinblastine (**71**) and paclitaxel (**73**), as was determined by the COMPARE program (See Table 3.4).

Reproduced with permission of the copyright owner. Further reproduction prohibited without permission.

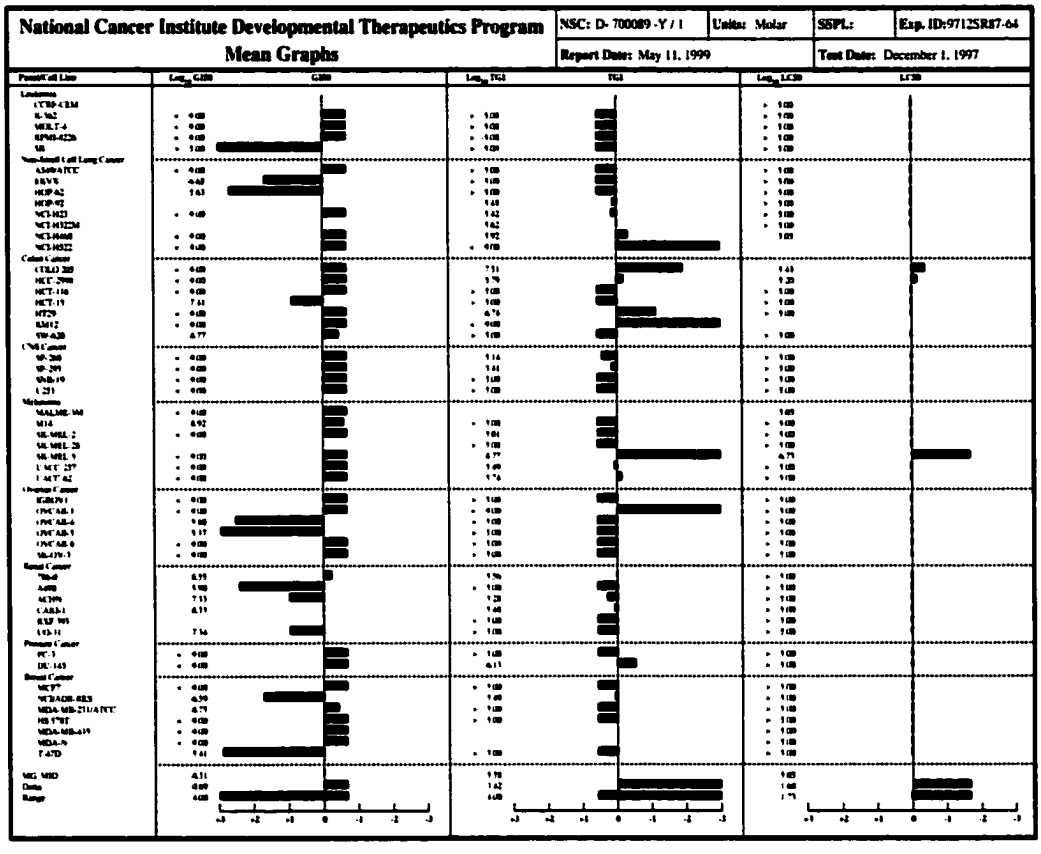

Figure 3.8: GI_{50}, TGI, and LC_{50} mean-graph profiles for diazonamide A (**75**). The selectivity profile shows a high degree of similarity with that of antimitotic agents such as vinblastine (**71**) and paclitaxel (**73**), as was determined by the COMPARE program (See Table 3.5).

Reproduced with permission of the copyright owner. Further reproduction prohibited without permission.

3.2 Materials and Methods

3.2.1 Drugs and Chemicals

The following compounds were obtained from the indicated sources: Vinblastine (sulfate) (**71**) solution (1.0 mg/mL in H_2O) was obtained from the UCSD Medical Center. Paclitaxel (**73**) (5 mg), the monoclonal mouse β-tubulin antibody (T-4026) and the FITC-labeled goat anti-mouse IgG antibody (F-3008) were obtained from Sigma Chemical Co., St. Louis, MO. Propidium iodide (P-3566) was obtained from Molecular Probes, Eugene, OR. DNAse-free RNAse was obtained from Sigma Chemical Co., boiled for 15 min. (10 mg/mL in Tris buffer tablet pH 7.6 (T-5030, Sigma Chemical Co.)) and cooled to room temperature before use. Stock solutions of paclitaxel (**73**), diazonamide A (**75**) and vinblastine (**71**) were maintained at -20°C in water and/or dilute DMSO.

3.2.2 Ascidian Collection and Identification

The ascidian was collected in the Philippines with the assistance of Pat Colins and Dr. David Newman of the National Cancer Institute. Seven specimens were recollected and immediately frozen until used.

3.2.3 Isolation and Purification of Diazonamide A

After collection, the seven *D. angulata* specimens were deep frozen at -20°C within three hours of collection, all the time being kept in seawater. Of each specimen, crude organic and aqueous axtracts were prepared at the NCI, as described below.

The frozen material was broken in the presence of crushed dry ice by passage through a grinder. The crushed mass was held at -20°C for two to three days until the dry ice had sublimed and the broken material was stirred with ~1 L of deionized water at 4°C for 30 minutes. The supernatant solution was removed from the pellet by means of a basket centrifuge and the aqueous solution was lyophilized. The remaining pellet was extracted at room temperature with a 50:50 v/v mix of methanol:methylene chloride, for 6 to 8 hours. The solution was removed by vacuum filtration, the pellet washed with approximately 10% of pellet volume of methanol, and all organic solutions were reduced to dryness at less than 30°C, followed by high vacuum drying overnight at

Reproduced with permission of the copyright owner. Further reproduction prohibited without permission.

room temperature.

The organic and aqueous extracts of the seven specimens were obtained from the NCI and tested in an *in vitro* cytotoxicity assay employing the HCT 116 human colon adenocarcinoma cell line. The organic crude extracts showed potent growth inhibition whereas the aqueous extracts showed no activity.

The organic crude (900 mg) of one specimen was fractionated using Sephadex LH-20 with a mixture of isooctane/methanol/toluene (3:1:1) and 7 mg of pure diazonamide A (**75**) was isolated from three of the obtained fractions using reversed phase (C_{18}) HPLC using 12% water in MeOH.

The organic fractions of the remaining six specimens were combined (3.18 grams) based on ^{1}H NMR spectral features and *in vitro* cytotoxicity data using the human colon adenocarcinoma cell line HCT 116, and the combined crude was fractionated between methanol and isooctane. The methanol fraction (2.36 grams) was partitioned between water and butanol. The butanol fraction (1.22 grams) was fractionated over Sephadex LH-20 using isooctane/methanol/toluene (3:1:1). Fractions containing diazonamides A-D (**75**)-(**78**), by ^{1}H NMR analysis were combined and separated over Sephadex LH-20 in 100% methanol. Diazonamide A (**75**) (20.0 mg) was purified by reversed phase (C_{18}) HPLC using 26% water in MeOH. The compound was dissolved in DMSO and stored at -20°C.

3.2.4 Cell Culture

The parental 2008 human ovarian carcinoma cell line used in these studies was maintained in tissue culture flasks in a humidified incubator at 37°C and 5% CO_2 atmosphere. Cells were maintained in complete medium consisting of RPMI 1640 supplemented with 5% heat-inactivated fetal bovine serum, 2 mM L-glutamine, 200 units/mL penicillin and 200 μg/mL streptomycin.

3.2.5 Inhibition of Cell Proliferation

The concentration dependence for inhibition of proliferation of 2008 human ovarian carcinoma cells by diazonamide A (**75**), paclitaxel (**73**), and vinblastine (**71**) was measured using colony-forming assays. Two hundred cells suspended in 3 ml medium

Reproduced with permission of the copyright owner. Further reproduction prohibited without permission.

were seeded per well in plastic 6-well plates (Corning Glass Works, Corning, NY). The cells were allowed to attach for 8-12 hours prior to drug addition and then treated with varying concentrations of paclitaxel (**73**), vinblastine (**71**) or diazonamide A (**75**). The plates were incubated at 37°C for 7-10 days, at which time the medium was aspirated and the cells were fixed with ethanol vapor. The colonies were stained with Trypan Blue Stain 0.4%, and scored. Survival as a function of concentration was expressed as a percentage of the number of control colonies. The experiments were run in triplicate and IC_{50} values were calculated for all drugs drug.

3.2.6 Cell Cycle Analysis

Cells of the 2008 human ovarian carcinoma line were grown in 10 ml complete medium (RPMI 1640) supplemented with 5% heat-inactivated fetal bovine serum, 2 mM L-glutamine, 200 units/mL penicillin and 200 μg/mL streptomycin in plastic tissue culture dishes to a density of approximately 2×10^6 cells per dish. The cells were treated with 40 nM paclitaxel (**73**), 10 nM vinblastine (**71**), 40 nM diazonamide A (**75**) or vehicle alone for the times indicated. Cells were harvested by brief trypsinization (10 min.), washed three times with ice cold PBS and fixed in ice cold 100% ethanol. Cells were kept at 4°C for up to 5 days prior to analysis. The cells were counted, 10^6 cells were resuspended in 300 μL ice cold PBS, treated with RNAse at 1.0 mg/mL (20-30 min. at 37°C) and stained with propidium iodide (50 μg/mL at 0°C) for a minimum of 30 min. before analysis. DNA content was measured using a FACScan (Becton-Dickinson Immunocytometry Systems (San Jose, CA)). The DNA cell cycle was analyzed with a Phoenix Flow Systems (San Diego, CA) MultiCycleAV software. The proportion of cells in G_0-G_1, S, and G_2-M phases, as well as apoptotic cells were estimated from their histograms using CELLQuest software.

3.2.7 Mitotic Index Determination

Cells of the 2008 human ovarian carcinoma line were seeded in 10 mL tissue culture dishes containing 2 cover slips (0.17 mm thickness) per dish. Cells were grown to approximately 2×10^6 cells per dish, then treated with 40 nM paclitaxel (**73**), 10 nM vinblastine (**71**), 40 nM diazonamide A (**75**) or vehicle. At the indicated times, cover

Reproduced with permission of the copyright owner. Further reproduction prohibited without permission.

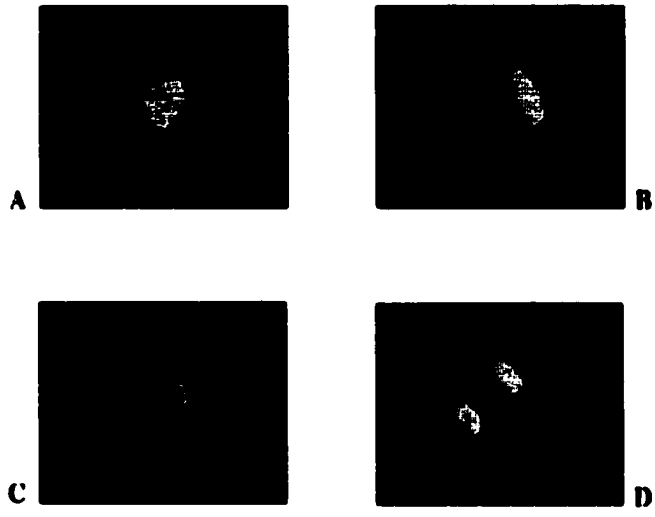

Figure 3.9: Mitotic 2008 human ovarian carcinoma cells, indicating (A) prophase, (B) metaphase, (C) anaphase, and (D) telophase.

slips were removed, fixed in a solution containing 3.7% formaldehyde, 0.5% Nonidet P-40, and Hoechst 33258 (10 μg/mL) in PBS. Cells were visualized by fluorescence microscopy. They were scored as mitotic when they were rounded and the nuclear membrane had disappeared. In such cells, condensed evenly staining chromosomes could be seen, indicating prophase, metaphase, anaphase, or telophase Fig. 3.9. At least 300 cells were counted for each determination.

3.2.8 Indirect Immunofluorescence

Cells of the 2008 human ovarian carcinoma line were grown in 10 mL complete medium to approximately 80% confluence in 4 plastic tissue culture plates containing three cover slips per plate. The coverslips were transfered to 2 six-well plates and treated for 24 hours with varying concentrations (100 nM, 1 μM) of paclitaxel (**73**), vinblastine (**71**), diazonamide A (**75**) or vehicle. Cells were fixed in 3.7% formaldehyde with 0.1% Nonidet P-40 for 30 min, plunged into -20°C methanol for 10 min, and incubated for 2 hours with 20 μL undiluted mouse β-tubulin antibody. After a series of washes with PBS, the cells were incubated for several hours with fluorescein isothiocyanate (FITC)-conjugated sheep anti-mouse IgG (dilution 1/100). The coverslips were washed, air-

Reproduced with permission of the copyright owner. Further reproduction prohibited without permission.

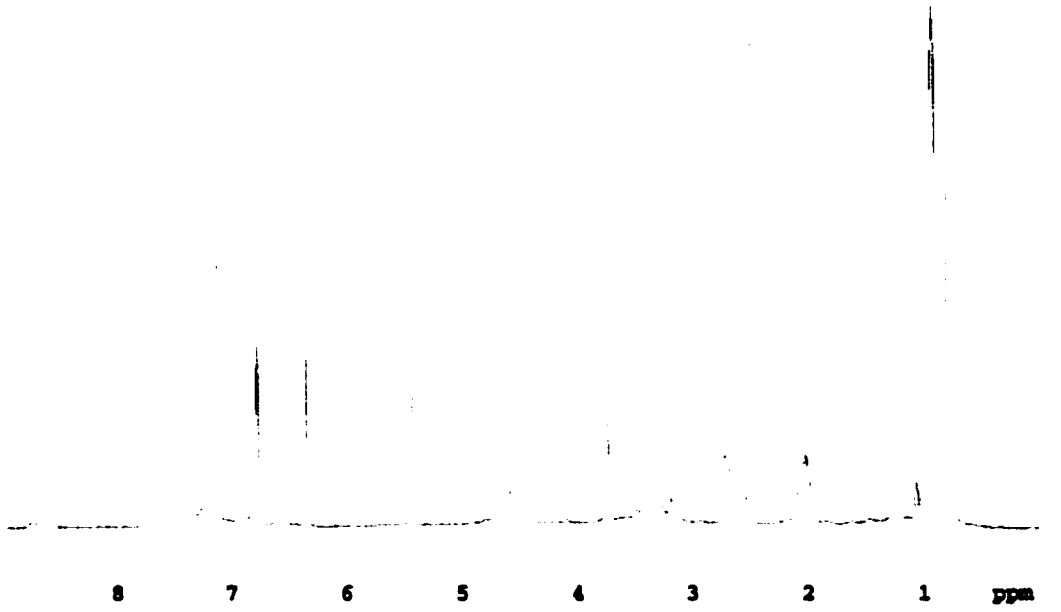

Figure 3.10: ^{1}H NMR spectrum of diazonamide A (**75**) (DMSO-d_6, 300MHz).

dried, and mounted using 90% glycerol in PBS with 1 mg/mL *p*-phenylenediamine. Cellular microtubules were visualized using a Nikon fluorescence microscope with optics for fluorescein.

3.3 Results

3.3.1 Isolation and Purification of Diazonamide A

Diazonamide A (**75**) was isolated as a tan-colored, amorphous solid. Its ^{1}H NMR spectrum at 300 MHz in MeOH was identical to that reported in the literature. A ^{1}H NMR spectrum of diazonamide A (**75**) in DMSO is shown in Fig. 3.10.

Reproduced with permission of the copyright owner. Further reproduction prohibited without permission.

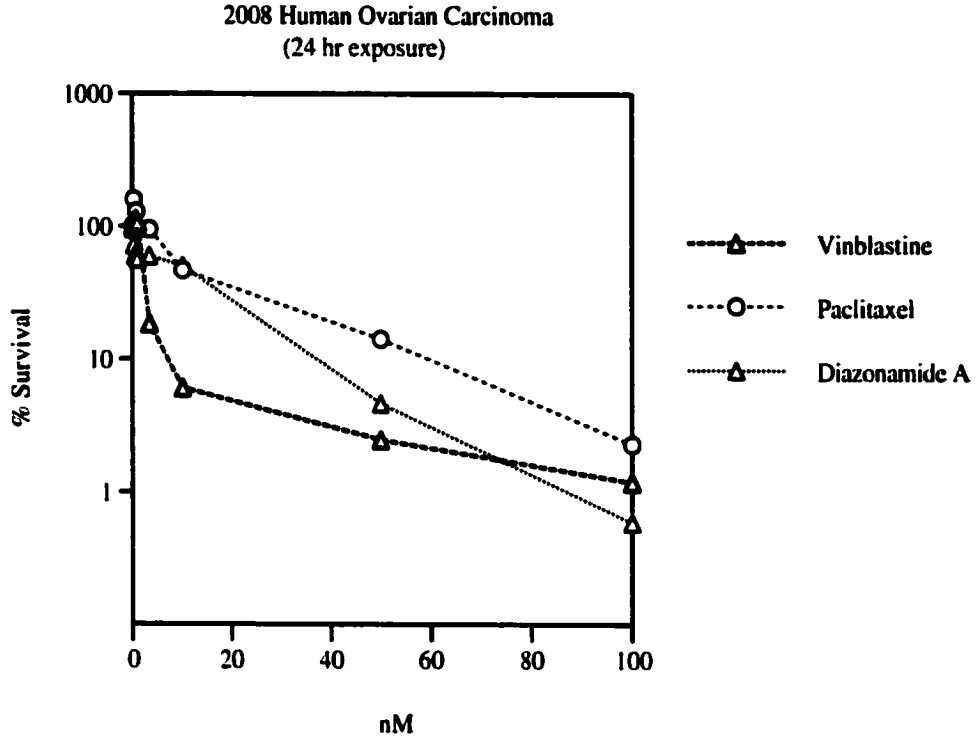

Figure 3.11: Clonogenic (colony forming) assays show that diazonamide A (**75**), paclitaxel (**73**), and vinblastine (**71**) inhibit proliferation of 2008 human ovarian carcinoma cells in a concentration-dependent manner.

3.3.2 Cell Proliferation

Diazonamide A (**75**), paclitaxel (**73**), and vinblastine (**71**) inhibited proliferation of 2008 human ovarian carcinoma cells in a concentration-dependent manner. The cytotoxic potencies of the three drugs differed less than an order of magnitude. The obtained dose-response curves for the three drugs are shown in Fig. 3.11 and the IC_{50} values are summarized in Table 3.6.

3.3.3 Cell Cycle Progression

Treatment of 2008 human ovarian carcinoma cells with diazonamide A (**75**), paclitaxel (**73**), or vinblastine (**71**) for up to 96 hours, caused an increase in G_2-M phase cells at concentrations of 10 nM, 10 nM and 4 nM respectively, Fig. 3.12-Fig. 3.14. The effect was most pronounced after 24 hrs.

Reproduced with permission of the copyright owner. Further reproduction prohibited without permission.

Table 3.6: IC_{50} values for Diazonamide A (**75**), Paclitaxel (**73**), and Vinblastine (**71**), determined by clonogenic (colony forming) assays using 2008 human ovarian carcinoma cells

Compound	nM
Diazonamide A (**75**)	10.0
Paclitaxel (**73**)	9.6
Vinblastine (**71**)	2.5

3.3.4 Mitotic Index

Cells of the 2008 human ovarian carcinoma cell line were grown on glass coverslips and treated with vehicle (0.01% DMSO), 40 nM diazonamide A (**75**), 10 nM vinblastine (**71**), or 40 nM paclitaxel (**73**). The doses of all three drugs correspond to approximately 4 times the IC_{50} values for this cell line. Morphological examination revealed that at least 97% of the untreated cells were in interphase throughout the duration of the experiment, Fig. 3.15. Treatment with vinblastine (**71**) resulted in a sharp increase in the number of cells in mitosis over the first 12 hours of the experiment to almost 30%, followed by a decline of the mitotic figure to an average of 8% over the remainder of the experiment. Diazonamide A (**75**) showed a similar pattern, although the mitotic index peaked at 12 hours at about 20%, then leveled off at about 6% at t=48 hrs. Paclitaxel (**73**) also induced an increase in mitotic index to approximately 12% over the first 12 hours and fluctuated around 7% after 48 hours. The cells blocked in mitosis under the influence of the three drugs were rounded with highly condensed round masses of chromatin, resembling most closely prophase since no formation of the metaphase plate seemed to take place Fig. 3.9.

3.3.5 Cellular Microtubule Structure

The ability of diazonamide A (**75**) to initiate microtubule changes coincident with mitotic arrest was studied by immunofluorescence techniques. Fig. 3.16 A shows control cells with normal interphase microtubule networks and cells in mitosis with normal bipolar mitotic spindles. As can be seen in Fig. 3.16 B and C, treatment of 2008 human ovarian carcinoma cells with diazonamide A (**75**) resulted in the disappearance

Reproduced with permission of the copyright owner. Further reproduction prohibited without permission.

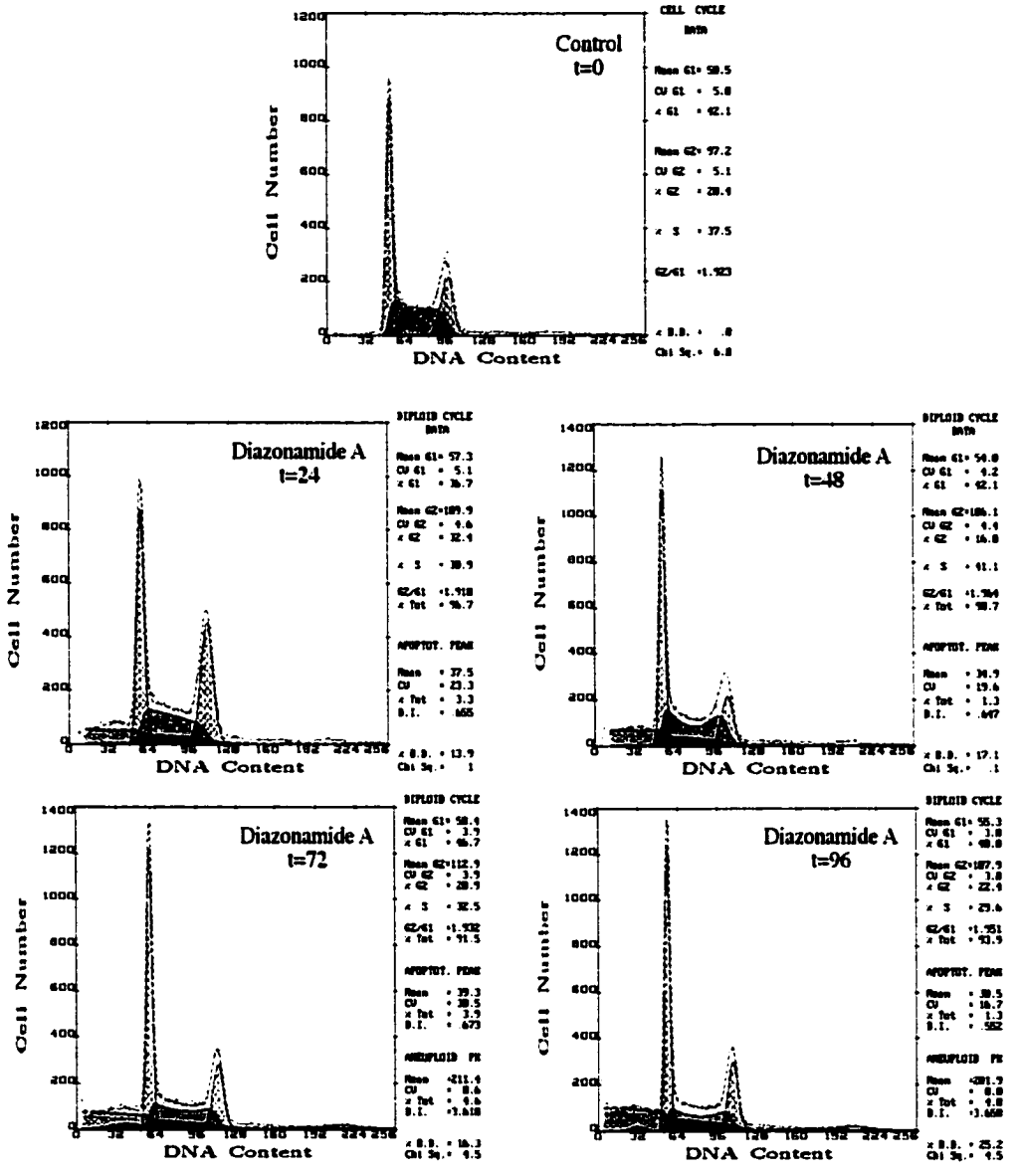

Figure 3.12: Flow cytometric analysis reveals that treatment of 2008 human ovarian carcinoma cells with 40 nM diazonamide A (**75**) results in an increase in the number of cells in the G_2-M phase of the cell cycle. The effect is most pronounced after 24 hours.

of microtubules at concentrations of 100 nM and 1 μM. At the highest concentration, 1 μM Fig. 3.16 C, the formation of some amorphous aggregates of tubulin in the periphery of the cell can be observed. At both concentrations, diazonamide A (**75**) caused mitotic block in over 95% of the cells, with no visibly staining microtubules in the remaining interphase cells.

Reproduced with permission of the copyright owner. Further reproduction prohibited without permission.

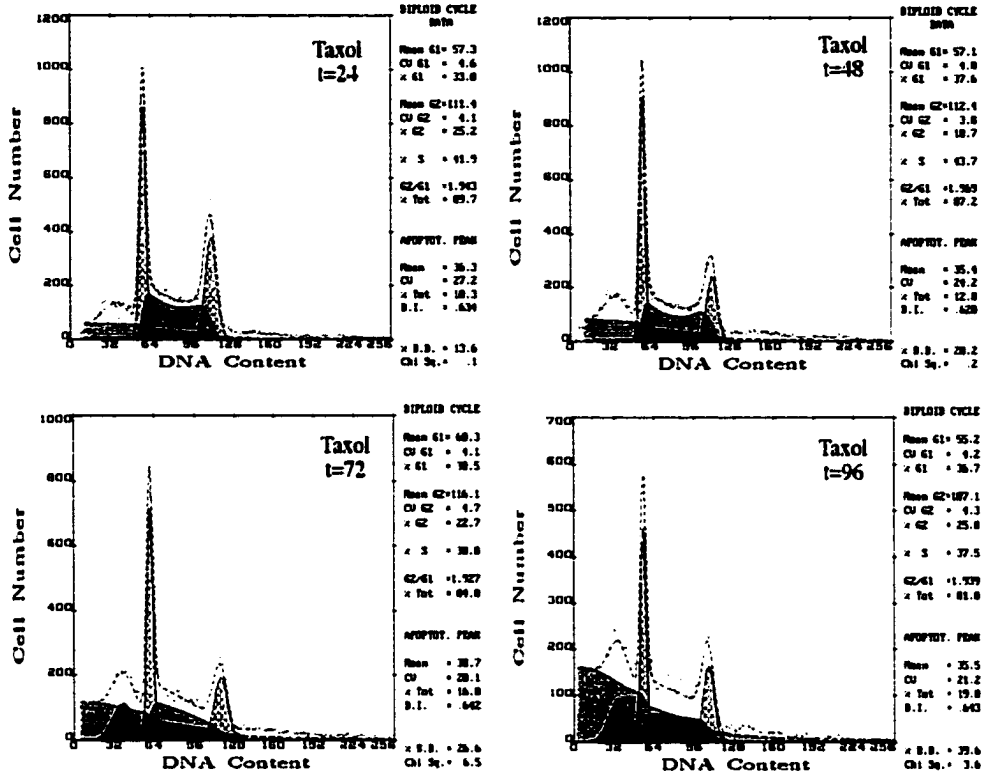

Figure 3.13: Flow cytometric analysis of 2008 human ovarian carcinoma cells treated with 40 nM paclitaxel (**73**) results in an increase in the number of cells in the G_2-M phase of the cell cycle. The effect is most pronounced after 24 hours.

Treatment of cells with paclitaxel (100 nM, Fig. 3.16 D) resulted in the formation of more intensely staining microtubules, although no microtubule bundling was observed. At higher concentrations of paclitaxel (1 μM, Fig. 3.16 E), tubulin asters formed in the mitotic cells and the few interphase cells appeared apoptotic with no visibly staining microtubules.

Treatment with vinblastine (**71**) on the other hand resulted in the disappearance of microtubules at the lower concentration of 100 nM, Fig. 3.16 F) and the formation of several large paracrystals of tubulin in mitotic cells at high concentration (1 μM, Fig. 3.16 G). Over 95% of the cells appeared mitotic at 100 nM and 1 μM, with no visibly staining microtubules in the remaining interphase cells.

Reproduced with permission of the copyright owner. Further reproduction prohibited without permission.

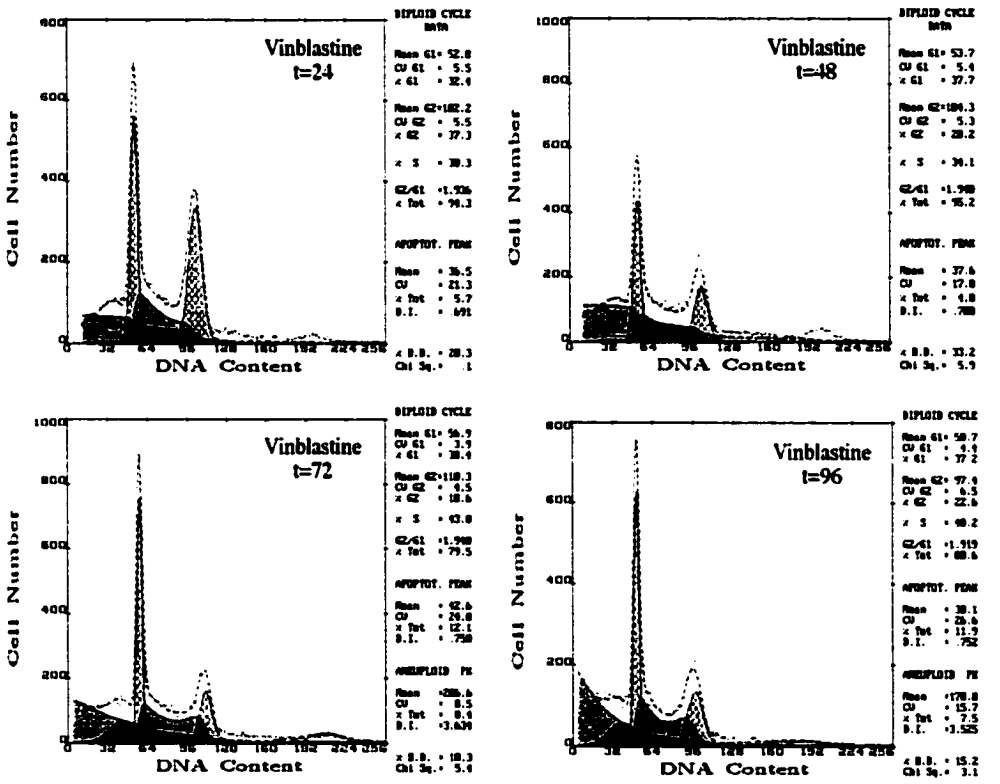

Figure 3.14: Flow cytometric analysis of 2008 human ovarian carcinoma cells treated with 10 nM vinblastine (**71**) results in an increase in the number of cells in the G_2-M phase of the cell cycle. The effect is most pronounced after 24 hours.

Reproduced with permission of the copyright owner. Further reproduction prohibited without permission.

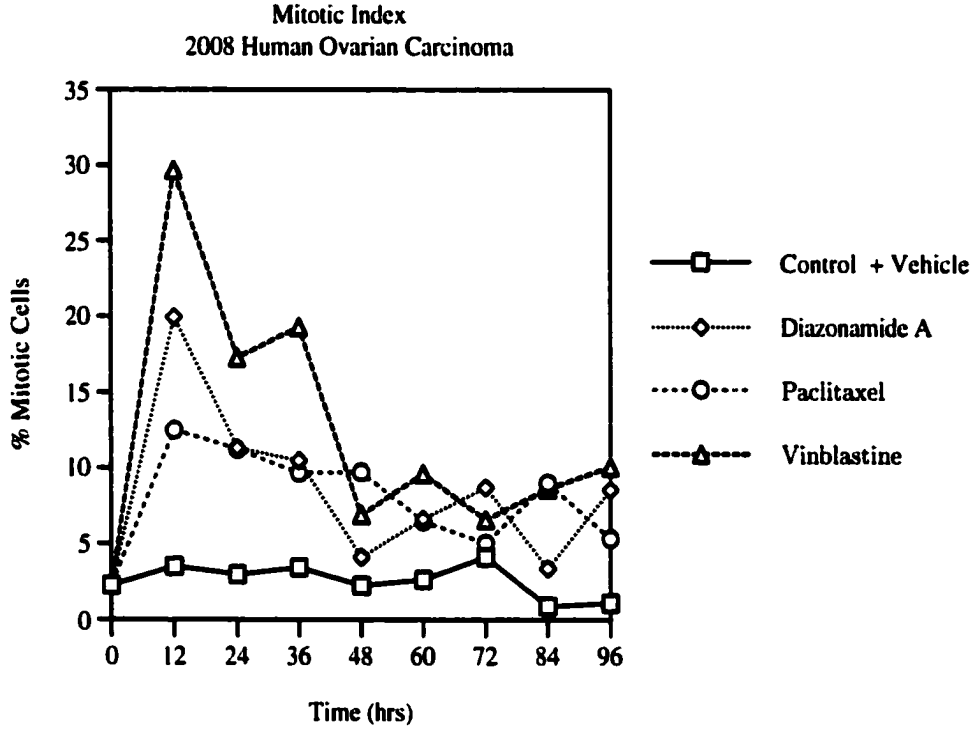

Figure 3.15: Mitotic index determination reveals that treatment of 2008 human ovarian carcinoma cells with 40 nM paclitaxel (**73**), 10 nM vinblastine (**71**), and 40 nM diazonamide A (**75**) results in an increase in the number of mitotic cells.

Reproduced with permission of the copyright owner. Further reproduction prohibited without permission.

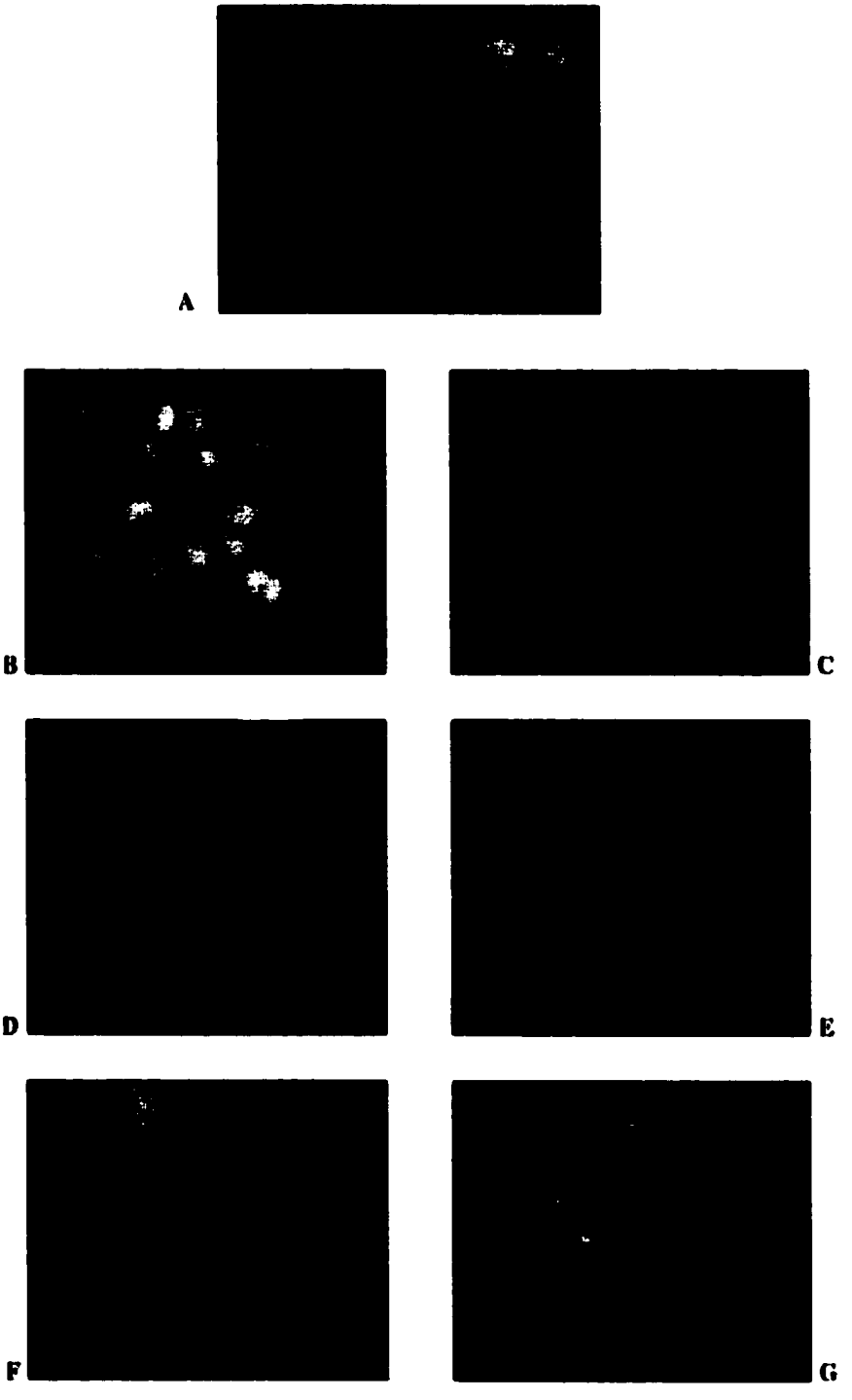

Figure 3.16: Immunofluorescence micrographs of 2008 human ovarian carcinoma cells treated with vehicle (A), diazonamide A (**75**) (B: 100 nM and C: 1μM), vinblastine (**71**) (D: 100 nM and E: 1μM) and paclitaxel (**73**) (F: 100 nM and G: 1μM).

Reproduced with permission of the copyright owner. Further reproduction prohibited without permission.

3.4 Discussion

Microtubules are an integral structural component of eukaryotic cells [187]. They have been implicated in a variety of cellular functions such as the regulation of cell shape, strength, and rigidity, the anchorage of surface receptors in the plasma membrane, and cell motility either of the cell as a whole or associated with cilia and flagella. In addition, they serve as guiding rails for the transport of organelles in association with the motor proteins dynein and kinesin. Most importantly though, microtubules are known to play an essential role in cell division, mitosis, when they form the mitotic spindle that facilitates the segregation of the chromosomes before division into two daughter cells.

Tubulin is a heterodimeric protein, consisting of two $\alpha - \beta$ subunits of 50kD each. Each dimer has two tightly bound GTPs, one at an exchangeable site, the E-site, which hydrolyzes during microtubule assembly, the other at a non-exchangeable site, the N-site. Under certain circumstances tubulin will co-purify with a series of proteins, called MAPs or "Microtubule Associated Proteins", and these proteins are believed to play an important role in the assembly of microtubules *in vitro* and in the cell.

Microtubules are in complex dynamic equilibrium with free tubulin, both in the cell [188–190] and in *in vitro* cell-free assays in which microtubules can been grown to steady-state from free tubulin. *In vitro*, tubulin will spontaneously self-assemble into microtubules, in the presence of MAPs and GTP, above a required minimum concentration of tubulin, the "critical concentration" or C_c. Thus, when steady state microtubules have grown, the amount of tubulin that remains unassembled is C_c. *In vitro* dilution will cause the disassembly of steady state microtubules whereas the addition of tubulin causes an increase in microtubule mass.

Microtubules are long hollow cylinders of 13 helically twisted protofilaments that are aligned longitudinally along the axis of the cylinder. In interphase cells, microtubules stretch from an area close to the nucleus, the microtubule organizing center or MTOC, to the cell membrane. During mitosis the interphase microtubule network breaks down and is replaced with mitotic spindle microtubules. During the G_2-phase of the cell cycle, the MTOC has been duplicated and the mitotic spindle microtubules extend from the two MTOCs at the poles of the cells to the chromosomes in the cen-

Reproduced with permission of the copyright owner. Further reproduction prohibited without permission.

ter. GTP is required for *in vitro* assembly of tubulin into microtubules although its hydrolysis appears not to be required, since microtubules will form in the presence of nonhydrolyzable GTP analogs.

The energy provided by the hydrolysis of GTP during the addition of tubulin to microtubule ends confers them two unusual dynamic properties. One such property, called "treadmilling" or flux, is the net addition of tubulin at one microtubule end and the balanced loss of tubulin at the opposite end, at polymer-mass steady state. The two ends of the individual microtubules differ structurally and kinetically, and the dynamics of tubulin exchange at one end, the plus (+) end, are much more rapid than the dynamics of the opposite or minus (-) end. The end that grows at steady state is called the net assembly or A end and appears to be the kinetically rapid or plus (+) end. Thus, at the plus (+) end, addition and loss of tubulin results in a net growth of the microtubule, whereas at the minus (-) end, a net loss of tubulin takes place. Thus, tubulin that is added on one site of the microtubule is eventually released on the other site, causing this so-called flux.

The second remarkable property, called dynamic instability, can be described as the switching at individual microtubule ends between phases of shortening and growing. Mitotic spindle microtubules are especially dynamic and more rapid exchange with free tubulin at the microtubule ends takes place. Both dynamic properties, the growing and shortening dynamics, as well as the treadmilling dynamics of microtubules, are critical to mitotic spindle function.

The proper functioning of the dynamic equilibrium between free cytoplasmic tubulin and microtubules in the cell is critical for cell proliferation. Antimitotic agents invariably have been found to interact with tubulin or microtubules, rather than with MAPs or other proteins involved in mitosis, and these agents have a long history both as poisons and in the treatment of human disease.

Although antimitotic agents play a significant role in the treatment of inflammatory diseases (*e.g.*, colchicine [191]), fungal diseases (*e.g.*, griseofulvin [192]), and parasitic diseases (*e.g.*, benzimidazole carbamates [193]), the greatest current interest derives from their role in the treatment of cancer. Most chemotherapeutic agents that exhibit antimitotic activity target the cellular regulation of microtubules and the most

Reproduced with permission of the copyright owner. Further reproduction prohibited without permission.

important antimitotic antitumor agents used in the clinic today are vinblastine (**71**) and paclitaxel (**73**).

For many years the antiproliferative activities of vinblastine (**71**) and paclitaxel (**73**) have been attributed to their ability to destabilize and stabilize microtubules, respectively. However, more detailed investigations into their mechanisms of action have revealed that their interaction with microtubules is much more complex.

Vinblastine (**71**) and other *Vinca* alkaloids were first found to interact with microtubules and tubulin as was indicated by their effect on the mitotic spindle in cultured cells [194, 195] and their ability to induce the formation of paracrystalline structures *in vivo* and *in vitro* [196–204]. They bind with high affinity to tubulin and at high concentrations inhibit the polymerization of tubulin into microtubules, both *in vitro* and *in vivo* [194, 205–208]. They are also capable of depolymerizing microtubules *in vitro* by fraying and peeling protofilaments at both microtubule ends [206, 209]. For this reason, it was generally accepted that the *Vinca* alkaloids inhibit mitosis [210, 211] by depolymerizing existing mitotic spindle microtubules required for chromosome movement, or by inhibiting the formation of new ones [212–217].

After the first observation of mitotic arrest caused by paclitaxel (**73**) [218], it was noted that the drug interferes with microtubules in the cell by enhancing polymer stability and assembly [219–221] rather than inhibiting assembly and destabilizing microtubules like vinblastine (**71**). In cell free preparations, paclitaxel (**73**) causes the self-assembly of tubulin at lower protein concentrations and temperatures [222–224] and in the absence of MAPs or GTP. The polymer that forms under the influence of paclitaxel (**73**) is stable to dilution and shorter than normal although more protein is polymerized. In cells, paclitaxel (**73**) often causes characteristic thick bundles of parallel microtubules that do not originate from microtubule organizing centers, the MTOCs [225]. For this reason, paclitaxel (**73**) and docetaxel (**74**) are generally believed to cause mitotic arrest with a completely different mechanism of action in that they enhance microtubule polymerization, increasing the mass of microtubules both in cells and *in vitro* [187].

However, it was found that the inhibition of cell proliferation and the interaction with microtubules and tubulin are not well correlated. The concentrations of vinblastine (**71**) or paclitaxel (**73**) needed to inhibit 50% cell proliferation are much lower than

Reproduced with permission of the copyright owner. Further reproduction prohibited without permission.

those needed for a 50% change in the mass of microtubules. It was found that these drugs accumulate inside the cell to concentrations that are observed *in vitro* to affect the exchange of tubulin at the microtubule ends. The most sensitive antiproliferative and antimitotic effects seen for vinblastine (**71**) and paclitaxel (**73**) occur at nanomolar concentrations, which closely resemble the steady-state serum concentrations that are reached during intravenous infusion of vinblastine (**71**) or paclitaxel (**73**).

Inhibition of cell proliferation and blockage of cells in mitosis at the lowest effective concentration of vinblastine (**71**) or paclitaxel (**73**) occurs with little or no change in microtubule polymerization or spindle organization [210,211]. Thus antiproliferative activity of these drugs at the lowest effective concentration is due to the inhibition of mitotic spindle *function*. Vinblastine (**71**) and paclitaxel (**73**) are now believed to inhibit cell proliferation by altering the dynamics of tubulin addition and loss at the ends of mitotic spindle microtubules, rather than by depolymerizing or polymerizing microtubules. At their lowest effective concentrations *in vitro* they kinetically stabilize microtubule dynamics by reducing the rate of tubulin addition and loss at the microtubule ends [226,227].

Therefore, antimitotic drugs like vinblastine (**71**) and paclitaxel (**73**) may in fact exert their chemotherapeutic actions clinically via the same mechanism of action, by affecting the dynamics of mitotic spindle microtubules and not by depolymerizing or excessively polymerizing microtubules [190].

In spite of their clinical success, vinblastine (**71**) and paclitaxel (**73**) suffer from several serious drawbacks. Vinblastine (**71**) and paclitaxel (**73**) are good substrates for transport by the P-glycoprotein efflux pump, which mediates acquired or *de novo* multidrug resistance (MDR) [228]. This limits the ability of the *Vinca* alkaloids, the taxanes, and other natural product anticancer drugs to inhibit tumor growth. In addition, resistance to paclitaxel (**73**) can be acquired through the expression of altered forms of α- or β-tubulin that exhibit impaired capacity to polymerize into microtubules, have a lower affinity for paclitaxel (**73**), or an intrinsically lower rate of microtubule assembly [229].

Even though vinblastine (**71**) and paclitaxel (**73**) might share their clinical mode of action, the discovery of paclitaxel (**73**) and its pharmacological properties has sparked a continued interest in the discovery of novel antimitotic chemotypes that may

Reproduced with permission of the copyright owner. Further reproduction prohibited without permission.

avoid these mechanisms of drug resistance. Before 1984, generally all antimitotic natural products were isolated from higher plants. Since then a large number of new ones has been discovered from many different classes of organisms [230]. The relatively unexplored environment of the ocean has been especially prolific and marine metabolites have shown a particularly high propensity toward potent antimitotic activity [15, 180, 231].

Several compounds from marine origin, the halichondrins (**4–81**) [232–235], cryptophycin 1 (**82**) [236–243], the spongistatins (**83–86**) [232, 244–247], and dolastatin 10 (**3**) [248–254] that interact at the *Vinca* domain of tubulin, are at the moment in preclinical and clinical evaluation against cancer.

The halichondrins and halistatins (**4–81**), Fig. 3.17, are lactone polyethers isolated from the marine sponges *Halichondria okadai*, *Axinella* sp., *Axinella carteri*, and *Phakellia carteri* [233–235, 255]. Of the four compounds, halichondrin B (**4**) has been studied most extensively. It is highly cytotoxic, causes mitotic arrest and the disappearance of intracellular microtubules, and it inhibits tubulin polymerization *in vitro*.

Cryptophycin 1 (**82**), Fig. 3.17, and its analogs were isolated from the terrestrial cyanobacterium *Nostoc* sp. [256–258]. Cryptophycin 1 (**82**) inhibits microtubule assembly, causes the disappearance of intracellular microtubules. It suppresses microtubule dynamic instability and it causes rapid apoptosis [239]. Cryptophycin 1 (**82**) differs from other antimitotic agents as it is not a substrate for transport by the P-glycoprotein efflux pump and thus is active against multiple drug resistant (MDR) cell lines.

The spongistatins (**83–86**), Fig. 3.18, are also lactone polyethers isolated from the sponges *Spongia* sp. and *Spirastrella spinispirulifera* [245–247, 259], and others [260, 261]. They are potent cytotoxins *in vitro*, cause mitotic arrest, and the disappearance of intracellular microtubules. They also inhibit the assembly of microtubules *in vitro*.

The dolastatins were isolated from the shell-less opistobranch mollusc *Dolabella auricularia*. This sea hare contains several of these unusual depsipeptides, the most potent of which is dolastatin 10 (**3**), Fig. 3.18, [254]. The peptide causes cells to accumulate in mitotic arrest and at higher concentrations intracellular microtubules disappear. Dolastatin 10 (**3**) inhibits tubulin polymerization *in vitro* and non-competitively inhibits the binding of vinblastine (**71**) to tubulin. The non-competitive behavior is usu-

Reproduced with permission of the copyright owner. Further reproduction prohibited without permission.

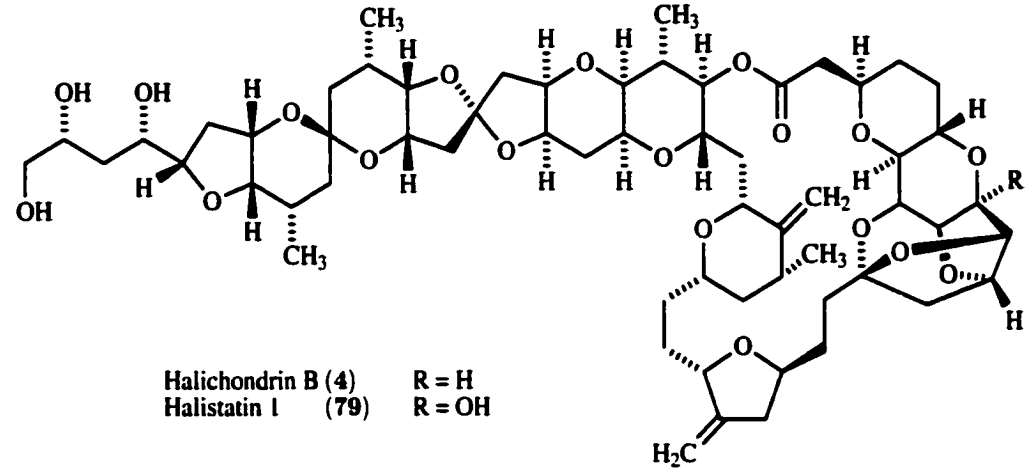

Halichondrin B (4) R = H
Halistatin 1 (79) R = OH

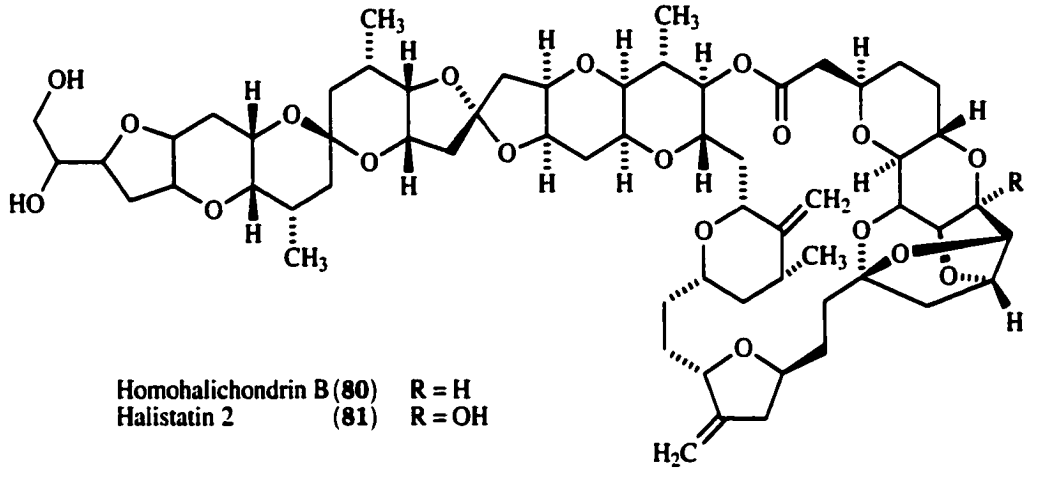

Homohalichondrin B (80) R = H
Halistatin 2 (81) R = OH

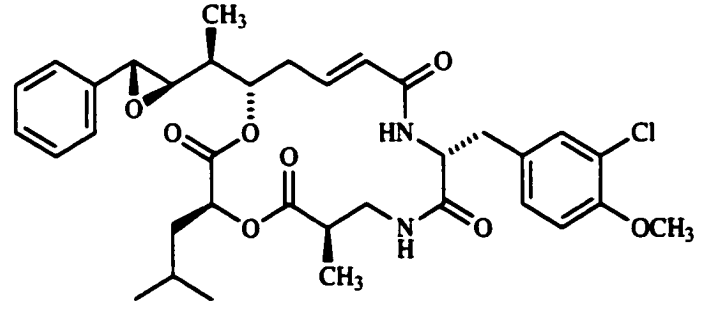

Cryptophycin 1 (82)

Figure 3.17: Antimitotic marine natural products, interacting at the *Vinca* domain, that are currently under investigation by the NCI.

Reproduced with permission of the copyright owner. Further reproduction prohibited without permission.

ally explained with a close proximity of the binding sites of the *Vinca* alkaloids and peptide binding site and GTP. Therefore the partially overlapping binding regions of these molecules is collectively called the *Vinca* domain. *In vitro*, dolastatin 10 (**3**) causes tubulin aggregation at higher concentration, but the morphology of the formed precipitate is distinct from that formed by the *Vinca* alkaloids.

Several other marine metabolites interacting with tubulin at the paclitaxel binding site, the epothilones (**87–88**) [262–264], discodermolide (**89**) [265–269], eleutherobin (**90**) [270, 271], and the laulimalides (**91–92**) [272], are also in preclinical evaluation against cancer.

The epothilones A (**87**) and B (**88**), Fig. 3.19, where isolated from the myxobacterium *Sorangium cellulosum*, after the crude extract was found to stabilize microtubules [264], although they had previously been isolated as antifungal cytotoxins [273]. Their cytotoxicity is mediated through the induction of mitotic arrest, with the concomitant appearance of microtubules bundles in the cells. *In vitro*, microtubules assemble from tubulin in the presence of epothilone B (**88**) in the absence of the usually required GTP. The polymers formed are stable to cold and calcium.

Discodermolide (**89**), Fig. 3.19, is a lactone isolated from the marine sponge *Discodermia dissoluta* [274]. It was originally identified as an immunosuppressive agent [275–278], but was later found by flow cytometry to cause cell cycle arrest in the G_2-M phase in several cells lines [268,275,279]. Mitotic arrest was accompanied by microtubule bundling at concentrations much lower than those required for the same effect with paclitaxel (**73**) [267].

Eleutherobin (**90**), Fig. 3.19, was isolated from the rare Western Australian soft coral *Eleutherobia* sp. (order Alcyonacea, family Alcyoniidea) [271]. The molecule is a diterpene glycoside exhibiting significant *in vitro* cytotoxicity with IC_{50} values around 10-15 nM. It was found to stabilize microtubules by competing for the paclitaxel binding site on the microtubule polymer [270]. Eleutherobin (**90**) exhibits enhanced selectivity against breast, renal, ovarian and lung cancer cell lines in the NCI sixty cell line *in vitro* primary screen and an 84% correlation coefficient with paclitaxel (**73**) was calculated in the COMPARE program. Eleutherobin (**90**) is a substrate for P-glycoprotein efflux pump which mediates multiple drug resistance and thus it shows cross resistance with

Reproduced with permission of the copyright owner. Further reproduction prohibited without permission.

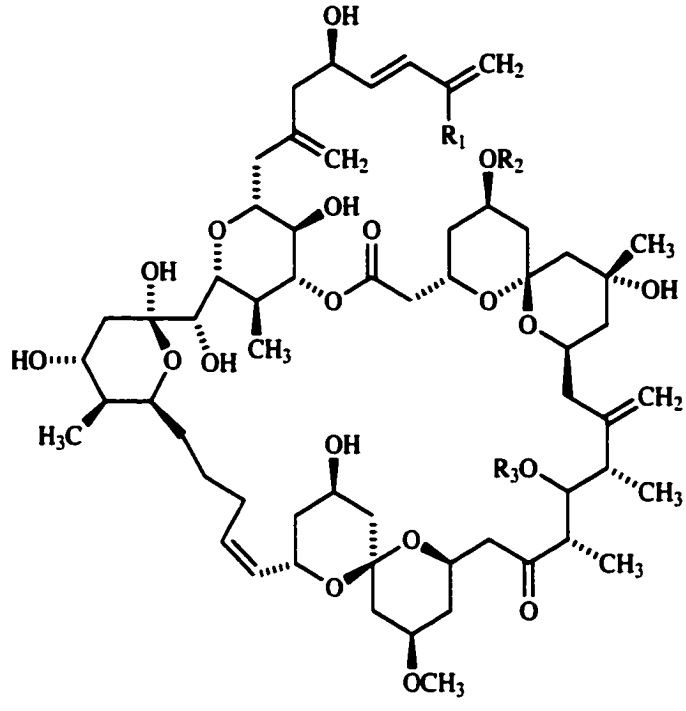

Spongistatin 1 (**83**) $R_1 = Cl$, $R_2 = R_3 = COCH_3$
Spongistatin 2 (**84**) $R_1 = H$, $R_2 = R_3 = COCH_3$
Spongistatin 3 (**85**) $R_1 = Cl$, $R_2 = H$, $R_3 = COCH_3$
Spongistatin 4 (**86**) $R_1 = Cl$, $R_2 = COCH_3$, $R_3 = H$

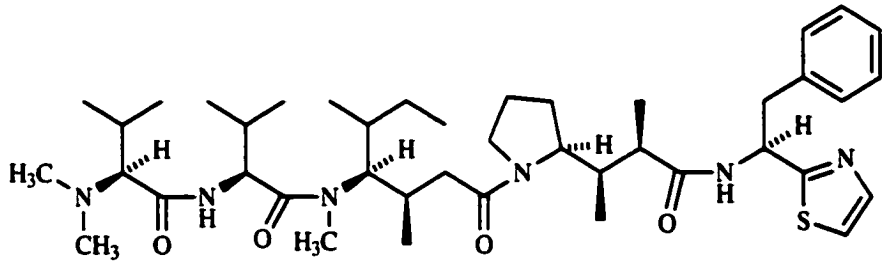

Dolastatin 10 (**3**)

Figure 3.18: Antimitotic marine natural products, interacting at the *Vinca* domain, that are currently under investigation by the NCI (Continued).

Reproduced with permission of the copyright owner. Further reproduction prohibited without permission.

paclitaxel-resistant cell lines.

Laulimalide (**91**) and isolaulimalide (**92**), Fig. 3.19, are macrocyclic lactones, originally isolated from sponges from Indonesia [280], Vanuatu [281], and Okinawa [282]. During a mechanism-based screening program their antimicrotubule activity, similar to that of paclitaxel (**73**), was discovered and although they are not as potent as paclitaxel (**73**) they are more effective at inducing intracellular microtubule bundles. In contrast to paclitaxel (**73**) the laulimalides (**91–92**) inhibit the proliferation of multiple drug resistant cells, suggesting they are poor substrates for transport by the P-glycoprotein efflux pump.

In order to unravel the mechanism of action of diazonamide A (**75**) and to place it among the other marine drugs interacting either at the *Vinca* domain or the paclitaxel binding site, three experiments were performed.

First, cells treated with diazonamide A (**75**), paclitaxel (**73**), and vinblastine (**71**) were analyzed using flow cytometry to determine whether diazonamide A (**75**), like paclitaxel (**73**) and vinblastine (**71**), is capable of arresting cells in the G_2-M phase of the cell cycle. G_2-M arrest is caused by direct interaction of antimitotic agents with the functioning of microtubules causing cells to arrest in mitosis. However, G_2-M arrest can also occur due to check point activation in response to DNA-damaging agents or incomplete chromosome replication. Flow cytometry will not discriminate between cells blocked in mitosis (M phase) and cells arrested at the G_2-M border due to check point activation. Therefore, concomitant mitotic index determination was carried out on the treated cells and all three drugs showed an increase in the number of cells exhibiting the characteristic condensed chromatin pattern of mitotic cells, Fig. 3.9. Diazonamide A (**75**), like paclitaxel (**73**) and vinblastine (**71**), blocks cells in mitosis.

The effect of diazonamide A (**75**) on microtubule structure in the 2008 cell line was similar to that of vinblastine (**71**). At a concentration of 100 nM, no microtubules were visible whereas those in paclitaxel (**73**) treated cells were more dense. At a concentration of 1 μM, diazonamide A (**75**) did not induce the formation of paracrystals like vinblastine (**71**), although some aberrant polymerization was observed. This may be due to the fact that diazonamide A (**75**) is 4-fold less potent than vinblastine (**71**) in this cell line and concentrations higher than 1 μM were not investigated.

Reproduced with permission of the copyright owner. Further reproduction prohibited without permission.

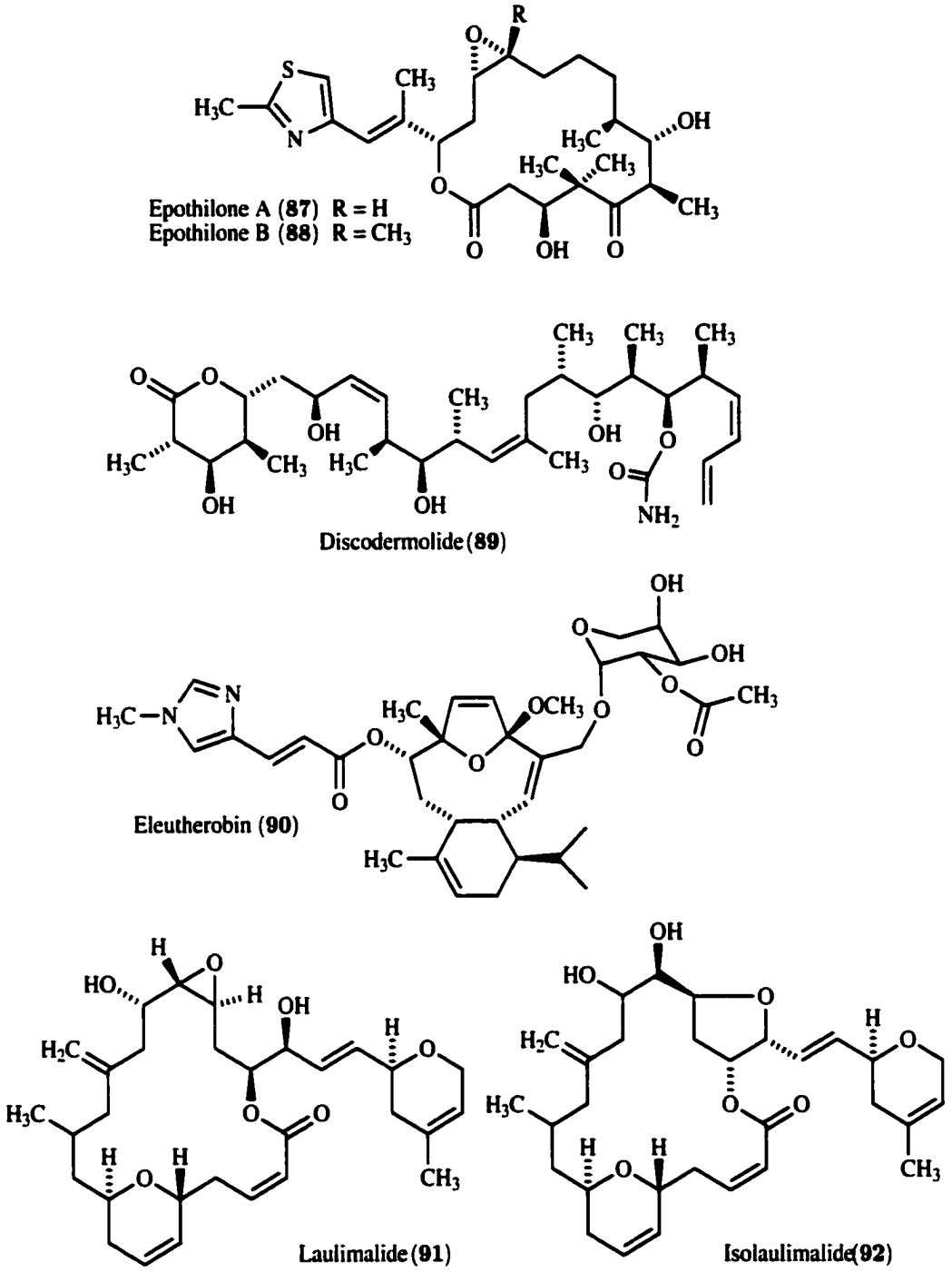

Figure 3.19: Antimitotic marine natural products, interacting at the paclitaxel binding site, that are currently under investigation by the NCI.

Reproduced with permission of the copyright owner. Further reproduction prohibited without permission.

The effect of diazonamide A (**75**) on microtubule dynamics will be further investigated in future *in vitro* polymerization experiments. These assays, using purified free tubulin protein or steady-state microtubules, will be performed to confirm the ability of diazonamide A (**75**) to interfere with microtubule dynamics in a manner analogous to vinblastine (**71**). Diazonamide A (**75**) is expected to inhibit the polymerization of tubulin into microtubules and cause the depolymerization of steady-state microtubules at high concentrations.

The actual binding site for diazonamide A (**75**) on tubulin (or microtubules) will need to be determined be means of competitive binding assays using tritiated drugs that are known to bind the three distinct binding areas on tubulin, such as colchicine, vinblastine (**71**), and paclitaxel (**73**). Diazonamide A (**75**) is likely to (non-)competitively inhibit the binding of vinblastine (**71**) in such assays although the possibility for inhibition of colchicine binding should not be discarded. Diazonamide A (**75**) may, however, bind tubulin or microtubules at a binding site completely different from those known today.

3.5 Conclusion

In summary, diazonamide A (**75**) is a potent inhibitor of cell proliferation and causes cells to accumulate in mitosis. Indirect immunofluorescence studies demonstrated that treatment of 2008 human ovarian carcinoma cells with diazonamide A (**75**) results in marked depletion of cellular microtubules at higher concentrations. These results indicate that diazonamide A (**75**) may exert its antimitotic effect through interaction with tubulin at the *Vinca* domain, in a fashion similar to vinblastine (**71**). Tubulin polymerization studies and competitive binding assays will be needed to further investigate the mechanism of action of diazonamide A (**75**).

Reproduced with permission of the copyright owner. Further reproduction prohibited without permission.

Chapter 4

Targeted Delivery Using Tumor Homing Peptides

4.1 Introduction

Current chemotherapy consists of the intravenous administration of a cocktail of cytotoxic anticancer drugs. This treatment is often unsuccessful for two reasons. First, even the most selective clinically available anticancer drugs cause severe toxicity to healthy tissues, which limits the doses at which they can be given. Second, conventional chemotherapy targets the tumor cells which are inherently genetically unstable. Due to their elevated rate of mutation, cancer cells often quickly become resistant to the administered drugs, as well as to drugs to which the tumor has not been exposed but to which resistance may occur via a common mechanism. A great deal of effort has gone into the development of alternative treatments such as biological treatments (gene therapy [283], immunotherapy [284–286], and cancer vaccines [287, 288]) and the treatment through the inhibition of angiogenesis [289–295]. At the same time, research has focussed on finding more selective cytotoxic drugs or ones that have fewer toxic side effects.

Reproduced with permission of the copyright owner. Further reproduction prohibited without permission.

4.1.1 Angiogenesis

Angiogenesis is the formation of new capillary blood vessels from existing vasculature by the migration and proliferation of endothelial cells [296]. Capillary blood vessels reach virtually all cells in the body and they replenish nutrients and oxygen and carry off waste products. The endothelial cells that form these vessels do usually not divide [297] although occasionally, for example during wound healing, they will proliferate rapidly. In the adult body under normal physiological conditions, angiogenesis is rare and it is highly regulated by angiogenic stimulators and inhibitors in direct response to tissue demands.

Tumors can exist as small localized masses for many months or years, the rapid proliferation of the tumor cells [298] balanced by a high rate of apoptosis (programmed cell death) [299]. Since these tumors are avascular, they are incapable of growing beyond 2 to 3 mm in size, limited by the diffusion of oxygen and nutrients into the tumor bed [300, 301]. At the microscopic stage, these tumors excrete angiogenic growth factors that promote the process of angiogenesis, but it is balanced by their induction or secretion of inhibitory factors, such as angiostatin [302, 303], that prevent the process of angiogenesis. Over time however, a tumor may abruptly switch to the angiogenic phenotype via mechanisms presently not fully understood and tumor growth is accelerated aided by neovascularization [304].

The process of angiogenesis begins with the degradation of the basement membrane, the structure overlying the endothelium of a pre-existing blood vessel, through the upregulation of matrix metalloproteinases (MMPs) produced by the tumor cells [305]. This is followed by the proliferation and migration of endothelial cells towards the tumor. As canals and branches are laid out, a new basement membrane is formed on which the endothelial cells reside [306].

Tumor blood vessels are very different from those in normal tissues. They are often "leaky" and nonfunctional, and blood flow is erratic with stasis and reversal of blood flow occurring within individual vessels. Nevertheless, tumor growth is dependent on angiogenesis and the formation of new blood vessels toward the tumor allows it to become more aggressively invasive. Moreover, the presence of blood vessels in the tumor provides a route for the spread of detached tumor cells via the blood circulatory

Reproduced with permission of the copyright owner. Further reproduction prohibited without permission.

system to distant sites [307]. Thus, angiogenesis is a requirement for malignant tumor growth, invasion, and metastasis [300, 308, 309] and clinical studies have demonstrated that the degree of angiogenesis is correlated with the malignant potential of several cancers, including breast cancer and malignant melanoma [307].

4.1.2 Anti-angiogenic Treatment

The process of angiogenesis constitutes a prominent target for therapeutic intervention. Anti-angiogenic treatment has recently gained considerable attention, since it has the potential to overcome many of the shortcomings of conventional chemotherapy and the alternative treatments mentioned earlier. Chemotherapy and most alternative treatments are hindered by limited access to tumor cells, heterogeneity of tumor cells, the emergence of resistant tumor cells, and the limited activity against widespread metastasis. Whereas these treatments are directed mainly to tumor cells, anti-angiogenic therapy is directed specifically against the endothelial cells of the capillary tumor vasculature. These cells are derived from the resting vasculature of the host and consist of normal, genetically stable cells. Anti-angiogenic treatment therefore does not induce acquired drug resistance and, since angiogenesis is normally rare, anti-angiogenic treatment shows very few toxic side effects.

Since Folkman, in the early 1970's, first hypothesized that neovascularization is required for tumor growth, a large number of angiogenic factors produced by tumor cells has been identified. More recently, attention has turned to the isolation and characterization of angiogenesis inhibitors that may have potential usefulness as antitumor agents. These compounds include naturally occurring proteins such as thrombospondin, interferon and metalloproteinase inhibitors that can be isolated from human tissues or blood. But, tumors themselves are also known to produce or induce the production of anti-angiogenic factors, the most recent examples being angiostatin [302, 310] and endostatin [311], potent inhibitors of endothelial proliferation. These molecules are cleavage products of plasminogen, secreted by the liver, and collagen XVIII, an extracellular matrix protein, respectively. Several synthetic angiogenesis inhibitors, often analogs of natural products, are being developed such as the fumagillin analog TNP-470 [312] and batimastat (BB94) [313] which may become useful clinical agents. Several conventional

Reproduced with permission of the copyright owner. Further reproduction prohibited without permission.

chemotherapeutic agents, doxorubicin (**67**), taxol (**73**), and tamoxifen [314] have also shown anti-angiogenic activity and angiostatic steroids [315] and antibiotics [316] are also known.

Anti-angiogenic therapy takes a fundamentally different approach to cancer treatment. Whereas conventional chemotherapy strives to eradicate *all* tumor cells, anti-angiogenesis is aimed at shrinking the tumor into dormancy by limiting its blood supply, as well as inhibiting new tumors from forming through metastasis. Since each endothelial cell supports ten to one hundred tumor cells, the targeting of tumor cells has an intrinsic amplification mechanism. It is likely that anti-angiogenic treatment will be particularly successful in conjunction with other treatments such as chemotherapy, radiation and other treatments. Angiogenic treatment may be used as a long-term treatment after other treatments are completed, to prevent previously metastasized tumors from becoming angiogenic and invasive.

4.1.3 Increasing Selectivity

Much effort has gone into searching for ways to more selectively deliver anti-cancer treatments to tumor cells, in order to increase efficacy and reduce dose limiting toxicity. Several delivery strategies using liposomes, viral vectors, or antibodies for the targeted delivery of both conventional chemotherapeutic agents and alternative treatments are the focus of intense research today.

Liposomal Delivery

Liposomes [317] are small vesicles made of natural phospholipids and cholesterol, capable of targeting encapsulated small drug molecules, proteins, nucleotides, and even DNA plasmids to selected tissues, either by passive mechanisms or by active mechanisms after chemical modification of the lipid bilayer. For example, certain liposomes leave the vasculature specifically in tissues characterized by leaky vessels, such as solid tumors, and can exhibit target specificity with negligible adverse effects to normal tissues. Despite success in the development of clinically useful liposomal anticancer drugs, the advancement has been limited to only a few successful studies in animal models of cancer. Conventional liposomes are limited in effectiveness due to their rapid uptake by

Reproduced with permission of the copyright owner. Further reproduction prohibited without permission.

macrophage cells of the immune system, predominantly in the liver and spleen, before they can reach the tumor.

Viral Delivery

Viral vectors are the most frequently used vehicles for the delivery of genes in gene therapy [283]. Gene therapy in cancer is aimed at the alteration of the cell phenotype by insertion of the "correct" or removal of the "incorrect" genetic information in order to control the disease. Viruses can infect a variety of mammalian cells and the viral particle can be modified to enter only the target cell through the interaction of engineered viral envelope proteins with the appropriate receptors on the cell surface. Viral delivery to tumor cells poses several problems. Virus particles are rapidly removed via immune clearance and other mechanisms and systemically injected viruses often fail to reach the tumor. Thus, for anti-cancer gene therapy, direct injection into tumors is currently used [283]. However, this is impractical for some sites and multiple tumors and misses small metastases. In addition, viruses have their own "target" cells and can naturally cause deleterious diseases in humans. Changing this innate targeting and rendering the virus non-infectious can be very difficult.

Antibody Delivery

In the 1980's, shortly after Köhler and Milstein invented the technique for making them, monoclonal antibodies (MAbs) were hailed as the "magic bullets" for the treatment of cancer and other diseases. MAbs bind their target antigens with high affinity and are capable of marshaling immune cells to destroy the cells carrying them. In addition, they can be used as highly specific carriers of cytotoxins, radioisotopes, or other cytotoxic messages. However, MAbs are large protein structures and mouse-derived MAbs are recognized by the human immune system as foreign, which drastically reduces their half-lives in the blood. In addition, even though these immunoglobulin proteins are broadly conserved among different mammalian species, mouse MAbs fail to significantly interact with the human immune system. Humanized mouse MAbs are now being developed, using a combination of genetic engineering and computer modeling, and at least one humanized antibody, Herceptin [318–321], has received FDA approval

Reproduced with permission of the copyright owner. Further reproduction prohibited without permission.

for the treatment of breast cancer. Several other MAbs are at the moment in clinical trials against a variety of cancers.

Ever since their discovery, researchers have been trying to use antibodies to target cytotoxic treatment specifically to the tumor. Currently, several conjugates between humanized MAbs and cytotoxins are in clinical trails against cancer. The antibodies are typically designed to target known receptors that are overexpressed on tumor cells versus normal cells, in particular those involved in cell proliferation. Such MAb-cytotoxin conjugates exhibit a very attractive mechanism of action. Apart from carrying the cytotoxin to the tumor, binding of the MAb to its target cell surface receptor disturbs the proper functioning of the antigen such that the antibody itself may exerts anticancer activity.

Several impressive results were obtained with immunoconjugates between the anticancer drug doxorubicin (**67**) and the MAb BR96 [285]. BR96 binds to an antigen that is abundantly expressed on the surface of a number of different tumor types and complete regressions and several cures were obtained in mice. However, the required doses of antibody are very high and an alternative approach to tumor killing with cytotoxic drug-antibody conjugates is to select a more potent drug molecule [284]. One such molecule is calicheamicin [59,60], a member of the enediyne family. Enediynes are potent microbial products that, due to their unique structure, can form biradicals that cleave DNA. Calicheamicin γ is more than 100-fold more potent then doxorubicin (**67**) and is too toxic to be used as an unconjugated drug for cancer therapy. Calicheamicin γ has been conjugated to a number of humanized MAbs and the results of phase I clinical trials are encouraging [322].

Thus, (humanized) antibodies that target antigens specifically expressed on tumor cells show promise as anticancer agents by virtue of their intrinsic anticancer activity, their ability to tag tumor cells for destruction by the immune system, and as vehicles to carry toxins, radioisotopes, chemotherapeutics, or other more potent drugs to the tumor.

Tumor targeting by MAbs suffers several drawbacks. Although tumor-associated antigens are used to raise tumor-targeting antibodies, their expression is rarely restricted to tumor cells. In addition, tumor cells are inherently genetically unstable and can quickly develop resistance to antibody treatment by mechanisms similar to some

Reproduced with permission of the copyright owner. Further reproduction prohibited without permission.

of those used to avoid cytotoxic drugs and through complex mechanisms to evade or suppress antigen immune recognition. A severe limitation to the generation of potent immunoconjugates is the linking technology and the number of drug molecules per antibody molecule. Increasing the number of drug molecules above approximately 5 per antibody results in loss of antigen-binding. In addition, the major solid tumors remain a difficult target for MAb therapy. Often only a small percentage of the systemic dose of antibody conjugate reaches the tumor site due to the size of the molecule, resulting in poor tumor penetration.

Delivery using Tumor Homing Peptides

A promising new cancer treatment is currently being developed that may overcome the problems of toxicity, selectivity, and drug resistance that normal chemotherapeutic regimes pose, as well as some of the difficulties encountered with the use of the targeted delivery systems outlined above. The molecular basis of this treatment is a series of molecules that the body uses to identify and distinguish the cells in the various tissues and organs [323]. The existence of such "address" systems enables the delivery of cytotoxic messages, targeted specifically to the tumor cells and/or the cells comprising their supportive structures such as the blood vessels.

The presence of tissue specific marker molecules was suspected early with the observation that tumors of a certain kind tend to metastasize to specific tissues [324,325]. Some of these metastases can be explained by the route the blood circulation takes through the body. However, not all metastases can be explained by the simple assumption that tumor cells get trapped in the first vascular bed they encounter downstream of the primary tumor site. The preferential homing of circulating tumor cells stems from a positive interaction between molecular markers on the cell surface of the tumor cell with tissue specific marker molecules displayed on the endothelial cells [325].

Like endothelial cells and tumor cells, all mammalian cells carry such marker molecules (e.g. [326–328]) and these receptor proteins play an important role in cell adhesion, both intercellular between different cell surface receptors, and between cells and their surrounding extracellular matrix (ECM). The ECM is a proteinacious network whose composition and structure differ for different cell types and their location. Some

Reproduced with permission of the copyright owner. Further reproduction prohibited without permission.

typical components of the ECM are fibronectin, vitronectin and collagen. The ECM forms a highly organized three-dimensional matrix in which the proteins associate with each other and with cells.

Integrins Adhesion of cells to the ECM is mediated through integrins [329], which are large membrane-spanning α-β heterodimeric proteins. There are presently 16 known α-subunits and 9 known β-subunits that together form at least 24 different integrins. The binding of cells to the ECM is mediated through the recognition of the ECM protein ligands by integrins, which is often based on the three amino acid sequence RGD (Arginine-Glycine-Aspartic acid) within the ECM proteins [330, 331]. Many integrins bind this RGD sequence but other peptide motifs have been identified as well.

The interaction between cells and ECM proteins via integrins is essential for cell growth and survival. Binding of the ECM to integrins elicits intracellular signal-transduction events that regulate cellular functions, such as cell shape and motility, but most importantly apoptosis and cell proliferation [332, 333]. When the integrins of a cell are denied binding to its proper ECM substrate, the cell stops proliferation and undergoes apoptosis [334].

This phenomenon is called anchorage-dependence and the acquisition of anchorage-independent growth is a hallmark of malignancy. Tumors are believed to descend from a single ancestral cell that over time accumulated, and survived, a series of mutations in important genes regulating cell growth and proliferation. A primary tumor is formed by the anchorage-independent proliferation of this cell. During tumor invasion and metastasis, the interactions of cell surface receptors on the tumor cells with ECM proteins induce the expression and secretion of matrix metalloproteinases (MMPs) which degrade the ECM components, allowing for the invasion of tumor cells through the matrix. This implies the dysregulation of growth signals emanating from the cell-ECM interaction and the expression of integrin receptors is often altered in malignant cells. There is, however, no simple correlation between the expression of integrins and malignant transformation. The influence of integrin function on tumor invasion and metastasis appears to differ per tumor type and per integrin.

Hence, integrins on the cell surfaces of tumor cells play an important role in the

Reproduced with permission of the copyright owner. Further reproduction prohibited without permission.

invasion and metastasis of cancer. In addition, integrins displayed on the cell surfaces of endothelial cells play an important role in angiogenesis. Tumor vasculature undergoes continuous angiogenesis and the proliferating endothelial cells in these angiogenic vessels express specific marker molecules, such as $\alpha_V\beta_3$ integrins, that are not displayed in normal resting vasculature. The interactions between endothelial integrins and the ECM (basement membrane) have been identified as important regulators of vascular cell survival, proliferation and invasion during angiogenesis [329].

Phage-Display Peptide Libraries Thus, the molecular markers expressed on endothelial cells in the vasculature of various organs and tissues differ from one another and vary between proliferating and non-proliferating endothelial cells. The existence of molecular markers on tumor cells and proliferating endothelial cells offers new possibilities for tumor therapies. In order to study the availability of tissue specific marker molecules for possible targeting of cancer therapy to tumors and their vasculature, a technique known as phage display peptide libraries was used to screen for peptides that show affinity for these cell surface receptors [12, 13].

A phage is a viral particle that normally infects bacteria. Infection is initiated by attachment of the phage to the bacterial envelop via the phage coat protein. Each phage particle displays five copies of the coat proteins used for attachment. Each copy carries a specific sequence that mediates the molecular interaction between phage and bacterium. Synthetic strands of DNA can be incorporated into the gene coding for the particular coat protein, such that the corresponding peptide sequence is displayed as part of the coat protein. If during synthesis of the DNA-insert mixtures of nucleotides are used, an enormous diversity of gene variants is obtained that code for a large variety of peptides, with each peptide displayed five times on the coat of a single phage particle.

To identify small peptide sequences with affinity for specific tissues and organs in the mouse, Pasqualini *et al.* performed the *in vivo* screening of large libraries of phage displaying billions of random peptides by injecting them into mice [12, 13]. The phage do not infect the eukaryotic cells of the mouse, but if a peptide carried by the phage shows affinity for the marker molecules on the endothelium of a particular tissue, it will causes the phage to stick. Phage particles that preferentially home to certain organs

Reproduced with permission of the copyright owner. Further reproduction prohibited without permission.

can subsequently be recovered from the organs of the mouse and replicated in *E. coli* for amplification. Thus, from a library of billions of phage-displayed peptides, one can isolate a single peptide sequence that can specifically bind to certain tissues of the mouse. Using this method, Pasqualini *et al.* discovered a series of small peptide sequences that selectively home to the brain and the kidney of the mouse and they invariably found that the phage bind to the vasculature of the specific organs [12, 13].

Subsequently, the *in vivo* screening of phage displayed peptide libraries was adapted to identify peptide sequences that specifically bind to the vasculature of human tumor xenografts carried by mice [14, 335]. Three main peptide motifs have been identified that target the vasculature of various human and murine tumors in mice [14]. One such motif is the sequence Arg-Gly-Asp (RGD) embedded in a double cyclic structure CDCRGDCFC or RGD-4C [336]. The RGD motif had previously been identified as the recognition sequence for integrin binding to ECM proteins and the RGD-binding integrin $\alpha_V\beta_3$ is known to be overexpressed on tumor vasculature. A second peptide motif is the sequence NGR, which has also been identified as a cell adhesion motif [337–339]. NGR-motif peptides also bind integrins but with much lower affinity than RGD peptides. The receptor in tumor vasculature for NGR containing peptides has recently been identified as the aminopeptidase N, a highly conserved transmembrane metalloproteinase also known as CD13 [340]. CD13 appears to be exposed to the circulation primarily in angiogenic blood vessels, although it is expressed outside the vascular system in various epithelial and hematopoietic cells. Among other cellular processes, overexpression of CD13 has been linked to enhanced tumor invasion and metastasis [341, 342]. The third tumor homing sequence, GSL (Glycine-Serine-Leucine), was not further investigated [14].

Synthetic versions of these peptides specifically home to the vasculature of tumors due to the high affinity for their receptors and the fact that these are overexpressed on proliferating endothelial cells as well as, in some cases, the tumor cells themselves [14]. The homing of these peptides is independent of tumor type and species and tumor homing peptides have been used successfully to target phage, cells and chemotherapeutic drugs [14] to tumor vasculature in the mouse model.

The anticancer drug doxorubicin (**67**) was chemically linked to the tumor homing peptides RGC-4C and CNGRC, allowing it to be targeted to human breast tumors

Reproduced with permission of the copyright owner. Further reproduction prohibited without permission.

carried by mice. Each peptide markedly increased the efficacy of the drug by 10 to 40 times (50 to 200 μg/week for doxorubicin alone versus 5 μg/week for conjugates) and significantly reduced its toxicity [14]. Mice treated with conjugates outlived control mice treated with doxorubicin by more than six months and upon necropsy conjugate-treated mice showed smaller tumors and fewer metastases.

It is believed that tumor-targeted drugs exhibit a dual mechanism of action. First, they act against the tumor cells by targeting the parent cytotoxin directly to the tumor. Since actively proliferating endothelial cells normally occur predominantly in the tumor, they may exhibit a high degree of selectivity and thus minimal toxicity. Second, they act by destroying the newly formed blood vessels that were induced by the tumor to provide it with oxygen and nutrients from the blood. Since angiogenic vessels are composed of normal endothelial cells that were induced to proliferate by growth factors released by the tumor, these cells are genetically stable and are less likely to develop drug resistance.

The use of tumor homing peptides in cancer treatment may have several advantages over conventional cancer therapies. First, tumor homing peptides are applicable to many tumor types because they all require blood supply for survival and growth and they all express the same marker molecules in their endothelia that identify them as angiogenic. Second, target endothelial cells are directly accessible through the blood and are normal, genetically stable cells, making the arising of resistant mutants unlikely. Third, there is an in-built amplification mechanism because thousands of tumor cells are reliant on each capillary for nutrients and oxygen. In addition, tumor homing peptides also overcome some of the disadvantages encountered in other therapies. First, the molecules are small and do not evoke an immune response. Second, they are relatively easy to make and stable enough in the blood to reach the tumor in significant amounts. Third, due to their high specificity they can be used to target toxic compounds to the tumor. As has been shown with the tumor homing peptide-doxorubicin conjugate, lower concentration of conjugate drug can be used and its toxicity is reduced compared to the parent toxin.

Reproduced with permission of the copyright owner. Further reproduction prohibited without permission.

4.1.4 Dianestatin 1: The First Marine Derived Tumor Homing Conjugate

Organic synthesis and the isolation of natural products has yielded many thousands of structures, a fraction of which play a role in cancer treatment today. However, many of these compounds are potent cytotoxins but are not useful in the treatment of cancer due to their lack of selectivity for cancer cells over normal tissues. The concept of targeting by means of tumor homing peptides can vastly expand the arsenal of potentially clinically useful anticancer drugs by overcoming toxicity with direct delivery to tumors. The ground breaking work of targeting doxorubicin to tumor vasculature by means of highly selective homing peptides [14], represents but the tip of an iceberg of what can be done with this technique, considering the large number of very potent cytotoxic compounds that are known today.

The marine environment constitutes over 70% of the worlds surface area. Only over the past few decades, medicinal chemists have been able to assess this new frontier in drug discovery and it has proven to be an exceptionally rich source for novel potent cytotoxins. Evolutionary pressures in the aquatic environment, such as defense against predation, fouling, and overgrowth have yielded unprecedented molecular structures that because of their unusual constitution show such strong bioactivity in the human body. Some of the most important recent discoveries in the search for novel anticancer leads are in fact from the marine environment, Fig. 2.1 Chapter II, and consistent with the concept of chemical defense most of these bioactive compounds are isolated from softbodied, vulnerable organisms that are most likely to have developed chemical defenses.

This chapter describes the synthesis of the first conjugate, dianestatin 1 (**102**), between a tumor homing peptide and the potent but non-selective cytotoxin, didemnin B (**11**), Fig. 4.1. Didemnin B (**11**) was the first marine derived compound to reach phase II clinical trials against cancer. It was ultimately dropped from further development lacking sufficient clinical efficacy (For more details see Chapter II). In retrospect, although didemnin B (**11**) is one of the most potent cytotoxins acting by the inhibition of protein synthesis, the molecule showed almost no selectivity in the NCI's 60 cancer cell line bioassay. Thus, didemnin B (**11**) was concluded to be of no future interest for the treatment of cancer. The hypothesis that is being tested with the synthesis of

Reproduced with permission of the copyright owner. Further reproduction prohibited without permission.

dianestatin 1 (**102**) is that by linkage with a tumor homing peptide, selective anticancer agents can be created from non-selective cytotoxins.

Since didemnin B (**11**) carries two hydroxy functionalities instead of an amino group as in doxorubicin (**67**), conjugation involves the formation of an ester bond rather than a amide bond, which may facilitate release of the parent cytotoxin *in situ*. The second hypothesis that is being tested with the synthesis of dianestatin 1 (**102**), is that with the use of an ester bond, an *in vivo* active reagent can be created which releases the parent cytotoxin in the tumor by an expected enzymatic ester bond hydrolysis [343]. Selection of the proper chemical link between tumor homing peptide and cytotoxin can be used to influence the stability of the conjugate. Thus, its lifetime can be designed such that the cytotoxin is not released until diffusion into the tumor is complete.

Tumor homing peptides are short sequences, usually containing five to nine amino acids. The actual homing sequence which binds to the receptor displayed on the tumor vasculature, is even shorter, as little as three amino acids. The remaining amino acids flanking the tripeptide sequence are often rich in cysteine providing cyclization via one or more disulfide bridges. Both linear and cyclized tumor homing sequences are known, but in certain cyclized sequences the additional conformational strain increases the avidity for tumor vasculature when compared to their linear counterparts.

In this study, the acetylated minimum cyclized NGR-motif peptide AcCNGRC (Ac-Cys-Asp-Gly-Arg-Cys) (**93**) was used for coupling to didemnin B (**11**). This disulfide bridged pentapeptide is blocked on the amino terminus by an acetate group and is available for binding via its carboxyl terminus. The tumor homing peptide was coupled to the cytotoxin via a linker molecule which carries both the proper functionality for coupling to the cytotoxin as well as one for coupling to the peptide. A commonly used linker molecule is glycine [344] and the presence of the linker in the molecule was not expected to significantly alter the specificity of tumor homing.

Reproduced with permission of the copyright owner. Further reproduction prohibited without permission.

4.2 Results

4.2.1 Synthesis of Dianestatin 1

Synthesis of [Fmoc-Gly^{10}]didemnin B (95)

The first step in the synthesis of dianestatin 1 (**102**) was the ester coupling of the linker molecule glycine to didemnin B (**11**), preferably via its most accessible lactic acid unit, Lac^9. For this purpose, an amino protected 9-fluorenylmethyloxycarbonyl (Fmoc) glycine unit was coupled to the hydroxy functionalities of didemnin B (**11**) by means of its pentafluorophenyl(Pfp)-activated ester Fig. 4.1. The protective Fmoc group is base-labile and has the advantage that it can be removed at room temperature, since the coupling product at Lac^9 was expected to be temperature sensitive [48]. OPfp-activated esters are commonly used in peptide synthesis in the formation of amide bonds and Fmoc-Gly-OPfp (**94**) was expected to show sufficient activity towards the hydroxy functionalities of didemnin B (**11**) in the formation of the ester bond. In addition, the bulkiness of the activated ester lowers its affinity for the more sterically hindered hydroxy group in the Ist^1 group, thus the coupling product with the glycine attached to the Lac^9 unit was obtained in excess. A 3-fold excess of Fmoc-Gly-OPfp (**94**) was stirred with didemnin B (**11**) in the presence of a catalytic amount of dimethylaminopyridine (DMAP) at room temperature for 6 days and the desired [Fmoc-Gly^{10}]didemnin B (**95**) (coupling at Lac^9) was obtained as the major product together with the minor product didemnin B[Gly^{10}-Fmoc] (coupling at Ist^1).

There are many alternative coupling reagents available from peptide synthesis that could be used in the formation of the ester bond in the coupling of glycine to didemnin B (**11**). Two alternative coupling strategies were tried before the activated OPfp ester yielded moderate success in the coupling reaction Fig. 4.3. Coupling of Fmoc-Gly-OH (**99**) to didemnin B (**11**) using isopropenyl chloroformate (IPCF) [139] in the presence of base (triethylamine (TEA) and catalytic DMAP (dimethylaminopyridine), suffered from moisture sensitivity on the micromolar scale at which the reaction was carried out and no yields higher than 25% were obtained. An alternative activated ester was also investigated, Fig. 4.3. Cbz-Gly-OSu (**100**), amino protected by the acid labile benzyloxycarbonyl (Cbz) group and activated with the *N*-hydroxysuccinimide (Su)

Reproduced with permission of the copyright owner. Further reproduction prohibited without permission.

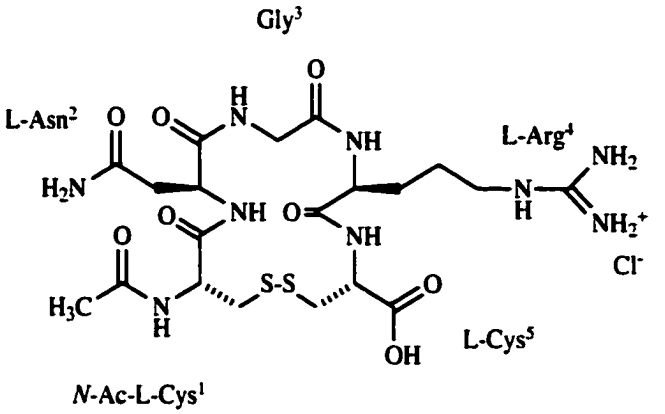

CNGRC (**93**)

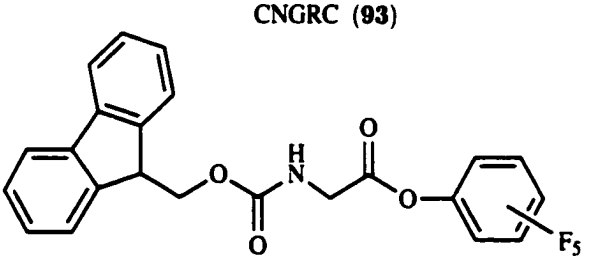

Fmoc-Gly-OPfp (**94**)

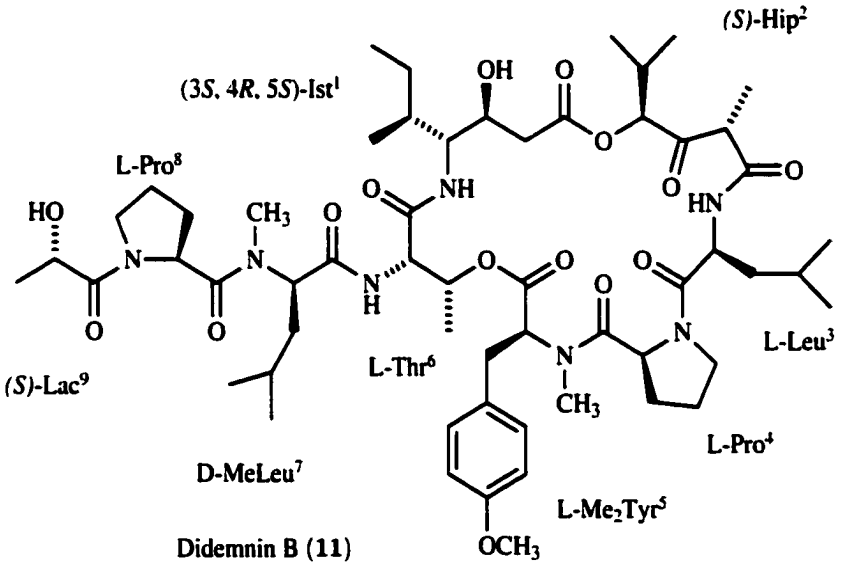

Figure 4.1: Starting materials for the synthesis of dianestatin 1 (**102**). The tumor homing peptide AcCNGRC (**93**), the *N*-protected activated ester of the glycine linker (*N*-(9-fluorenylmethoxycarbonyl)glycine pentafluorophenyl ester (Fmoc-Gly-OPfp **94**), and the ascidian natural product didemnin B (**11**).

Reproduced with permission of the copyright owner. Further reproduction prohibited without permission.

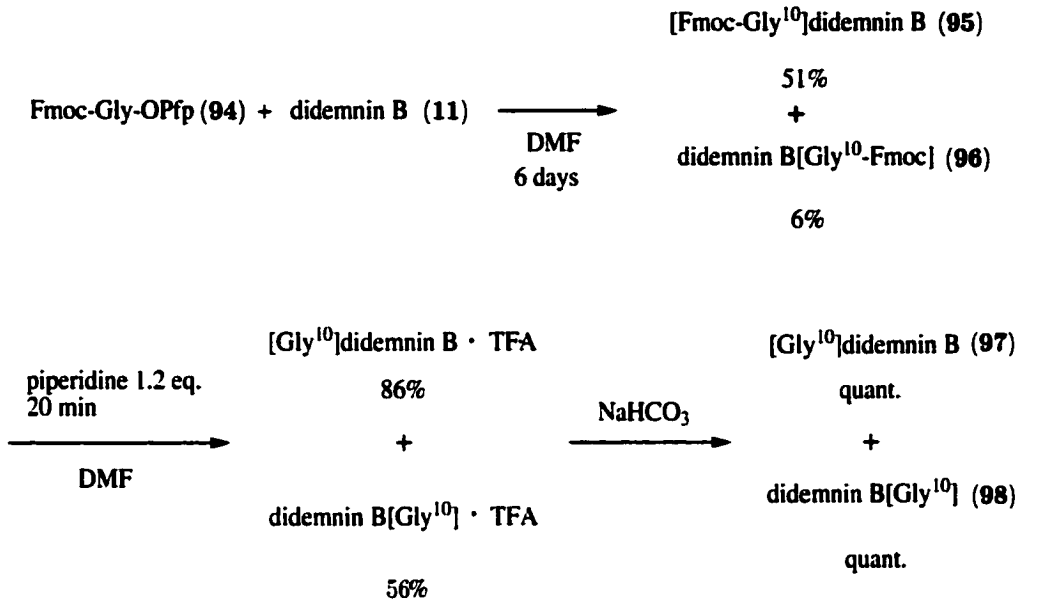

Figure 4.2: Synthesis of the intermediates [Fmoc-Gly^{10}]didemnin B (**95**) and didemnin B[Fmoc-Gly^{10}] (**96**), and [Gly^{10}]didemnin B (**97**) and didemnin B[Gly^{10}] (**98**).

group, stirred in excess at room temperature with didemnin B (**11**) for 6 days, yielded no detectable coupling product.

Deprotection of [Fmoc-Gly^{10}]didemnin B (95)

Deprotection of [Fmoc-Gly^{10}]didemnin B was achieved using a slight excess, 1.2 equivalents, of piperidine in contrast with the usual deprotection protocol of 20% piperidine in dimethyl formamide (DMF). The ester bond created between Lac^9 and the newly introduced Gly^{10} showed not only sensitivity towards temperatures above approximately 40°C but also base sensitivity in the standard protocol. However, the ester bond is sufficiently stable in acid and [Gly^{10}]didemnin B (**97**) was obtained as its TFA salt. [Gly^{10}]didemnin B (**97**), Fig. 4.4 and Fig. 4.5, was subsequently quantitatively liberated by treatment with saturated $NaHCO_3$ solution. Since TFA is a carboxylic acid and will therefore compete with the tumor homing peptide for coupling to [Gly^{10}]didemnin B (**97**) (yielding [TFA^{11}-Gly^{10}]didemnin B !), any TFA contaminants in either the [Gly^{10}]didemnin B (**97**) or AcCNGRC (**93**) (see further) were carefully removed.

Reproduced with permission of the copyright owner. Further reproduction prohibited without permission.

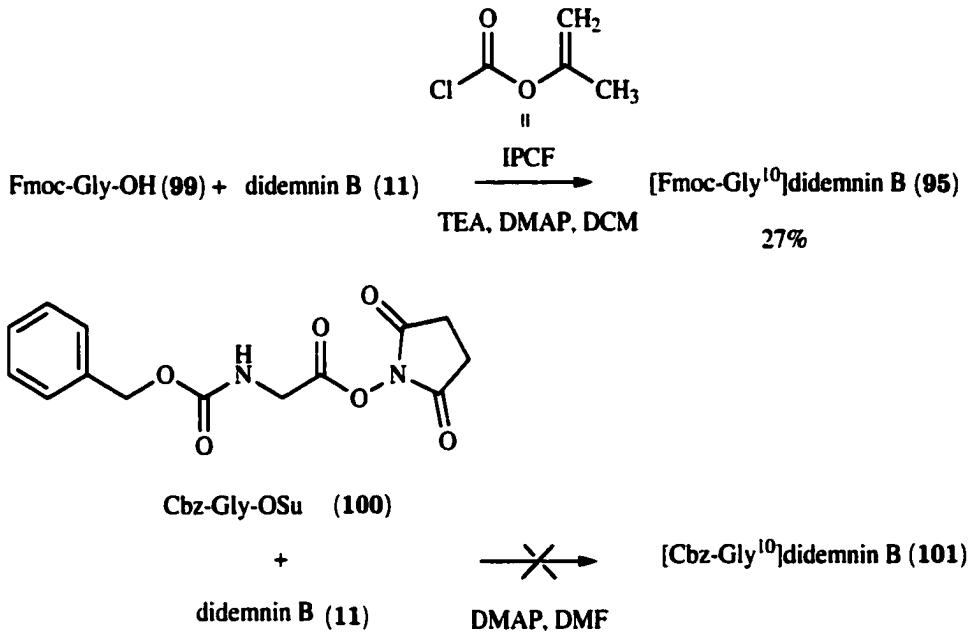

Figure 4.3: Alternative coupling strategies used for the preparation of *N*-protected [Gly[10]]didemnin B.

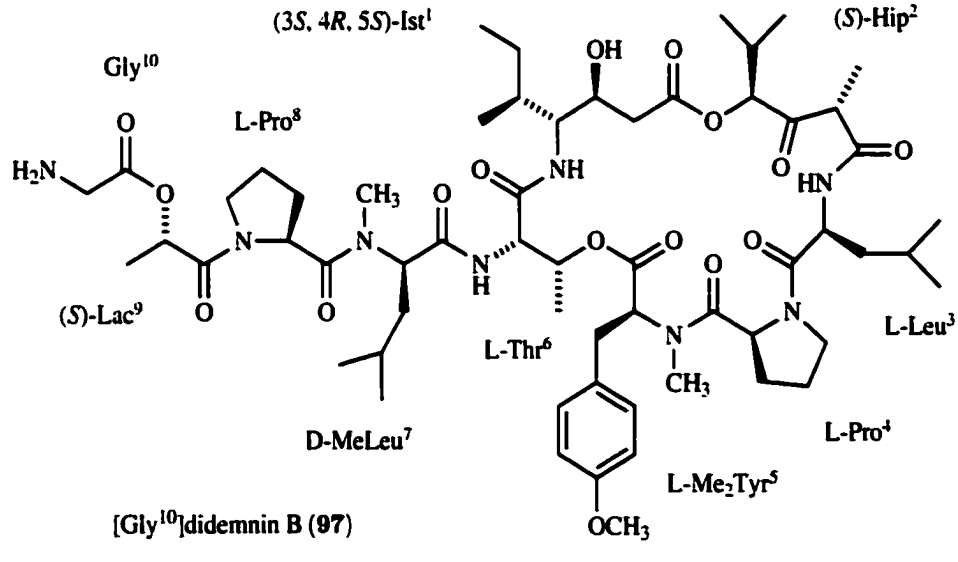

Figure 4.4: Major coupling product with the glycine linker attached to the hydroxy group of Lac[9].

Reproduced with permission of the copyright owner. Further reproduction prohibited without permission.

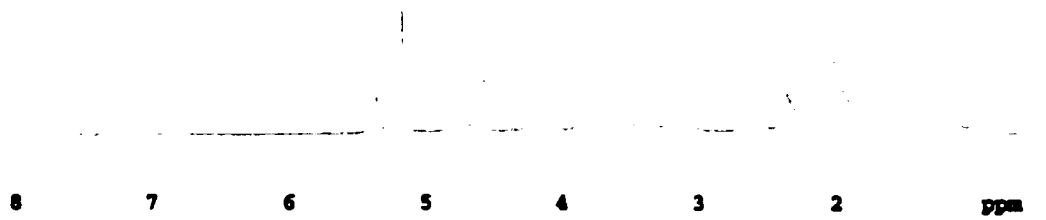

Figure 4.5: ^{1}H NMR spectrum of [Gly^{10}]didemnin B (**97**) ($CDCl_3$, 300MHz).

Deprotection of didemnin B[Fmoc-Gly^{10}] (96)

By the same methods, didemnin B[Fmoc-Gly^{10}] (**96**) was deprotected to yield the free amine, didemnin B[Gly^{10}] (**98**), Fig. 4.6 and Fig. 4.7. This molecule was not futher investigated here, but it may in the future serve as the precursor to dianestatins 2 and 3, carrying one tumor-homing peptide on the Ist^1 unit or two tumor-homing peptides on both Ist^1 and Lac^9, respectively.

Preparation of the Tumor Homing Peptide AcCNGRC (93)

The tumor homing peptide AcCNGRC · TFA Fig. 4.1 was obtained from AnaSpec Inc. San Jose, CA. Its ^{1}H NMR spectrum in DMSO is shown in Fig. 4.8.

Reproduced with permission of the copyright owner. Further reproduction prohibited without permission.

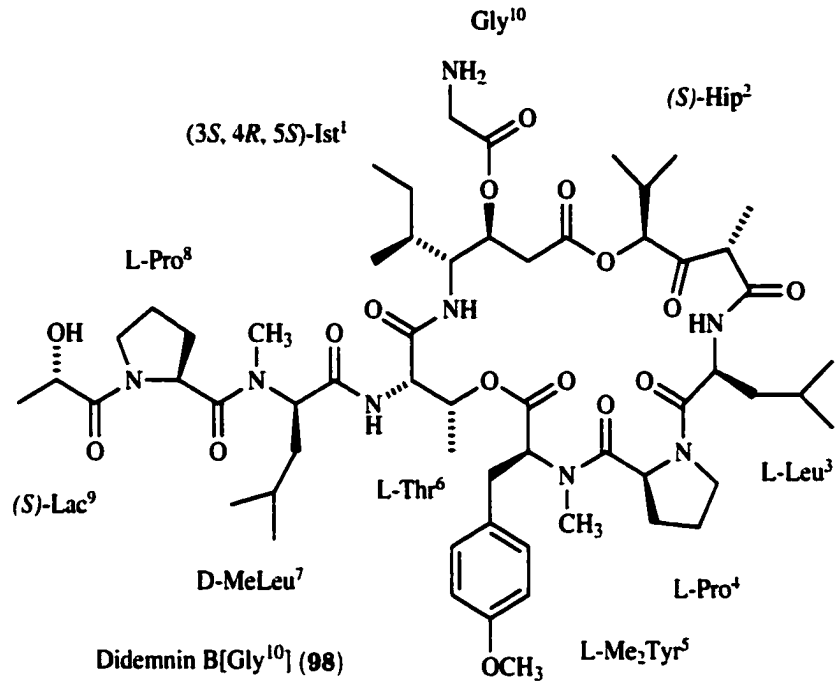

Figure 4.6: Minor coupling product with the glycine linker attached to the hydroxy group of Ist[1].

This disulfide bridged pentapeptide contains an asparagine group and thus possesses a carboxamide side chain. Due to the resistance of the carboxamide nitrogen to acylation or alkylation, this group is usually left unprotected unless one expects intramolecular side reactions with the carboxyl or amino moieties of the same asparagine unit during activation or deprotection reactions. Since the asparagine unit is separated from the carboxylic end of AcCNGRC (**93**) by two amino acids and neighbors an acylated cysteine on the amino end of AcCNGRC (**93**), this unit was left unprotected during coupling to [Gly[10]]didemnin B (**97**).

Disulfide bridges are often used in the protection of the sulfhydryl group of cysteine [345] and the disulfide bridge in AcCNGRC was assumed sufficiently stable to the reaction conditions.

AcCNGRC (**93**) also contains an arginine residue in its sequence and the three amino functionalities of the guanidine group of this amino acid form a single, monoacidic cation. Hence arginine is extremely basic and it remains protonated under the conditions of peptide synthesis and coupling of AcCNGRC (**93**) to [Gly[10]]didemnin B (**97**). Thus,

Reproduced with permission of the copyright owner. Further reproduction prohibited without permission.

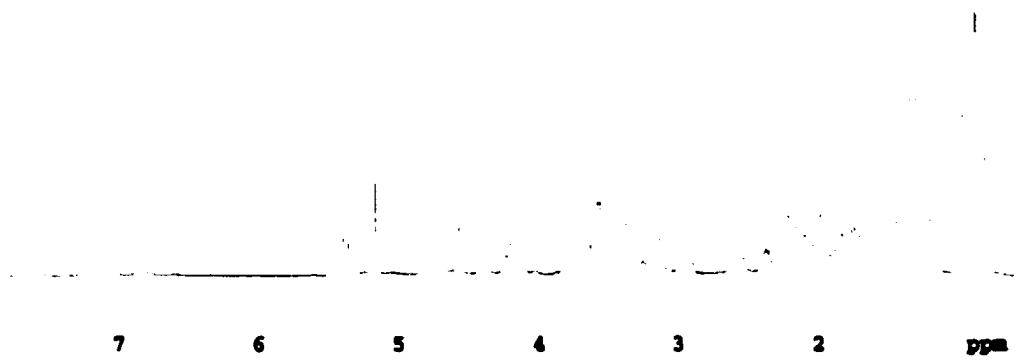

Figure 4.7: ^{1}H NMR spectrum of didemnin B[Gly^{10}] (**98**) ($CDCl_3$, 300MHz).

protonation offers sufficient protection against competing intermolecular coupling reactions at the arginine side chain, however, one has to be concerned about the counter-ion associated with the guanidine group of arginine. The tumor homing peptide AcCNGRC (**93**) was obtained as its arginine · TFA salt and the peptide was therefore converted to its arginine· HCl salt by means of an ion-exchange raisin Fig. 4.9.

Synthesis of Dianestatin 1 (102)

The synthesis of dianestatin 1 (**102**) involves the coupling of [Gly^{10}]didemnin B (**97**) to AcCNGRC· HCl (**93**) through the formation of an peptide bond between the carboxylic end of AcCNGRC and the amino functionality of [Gly^{10}]didemnin B (**97**), Fig. 4.10. Numerous coupling reagents are known that can be used in this reaction

Reproduced with permission of the copyright owner. Further reproduction prohibited without permission.

Figure 4.8: ^{1}H NMR spectrum of AcCNGRC (**93**) (DMSO-d_6, 300MHz).

and the most commonly used reagent, 1-(3-dimethylaminopropyl)-3-ethylcarbodiimide hydrochloride (EDC) was chosen. Under the normal conditions of peptide synthesis. used during the coupling of [Gly^{10}]didemnin B (**97**) and AcCNGRC· HCl (**93**), this reagent activates the carboxyl group for rapid coupling to tertiary amines, minimally affecting primary and secondary amines.

In the absence of any additives, the formation of the peptide bond occurs through the addition of the carboxyl group to the N=C double bond of the carbodiimide, Fig. 4.11, to form a *O*-acylisourea intermediate in the presence of the amine [345]. Then, the reaction can proceed via several different competing mechanisms. The first pathway, 1 Fig. 4.11, involves nucleophilic attack of the amino-component on the *O*-acylisourea intermediate giving a urea by-product which is usually easily removed. How-

Reproduced with permission of the copyright owner. Further reproduction prohibited without permission.

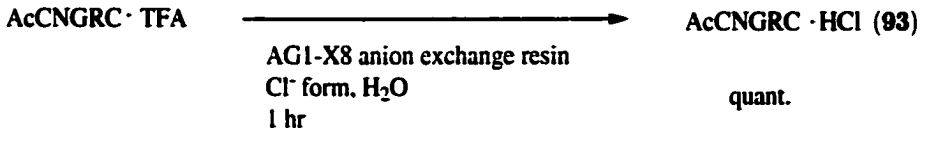

Figure 4.9: The tumor homing peptide AcCNGRC (**93**) is obtained as its arginine · TFA salt. Since TFA is a carboxylic acid, it will compete with the tumor homing peptide for coupling to [Gly^{10}]didemnin B (**97**). The peptide is therefore converted to its arginine · HCl salt by means of an ion-exchange resin.

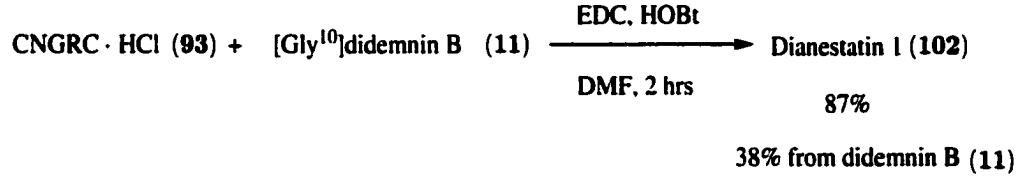

Figure 4.10: Dianestatin 1 (**102**) was synthesized by coupling AcCNGRC (**93**) to [Gly^{10}]didemnin B (**97**) using 1-(3-dimethylaminopropyl)-3-ethylcarbodiimide hydrochloride (EDC) and the auxiliary nucleophile 1-hydroxybenzotriazole (HOBt) in dimethyl formamide (DMF).

ever, an undesirable side reaction, (2) Fig. 4.11, is the intramolecular rearrangement of the *O*-acylisourea to the unreactive *N*-acylurea by-product, Fig. 4.11. In addition, over-activation by carbodiimides causes some racemization (4) of the carboxyl-terminal amino acid residue [345].

An alternative mechanism is equally important and involves reaction of the *O*-acylisourea intermediate with unreacted carboxyl-component yielding a symmetrical anhydride, (5) Fig. 4.11, also a potent acylating reagent. When two moles of carboxylic acid for each mole of carbodiimide are used, the formation of a symmetric anhydride is favored and the formation of the *N*-acylurea by-product is suppressed.

The coupling reaction using carbodiimides is markedly improved by the use of additives such as e.g. 1-hydroxybenzotriazole (HOBt), (5) Fig. 4.11 [345]. The additive is usually is an auxiliary nucleophile that is applied in equimolar amount with the carboxyl and amino components and thus two moles of nucleophiles are present for each mole of carboxyl component or carbodiimide. Therefore, the lifetime of the highly reactive *O*-acylisourea or symmetrical anhydride is significantly reduced. The nucleophilic additive is constantly regenerated and accelerates the reaction but most importantly, converts

Reproduced with permission of the copyright owner. Further reproduction prohibited without permission.

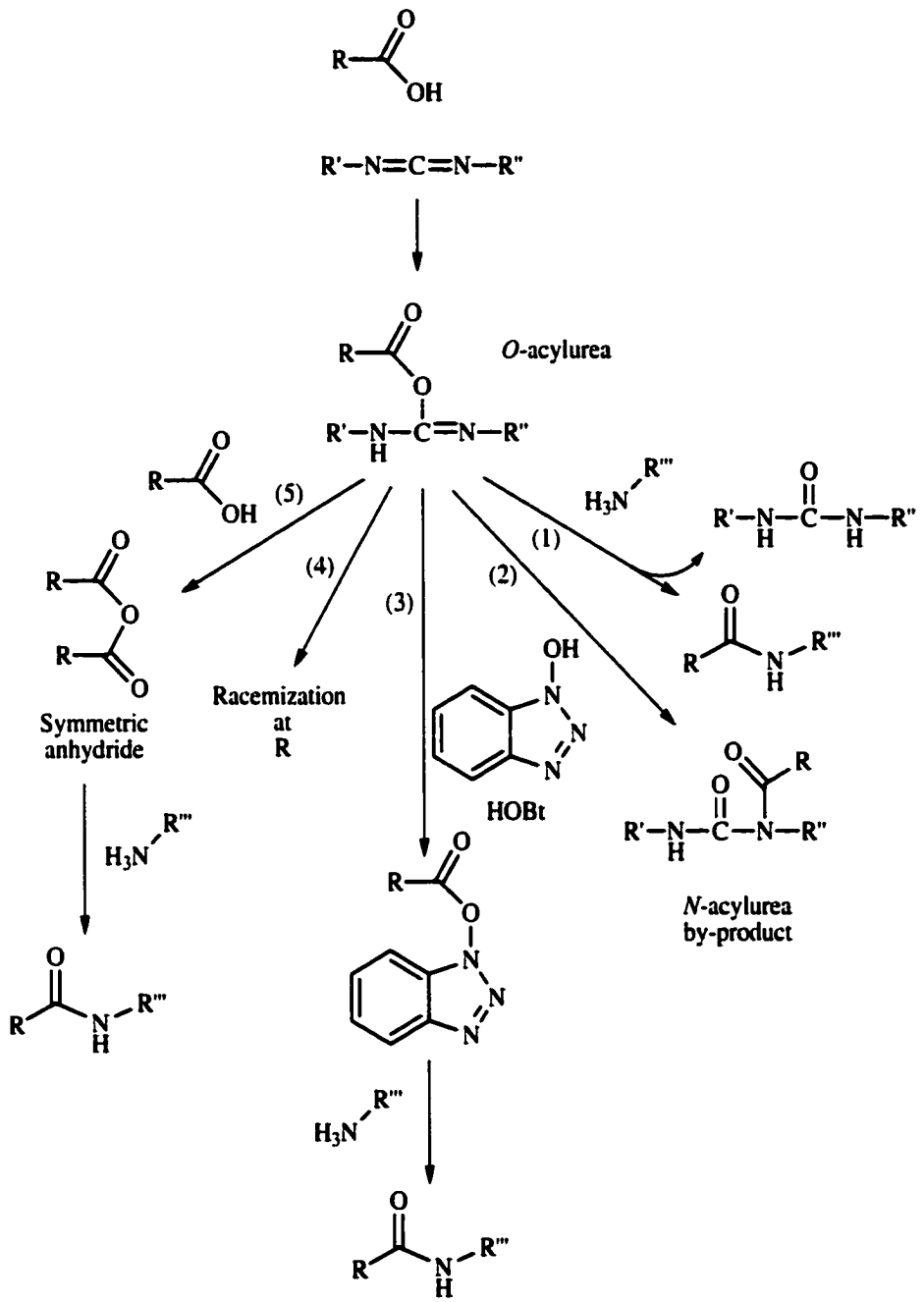

Figure 4.11: Alternative competing reaction mechanisms for the formation of a peptide bond using carbodiimide coupling reagents. Addition of HOBt suppresses the occurence of all other pathways, avoiding undesirable reactions such as racemization and *N*-acylurea formation.

Reproduced with permission of the copyright owner. Further reproduction prohibited without permission.

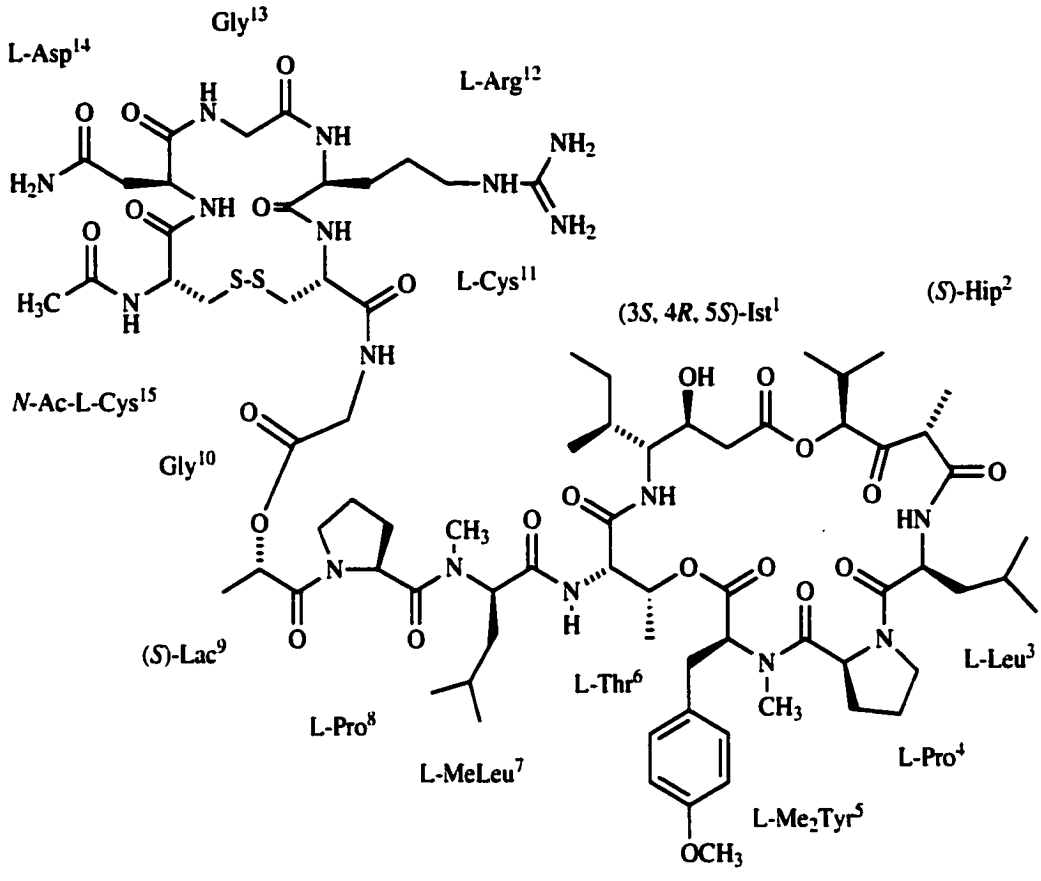

Dianestatin 1 (**102**)

Figure 4.12: Dianestatin 1 (**102**), the first conjugate between a tumor homing peptide and a marine natural product.

the overactivated intermediates into less reactive esters of the additive, thus avoiding the undesired side reactions described above.

AcCNGRC· HCl (**93**) was coupled to [Gly^{10}]didemnin B (**97**) using approximately equimolar amounts of EDC and HOBt at room temperature in DMF, Fig. 4.10 and the TFA salt of Dianestatin 1 ([[Cys^{11} →Cys^{1}5]; Ac-L-Cys^{15}-L-Arg^{14}-Gly^{13}-L-Asn^{12}-L-Cys^{11}-Gly^{10}]didemnin B (**102**)), was obtained. Dianestatin 1 (**102**), Fig. 4.13, was identified as the desired product and was fully characterized using spectroscopic techniques, especially extensive 2D NMR experiments such as gHMQC, gHMBC, TOCSY, and ROESY, Table 4.2.

Reproduced with permission of the copyright owner. Further reproduction prohibited without permission.

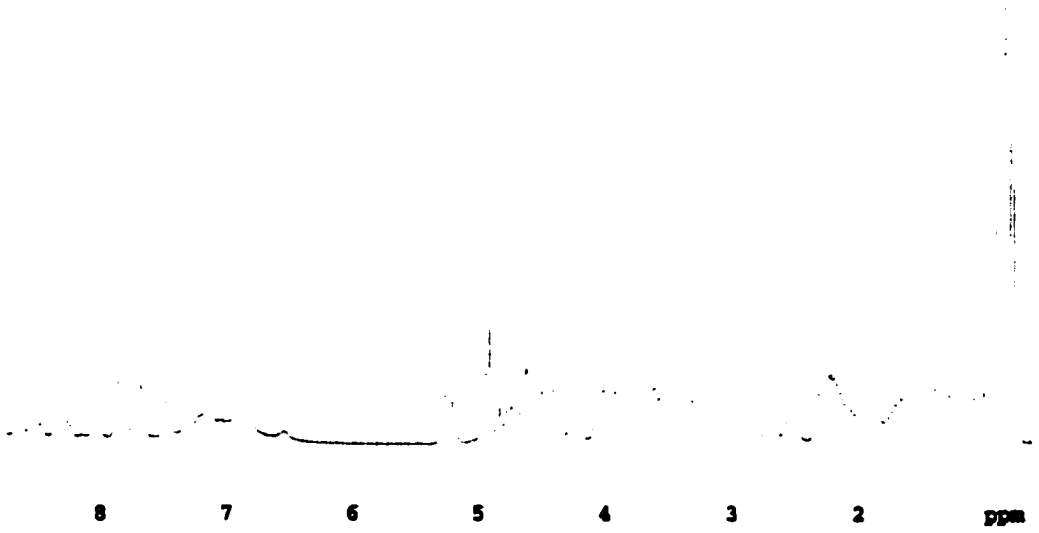

Figure 4.13: ^{1}H NMR spectrum of dianestatin 1 (**102**) (DMSO-d_6, 300MHz).

4.2.2 Cytotoxicities of Dianestatin 1 and [Gly^{10}]didemnin B

Since the synthesis of dianestatin 1 (**102**) involves the coupling of [Gly^{10}]didemnin B (**97**) to the tumor homing peptide AcCNGRC (**93**), the cytotoxic activities of dianestatin 1 (**102**), [Gly^{10}]didemnin B (**97**) and didemnin B (**11**) were assessed by means of colony forming assays using the human colon adenocarcinoma HCT 116. The cytotoxic potencies of didemnin B (**11**) and [Gly^{10}]didemnin B (**97**) are practically identical with IC_{50} values of 0.4 ng/mL and 0.3 ng/mL respectively, Table 4.1. Dianestatin 1 (**102**) is an order magnitude less potent with an IC_{50} value of 16.4 ng/mL. The obtained dose-response curves for the three drugs are shown in Fig. 4.14.

Reproduced with permission of the copyright owner. Further reproduction prohibited without permission.

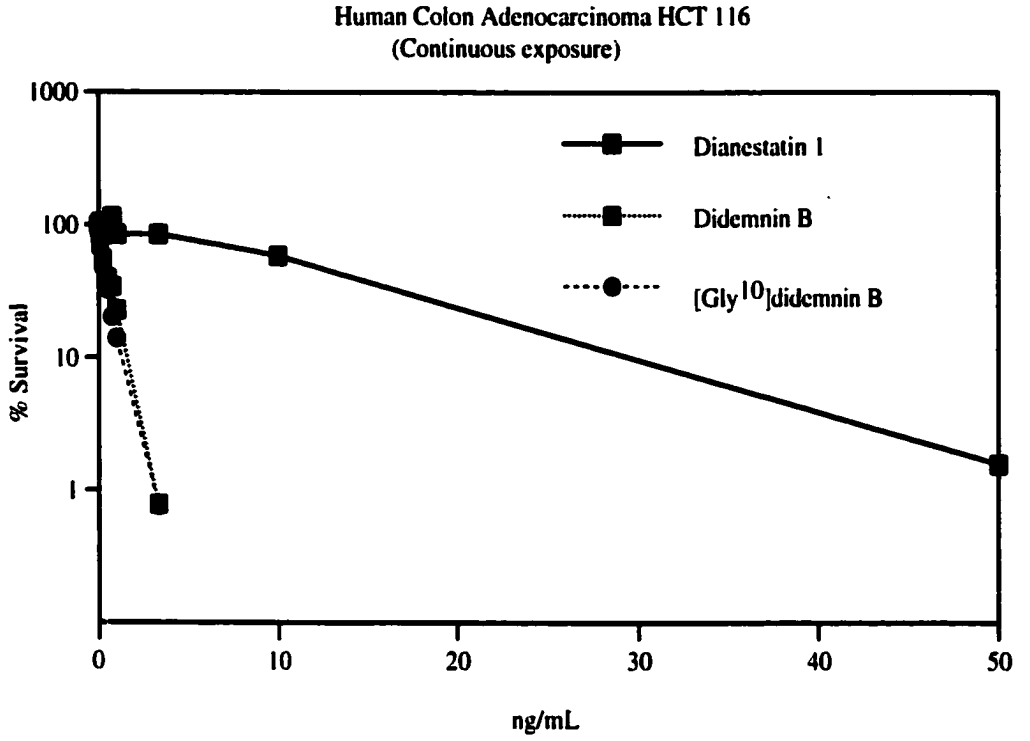

Figure 4.14: Clonogenic (colony forming) assays show that didemnin B (**11**), [Gly^{10}]didemnin B (**97**), and dianestatin 1 (**102**) inhibit proliferation of human colon adenocarcinoma (HCT 116) cells in a concentration-dependent manner.

Table 4.1: IC_{50} values for Didemnin B (**11**), [Gly^{10}]didemnin B (**97**), and Dianestatin 1 (**102**), determined by clonogenic (colony forming) assays using human colon adenocarcinoma HCT 116.

Compound	ng/mL
Didemnin B (**11**)	0.4
[Gly^{10}]didemnin B (**97**)	0.3
Dianestatin 1 (**102**)	16.4

Reproduced with permission of the copyright owner. Further reproduction prohibited without permission.

Table 4.2: NMR Assignments for Dianestatin 1 (**102**).

(3*S*, 4*R*, 5*S*)-Ist[1]						
CO	171.1	(C)				3.40, 4.90
1	39.5	(CH_2)	2.29	(m, 1H)	3.40, 3.78	2.29
			3.40	(m, 1H)		
2	65.8	(CH)	3.78	(m, 1H)	2.29, 6.91	0.86, 0.89, 1.14
						1.24, 2.29, 3.76
3	54.8	(CH)	3.78	(m, 1H)		0.86
4	33.2	(CH)	1.87	(m, 1H)	0.86, 0.89	
5	27.2	(CH_2)	1.24	(m, 1H)	0.89, 1.14	0.86, 0.89
			1.14	(m, 1H)	0.89, 1.24	
6	12.0	(CH_3)	0.89	(m, 3H)	1.14, 1.24	1.14, 1.24
7	13.9	(CH_3)	0.86	(d, 6.6, 3H)	1.87	1.14, 1.24
NH			6.91	(br d, 9.6, 1H)	3.78	
(S)-Hip[2]						
CO	168.3	(C)				1.16, 3.93
α	48.0	(CH)	3.93	(q, 6.9, 1H)	1.16	1.16
α-CH_3	15.1	(CH_3)	1.16	(d, 6.6, 3H)	3.93	3.93
CO	204.6	(C)				1.16, 3.93, 4.90
α	79.9	(CH)	4.90	(d, 3.6, 1H)	2.21	0.77, 0.83
β	29.5	(CH)	2.21	(m, 1H)	4.90	0.77, 0.83, 4.90
β-CH_3	16.6	(CH_3)	0.77	(d, 6.6, 3H)	2.21	4.90
β-CH_3	18.9	(CH_3)	0.83	(d, 6.6, 3H)	2.21	4.90
L-Leu3						
CO	168.6	(C)				7.85
α	48.5	(CH)	4.63	(m, 1H)	7.85, 1.08	
β	40.4	(CH_2)	1.08	(m, 1H)	1.47	0.86
			1.47	(m, 1H)	1.08	
γ	24.1	(CH)	1.47	(m, 1H)	0.86	
γ-CH_3	20.5	(CH_3)	0.86	(d, 6.6, 3H)	1.47	0.86
γ-CH_3	23.6	(CH_3)	0.86	(d, 6.6, 3H)	1.47	0.86
NH			7.85	(br d, 8.7, 1H)	4.63	
L-Pro[4]						
CO	169.9	(C)				2.54
α	56.9	(CH)	4.61	(m, 1H)	1.47, 2.15	
β	27.4	(CH_2)	1.47	(m, 1H)	4.61	4.61
			2.15	(m, 1H)	4.61	
γ	25.1	(CH_2)	1.96	(m, 2H)	2.15	
			1.55	(m, 2H)		
delta	46.7	(CH_2)	3.60	(m, 2H)	3.46	
			3.46	(m, 2H)	3.60	
L-Me^2Tyr[5]						
CO	(C)					
α	62.4	(CH)	4.00	(m, 1H)	2.98, 3.18	2.54

...continued on next page

Reproduced with permission of the copyright owner. Further reproduction prohibited without permission.

...continued from previous page

β	33.4	(CH_2)	3.18	(m, 1H)	2.98	4.00, 7.15
			2.98	(m, 1H)	3.18	
γ	130.0	(C)				2.98, 3.18, 6.87, 7.15
δ	130.6	(CH)	7.15	(d, 8.4, 2H)	6.87	6.87, 7.15
ϵ	113.7	(CH)	6.87	(d, 8.4, 2H)	7.15	6.87, 7.15
ζ	158.0	(C)				6.87, 7.15, 3.72
γ-CH_3	55.0	(CH_3)	3.72	(s, 3H)		
N-CH_3	38.1	(CH_3)	2.54	(s, 3H)		4.00
L-Thr[6]						
CO	168.2	(C)				4.93
α	57.0	(CH)	4.38	(m, 1H)	4.93	4.93, 1.22
β	69.8	(CH)	4.93	(m, 1H)	4.38	4.38, 1.22
β-CH_3	16.2	(CH_3)	1.22	(d, 6.3, 3H)	4.93	4.38
NH			7.68	(br s, 1H)	4.38	
D-MeLeu[7]						
CO	171.2	(C)			5.21, 7.68	
α	53.6	(CH)	5.21	(d, 4.8, 1H)	1.69, 1.62	3.03
β	36.0	(CH_2)	1.69	(m, 1H)	5.21	0.79, 0.86
			1.62	(m, 1H)	5.21	
γ	24.3	(CH)	1.33	(m, 1H)	0.79, 0.86	
β-CH_3	23.6	(CH_3)	0.86	(d, 6.6, 3H)	1.33	0.79
β-CH_3	21.0	(CH_3)	0.79	(d, 6.6, 3H)	1.33	0.86
N-CH_3	30.6	(CH_3)	3.03	(s, 3H)		5.21
L-Pro[8]						
CO	172.4	(C)			2.21, 3.03, 4.75	
α	56.3	(CH)	4.75	(br t, 6.6, 1H)	1.78, 2.21	
β	28.2	(CH_2)	1.78	(m, 1H)		4.75
			2.21	(m, 1H)		
γ	25.2	(CH_2)	1.94	(m, 1H)		
			2.09	(m, 1H)		
γ	46.8	(CH_2)	3.51	(m, 1H)		
			3.74	(m, 1H)		
(S)-Lac[9]						
CO	168.3	(C)				1.34, 3.74
α	68.5	(CH)	5.24	(br q, 6.6, 1H)	1.34	1.34
α-CH_3	15.7	(CH_3)	1.34	(d, 6.9, 3H)	5.24	5.24
Gly[10]						
CO	170.3	(C)				3.78, 4.00, 8.53
α	40.2	(CH_2)	3.78	(m, 1H)	8.53	
			4.00	(m, 1H)	8.53	
NH			8.53	(br t, 7.2, 1H)	3.78, 4.00	170.3
L-Cys[11]						
CO	171.6					8.03, 4.52

...continued on next page

Reproduced with permission of the copyright owner. Further reproduction prohibited without permission.

...continued from previous page

α	51.5	(CH)	4.52	(br t, 6.0, 1H)	8.03, 3.24, 3.03	
β	40.8	(CH_2)	3.24	(m, 2H)	4.52	
			3.03	(m, 2H)	4.52	
NH			8.03	(d, 8.1, 1H)	4.52	
L-Arg[12]						
CO	169.6	(C)				7.72
α	51.7	(CH)	4.38	(m, 1H)	7.72	
β			1.47	(m, 1H)	1.94	
			1.94	(m, 1H)	1.47	
γ	24.5	(CH_2)	1.47	(m, 2H)	3.08, 1.94	
δ	40.4	(CH_2)	3.08	(m, 2H)	7.50	
ϵ-NH			7.50	(br d, 6.0, 1H)	3.08	
ζ	156.6	(C)				3.08
ζ-(NH_2)$_2$			7.00	(very br s, 4H)		
NH			7.72	(d, 8.7, 1H)	4.38	
Gly[13]						
CO	169.8	(C)				3.40, 4.23
α	42.7	(CH_2)	4.23	(dd, 16.5, 8.1, 1H)	7.85	
			3.40	(m, 1H)	7.85	
NH			7.85	(br d, 8.7, 1H)	3.40, 4.23	
L-Asn[14]						
CO	170.6	(C)			2.29, 2.71, 4.52, 8.65	
α	49.5	(CH)	4.52	(br t, 7.2, 1H)	8.65, 2.71, 2.29	2.29, 2.71
β	36.2	(CH_2)	2.29	(m, 1H)	4.52	4.52
			2.71	(dd, 15.6, 7.4, 1H)	4.52	
γ	171.6	(C)				2.29, 2.71
γ-NH_2			6.82	(s, 1H)	7.30	
			7.30	(s, 1H)	6.82	
NH			8.65	(br d, 7.5, 1H)	4.52	
N-Ac-L-Cys[15]						
CO						
α	52.9	(CH)	4.40	(m, 1H)	8.33, 3.18, 2.88	
β	40.7	(CH_2)	2.88	(m, 1H)	4.40	
			3.18	(m, 1H)	4.40	
NH			8.33	(br d, 7.8, 1H)	4.40	
N-CO	169.9	(C)				1.87, 8.33
CH_3	22.5	(CH_3)	1.87	(s, 3H)		

a) ^{1}H and ^{13}C NMR shifts were referenced to $CDCl_3$ (^{1}H δ 7.27 and ^{13}C δ 77.2 ppm).

Reproduced with permission of the copyright owner. Further reproduction prohibited without permission.

4.3 Discussion

This chapter describes the (semi-)synthesis of dianestatin 1 (**102**), the first conjugate between a marine natural product and a tumor homing peptide. The starting material in the synthesis of dianestatin 1 (**102**) is didemnin B (**11**), a secondary metabolite originally isolated from the Caribbean ascidian *Tridemnum solidum* [44] (For more details see Chapter II). Didemnin B (**11**) is a potent, but non-selective cytotoxin, acting through the inhibition of protein synthesis and to a lesser extent inhibition of DNA and RNA synthesis [132,346,347]. After many years of extensive preclinical and clinical evaluation, didemnin B (**11**) eventually failed to show efficacy as an anticancer drug, due to a lack of selectivity for cancer cells over normal healthy tissues.

The tumor homing peptide, which comprises the second part of dianestatin 1 (**102**), is AcCNGRC (**93**). This disulfide bridged pentapeptide homes specifically to the vasculature of murine and human tumors in a mouse model due to a high affinity for its receptor, the aminopeptidase N or CD13, which is overexpressed on tumor vasculature [340]. Homing peptides like AcCNGRC have been shown to be effective agents for the delivery of cytotoxic molecules, phage particles and whole cells to the vasculature of specific tissues including tumors. AcCNGRC coupled to the anticancer drug doxorubicin specifically homed to the vasculature of various human and murine tumors in mice, reducing the toxicity of the drug and enhancing its efficacy [14].

The synthesis of dianestatin 1 (**102**) was undertaken to test the following hypotheses. First, by coupling a tumor homing peptide to a potent but non-selective cytotoxin, such as didemnin B (**11**), an effective anticancer agent can be created that selectively homes to the tumor vasculature and accumulates there. This concept is based on the discovery that tumor vasculature expresses specific marker molecules that are not expressed in normal resting blood vessels since they are not undergoing angiogenesis. Since the tumor vasculature is normally the only tissue with affinity for the conjugate, it is hoped that a much lower dose may give the desired response level.

The coupling of AcCNGRC (**93**) to didemnin B (**11**) was accomplished using a glycine linker unit [344], yielding an ester bond between glycine and didemnin B (**11**) and an amide bond between AcCNGRC (**93**) and glycine. Preliminary testing has shown

Reproduced with permission of the copyright owner. Further reproduction prohibited without permission.

that coupling of the non-selective cytotoxin didemnin B (**11**) to a tumor homing peptide reduced its toxicity by an order of magnitude. Dianestatin 1 (**102**) awaits further *in vitro* and *in vivo* testing in order to evaluate stability, tumor targeting ability and potency.

4.4 Experimental

[Fmoc-Gly^{10}]didemnin B, didemnin B[Fmoc-Gly^{10}] (95-96). Under a dry, argon atmosphere, a mixture of 70 mg (151.1 μmol) *N*-(9-fluorenylmethoxycarbonyl)glycine pentafluorophenyl ester, Fmoc-Gly-OPfp (**94**) (Calbiochem-Novabiochem Corp., La Jolla, CA) and 56 mg (50.4 μmol) didemnin B (**11**), (National Cancer Institute, Bethesda, MD) in 500 μL dry dimethylformamide (DMF) was stirred in the presence of a catalytic amount (1 mg, 5.0 μmol) of dimethylaminopyridine (DMAP) for 6 days. The desired [Fmoc-Gly^{10}]didemnin B (36 mg, yield 51%) was separated from didemnin B[Gly^{10}-Fmoc] (4 mg, yield 6%) and the reaction mixture by reversed phase (C_{18}) HPLC using 15% H_2O in MeOH.

[Gly^{10}]didemnin B (97). [Fmoc-Gly^{10}]didemnin B (**95**, 30 mg, 21.6 μmol) was dissolved in 500μL dry DMF and 12 μL of a 20% piperidine solution in dry DMF (25.9 μmol, 1.2 eq.) was added. The mixture was stirred under argon for 20 minutes. The reaction was quenched by acidification with 1 mL CH_3CN (0.1% TFA). The solvents were evaporated *in vacuo* at a bath temperature no higher than 35°C and the TFA salt of [Gly^{10}]didemnin B (**97**) was purified by reversed phase (C_{18}) HPLC using 45% H_2O in CH_3CN (0.1% TFA, 24 mg, yield 86%). The TFA salt of [Gly^{10}]didemnin B (**97**) was dissolved in a minimum amount of CH_3CN and poured into a saturated $NaHCO_3$ solution. The aqueous solution was extracted three times with 10% isopropanol in dichloromethane. The organic fractions were combined, washed with brine, dried over $MgSO_4$ and the solvents were removed *in vacuo* (22 mg, quant, yield from **11**: 38%).

[Gly^{10}]didemnin B (**97**) was isolated as a white, amorphous solid. HRFABMS (NBA/CsI matrix) *m/z* 1301.5629 $[MCs]^+$, calcd for $C_{59}H_{92}N_8O_{16}$, 1301.5686 (Δ = 4.4 ppm); ^{1}H NMR ($CDCl_3$) is shown in Fig. 4.5.

Didemnin B[Gly^{10}] (98). Didemnin B[Fmoc-Gly^{10}] (**96**, 19 mg, 14.3 μmol) was dissolved in 500μL dry DMF and 6.5 μL of a 20% piperidine solution in dry DMF

Reproduced with permission of the copyright owner. Further reproduction prohibited without permission.

(17.2 μmol, 1.2 eq.) was added. The mixture was stirred under argon for 20 minutes. The reaction was quenched by acidification with 1 mL CH_3CN (0.1% TFA). The solvents were evaporated *in vacuo* at a bath temperature no higher than 35°C and the TFA salt of didemnin B[Gly^{10}] (**98**) was purified by reversed phase (C_{18}) HPLC using 45% H_2O in CH_3CN (0.1% TFA, 9 mg, yield 56%). The TFA salt of didemnin B[Gly^{10}] (**98**) was dissolved in a minimum amount of CH_3CN and poured into a saturated $NaHCO_3$ solution. The aqueous solution was extracted three times with 10% isopropanol in dichloromethane. The organic fractions were combined, washed with brine, dried over $MgSO_4$ and the solvents were removed *in vacuo* (8 mg, quant, yield from **11**: <1%).

Didemnin B[Gly^{10}] (**98**) was isolated as a white, amorphous solid. ^{1}H NMR ($CDCl_3$) is shown in Fig. 4.7.

AcCNGRC·HCl (93). The TFA salt of synthetic AcCNGRC ([Ac-Cys^1 → Cys^5]; *N*-Ac-L-Cys^1-L-Asn-Gly-L-Arg-L-Cys^5, 21.6 mg, AnaSpec Inc., San Jose, CA) was dissolved in 10 mL H_2O. Then, 0.55 g AG1-X8 strong anion exchange resin (Bio-Rad Laboratories, Hercules, CA), in the Cl^--form, was added. The mixture was stirred for 1 hour, filtered over fresh resin and the remaining aqueous solution of AcCNGRC·HCl (**93**) was lyophilized (20 mg, quant.).

Dianestatin 1 (102). AcCNGRC·HCl (**93**) (11 mg, 16.9 μmol) was dissolved in 350 μL dry DMF. 1-(3-Dimethylaminopropyl)-3-ethylcarbodiimide hydrochloride (EDC, 12 mg, 23.1 μmol) and 1-hydroxybenzotriazole (HOBt, 3 mg, 23.1 μmol) were added to the reaction mixture, which was stirred for approximately 30 minutes. [Gly^{10}]didemnin B (**97**) was added with an additional 150 μL dry DMF. The mixture was stirred for 1 hour. Dianestatin 1 (**102**) ([[Cys^{11} →Cys^{1}5]; L-Cys^{15}-L-Arg^{14}-Gly^{13}-L-Asn^{12}-L-Cys^{11}-Gly^{10}]didemnin B, 29 mg, 87%.) was purified from the reaction mixture by reversed phase (C_{18}) HPLC using 53% H_2O in CH_3CN (0.1% TFA).

Dianestatin 1 (**102**) was isolated as a white amorphous solid. $[\alpha]_D$ = -45°, c = 0.08; HRFABMS (NBA/CsI matrix) m/z 1874.7337 $[MCs]^+$, calcd for $C_{79}H_{123}N_{17}O_{23}S_2$, 1874.7474 ($\Delta$ = 7.3 ppm); ^{1}H and ^{13}C NMR data ($CDCl_3$) are shown in Table 4.2.

Clonogenic Assays. Cytotoxicity of dianestatin 1 (**102**), [Gly^{10}]didemnin B (**97**), and the parent compound didemnin B (**11**) were evaluated using clonogenic (colony

Reproduced with permission of the copyright owner. Further reproduction prohibited without permission.

forming) assays. Human colon adenocarcinoma cells (HCT 116) growing in log-phase in IMDM medium (Iscove's Modified Dulbecco's Medium, 25mM HEPES buffer, Irvine Scientific, Santa Ana, CA) containing 10% Fetal Calf Serum (FCS) and L-Glu, were harvested by trypsinization (5 minutes at 37°C). The cells were pelleted and resuspended in fresh medium. The cells, approximately 200 per well containing 3 mL fresh medium each, were grown under continuous exposure to dianestatin 1 (**102**), [Gly^{10}]didemnin B (**97**), and didemnin B (**11**). The assay was run in triplicate and concentrations ranged from 0-10 ng/mL. Percent survival was measured by counting the number of colonies (>100 cells) after 7 days.

Reproduced with permission of the copyright owner. Further reproduction prohibited without permission.

Bibliography

[1] R.C. Brusca and G.J. Brusca. *Invertebrates.* Sinauer Associates, Inc. Publishers, Sunderland, Massachusetts, 1990.

[2] N.L. Lindquist. *Secondary Metabolite Production and Chemical Adaptations in the Class Ascidiacea.* PhD thesis, University of San Diego, California, 1989.

[3] N. Lindquist, W. Fenical, G.D. Van Duyne, and J. Clardy. Isolation and structure determination of diazonamides A and B, unusual cytotoxic metabolites from the marine ascidian *Diazona chinensis. J. Am. Chem. Soc.*, 113(6):2303–2304, 1991.

[4] D.J. Faulkner. Marine natural products. *Nat. Prod. Rep.*, 3(1):1–33, 1986.

[5] D.J. Faulkner. Marine natural products. *Nat. Prod. Rep.*, 4(5):539–576, 1987.

[6] D.J. Faulkner. Marine natural products. *Nat. Prod. Rep.*, 5(6):613–663, 1988.

[7] D.J. Faulkner. Marine natural products. *Nat. Prod. Rep.*, 7(4):269–309, 1990.

[8] D.J. Faulkner. Marine natural products. *Nat. Prod. Rep.*, 8(2):97–147, 1991.

[9] D.J. Faulkner. Marine natural products. *Nat. Prod. Rep.*, 10(5):497–539, 1993.

[10] D.J. Faulkner. Marine natural products. *Nat. Prod. Rep.*, 13(2):75–125, 1996.

[11] D.J. Faulkner. Marine natural products. *Nat. Prod. Rep.*, 15(2):113–158, 1998.

[12] R. Pasqualini and E. Ruoslahti. Tissue targeting with phage peptide libraries. *Mol. Psych.*, 1(6):423–423, 1996.

[13] R. Pasqualini and E. Ruoslahti. Organ targeting *in vivo* using phage display peptide libraries. *Nature*, 380(6572):364–366, 1996.

[14] W. Arap, R. Pasqualini, and E. Ruoslahti. Cancer treatment by targeted drug delivery to tumor vasculature in a mouse model. *Science*, 279(5349):377–380, 1998.

[15] W. Fenical. Marine biodiversity and the medicine cabinet; the status of new drugs from marine organisms. *Oceanography*, 9:23–27, 1996.

[16] F. Monniot, F. Monniot, and P. Laboute. *Coral Reef Ascidians of New Caledonia.* Editions de l'ORSTOM, Institut Français de Recherche Scientifique pour le Développement en Coopération, 1991.

Reproduced with permission of the copyright owner. Further reproduction prohibited without permission.

[17] S.L. Schreiber. Chemical genetics resulting from a passion for synthetic organic chemistry. *Bioorg. Med. Chem.*, 6(8):1127–1152, 1998.

[18] B.S. Davidson. Ascidians; producers of amino acid derived metabolites. *Chem. Rev.*, 93(5):1771–1791, 1993.

[19] M.M. Sigel, L.L. Wellham, W. Lichter, L.E. Dudeck, J.L. Gargus, and A.H. Lucas. Anticellular and antitumor activity of extracts from tropical marine invertebrates. In H.W. Younghen Jr., editor, *Food-Drugs from the Sea. Proceedings 1969*, pages 281–294, Washington, D.C., 1970. Marine Technology Soc.

[20] T.G. Holt. PhD thesis, University of Illinois, Urbana, 1986.

[21] K.L. Rinehart, T.G. Holt, N.L. Fregeau, J.G. Stroh, P.A. Keifer, F. Sun, L.H. Li, and D.G. Martin. Ecteinascidin 729, 743, 745, 759A, 759B, 770: Potent antitumor agents from the Caribbean tunicate *Ecteinascidia turbinata*. *J. Org. Chem.*, 55(15):4512–4515, 1990.

[22] A.E. Wright, D.A. Forleo, G.P. Gunawardana, S.P. Gunasekera, F.E. Koehn, and O.J. McConnell. Antitumor tetrahydroisoquinoline alkaloids from the colonial ascidian *Ecteinascidia turbinata*. *J. Org. Chem.*, 55(15):4508–4512, 1990.

[23] J.M. Reid, D.L. Walker, and M.M. Ames. Preclinical pharmacology of ecteinascidin 729, a marine natural product with potent antitumor activity. *Cancer Chemother. Pharm.*, 38(4):329–334, 1996.

[24] W. Lichter, A. Ghaffar, L.L. Wellham, and M.M. Sigel. Immunomodulation by extracts of *Ecteinascidia turbinata*. In *Drugs & Food from the Sea. Myth or Reality?*, pages 137–144, Norman, OK, 1978. Univ. Oklahoma.

[25] T. Arai, K. Takahashi, and A. Kubo. New antibiotics saframycins A, B, C, D and E. *J. Antibiot.*, 30(11):1015–1018, 1977.

[26] R. Sakai, K.L. Rinehart, Y. Guan, and A.H. Wang. Additional antitumor ecteinascidins from a Caribbean tunicate: crystal structures and activities *in vivo*. *Proc. Natl. Acad. Sci. USA*, 89(23):11456–11460, 1992.

[27] K.L. Rinehart, L.G. Gravalos, G. Faircloth, and J. Jimeno. Preclinical antitumor development of a marine derived natural product. *Proc. Am. Assoc. Cancer Res.*, 36:2322, 1995.

[28] Y. Pommier, G. Kohlhagen, C. Bailly, M. Waring, A. Mazumder, and K.W. Kohn. DNA sequence- and structure-selective alkylation of guanine N2 in the DNA minor groove by ecteinascidin 743, a potent antitumor compound from the Caribbean Tunicate *Ecteinascidia turbinata*. *Biochemistry*, 35(41):13303–13309, 1996.

[29] M. Ghielmini, E. Colli, E. Erba, D. Bergamaschi, S. Pampallona, J. Jimeno, G. Faircloth, and C. Sessa. *In vitro* schedule-dependency of myelotoxicity and cytotoxicity of ecteinascidin 743 (ET-743). *Annals Oncol.*, 9(9):989–993, 1998.

Reproduced with permission of the copyright owner. Further reproduction prohibited without permission.

[30] M. Garcia Rocha, M. Garcia Gravalos, and J. Avila. Characterisation of antimitotic products from marine organisms that disorganise the microtubule network: Ecteinascidin 743, isohomohalichondrin B and LL-15. *Brit. J. Cancer*, 73(8):875–883, 1996.

[31] R. Sakai, E.A. Jares-Erijman, I. Manzanares, M.V.S. Elipe, and K.L. Rinehart. Ecteinascidins: Putative biosynthetic precursors and absolute stereochemistry. *J. Am. Chem. Soc.*, 118(38):9017–9023, 1996.

[32] A. Lansiaux and C. Bailly. Ecteinascidin 743. *Bull. Cancer*, 86(2):139–141, 1999.

[33] M. Riofrio, A. Taamma, B. McKranter, F. Goldwasser, J. Jimeno, C. Jasmin, J.L. Misset, and E. Cvitkovic. Ecteinascidin-743 (ET-743) 24 hours continuous infusion (CI): Clinical and pharmacokinetic phase I study progressive report. *Annals Oncol.*, 9(4):133–133, 1998.

[34] A. Bowman, C. Twelves, K. Hoekman, A. Simpson, J. Smyth, J. Vermorken, F. Hoppener, J. Beijnen, E. Vega, J. Jimeno, and A.R. Hanauske. Phase I clinical and pharmacokinetic (PK) study of ecteinascidin-743 (ET-743) given as a one hour infusion every 21 days. *Annals Oncol.*, 9(2):118–118, 1998.

[35] M.J.X. Hillebrand, J. Jimeno, E. Cvitkovic, K. Hoekman, F. Hoppener, C. Twelves, M. Villalona, H. Rosing, and J.H. Beijnen. Pharmacokinetics of ecteinascidin-743 (ET-743) in three phase I studies. *Annals Oncol.*, 9(2):119–119, 1998.

[36] E. Cvitkovic, B. Mekranter, A. Taamma, F. Goldwasser, J.H. Beijnen, J. Jimeno, M. Riofrio, E. Vega, J.L. Misset, and P. Hop. Ecteinascidin-743 (ET-743) 24 hour continuous intravenous infusion (CI) phase I study in solid tumors (ST) patients. *Annals Oncol.*, 9(2):119–119, 1998.

[37] C.J. Twelves, J. Vermorken, A. Bowman, A. Simpson, J. Smyth, F. Hoppener, J. Beijnen, J. Jimeno, and A.R. Hanauske. Phase I and pharmacokinetic study of ecteinascidin- 743 (ET-743) given as a one hour infusion every 21 days. *Eur. J. Cancer*, 33(8):1107–1107, 1997.

[38] A. Taamma, E. Cvitkovic, J. Jimeno, M. Gasparetto, K. Meeley, E. Vega, L. Cameron, and J.L. Misset. Phase I clinical study of ecteinascidin-743 (ET-743) as a 24 hours continuous intravenous infusion (CI) in patients (pts) with solid tumors (ST): A progress report. *Eur. J. Cancer*, 33(8):1119–1119, 1997.

[39] E. Izbicka, R. Lawrence, E. Raymond, G. Eckhardt, G. Faircloth, J. Jimeno, G. Clark, and D.D. Von Hoff. *In vitro* antitumor activity of the novel marine agent, ecteinascidin-743 (ET-743, NSC-648766) against human tumors explanted from patients. *Annals Oncol.*, 9(9):981–987, 1998.

[40] G. Valoti, M.I. Nicoletti, A. Pellegrino, J. Jimeno, H. Hendriks, M. D'Incalci, G. Faircloth, and R. Giavazzi. Ecteinascidin-743, a new marine natural product with potent antitumor activity on human ovarian carcinoma xenografts. *Clin. Cancer Res.*, 4(8):1977–83, 1998.

Reproduced with permission of the copyright owner. Further reproduction prohibited without permission.

[41] B.V. SirDeshpande and P.L. Toogood. Constitution of ribosomal complex in presence of didemnin B, an inhibitor of protein synthesis. *FASEB J.*, 10(6):2355–2355, 1996.

[42] B.V. SiDeshpande and P.L. Toogood. Didemnin B inhibits polypeptide elongation in cell- free translation systems. *FASEB J.*, 7(7):A1083–A1083, 1993.

[43] K.L. Rinehart Jr., J.B. Gloer, R.G. Hughes Jr., H.E. Renis, J.P. McGovren, E.B. Swynenberg, D.A. Stringfellow, S.L. Kuentzel, and L.H. Li. Didemnins: antiviral and antitumor depsipeptides from a Caribbean tunicate. *Science*, 212(4497):933–935, 1981.

[44] K.L. Rinehart Jr., J.B. Gloer, J.C.Jr. Cook, S.A. Mizsak, and T.A. Scahill. Structures of the didemnins, antiviral and cytotoxic depsipeptides from a caribbean tunicate. *J. Am. Chem. Soc.*, 103(7):1857–1859, 1981.

[45] K.L. Rinehart. U.S. Patent 4,493,796. 1985.

[46] K.L. Rinehart. U.S. Patent 4,548,814. 1985.

[47] M. Guyot, D. Davoust, and E. Morel. Isodidemnine I, a cytotoxic cyclodepsipeptide isolated from the tunicate, *Tridemnum cyanophorum* (Didemnidae). *Comptes Rendus Ac. Sci. Serie II*, 305(8):681–686, 1987.

[48] J.B. Gloer. PhD thesis, University of Illinois, Urbana, IL, 1983.

[49] R.E. Gutowsky. Master's thesis, University of Illinois, Urbana, IL, 1984.

[50] F. Sakai, J.G. Stroh, D.W. Sullins, and K.L. Rinehart. Seven new didemnins from the marine tunicate *Tridemnum solidum*. *J. Am. Chem. Soc.*, 117(13):3734–3748, 1995.

[51] A. Boulanger, E. Aboumansour, A. Badre, B. Banaigs, G. Combaut, and C. Francisco. The complete spectral assignment of didemnin H, new constituent of the tunicate *Tridemnum cyanophorum*. *Tetrahedron Lett.*, 35(25):4345–4348, 1994.

[52] K.L. Rinehart. Brittish Patent Application # 8922026.3. 1989.

[53] E. Aboumansour, A. Boulanger, A. Badre, I. Bonnard, B. Banaigs, G. Combaut, and C. Francisco. [Tyr(5)]didemnin B and [D-Pro(4)]didemnin B; 2 New natural didemnins with a modified macrocycle. *Tetrahedron*, 51(46):12591–12600, 1995.

[54] V. Fimiani. *In vivo* effect of didemnin B on two tumors of the rat. *Oncol.*, 44(1):42–46, 1987.

[55] J.L. Urdiales, P. Morata, I. Núñez De Castro, and F. Sánchez-Jiménez. Antiproliferative effect of dehydrodidemnin B (DDB), a depsipeptide isolated from Mediterranean tunicates. *Cancer Lett.*, 102(1-2):31–7, 1996.

[56] R. Sakai, K.L. Rinehart, V. Kishore, B. Kundu, G. Faircloth, J.B. Gloer, J.R. Carney, M. Namikoshi, F. Sun, R.G. Hughes, D.G. Gravalos, T.G. de Quesada, G.R. Wilson, and R.M. Heid. Structure-activity relationships of the didemnins. *J. Med. Chem.*, 39(14):2819–2834, 1996.

Reproduced with permission of the copyright owner. Further reproduction prohibited without permission.

[57] C. Lobo, S.G. García-Pozo, I. Núñez de Castro, and F.J. Alonso. Effect of dehydrodidemnin B on human colon carcinoma cell lines. *Anticancer Res.*, 17(1A):333–6, 1997.

[58] H. Depenbrock, R. Peter, G.T. Faircloth, I. Manzanares, J. Jimeno, and A.R. Hanauske. *In vitro* activity of aplidine, a new marine-derived anti-cancer compound, on freshly explanted clonogenic human tumour cells and haematopoietic precursor cells. *Brit. J. Cancer*, 78(6):739–744, 1998.

[59] M.D. Lee, G.A. Ellestad, and D.B. Borders. Calicheamicins; discovery, structure, chemistry, and interaction with DNA. *Acc. Chem. Res.*, 24(8):235–243, 1991.

[60] W.M. Maiese, M.P. Lechevalier, H.A. Lechevalier, J. Korshalla, N. Kuck, A. Fantini, M.J. Wildey, J. Thomas, and M. Greenstein. Calicheamicins, a novel family of antitumor antibiotics: Taxonomy, fermentation and biological properties. *J. Antibiotics (Tokyo)*, 42:558–563, 1989.

[61] L.A. McDonald, T.L. Capson, G. Krishnamurthy, W.D. Ding, G.A. Ellestad, V.S. Bernan, W.M. Maiese, P. Lassota, C. Discafani, R.A. Kramer, and C.M. Ireland. Namenamicin, a new enediyne antitumor antibiotic from the marine ascidian *Polysyncraton lithostrotum*. *J. Am. Chem. Soc.*, 118(44):10898–10899, 1996.

[62] D. Gouiffes, M. Juge, N. Grimaud, L. Welin, M.P Sauviat, Y. Barbin, D. Laurent, C. Roussakis, J.P. Henichart, and J.F. Verbist. Bistramide A, a new toxin from the Urochordata *Lissoclinum bistratum* Sluiter: Isolation and preliminary characterization. *Toxicon*, 26(12):1129–1136, 1988.

[63] D. Watters, K. Marshall, S. Hamilton, J. Michael, M. McArthur, G Seymour, C. Hawkins, R. Gardiner, and M. Lavin. The bistratenes: new cytotoxic marine macrolides which induce some properties indicative of differentiation in HL-60 cells. *Biochem. Pharmacol.*, 39(10):1609–1614, 1990.

[64] J.-F. Biard, C. Roussakis, J.-M. Kornprobst, D. Gouiffes-Barbin, J.-F. Verbist, P. Cotelle, M.P. Foster, C.M. Ireland, and C. Debitus. Bistramide A, B, C, D, and K: A new class of bioactive cyclic polyethers from *Lissoclinum bistratum*. *J. Nat. Prod.*, 57(10):1336–1345, 1994.

[65] G. Griffiths, B. Garrone, E. Deacon, P. Owen, J. Pongracz, G. Mead, A. Bradwell, D. Watters, and J. Lord. The polyether bistratene A activates protein kinase C-delta and induces growth arrest in HL-60 cells. *Biochem. Biophys. Res. Commun.*, 222(3):802–8, 1996.

[66] B. Garrone, P. Kedar, I. Elarova, M. Lavin, and D. Watters. Approaches to determine the specific role of the delta isoform of protein kinase C. *J. Biochem. Biophys. Meth.*, 36(1):51–61, 1997.

[67] D. Watters, B. Garrone, G. Gobert, S. Williams, R. Gardiner, and M. Lavin. Bistratene A causes phosphorylation of talin and redistribution of actin microfilaments in fibroblasts: possible role for PKC-delta. *Exp. Cell Res.*, 229(2):327–335, 1996.

Reproduced with permission of the copyright owner. Further reproduction prohibited without permission.

[68] T.M. Zabriskie, C.L. Mayne, and C.M. Ireland. Patellazole C: A novel cytotoxic macrolide from *Lissoclinum patella*. *J. Am. Chem. Soc.*, 110(23):7919–7920, 1988.

[69] D.G. Corley, R.E. Moore, and V.J. Paul. Patellazole B; A novel cytotoxic thiazole-containing macrolide from the marine tunicate *Lissoclinum patella*. *J. Am. Chem. Soc.*, 110(23):7920–7922, 1988.

[70] B.S. Davidson, T.F. Molinski, L.R. Barrows, and C.M. Ireland. Varacin A: Novel benzopentathiepin from *Lissoclinum vareau* that is cytotoxic toward a human colon tumor. *J. Am. Chem. Soc.*, 113(12):4709–4712, 1991.

[71] C.J. Hawkins, M.F. Lavin, K.A. Marshall, A.L. van den Brenk, and D.J. Watters. Structure-activity relationships of the lissoclinamides, cytotoxic cyclic peptides from the ascidian *Lissoclinum patella*. *J. Med. Chem.*, 33(6):1634–1638, 1990.

[72] D.F. Sesin, S.J. Gaskell, and C.M. Ireland. The chemistry of *Lissoclinum patella*. *Bull. Soc. Chim. Belg.*, 95(9-10):853–867, 1986.

[73] B.M. Degnan, C.J. Hawkins, M.F. Lavin, E.J. McCaffrey, D.L. Parry, and D.J. Watters. Novel cytotoxic compounds from the ascidian *Lissoclinum bistratum*. *J. Med. Chem.*, 32(6):1354–1359, 1989.

[74] F.J. Schmitz, M.B. Ksebati, J.S. Chang, J.L. Wang, M.B. Hossain, D. van der Helm, M.H. Engel, A. Serban, and J.A. Silfer. Cyclic-peptides from the ascidian *Lissoclinum- patella*: Conformational analysis of patellamide D by X-ray analysis and molecular modeling. *J. Org. Chem.*, 54(14):3463–3472, 1989.

[75] J.M. Wasylyk, J.E. Biskupiak, and C.E. Costello. Cyclic peptide structures from the tunicate *Lissoclinum patella* by FAB mass spectrometry. *J. Org. Chem.*, 48(24):4445–4449, 1983.

[76] D.E. Williams, R.E. Moore, and V.J. Paul. The structure of ulithiacyclamide B. antitumor evaluation of cyclic peptides and macrolides from *Lissoclinum patella*. *J. Nat. Prod.*, 52(4):732–9, 1989.

[77] U. Schmidt, R. Utz, and P. Gleich. What is the structure of the patellamides? *Tetrahedron Lett.*, 26:4367–4370, 1985.

[78] B.M. Degnan, C.J. Hawkins, M.F. Lavin, E.J. McCaffrey, D.L. Parry, A.L. Vandenbrenk, and D.J. Watters. New cyclic peptides with cytotoxic activity from the ascidian *Lissoclinum patella*. *J. Med. Chem.*, 32(6):1349–1354, 1989.

[79] L.A. McDonald and C.M. Ireland. Patellamide E; a new cyclic peptide from the ascidian *Lissoclinum patella*. *J. Nat. Prod.*, 55(3):376–379, 1992.

[80] C.M. Ireland, A.R. Durso Jr., R.A. Newman, and M.P. Hacker. Antineoplastic cyclic peptides from the marine tunicate *Lissoclinum patella*. *J. Org. Chem.*, 47:1807–1811, 1982.

[81] C.M. Ireland and P.J. Scheuer. Ulicyclamide and ulithiacyclamide, two new small peptides from a marine tunicate. *J. Am. Chem. Soc.*, 102(17):5688–5691, 1980.

Reproduced with permission of the copyright owner. Further reproduction prohibited without permission.

[82] N.R. Shochet, A. Rudi, Y. Kashman, Y. Hod, M.R. Elmaghrabi, and I. Spector. Novel marine alkaloids from the tunicate *Eudistoma* sp. are potent regulators of cellular growth and differentiation and affect cAMP mediated processes. *J. Cell. Physiol.*, 157(3):481–492, 1993.

[83] M. Einat, M. Lishner, A. Amiel, A. Nagler, S. Yarkorli, A. Rudi, Y. Kashman, D. Markel, and I. Fabian. Eilatin: A novel marine alkaloid inhibits *in vitro* proliferation of progenitor cells in chronic myeloid leukemia patients. *Exp. Hematol.*, 23(14):1439–1444, 1995.

[84] M. Lishner, I. Shur, I. Bleiberg, A. Rudi, Y. Kashman, and I. Fabian. Sensitivity of hematopoietic progenitors of acute myeloblastic leukemia to new compounds derived from marine organisms. *Leukemia*, 9(9):1543–8, 1995.

[85] H. Kessler, M. Will, G.M. Sheldrick, and J. Antel. Assignment of proton and carbon NMR signals of didemnin A in solution. *Magn. Reson. Chem.*, 26(6):501–506, 1988.

[86] H. Kessler, M. Will, J. Antel, H. Beck, and G.M. Sheldrick. Conformational analysis of didemnins; a multidisciplinary approach by means of X-ray, NMR, molecular dynamics, and molecular mechanics techniques. *Helv. Chim. Acta*, 72(3):530–555, 1989.

[87] B. Banaigs, G. Jeanty, C. Francisco, P. Jouin, J. Poncet, A. Heitz, A. Cave, J.C. Prome, M. Wahl, and F. Lafargue. Didemnin B; comparative study and conformational approach in solution. *Tetrahedron*, 45(1):181–190, 1989.

[88] P. Marfey. Determination of D-amino acids. II. Use of a bifunctional reagent, 1,5-difluoro-2,4-dinitrobenzene. *Carlsberg Res. Commun.*, 49:591–596, 1984.

[89] M.J. Rieser, Y.-H. Hui, J.K. Rupprecht, J.F. Kozlowski, K.V. Wood, J.L. McLaughlin, P.R. Hanson, Z. Zhuang, and T.R. Hoye. Determination of absolute configuration of stereogenic carbinol centers in annonaceous acetogenins by ^{1}H- and ^{19}F-NMR analysis of Mosher ester derivatives. *J. Am. Chem. Soc.*, 114(26):10203–10213, 1992.

[90] J.A. Dale and H.S. Mosher. Nuclear Magnetic Resonance enantiomer reagents. Configurational correlations *via* Nuclear Magnetic Resonance chemical shifts of diastereomeric mandelate, *O*-methylmandelate, and α-methoxy-α-trifluoromethylphenylacetate (MTPA) esters. *J. Am. Chem. Soc.*, 95(2):512–519, 1973.

[91] M.B. Hossain, D. van der Helm, J. Antel, G.M. Sheldrick, S.K. Sanduja, and A.J. Weinheimer. Crystal and molecular structure of didemnin B, an antiviral and cytotoxic depsipeptide. *Proc. Natl. Acad. Sci. USA*, 85(12):4118–4122, 1988.

[92] M.S. Searle, J.G. Hall, I. Kyratzis, and L.P.G. Wakelin. Didemnin B, conformation and dynamics of an antitumour and antiviral depsipeptide studied in solution by ^{1}H and ^{13}C-NMR spectroscopy. *Int. J. Peptide Protein Research*, 34(6):445–454, 1989.

Reproduced with permission of the copyright owner. Further reproduction prohibited without permission.

[93] H. Kessler, S. Mronga, M. Will, and U. Schmidt. Solution structure of [Me-L-Leu^7]didemnin B determined by NMR spectroscopy and refined by MD calculation. *Helv. Chim. Acta*, 73(1):25–47, 1990.

[94] L.G. Pease, C.H. Niu, and G. Zimmermann. Solution conformation of *cyclo*-(Gly-Pro-Ser-D-Ala-pro). Hydrogen-bonded reverse turns in cyclic pentapeptides. *J. Am. Chem. Soc.*, 101(1):184–191, 1979.

[95] E.S. Stevens, N. Sugawara, G.M. Bonara, and C. Toniolo. Conformational analysis of linear peptides. 3. Temperature dependence of NH chemical shifts in chloroform. *J. Am. Chem. Soc.*, 102(23):7048–7050, 1980.

[96] K.L. Rinehart. *Peptides, Chemistry and Biology, G.R. Marshall (Ed)*, pages 626–631. ESCOM, Leiden, 1988.

[97] P.G. Canonico, W.L. Pannier, J.W. Huggins, and K.L. Rinehart. Inhibition of RNA viruses *in vitro* and in Rift Valley fever infected mice by didemnin A and didemnin B. *Antimicr. Agents Chemother.*, 22(4):696–697, 1982.

[98] D.W. Montgomery, G.K. Shen, E.D. Ulrich, and C.F. Zukoski. Immunomodulation by didemnins. Invertebrate marine natural products. *Ann. N. Y. Ac. Sci.*, 712:301–314, 1994.

[99] M.B. Teunissen, F.H. Pistoor, H.A. Rongen, M.L. Kapsenberg, and J.D. Bos. A comparison of the inhibitory effects of immunosuppressive agents cyclosporine, tetranactin, and didemnin B on human T cell responses *in vitro*. *Transplantation*, 53(4):875–881, 1992.

[100] M.B. Teunissen, F.H. Pistoor, H.A. Rongen, M.L. Kapsenberg, and J.D. Bos. Comparison of the inhibitory effects of immunosuppressive drugs cyclosporin A, tetranactin, and didemnin B on human T cell responses *in vitro*. *J. Autoimmun.*, 5(Suppl. A):XXVI, 1992.

[101] G.K. Shen, C.F. Zukoski, and D.W. Montgomery. A specific binding site in Nb2 node lymphoma cells mediates the effects of didemnin B, an immunosuppressive cyclic peptide. *Int. J. Immunopharmacol.*, 14(1):63–73, 1992.

[102] G.K. Shen, D.W. Montgomery, and C.F. Zukoski. Identification of didemnin B binding site on Nb2 node lymphoma cells. *FASEB J.*, 5(6):A1637, 1991.

[103] D.W. Montgomery and C.F. Zukoski. Didemnin B: a new immunosuppressive cyclic peptide with potent activity *in vitro* and *in vivo*. *Transplantation*, 40(1):49–56, 1985.

[104] S.W. Wynn, E.W. Nelson, D. Alexander, E.J. Eichwald, and J. Shelby. Immunosuppressive properties of didemnin B. *Clin. Res.*, 38(1):A216, 1990.

[105] D.D. Yuh, R.P. Zurcher, P.G. Carmichael, and R.E. Morris. Efficacy of didemnin B in suppressing allograft rejection in mice and rats. *Transplantation Proc.*, 21(1):1141–1143, 1989.

Reproduced with permission of the copyright owner. Further reproduction prohibited without permission.

[106] S.J. LeGrue, T.L. Sheu, D.D. Carson, J.L. Laidlaw, and S.K. Sanduja. Inhibition of lymphocyte T proliferation by the cyclic polypeptide didemnin B: No inhibition of lymphokine stimulation. *Lymphokine Res.*, 7(1):21–29, 1988.

[107] S.J. LeGrue, T.L. Sheu, and S.K. Sanduja. Immunosuppression by the cyclic peptide didemnin B: Effects on interleukin 2. *J. Cell. Biochem. Suppl.*, 12(A):226, 1988.

[108] D.W. Stevens, R.M. Jensen, and L.E. Stevens. Didemnin B prolongs rat heart allograft survival. *Transplantation Proc.*, 21(1):1139–1140, 1989.

[109] E.J. Alfrey, C.F. Zukoski, and D.W. Montgomery. Prolongation of skin allograft survival in mice by didemnin B. *Transplantation*, 54(1):188–189, 1992.

[110] T.L. Jiang, R.H. Liu, and S.E. Salmon. Antitumor activity of didemnin B in the human tumor stem cell assay. *Cancer Chemother. Pharm.*, 11(1):1–4, 1983.

[111] J.A. Stewart, W.P. Tong, J.N. Hartshorn, and J.J. McCormack. Phase I evaluation of didemnin B (NSC 325319). *Proc. Am. Soc. Clin. Oncol.*, 5:33 (A128), 1986.

[112] F.A. Dorr, R. Schwartz, J.G. Kuhn, J. Bayne, and D.D. Von Hoff. Phase I clinical trial of didemnin B. *Proc. Am. Soc. Clin. Oncol.*, 5:39 (A151), 1986.

[113] H.G. Chun, B. Davies, D. Hoth, M. Suffness, J. Plowman, K. Flora, C. Grieshaber, and B. Leyland-Jones. Didemnin B. The first marine compound entering clinical trials as an antineoplastic agent. *Invest. New Drugs*, 4(3):279–284, 1986.

[114] J.A. Stewart, J.B. Low, J.D. Roberts, and A. Blow. A phase I clinical trial of didemnin B. *Cancer*, 68(12):2550–2554, 1991.

[115] P.Y. Holoye, M.N. Raber, and D.G. Jeffries. Phase I study of didemnin B in non-small-cell bronchogenic carcinoma. *Invest. New Drugs*, 7(4):369, 1989.

[116] D.M. Shin, P.Y. Holoye, W.K. Murphy, A. Forman, S.C. Papasozomenos, W.K. Hong, and M. Raber. Phase I/II clinical trial of didemnin B in non-small-cell lung cancer: Neuromuscular toxicity is dose-limiting. *Cancer Chemother. Pharm.*, 29(2):145–149, 1991.

[117] F.A. Dorr, J.G. Kuhn, J. Phillips, and D.D. VonHoff. Phase I clinical and pharmacokinetic investigation of didemnin B, a cyclic depsipeptide. *Eur. J. Cancer Clin. Oncol.*, 24(11):1699–1706, 1988.

[118] J.H. Malfetano, J.A. Blessing, H.D. Homesley, K.Y. Look, and R. McGehee. A phase II trial of didemnin B (NSC 325319) in patients with advanced squamous cell carcinoma of the cervix. A Gynecologic Oncology Group Study. *Am. J. Clin. Oncol. Cancer Clin. Trials*, 19(2):184–186, 1996.

[119] A.J. Jacobs, J.A. Blessing, and A. Munoz. A phase II trial of didemnin B (NSC 325319) in advanced and recurrent cervical carcinoma. A Gynecologic Oncology Group Study. *Gyn. Oncol.*, 44(3):268–270, 1992.

Reproduced with permission of the copyright owner. Further reproduction prohibited without permission.

[120] S.K. Williamson, M.K. Wolf, M.A. Eisenberger, M. O'Rourke, W. Brannon, and E.D. Crawford. Phase II evaluation of didemnin B in hormonally refractory metastatic prostate cancer. A Southwest Oncology Group study. *Invest. New Drugs*, 13(2):167–170, 1995.

[121] D.M. Shin, P.Y. Holoye, A. Forman, R. Winn, R. Perezsoler, S. Dakhil, J. Rosenthal, M.N. Raber, and W.K. Hong. Phase II clinical trial of didemnin B in previously treated small-cell lung cancer. *Invest. New Drugs*, 12(3):243–249, 1994.

[122] R.B. Weiss, B.L. Peterson, S.L. Allen, S.M. Browning, D.B. Duggan, and C.A. Schiffer. A phase II trial of didemnin B in myeloma. *Invest. New Drugs*, 12(1):41–43, 1994.

[123] V.K. Sondak, K.J. Kopecky, P.Y. Liu, W.S. Fletcher, W.H. Harvey, and L.R. Laufman. Didemnin B in metastatic malignant melanoma: A phase II trial of the Southwest Oncology Group. *Anti-Cancer Drugs*, 5(2):147–150, 1994.

[124] J.H. Malfetano, J.A. Blessing, and A.J. Jacobs. A phase II trial of didemnin B (NSC 325319) in patients with previously treated epithelial ovarian- cancer - A Gynecologic Oncology Group Study. *Am. J. Clin. Oncol. Cancer Clin. Trials*, 16(1):47–49, 1993.

[125] J.M. Cain, P.Y. Liu, D.E. Alberts, H.H. Gallion, L. Laufman, J. O'Sullivan, G. Weiss, and J.N. Bickers. Phase II trial of didemnin B in advanced epithelial ovarian cancer. A Southwest Oncology Group study. *Invest. New Drugs*, 10(1):23–24, 1992.

[126] J.A. Benvenuto, R.A. Newman, G.S. Bignami, T.J.G. Raybould, M.N. Raber, L. Esparza, and R.S. Walters. Phase II clinical and pharmacological study of didemnin B in patients with metastatic breast cancer. *Invest. New Drugs*, 10(2):113–117, 1992.

[127] S.A. Taylor, P. Goodman, E.D. Crawford, W.J. Stuckey, R.L. Stephens, and E.R. Gaynor. Phase II evaluation of didemnin B in advanced adenocarcinoma of the kidney. A Southwest Oncology Group Study. *Invest. New Drugs*, 10(1):55–56, 1992.

[128] R. Motzer, H. Scher, D. Bajorin, C. Sternberg, and G.J. Bosl. Phase II trial of didemnin B in patients with advanced renal cell carcinoma. *Invest. New Drugs*, 8(4):391–392, 1990.

[129] G.R. Weiss, P.Y. Liu, J. O'Sullivan, D.S. Alberts, T.D. Brown, J.R. Neefe, and L.F. Hutchins. A randomized phase II trial of trimetrexate or didemnin B for the treatment of metastatic or recurrent squamous carcinoma of the uterine cervix. A Southwest Oncology Group Trial. *Gynecol. Oncol.*, 45(3):303–306, 1992.

[130] G. Goss, A. Muldal, R. Lohmann, M. Taylor, P. Lopez, G. Armitage, and W.P. Steward. Didemnin B in favourable histology non-Hodgkin's lymphoma. A phase II study of the National Cancer Institute of Canada Clinical Trials Group. *Invest. New Drugs*, 13(3):257–260, 1995.

Reproduced with permission of the copyright owner. Further reproduction prohibited without permission.

[131] S.L. Crampton, E.G. Adams, S.L. Kuentzel, L.H. Li, G. Badiner, and B.K. Bhuyan. Biochemical and cellular effects of didemnins A and B. *Cancer Res.*, 44(5):1796–1801, 1984.

[132] B.V. SirDeshpande and P.L. Toogood. Mechanism of protein synthesis inhibition by didemnin B *in vitro*. *Biochemistry*, 34(28):9177–9184, 1995.

[133] C.M. Crews, J.L. Collins, W.S. Lane, M.L. Snapper, and S.L. Schreiber. GTP-dependent binding of the antiproliferative agent didemnin B to elongation factor 1-alpha. *J. Biol. Chem.*, 269(22):15411–15414, 1994.

[134] K.L. Rinehart, V. Kishore, S. Nagarajan, R.J. Lake, J.B. Gloer, F.A. Bozich, K.M. Li, R.E. Maleczka, W.L. Todsen, M.H.G. Munro, D.W. Sullins, and R. Sakai. Total synthesis of didemnin A, B, and C. *J. Am. Chem. Soc.*, 109(22):6846–6848, 1987.

[135] K.L. Rinehart, R. Sakai, V. Kishore, D.W. Sullins, and K.M. Li. Synthesis and properties of the 8 isostatine stereoisomers. *J. Org. Chem.*, 57(11):3007–3013, 1992.

[136] Y. Hamada, Y. Kondo, M. Shibata, and T. Shioiri. Efficient total synthesis of didemnins A and B. *J. Am. Chem. Soc.*, 111(2):669–673, 1989.

[137] Y. Hamada, Y. Kondo, M. Shibata, and T. Shioiri. Synthetic studies on didemnins, antiviral and cytotoxic cyclic depsipeptides from a Caribbean tunicate. In T. Shiba and S. Sakakibara, editors, *Peptide Chemistry 1987*, pages 359–362. Protein Research Foundation, Osaka, 1988.

[138] W.R. Ewing, B.D. Harris, W.R. Li, and M.M. Joullié. Synthetic studies of didemnins. iv. Synthesis of the macrocycle. *Tetrahedron Lett.*, 30(29):3757–3760, 1989.

[139] W.R. Li, W.R. Ewing, B.D. Harris, and M.M. Joullié. Total synthesis and structural investigations of didemnin A, B, and C. *J. Am. Chem. Soc.*, 112(21):7659–7672, 1990.

[140] P. Jouin, J. Poncet, M.N. Dufour, I. Maugras, A. Pantaloni, and B. Castro. An improved synthesis of beta keto ester units in didemnin using 2,2-carbonylbis-3,5-dioxo-4-methyl-1,2,4 -oxadiazolidine. *Tetrahedron Lett.*, 29(22):2661–2664, 1988.

[141] P. Jouin, J. Poncet, M.N. Dufour, A. Pantaloni, and B. Castro. Synthesis of the cyclodepsipeptide nordidemnin B, a cytotoxic minor product isolated from the sea tunicate *Trididemnum cyanophorum*. *J. Org. Chem.*, 54(3):617–627, 1989.

[142] W.R. Ewing, K.L. Bhat, and M.M. Joullié. Synthetic studies of didemnins. I. Revision of the stereochemistry of the hydroxyisovalerylpropionyl (Hip) unit. *Tetrahedron*, 42(21):5863–5868, 1986.

[143] B.D. Harris, K.L. Bhat, and M.M. Joullié. Synthetic studies of didemnins. II. Approaches to statine diastereomers. *Tetrahedron Lett.*, 28(25):2837–2840, 1987.

[144] S.C. Mayer, J. Ramanjulu, M.D. Vera, A.J. Pfizenmayer, and M.M. Joullié. Synthesis of new didemnin B analogs for investigations of structure biological activity relationships. *J. Org. Chem.*, 59(18):5192–5205, 1994.

Reproduced with permission of the copyright owner. Further reproduction prohibited without permission.

[145] A.J. Pfizenmayer, J. Ramanjulu, M.D. Vera, X.B. Ding, D. Xiao, W.C. Chen, and M.M. Joullié. Synthesis and biological activities of (N-MeLeu^5)didemnin B. *Bioorg. Med. Chem. Lett.*, 6:2713–2716, 1996.

[146] A.J. Pfizenmayer, J. Ramanjulu, M.D. Vera, X.B. Ding, D. Xiao, W.C. Chen, and M.M. Joullié. The *N,O*-dimethyltyrosine unit of didemnin B: Replacements with natural and unnatural amino acids. *Abstr. Am. Chem. Soc.*, 212(2):172, 1996.

[147] J.M. Ramanjulu and M.M. Joullie. Analogs of the beta-turn of the cyclodepsipeptide didemnin B. *Tetrahedron Lett.*, 37(3):311–314, 1996.

[148] K. Gerzon. Anticancer agents based on natural product models. In J.M. Cassady and J.D. Douros, editors, *Dimeric Catharanthus alkaloids*, pages 271–317. Academic press, Inc., New York, 1980.

[149] J.J. McCormack. Pharmacology of Antitumor Bisindole Alkaloids from *Catharanthus*. In *Antitumor Bisindole Alkaloids from Catharanthus roseus (L.)*., volume 37 of *Alkaloids (San Diego)*, pages 205–228. Academic Press, Inc., Chicago, Illinois, USA; London, England, UK., 1990.

[150] E.K. Rowinsky and R.C. Donehower. The clinical pharmacology and use of antimicrotubule agents in cancer. *Chemother. Pharm. Ther.*, 52(1):35–84, 1991.

[151] R.L. Noble, C.T. Beer, and J.H. Cutts. Role of chance observations on chemotherapy: *Vinca rosea*. *Ann. N.Y. Acad. Sci.*, 76:882–894, 1958.

[152] R.L. Noble, C.T. Beer, and J.H. Cutts. Further biological activities of vincaleukoblastine, an alkaloid isolated from *Vinca rosea* (L). *Biochem. Pharmacol.*, 1:347–348, 1958.

[153] I.S. Johnson, H.F. Wright, G.H. Svoboda, and J. Vlantis. Antitumor principles derived from *Vinca rosea* Linn. I. Vincaleukoblastine and leurosine. *Cancer Res.*, 20:1016–1022, 1960.

[154] I.S. Johnson, J.G. Armstrong, M. Gorman, and J.P. Burnett. The *Vinca* alkaloids: a new class of oncolytic agents. *Cancer Res.*, 23:1390–1427, 1963.

[155] J.H. Cutts, C.T. Beer, and R.L. Noble. Biological properties of vincaleukoblastine, an alkaloid in *Vinca rosea* Linn, with reference to its antitumor action. *Cancer Res.*, 20:1023–1031, 1960.

[156] G.H. Svoboda. Alkaloids of *Vinca rosea* (*Catharanthus roseus*). IX. Extraction and characterization of leurosidine and leurocristine. *Lloydia*, 24:173–178, 1961.

[157] E.K. Rowinsky. The development and clinical utility of the taxane class of antimicrotubule chemotherapy agents. *Annu. Rev. Med.*, 48:353–374, 1997.

[158] M. Suffness. Overview of paclitaxel research. Progress on many fronts. *Taxane Anticancer Agents*, 583:1–17, 1995.

Reproduced with permission of the copyright owner. Further reproduction prohibited without permission.

[159] M.T. Huizing, V.H.S. Misser, R.C. Pieters, W.W.T. Huinink, C.H.N. Veenhof, J.B. Vermorken, H.M. Pinedo, and J.H. Beijnen. Taxanes: A new class of antitumor agents. *Cancer Invest.*, 13(4):381–404, 1995.

[160] K.C. Nicolaou, W.M. Dai, and R.K. Guy. Chemistry and biology of Taxol. *Angew. Chem., Int. Ed. Eng*, 33(1):15–44, 1994.

[161] E.K. Rowinsky, N. Onetto, R.M. Canetta, and S.G. Arbuck. Taxol: the first of the taxanes, an important new class of antitumor agents. *Sem. Oncol.*, 19(6):646–662, 1992.

[162] S.J. Clarke and L.P. Rivory. Clinical pharmacokinetics of docetaxel. *Clin. Pharmacokin.*, 36(2):99–114, 1999.

[163] W.R. Martin. Focus on docetaxel: A new antineoplastic agent approved by the FDA for the treatment of locally advanced or metastatic breast cancer. *Formulary*, 31(10):891–905, 1996.

[164] M.C. Bissery, D. Guenard, F. Gueritte-Voegelein, and F. Lavelle. Experimental antitumor activity of Taxotere (RP- 56976, NSC 628503), a Taxol analog. *Cancer Res.*, 51(18):4845–4852, 1991.

[165] F. Cabral, E. Trimble. E. Reed, and G. Sarosy. Future directions with taxane therapy. *Hematol. Oncol. Clin. N. Am.*, 13(1):21–41, 1999.

[166] M.C. Wani, H.L. Taylor, M.E. Wall, P. Coggon, and A.T. McPhail. Plant antitumor agents. VI. The isolation and structure of Taxol, a novel antileukemic and antitumor agent from *Taxus brevifolia*. *J. Am. Chem. Soc.*, 93(9):2325–2327, 1971.

[167] V. Senilh, Blechert, M. Colin, D. Guénard, F. Picot, P. Potier, and P. Varenne. Taxoids. *J. Nat. Prod.*, 47:131, 1984.

[168] A. Stierle, G. Strobel, and D. Stierle. Taxol and taxane production by *Taxomyces andreanae*, an endophytic fungus of Pacific yew. *Science*, 260:214, 1993.

[169] P.A. Francis, J.R. Rigas, M.G. Kris, K.M. Oisters, J.P. Orazem, K.J. Woolley, and R.T Heelan. Phase II trial of docetaxel in patients with stage III and IV non-small-cell lung cancer. *J. Clin. Oncol.*, 12(6):1232–1237, 1994.

[170] E.L. Trimble, J.D. Adams, D. Vena, M.J. Hawkins, M.A. Friedman, J.S. Fisherman, M.C. Christian, R. Canetta, N. Onetto, R. Hayn, and S.J. Arbuck. Paclitaxel for platinum-refractory ovarian cancer: results from the first 1,000 patients registered to National Cancer Institute Treatment Referral Center 9103. *J. Clin. Oncol.*, 11(12):2405–2410, 1993.

[171] M.R. Boyd. The future of new drug development. In J.E. Neiderhuber, editor, *Current Therapy in Oncology*, pages 11–22. B.C. Decker, Inc., Philadelphia, 1992.

[172] Z. Fan and J. Mendelsohn. Therapeutic application of anti-growth factor receptor antibodies. *Curr. Opin. Oncol.*, 10(1):67–73, 1998.

Reproduced with permission of the copyright owner. Further reproduction prohibited without permission.

[173] A.M. Gewirtz. Antisense oligonucleotide therapeutics for human leukemia. *Curr. Opin. Hematol.*, 5(1):59–71, 1998.

[174] A.M. Gewirtz. Antisense oligonucleotide therapeutics for human leukemia. *Crit. Rev. Oncol.*, 8(1):93–109, 1997.

[175] L.D. Curcio, D.Y. Bouffard, and K.J. Scanlon. Oligonucleotides as modulators of cancer gene expression. *Pharmacol. Therapeut.*, 74(3):317–332, 1997.

[176] A. Calogero, G.A. Hospers, and N.H. Mulder. Synthetic oligonucleotides: useful molecules? A review. *Pharm. World Sci.*, 19(6):264–268, 1997.

[177] A. Alama, F. Barbieri, M. Cagnoli, and G. Schettini. Antisense oligonucleotides as therapeutic agents. *Pharmacol. Res.*, 36(3):171–178, 1997.

[178] M.R. Boyd and K.D. Paull. Some practical consideration and application of the National Cancer Institute *in vitro* drug discovery screen. *Drug Dev. Res.*, 34:91–109, 1995.

[179] B.A. Teicher. *Anticancer Drug Development Guide.* Humana Press, 1997.

[180] W. Fenical. New pharmaceuticals from marine organisms. *Trends in Biotech.*, 15(9):339–341, 1997.

[181] S. Jeong, X. Chen, and P.G. Harran. Macrocyclic triarylethylenes vai Heck endocyclization: A system relevant to diazonamide synthesis. *J. Org. Chem.*, 63(24):8640–8641, 1998.

[182] P. Wipf and F. Yokokawa. Synthetic studies toward diazonamide A. Preparation of the benzofuranone-indolyloxazole fragment. *Tetrahedron Lett.*, 39(16):2223–2226, 1998.

[183] A. Boto, M. Ling, G. Meek, and G. Pattenden. A synthetic approach towards the aromatic macrocyclic core of diazonamide A based on sp(2)-sp(2) coupling protocols. *Tetrahedron Lett.*, 39(44):8167–8170, 1998.

[184] C.J. Moody, K.J. Doyle, M.C. Elliott, and T.J. Mowlem. Studies toward the synthesis of diazonamide A. Unexpected formation of a 3,4-bridged indole. *J. Chem. Soc. Perkin Trans. 1*, 16:2413–2419, 1997.

[185] J.P. Konopelski, J.M. Hottenroth, H.M. Oltra, E.A. Veliz, and Z.C. Yang. Synthetic studies on diazonamide A. Benzofuranone-tyrosine and indole-oxazole fragment support studies. *Synlett*, N7:609–611, 1996.

[186] C.J. Moody, K.J. Doyle, M.C. Elliott, and T.J. Mowlem. Synthesis of heterocyclic natural products. Model studies towards diazonamide A. *Pure Applied. Chem.*, 66(10-11):2107–2110, 1994.

[187] J.J. Manfredi and S.B. Horwitz. Taxol: An antimitotic agent with a new mechanism of action. *Pharm. Ther.*, 24:83–125, 1984.

Reproduced with permission of the copyright owner. Further reproduction prohibited without permission.

[188] M.A. Jordan and L. Wilson. The use and action of drugs in analyzing mitosis. *Meth. Cell Biol.*, 61:267–9, 1999.

[189] M.A. Jordan and L. Wilson. Use of drugs to study role of microtubule assembly dynamics in living cells. In R. B. Vallee, editor, *Methods in Enzymology; Molecular motors and the cytoskeleton, Part B.*, volume 298, pages 252–276. Academic Press, Inc., San Diego, CA, USA; London, England, UK, 1998.

[190] M.A. Jordan and L. Wilson. Microtubules and actin filaments: dynamic targets for cancer chemotherapy. *Curr. Opin. Cell Biol.*, 10(1):123–130, 1998.

[191] Y. Adler, Y. Finkelstein, J. Guindo, A. Rodriguez de la Serna, Y. Shoenfeld, A. Bayes-Genis, A. Sagie, A. Bayes de Luna, and D.H. Spodick. Colchicine treatment for recurrent pericarditis. A decade of experience. *Circulation*, 97(21):2183–2185, 1998.

[192] S.M. Abdel-Rahman, M.C. Nahata, and D.A. Powell. Response to initial griseofulvin therapy in pediatric patients with *tinea capitis*. *Ann. Pharmacother.*, 31(4):406–410, 1997.

[193] S. Gupta, N.L. Pal, S. Chandra, G.K. Jain, and J.C. Katiyar. Substituted methyl benzimidazole carbamate (CDRI Compound 81-470) in the mass treatment of poultry round worms. *Tropical Medicin*, 39(2):51–56, 1997.

[194] P. George, L.J. Journey, and M.N. Goldstein. Effects of vincristine on the fine structure of HeLa cell during mitosis. *J. Natl. Cancer Inst.*, 35:355–361, 1965.

[195] A. Krishan. Time-lapsed and ultrastructure studies on the reversal of mitotic arrest induced by vinblastine sulfate in Earle's L cells. *J. Natl. Cancer Inst.*, 41:581–586, 1968.

[196] S.S. Schochet Jr., P.W. Lampert, and K.M. Earle. Neuronal changes induced by intrathecal vincristine sulfate. *J. Neuropath. Exp. Neurol.*, 27:645–658, 1968.

[197] K.G. Bensch, R. Marantz, H. Wisniewski, and M. Shelanski. Induction *in vitro* of microtubular crystals by *Vinca* alkaloids. *Science*, 165:495–496, 1969.

[198] K.G. Bensch and S.E. Malawista. Microtubular crystals in mammalian cells. *J. Cell Biol.*, 40:95–107, 1969.

[199] H. Stebbings. Influence of vinblastine sulphate on the deployment of microtubules and ribosomes in telotrophic ovarioles. *J. Cell Biol.*, 8:111–125, 1971.

[200] J. Bryan. Vinblastine and microtubules. I. Induction and isolation of crystals from sea urchin oocytes. *Exp. Cell Res.*, 66:129–136, 1971.

[201] J. Bryan. Vinblastine and microtubules. II. Characterization of two protein subunits from the isolated crystals. *J. Mol. Biol.*, 66:157–168, 1972.

[202] J. Bryan. Defenition of three classes of binding sites in isolated microtubule crystals. *Biochemistry*, 11:2611–2616, 1972.

Reproduced with permission of the copyright owner. Further reproduction prohibited without permission.

[203] L. Wilson, A.N.C. Morse, and J. Bryan. Characterization of acetyl-^{3}H-labeled vinblastine binding to vinblastine-tubulin crystals. *J. Mol. Biol.*, 121:255–268, 1978.

[204] G.C. Na and S.N. Timasheff. *In vitro* vinblastine induced tubulin paracrystals. *J. Biol. Chem.*, 257:10387–10391, 1982.

[205] R.J. Owellen, C.A. Hartke, R.M. Dickerson, and F.O. Hains. Inhibition of tubulin-microtubule polymerization by drugs of the *Vinca* alkaloid class. *Cancer Res.*, 36(4):1499–1502, 1976.

[206] R.H. Himes, R.N. Kersey, I. Heller-Bettinger, and F.E. Samson. Action of the *Vinca* alkaloids vincristine, vinblastine, and desacetyl vinblastine amide on microtubules *in vitro*. *Cancer Res.*, 36:3798–3802, 1976.

[207] L. Wilson, M.A. Jordan, A. Morse, and R.L. Margolis. Interaction of vinblastine with steady-state microtubules *in vitro*. *J. Mol. Biol.*, 159(1):125–149, 1982.

[208] M.A. Jordan, R.H. Himes, and L. Wilson. Comparison of the effects of vinblastine, vincristine, vindesine, and vinepidine on microtubule dynamics and cell-proliferation *in vitro*. *Cancer Res.*, 45(6):2741–2747, 1985.

[209] M.A. Jordan, R.L. Margolis, R.H. Himes, and L. Wilson. Identification of a distinct class of vinblastine binding sites on microtubules. *J. Mol. Biol.*, 187(1):61–73, 1986.

[210] M.A. Jordan, D. Thrower, and L. Wilson. Mechanism of inhibition of cell proliferation by *Vinca* alkaloids. *Cancer Res.*, 51(8):2212–2222, 1991.

[211] M.A. Jordan, D. Thrower, and L. Wilson. Effects of vinblastine, podophyllotoxin, and nocodazole on mitotic spindles; Implications for the role of microtubule dynamics in mitosis. *J. Cell Sci.*, 102(3):401–416, 1992.

[212] S.E. Malawista, K.G. Bensch, and H. Sato. Vinblastine and griseofulvin reversibly disrupt the living mitotic spindle. *Science*, 160:770–772, 1968.

[213] L. Wilson and J. Bryan. Biochemical and pharmacological properties of microtubules. *Advan. Cell. Mol. Biol.*, 3:21–72, 1974.

[214] M.J. de Brabander, R.M.L. van de Veire, F.E.M. Aerts, M. Borgers, and P.A.J. Janssen. The effects of nethyk [5-(2-thienylcarbonyl)-1h-benzimidazol -2-yl] carbamate (R 17 943: NSC 238159), a new synthetic antitumoral drug interfering with microtubules, on mammalian cells cultured *in vitro*. *Cancer Res.*, 36:905–916, 1981.

[215] G. Sluder. Role of spindle microtubules in the control of cell cycle timing. *J. Cell. Biol.*, 80:674–691, 1979.

[216] G.W. Zieve, D. Turnbull, J.M. Mullins, and J.R. McIntosh. Production of large numbers of mitotic mammalian cells by use of the reversible microtubule inhibitor nocodazole. *Exp. Cell. Res.*, 126:397–405, 1980.

[217] P. Dustin. *Microtubules*. Springer-Verlag, Berlin, 2nd edition, 1984.

Reproduced with permission of the copyright owner. Further reproduction prohibited without permission.

[218] D.A. Fuchs and R.K. Johnson. Cytologic evidence that Taxol, an antineoplastic agent from *Taxus brevifolia*, acts as a mitotic spindle poison. *Cancer Treatment Rep.*, 62(8):1219–1222, 1978.

[219] P.B. Schiff, J. Fant, and S.B. Horwitz. Promotion of microtubule assembly *in vitro* by Taxol. *Nature*, 277(5698):665–667, 1979.

[220] P.B. Schiff and S.B. Horwitz. Taxol stabilizes microtubules in mouse fibroblast cells. *Proc. Natl. Acad. Sci. USA*, 77(3):1561–5, 1980.

[221] P.B. Schiff and S.B. Horwitz. Taxol assembles tubulin in the absence of exogenous guanosine 5'-triphosphate or microtubule-associated proteins. *Biochemistry*, 20(11):3247–52, 1981.

[222] N. Kumar. Taxol-induced polymerization of purified tubulin. Mechanism of action. *J. Biol. Chem.*, 256(20):10435–10441, 1981.

[223] E. Hamel, A.A. del Campo, M.C. Lowe, and C.M. Lin. Interactions of Taxol, microtubule-associated proteins, and guanine nucleotides in tubulin polymerization. *J. Biol. Chem.*, 256(22):11887–11894, 1981.

[224] W.C. Thompson, L. Wilson, and D.L. Purich. Taxol induces microtubule assembly at low temperature. *Cell Motility*, 1(4):445–454, 1981.

[225] M. de Brabander, G. Geuens, R. Nuydens, R. Willebrords, and J. de Mey. Taxol induces the assembly of free microtubules in living cells and blocks the organizing capacity of centrosomes and kinetochores. *Proc. Natl. Acad. Sci. USA*, 78:5608–5612, 1981.

[226] W.B. Derry, L. Wilson, and M.A. Jordan. Substoichiometric binding of Taxol suppresses microtubule dynamics. *Biochemistry*, 34(7):2203–2211, 1995.

[227] M.A. Jordan and L. Wilson. Kinetic analysis of tubulin exchange at microtubule ends at low vinblastine concentrations. *Biochemistry*, 29(11):2730–2739, 1990.

[228] S.B. Horwitz, D. Cohen, and S. Rao. Taxol: Mechanism of action and resistance. *Monogr. Natl. Cancer Inst.*, 15:63–67, 1993.

[229] F. Cabral and S.B. Barlow. Resistance to antimitotic agents as a gentic probe of mirotubule structure and function. *Pharm. Ther.*, 52:159–171, 1991.

[230] E. Hamel. Antimitotic natural products and their interaction with tubulin. *Med. Res. Rev.*, 16(2):207–231, 1996.

[231] D.J. de Vries and P.M. Beart. Fishing for drugs from the sea: status and strategies. *Trends in Pharmacol. Sci.*, 16(8):275–279, 1995.

[232] R.F. Ludueña, M.C. Roach, V. Prasad, G.R. Pettit, Z.A. Cichacz, and C.L. Herald. Interaction of 3 sponge-derived macrocyclic lactone polyethers (spongistatin 3, halistatin 1 and halistatin 2) with tubulin. *Drug Dev. Res.*, 35(1):40–48, 1995.

Reproduced with permission of the copyright owner. Further reproduction prohibited without permission.

[233] G.R. Pettit, F. Gao, D.L Doubek, M.R. Boyd, E. Hamel, R.L. Bai, J.M. Schmidt, L.P. Tackett, and K. Rutzler. Antineoplastic agents 252. Isolation and structure of halistatin 2 from the Comoros marine sponge *Axinella carteri*. *Gazz. Chim. Ital.*, 123(7):371–377, 1993.

[234] G.R. Pettit, R. Tan, F. Gao, M.D. Williams, D.L. Doubek, M.R. Boyd, J.M. Schmidt, J.-C. Chapuis, E. Hamel, R. Bai, J.N.A. Hooper, and L.P. Tackett. Isolation and structure of halistatin 1 from the Eastern Indian Ocean marine sponge textitPhakellia carteri. *J. Org. Chem.*, 58:2538–2543, 1993.

[235] G.R. Pettit, C.L. Herald, M.R. Boyd, J.E. Leet, C. Dufresne, D.L Doubek, J.M. Schmidt, R.L. Cerny, J.N.A. Hooper, and K.C. Rutzler. Isolation and structure of the cell growth inhibitory constituents from the Western Pacific marine sponge *Axinella* sp. *J. Med. Chem.*, 34(11):3339–3340, 1991.

[236] M.M. Wagner, D.C. Paul, C. Shih, M.A. Jordan, L. Wilson, and D.C. Williams. *In vitro* pharmacology of cryptophycin 52 (LY355703) in human tumor cell lines. *Cancer Chemother. Pharm.*, 43(2):115–125, 1999.

[237] D. Panda, K. DeLuca, D. Williams, M.A. Jordan, and L. Wilson. Antiproliferative mechanism of action of cryptophycin 52: Kinetic stabilization of microtubule dynamics by high-affinity binding to microtubule ends. *Proc. Natl. Acad. Sci. USA*, 95(16):9313–9318, 1998.

[238] D. Panda, R.H. Himes, R.E. Moore, L. Wilson, and M.A. Jordan. Mechanism of action of the unusually potent microtubule inhibitor cryptophycin 1. *Biochemistry*, 36(42):12948–12953, 1997.

[239] S.L. Mooberry, L. Busquets, and G. Tien. Induction of apoptosis by cryptophycin 1, a new antimicrotubule agent. *Int. J. Cancer*, 73(3):440–448, 1997.

[240] S.L. Mooberry, C.R. Taoka, and L. Busquets. Cryptophycin 1 binds to tubulin at a site distinct from the colchicine binding site and at a site that may overlap the *Vinca* binding site. *Cancer Lett.*, 107(1):53–57, 1996.

[241] C.D. Smith and X.Q. Zhang. Mechanism of action of cryptophycin: Interaction with the *Vinca* alkaloid domain of tubulin. *J. Biol. Chem.*, 271(11):6192–6198, 1996.

[242] K. Kerksiek, M.R. Mejillano, R.E. Schwartz, G.I. George, and R.H. Himes. Interaction of cryptophycin 1 with tubulin and microtubules. *FEBS Lett.*, 377(1):59–61, 1995.

[243] T. Golakoti, J. Ogino, C.E. Hetzel, T. Lehusebo, C.M. Jensen, L.K. Larsen, G.M.L. Patterson, R.E. Moore, S.L. Mooberry, T.H. Corbett, and F.A. Valeriote. Structure determination, conformational analysis, chemical stability studies, and antitumor evaluation of the cryptophycins. Isolation of 18 new analogs from *Nostoc* sp. strain GSV-224. *J. Am. Chem. Soc.*, 117(49):12030–12049, 1995.

Reproduced with permission of the copyright owner. Further reproduction prohibited without permission.

[244] R.L. Bai, G.F. Taylor, Z.A. Cichacz, C.L. Herald, J.A. Kepler, G.R. Pettit, and E. Hamel. The spongistatins, potently cytotoxic inhibitors of tubulin polymerization, bind in a distinct region of the *Vinca* domain. *Biochemistry*, 34(30):9714–9721, 1995.

[245] G.R. Pettit, Z.A. Cichacz, F. Gao, C.L. Herald, M.R. Boyd, and J.M. Schmidt J.N.A. Hooper. Isolation and structure of spongistatin 1. *J. Org. Chem.*, 58(6):1302–1304, 1993.

[246] G.R. Pettit, Z.A. Cichacz, F. Gao, C.L. Herald, and M.R. Boyd. Isolation and structure of the remarkable human cancer cell growth inhibitors spongistatin 2 and spongistatin 3 from an Eastern Indian Ocean *Spongia* sp. *J. Chem. Soc. Chem. Commun.*, N14:1166–1168, 1993.

[247] G.R. Pettit, C.L. Herald, Z.A. Cichacz, F. Gao, M.R. Boyd, N.D. Christie, and J.M. Schmidt. Antineoplastic agents 293. The exceptional human cancer cell growth inhibitors spongistatins 6 and 7. *Nat. Prod. Lett.*, 3:239–244, 1993.

[248] R.M. Mohammad, M.L. Varterasian, V.P. Almatchy, G.N. Hannoudi, G.R. Pettit, and A. Al-Katib. Successful treatment of human chronic lymphocytic leukemia xenografts with combination biological agents auristatin PE and bryostatin 1. *Clin. Cancer Res.*, 4(5):1337–1343, 1998.

[249] S. Haldar, A. Basu, and C. M. Croce. Serine-70 is one of the critical sites for drug-induced Bcl2 phosphorylation in cancer cells. *Cancer Res.*, 58(8):1609–1615, 1998.

[250] S. Pathak, A.S. Multani, M. Ozen, M.A. Richardson, and R.A. Newman. Dolastatin 10 induces polyploidy, telomeric associations and apoptosis in a murine melanoma cell line. *Oncol. Rep.*, 5(2):373–6, 1998.

[251] T. Turner, W.H. Jackson, G.R. Pettit, A. Wells, and A.S. Kraft. Treatment of human prostate cancer cells with dolastatin 10, a peptide isolated from a marine shell-less mollusc. *Prostate*, 34(3):175–181, 1998.

[252] A. Maki, H. Diwakaran, B. Redman, S. al Asfar, G.R. Pettit, R.M. Mohammad, and A. al Katib. The Bcl-2 and p53 oncoproteins can be modulated by bryostatin 1 and dolastatins in human diffuse large cell lymphoma. *Anticancer Drugs*, 6(3):392–7, 1995.

[253] R. Bai, G.F. Taylor, J.M. Schmidt, M.D. Williams, J.A. Kepler, G.R. Pettit, and E. Hamel. Interaction of dolastatin 10 with tubulin: induction of aggregation and binding and dissociation reactions. *Mol. Pharmacol.*, 47(5):965–976, 1995.

[254] G.R. Pettit, Y. Kamano, C.L. Herald, A.A. Tuinman, F.E. Boettner, H. Kizu, J.M. Schmidt, L. Baczynskyj, K.B. Tomer, and R.J. Bontems. Dolastatin 10 from sea hare. *J. Am. Chem. Soc.*, 109(22):6883–6885, 1987.

[255] Y. Hirata and D. Uemura. Halichondrins: antitumour polyether macrolides from a marine sponge. *Pure Appl. Chem.*, 58:701–710, 1986.

Reproduced with permission of the copyright owner. Further reproduction prohibited without permission.

[256] R.E. Schwartz, C.F. Hirsch, D.F. Sesin, J.E. Flor, M. Chartrain, R.E. Fromtling, G.H. Harris, M.J. Salvatore, J.M. Liesch, and K. Yudin. Pharmaceuticals from cultured algae. *J. Indust. Microb.*, 5:113–124, 1990.

[257] G. Trimurtulu, I. Ohtani, G.M.L. Patterson, R.E. Moore, T.H. Corbett, F.A. Valeriote, and L. Demchik. Total structures of cryptophycins, potent antitumor depsipeptides from the blue-green alga *Nostoc* sp. strain GSV-224. *J. Am. Chem. Soc.*, 116(11):4729–4737, 1994.

[258] R.A. Barrow, T. Hemscheidt, J. Liang, S. Paik, R.E. Moore, and M.A. Tius. Total synthesis of cryptophycins. Revision of the structures of cryptophycin A and cryptophycin C. *J. Am. Chem. Soc.*, 117(9):2479–2490, 1995.

[259] G.R. Pettit, C.L. Herald, Z.A. Cichacz, F. Gao, J.M. Schmidt, M.R. Boyd, N.D. Christie, and F.E. Boettner. Isolation and structure of the powerful human cancer cell growth inhibitors spongistatins 4 and 5 from an African *Spirastrella spinispirulifera* (Porifera) 1. *J. Chem. Soc. Chem. Commun.*, 24:1805–1807, 1993.

[260] M. Kobayashi, S. Aoki, H. Sakai, K. Kawazoe, N. Kihara, T. Sasaki, and I. Kitagawa. Altohyrtin A, a potent anti-tumor macrolide from the Okinawan marine sponge *Hyrtios altum*. *Tetrahedron Lett.*, 34:2795–2798, 1993.

[261] N. Fusetani, K. Shinoda, and S. Matsunaga. Cinachyrolide A, a potent cytotoxic macrolide possessing two spiro ketals from marine sponge *Cinachyra* sp. *J. Am. Chem. Soc.*, 115:3977, 1993.

[262] P.F. Muhlradt and F. Sasse. Epothilone B stabilizes microtubuli of macrophages like Taxol without showing Taxol-like endotoxin activity. *Cancer Res.*, 57(16):3344–3346, 1997.

[263] R.J. Kowalski, P. Giannakakou, and E. Hamel. Activities of the microtubule-stabilizing agents epothilones A and B with purified tubulin and in cells resistant to paclitaxel (Taxol). *J. Biol. Chem.*, 272(4):2534–2541, 1997.

[264] D.M. Bollag, P.A. McQueney, J. Zhu, O. Hensen, L. Koupal, J. Liesch, M. Goetz, E. Lazarides, and C.M. Woods. Epothilones, a new class of microtubule-stabilizing agents with a taxol-like mechanism of action. *Cancer Res*, 55:2325–2333, 1995.

[265] R. Balachandran, E. ter Haar, M.J. Welsh, S.G. Grant, and B.W. Day. The potent microtubule-stabilizing agent (+)- discodermolide induces apoptosis in human breast carcinoma cells. Preliminary comparisons to paclitaxel. *Anti-Cancer Drugs*, 9(1):67–76, 1998.

[266] R.J. Kowalski, P. Giannakakou, S.P. Gunasekera, R.E. Longley, B.W. Day, and E. Hamel. The microtubule stabilizing agent discodermolide competitively inhibits the binding of paclitaxel (Taxol) to tubulin polymers, enhances tubulin nucleation reactions more potently than paclitaxel, and inhibits the growth of paclitaxel-resistant cells. *Mol. Pharmacol.*, 52(4):613–622, 1997.

Reproduced with permission of the copyright owner. Further reproduction prohibited without permission.

[267] E. ter Haar, R.J. Kowalski, E. Hamel, C.M. Lin, R.E. Longley, S.P. Gunasekera, H.S. Rosenkranz, and B.W. Day. Discodermolide, a cytotoxic marine agent that stabilizes microtubules more potently than Taxol. *Biochemistry*, 35(1):243–250, 1996.

[268] D.T. Hung, J.B. Nerenberg, and S.L. Schreiber. Distinct binding and cellular properties of synthetic (+)- and (-)-discodermolides. *Chem. Biol.*, 1:67–71, 1994.

[269] S.P. Gunasekera, M. Gunasekera, and P. McCarthy. Discodermolide: A new bioactive macrocyclic lactam from the marine sponge *Discodermia dissoluta*. *J. Org. Chem.*, 56(16):4830–4833, 1991.

[270] B.H. Long, J.M. Carboni, A.J. Wasserman, L.A. Cornell, A.M. Casazza, P.R. Jensen, T. Lindel, W. Fenical, and C.R. Fairchild. Eleutherobin, a novel cytotoxic agent that induces tubulin polymerization, is similar to paclitaxel (Taxol). *Cancer Res.*, 58(6):1111–1115, 1998.

[271] T. Lindel, P.R. Jensen, W. Fenical, B.H. Long, A.M. Casazza, J. Carboni, and C.R. Fairchild. Eleutherobin, a new cytotoxin that mimics paclitaxel (Taxol) by stabilizing microtubules. *J. Am. Chem. Soc.*, 119(37):8744–8745, 1997.

[272] S.L. Mooberry, G. Tien, A.H. Hernandez, A. Plubrukarn, and B.S. Davidson. Laulimalide and isolaulimalide, new paclitaxel-like microtubule stabilizing agents. *Cancer Res.*, 59(3):653–660, 1999.

[273] G. Höfle, N. Bedorf, and K. Gerth. *Patent DE 4138042*, 1993.

[274] S.P. Gunasekera, M. Gunasekera, R.E. Longley, and G.K. Schulte. Discodermolide, a new bioactive polyhydroxylated lactone from the marine sponge *Discodermia-dissoluta*. *J. Org. Chem.*, 55(16):4912–4915, 1990.

[275] R.E. Longley, D. Caddigan, D. Harmody, M. Gunasekera, and S.P. Gunasekera. Discodermolide, a new, marine-derived immunosuppressive compound 1. *Invitro* studies. *Transplantation*, 52(4):650–656, 1991.

[276] R.E. Longley, D. Caddigan, D. Harmody, M. Gunasekera, and S.P. Gunasekera. Discodermolide - a new, marine-derived immunosuppressive compound 2. *In vivo* studies. *Transplantation*, 52(4):656–661, 1991.

[277] R.E. Longley, D. Caddigan, and D. Harmody. Discodermolide, a new, marine-derived immunosuppressive compound 1. *In vitro* studies (transplantation, vol 52, pg 650, 1991). *Transplantation*, 55(1):236, 1993.

[278] R.E. Longley, S.P. Gunasekera, D. Faherty, J. McLane, and F. Dumont. Immunosuppression by discodermolide. *Immunosuppr. Antiinflam. Drugs*, 696:94–107, 1993.

[279] D.T. Hung, J. Chen, and S.L. Schreiber. (+)-Discodermolide binds to microtubules in stoichiometric ratio to tubulin dimers, blocks Taxol binding and results in mitotic arrest. *Chem. Biol.*, 3(4):287–293, 1996.

Reproduced with permission of the copyright owner. Further reproduction prohibited without permission.

[280] D.G. Corley, R. Herb, R.E. Moore, P.J. Scheuer, and V.J. Paul. Laulimalide. New potent cytotoxic macrolides from a marine sponge and a nudibranch predator. *J. Org. Chem.*, 53(15):3644–3646, 1991.

[281] E Quinoa, Y Kakou, and P. Crews. Fijianolides, polyketide heterocycles from a marine sponge. *J. Org. Chem.*, 53(15):3642–3644, 1992.

[282] C.W. Jefford, G. Bernardinelli, J. Tanaka, and T. Higa. Structures and absolute configurations of the marine toxins, latrunculin A and laulimalide. *Tetrahedron Lett.*, 37(2):159–162, 1996.

[283] Friedmann T. *The development of human gene therapy.* Cold Spring Harbor Laboratory Press, Cold Spring Harbor NY, 1999.

[284] W.J. Harris and J.R. Adair, editors. *Antibody Therapeutics.* CRC Press, Inc., Boca Raton, Fl, 1997.

[285] M.L. Grossbard. *Monoclonal Antibody-Based Therapy of Cancer.* Marcel Dekker, New York, 1998.

[286] G. Dranoff. The use of gene transfer in cancer immunotherapy. *Forum*, 8(4):357–364, 1998.

[287] B.R. Minev, F.L. Chavez, and M.S. Mitchell. New trends in the development of cancer vaccines. *In Vivo*, 12(6):629–638, 1998.

[288] M.P. Velders, H. Schreiber, and W.M. Kast. Active immunization against cancer cells: impediments and advances. *Sem. Oncol.*, 25(6):697–706, 1998.

[289] J. Folkman and D. Ingber. Inhibition of angiogenesis. *Sem. Cancer Biol.*, 3(2):89–96, 1992.

[290] W. Auerbach and R. Auerbach. Angiogenesis inhibition: a review. *Pharmacol. Therapeutics*, 63(3):265–311, 1994.

[291] J. Folkman. Seminars in medicine of the Beth Israel Hospital, Boston. Clinical applications of research on angiogenesis. *New England J. Med.*, 333(26):1757–63, 1995.

[292] J. Folkman. Angiogenesis in cancer, vascular, rheumatoid and other disease. *Nature Med.*, 1(1):27–31, 1995.

[293] J. Folkman. New perspectives in clinical oncology from angiogenesis research. *Eur. J. Cancer*, 32A(14):2534–2539, 1996.

[294] J. Folkman. Tumor angiogenesis and tissue factor. *Nature Med.*, 2(2):167–168, 1996.

[295] J. Folkman. Angiogenesis and angiogenesis inhibition: an overview. *Exs*, 79:1–8, 1997.

[296] L. Beck Jr. and P.A. D'Amore. Vascular development: cellular and molecular regulation. *FASEB J.*, 11(5):365–373, 1997.

Reproduced with permission of the copyright owner. Further reproduction prohibited without permission.

[297] J. Denekamp. Vascular attack as a therapeutic strategy for cancer. *Cancer Metastasis Rev.*, 9(3):267–282, 1990.

[298] L. Holmgren, M.S. O'Reilly, and J. Folkman. Dormancy of micrometastases: balanced proliferation and apoptosis in the presence of angiogenesis suppression. *Nature Med.*, 1(2):149–153, 1995.

[299] J.M. Pluda. Tumor-associated angiogenesis: mechanisms, clinical implications, and therapeutic strategies. *Sem. Oncol.*, 24(2):203–218, 1997.

[300] G. Gastl, T. Hermann, M. Steurer, J. Zmija, E. Gunsilius, C. Unger, and A. Kraft. Angiogenesis as a target for tumor treatment. *Oncol.*, 54(3):177–184, 1997.

[301] A. Hori, R. Sasada, E. Matsutani, K. Naito, Y. Sakura, T. Fujita, and Y. Kozai. Suppression of solid tumor growth by immunoneutralizing monoclonal antibody against human basic fibroblast growth factor. *Cancer Res.*, 51(22):6180–6184, 1991.

[302] O'Reilly M.S., L. Holmgren, Y. Shing, C. Chen, R.A. Rosenthal, M. Moses, W.S. Lane, Y. Cao, E.H. Sage, and J. Folkman. Angiostatin: a novel angiogenesis inhibitor that mediates the suppression of metastases by a lewis lung carcinoma. *Cell*, 79:315–328, 1994.

[303] Y. Cao, M.S. O'Reilly, B. Marshall, E. Flynn, R.W. Ji, and J. Folkman. Expression of angiostatin cdna in a murine fibrosarcoma suppresses primary tumor growth and produces long-term dormancy of metastases. *J. Clin. Invest.*, 101(5):1055–1063, 1998.

[304] J. Folkman. Tumor angiogenesis. In J. Mendelsohn, P.M. Howley, M.A. Isreal, and L.A. Liotta, editors, *The molecular basis of cancer*, pages 206–232. W.B. Sanders Co., Philadelphia, 1995.

[305] A.E. Yu, R.E. Hewitt, E.W. Connor, and W.G. Stetler-Stevenson. Matrix metalloproteinases. Novel targets for directed cancer therapy. *Drugs and Aging*, 11(3):229–244, 1997.

[306] D.H. Ausprunk and J. Folkman. Migration and proliferation of endothelial cells in preformed and newly formed blood vessels during tumor angiogenesis. *Microvascular Res.*, 14(1):53–65, 1977.

[307] D.A. Sipkins, D.A. Cheresh, M.R. Kazemi, L.M. Nevin, M.D. Bednarski, and K.C. Li. Detection of tumor angiogenesis *in vivo* by alphaVbeta3-targeted magnetic resonance imaging. *Nature Med.*, 4(5):623–6, 1998.

[308] J.W. Uhr, R.H. Scheuermann, N.E. Street, and E.S. Vitetta. Cancer dormancy: opportunities for new therapeutic approaches. *Nature Med.*, 3(5):505–509, 1997.

[309] R.Bicknell and A.L. Harris. Mechanisms and therapeutic implications of angiogenesis. *Curr. Opin. Oncol.*, 8(1):60–65, 1996.

Reproduced with permission of the copyright owner. Further reproduction prohibited without permission.

[310] M.S. O'Reilly, L. Holmgren, C. Chen, and J. Folkman. Angiostatin induces and sustains dormancy of human primary tumors in mice. *Nature Med.*, 2(6):689–692, 1996.

[311] M.S. O'Reilly, T. Boehm, Y. Shing, N. Fukai, G. Vasios, W.S. Lane, E. Flynn, J.R. Birkhead, B.R. Olsen, and J. Folkman. Endostatin: An endogenous inhibitor of angiogenesis and tumor growth. *Cell*, 88(2):277–285, 1997.

[312] Y. Takamiya, H. Brem, J. Ojeifo, T. Mineta, and R.L. Martuza. AGM-1470 inhibits the growth of human glioblastoma cells *in vitro* and *in vivo*. *Neurosurg.*, 34(5):869–875, 1994.

[313] H.S. Rasmussen and P.P. McCann. Matrix metalloproteinase inhibition as a novel anticancer strategy: a review with special focus on batimastat and marimastat. *Pharmacol. Therapeutics*, 75(1):69–75, 1997.

[314] I.N. Nomikos, J. Elemenoglou, and J. Papatheophanis. Tamoxifen-induced endometrial polyp. A case report and review of the literature. *Eur. J. Gynaecol. Oncol.*, 19(5):476–8, 1998.

[315] J.K. Lee, B. Choi, R.A. Sobel, E.A. Chiocca, and R.L. Martuza. Inhibition of growth and angiogenesis of human neurofibrosarcoma by heparin and hydrocortisone. *J. Neurosurg.*, 73(3):429–435, 1990.

[316] J.D. Weingart, E.P. Sipos, and H. Brem. The role of minocycline in the treatment of intracranial 9L glioma. *J. Neurosurg.*, 82(4):635–40, 1995.

[317] L.D. Mayer. Future developments in the selectivity of anticancer agents: drug delivery and molecular target strategies. *Cancer Metastasis Rev.*, 17(2):211–218, 1999.

[318] C. Graziano. HER-2 breast assay, linked to Herceptin, wins FDA's okay. *Cap Today*, 12(101):14–16, 1998.

[319] C. McNeil. Herceptin raises its sights beyond advanced breast cancer. *J. Nat. Cancer Inst.*, 90(12):882–883, 1998.

[320] J. Baselga, L. Norton, J. Albanell, Y.M. Kim, and J. Mendelsohn. Recombinant humanized anti-HER2 antibody (Herceptin) enhances the antitumor activity of paclitaxel and doxorubicin against HER2/neu overexpressing human breast cancer xenografts. *Cancer Res.*, 58(13):2825–2831, 1998.

[321] R. Repp, T. Valerius, G. Wieland, W. Becker, H. Steininger, Y. Deo, G. Helm, M. Gramatzki, J.G. van de Winkel, N. Lang, and *et al.* G-CSF-stimulated PMN in immunotherapy of breast cancer with a bispecific antibody to Fc gamma RI and to HER-2/neu (MDX-210). *J. Hematother.*, 4(5):415–421, 1995.

[322] H.N. Lode, R.A Reisfeld, R. Handgretinger, K.C. Nicolaou, G. Gaedicke, and W. Wrasidlo. Targeted therapy with a novel enediyene antibiotic calicheamicin θ_1^i effectively suppresses growth and dissemination of liver metastases in a syngeneic model of murine neuroblastoma. *Cancer Res.*, 58(14):2925–2928, 1998.

Reproduced with permission of the copyright owner. Further reproduction prohibited without permission.

[323] E. Ruoslahti. How cancer spreads. *Scientific American*, 275(3):72–77, 1996.

[324] I.J. Fidler and I.R. Hart. Biological diversity in metastatic neoplasms: origins and implications. *Science*, 217(4564):998–1003, 1982.

[325] R.C. Johnson, H.G. Augustin-Voss, D.Z. Zhu, and B.U. Pauli. Endothelial cell membrane vesicles in the study of organ preference of metastasis. *Cancer Res.*, 51(1):394–399, 1991.

[326] T.A Springer. Traffic signals for lymphocyte recirculation and leukocyte emigration: the multistep paradigm. *Cell*, 76(2):301–314, 1994.

[327] M. Salmi, K. Granfors, M. Leirisalo-Repo, M. Hämäläinen, R. MacDermott, R. Leino, T. Havia, and S. Jalkanen. Selective endothelial binding of interleukin-2-dependent human T-cell lines derived from different tissues. *Proc. Natl. Acad. Sci. U.S.A.*, 89(23):11436-40(89(23):11436-40):89(23):11436–40, 1992.

[328] K.L. Cepek, S.K. Shaw, C.M. Parker, G.J. Russell, J.S. Morrow, D.L. Rimm, and M.B. Brenner. Adhesion between epithelial cells and T lymphocytes mediated by E-cadherin and the alpha E beta 7 integrin. *Nature*, 372(6502):190–193, 1994.

[329] S. Stromblad and D.A. Cheresh. Integrins, angiogenesis and vascular cell survival. *Chem. Biol.*, 3(11):881–885, 1996.

[330] S. Dedhar, E. Ruoslahti, and M.D. Pierschbacher. A cell surface receptor complex for collagen type I recognizes the Arg-Gly-Asp sequence. *J. Cell Biol.*, 104(3):585–593, 1987.

[331] M.A. Bourdon and E. Ruoslahti. Tenascin mediates cell attachment through an RGD-dependent receptor. *J. Cell Biol.*, 108(3):1149–1155, 1989.

[332] J.A. Varner and D.A. Cheresh. Integrins and cancer. *Curr. Opin. Cell Biol.*, 8(5):724–730, 1996.

[333] S. Bourdoulous, G. Orend, R. Pasqualini, and E. Ruoslahti. Integrin activation by fibrillar fibronectin is required for Rho activation and cell cycle progression in adherant normal diploid cells. *Mol. Biol. Cell*, 8(S):2314–2314, 1997.

[334] M. Fornaro, M. Manzotti, G. Tallini, A.E. Slear, S. Bosari, E. Ruoslahti, and L.R. Languino. β_1^c Integrin in epithelial cells correlates with a nonproliferative phenotype - Forced expression of *beta*$_1^c$ inhibits prostate epithelial cell proliferation. *Am. J. Pathol.*, 153(4):1079–1087, 1998.

[335] R. Pasqualini, E. Koivunen, and E. Ruoslahti. αv Integrins as receptors for tumor targeting by circulating ligands. *Nature Biotech.*, 15(6):542–546, 1997.

[336] R. Pasqualini, E. Koivunen, and E. Ruoslahti. A peptide isolated from phage display libraries is a structural and functional mimic of an RGD-binding site on integrins. *J. Cell Biol.*, 130(5):1189–1196, 1995.

Reproduced with permission of the copyright owner. Further reproduction prohibited without permission.

[337] E. Koivunen, D.A. Gay, and E. Ruoslahti. Selection of peptides binding to the $\alpha 5\beta 1$ integrin from phage display library. *J. Biol. Chem.*, 268(27):20205–20210, 1993.

[338] E. Koivunen, B.C. Wang, and E. Ruoslahti. Isolation of a highly specific ligand for the $\alpha 5\beta 1$ integrin from a phage display library. *J. Cell Biol.*, 124(3):373–380, 1994.

[339] J.M. Healy, O. Murayama, T. Maeda, K. Yoshino, K. Sekiguchi, and M. Kikuchi. Peptide ligands for integrin $\alpha v\beta 3$ selected from random phage display libraries. *Biochemistry*, 34(12):3948–3955, 1995.

[340] R. Pasqualini, E. Koivunen, R. Kain, J. Lahderanta, M. Sakamoto, A. Stryhn, R.A. Ashmun, L.H. Shapiro, W. Arap, and E. Ruoslahti. Aminopeptidase N (CD13) regulates angiogenesis and functions as a receptor for peptides that home to activated blood vessels. *Submitted*, 1999.

[341] H. Fujii, M. Nakajima, I. Saiki, J. Yoneda, I. Azuma, and T. Tsuruo. Human melanoma invasion and metastasis enhancement by high expression of aminopeptidase N/CD13. *Clin. Exp. Metastasis*, 13(5):337–344, 1995.

[342] I. Saiki, H. Fujii, J. Yoneda, F. Abe, M. Nakajima, T. Tsuruo, and I. Azuma. Role of aminopeptidase N (CD13) in tumor-cell invasion and extracellular matrix degradation. *Int. J. Cancer*, 54(1):137–43, 1993.

[343] R.B. Greenwald, A. Pendri, C.D. Conover, C. Lee, Y.H. Choe, C. Gilbert, A. Martinez, J. Xia, D. Wu, and M. Hsue. Camptothecin-20-PEG ester transport forms: the effect of spacer groups on antitumor activity. *Bioorg. Med. Chem.*, 6(5):551–562, 1998.

[344] F.P. Svinarchuk, D.A. Konevetz, O.A. Pliasunova, A.G. Pokrovsky, and V.V. Vlassov. Inhibition of HIV proliferation in MT-4 cells by antisense oligonucleotide conjugated to lipophilic groups. *Biochimie*, 75(1-2):49–54, 1993.

[345] M. Bodanszky. *Peptide chemistry : a practical textbook.* Springer-Verlag, Berlin; New York, 2nd rev. edition, 1993.

[346] D. Tandon, B.V. SirDeshpande, and P.L. Toogood. Inhibition of protein synthesis by didemnin B. *FASEB J.*, 11(9):A1406–A1406, 1997.

[347] P.L. Toogood and B.V. SirDeshpande. Mechanistic studies of the inhibition of protein synthesis by antitumor agents. *J. Cell. Biochem.*, 18D:108, 1994.

Reproduced with permission of the copyright owner. Further reproduction prohibited without permission.